

DISSERTATION

ORGANOCATALYTIC, MICHAEL-STETTER REACTION AND
RHODIUM(I)-CATALYZED HYDROHETEROARYLATION OF ACRYLATES WITH BENZOXAZOLES:
REACTION DEVELOPMENT AND INVESTIGATIONS INTO ORIGINS OF ENANTIOSELECTIVITY

Submitted by

Claire M. Filloux

Department of Chemistry

In partial fulfillment of the requirements

For the Degree of Doctor of Philosophy

Colorado State University

Fort Collins, Colorado

Spring 2015

Doctoral Committee:

Advisor: Tomislav Rovis

Brian R. McNaughton

Amy L. Prieto

Debbie C. Crans

Shane T. Hentges

Copyright by Claire Marguerite Filloux 2015

All Rights Reserved

ABSTRACT

ORGANOCATALYTIC, MICHAEL-STETTER REACTION AND RHODIUM(I)-CATALYZED HYDROHETEROARYLATION OF ACRYLATES WITH BENZOXAZOLES: REACTION DEVELOPMENT AND INVESTIGATIONS INTO ORIGINS OF ENANTIOSELECTIVITY

The chapters that follow describe two independent investigations. Both relay the development of experimental methods for the catalytic, asymmetric addition of carbon–hydrogen bonds to alkenes. In the first chapter, nucleophilic amine and *N*-heterocyclic carbene cocatalysts cooperate in the organocatalytic, cascade synthesis of benzofuranone products in good yields and high enantioselectivities. Importantly, the cascade protocol is found to outperform a two-pot procedure in which reaction intermediates are isolated and purified before the second step. Mechanistic studies reveal that additives and geometry of an olefin intermediate crucially influence reaction enantioselectivity. In the second method, a bulky Rh(I)–bisphosphine complex catalyzes the asymmetric, intermolecular addition of benzoxazoles to methacrylate derivatives in fair to excellent yields and good to excellent enantioselectivities. Detailed deuterium labeling and epimerization studies provide considerable insight into the reaction mechanism: C–H activation is reversible; migratory insertion is likely enantiodetermining; and the bulky-bisphosphine ligand likely boosts reactivity and selectivity by discouraging deleterious ligation of benzoxazole starting materials to on- or off-cycle rhodium complexes and by impeding coordination-induced product epimerization.

ACKNOWLEDGMENTS

Tom, it can't be easy to mentor me. Some need a stick. Some need a carrot. I needed Campari, a very long leash and a 6-year supply of Croatian chocolate. With another advisor, I doubt I would have stuck it out. But you saw in me far more potential than I saw in myself. In the most patient of ways, you encouraged me to explore projects that harnessed my strengths. And the awesome thing is, you don't just do this for me. You do this for all of us. I respect you as a mentor and as a person, and I consider myself uncannily lucky to have had the chance learn from you.

Don, Chris, Ron, Tom, Mike and Pat, I have loved getting to know you over the past six years. Far more frequently than good results, my research generated stuck NMR samples, splintered glassware, motionless stir-plates, stalled vacuum pumps and clogged GC-MS needles. None of my work, none of any of our work, could be done without you. More importantly, you are my friends. On days when I felt particularly discouraged, I would find excuses to come see you in the basement to chat, even for just five minutes. I will miss those visits.

Marilyn, Johanna and Suzanne, thank you for your friendship. You helped me stay grounded, helped me remember who I am and helped me put one foot in front of the other.

Dave Freeman, you are a brother to me. You taught me about wireless routers and more than I ever wanted to know about pornography. On the grimmest days, we took bike rides over Bingham hill, watched Hot Tub Time Machine in bathrobes, and streamed every album ever produced by Elton John. You do everything without regret, and you inspire me to live my own life with gusto. If you're not married by the time you're 40, I will agree to enter into a platonic partnership with you.

Mom, Dad and Maddi, I love you with all my being. Mom, your section is by far the hardest to write. How can I possibly articulate what you mean to me? After all, you and I both hate clichés. But here goes—forgive me. No one's criticism cuts me so deep. No one's affection fills me so full. Before emergency surgery, no one else's hand will do. In no one else do I see so much of myself.

Dad, I've always felt we have a spiritual connection. When we run trails together it feels like church, but less boring. The way you live—in service of others—inspires me to do the same. I'll try to be good, dad.

Maddi, you are my tenderoni. I have loved watching you come into your own. You are a strong, observant and empathetic woman, and you are so tremendously easy to love. Remember that game we used to play? Well, in response to the question “if you had to be someone in the world besides yourself, who would you be?” I pick you.

Rovis group, you are a continuation of my family. Kevin Oberg, I believe you were a gift to me. You taught me to be a courteous and conscientious colleague. You, more than anyone else, helped me become a better scientist, not because you helped me do science like other people, but because you helped me do science like Claire. Intellectually, personally, even spiritually, you helped me grow into myself. No matter what career you decide to pursue, you are and will be a grade A mentor.

John, Natthawat, Dan, Oz, when I asked for help, you would drop whatever you doing, even if you were mid pipette. Stephen, you indulged so many ridiculous questions with kindness. Stéphane, you watched over me, and you trusted me with your son, even after I got shampoo in his eyes. Scott and Alexis, no matter how much I dreaded going to lab, I looked forward to seeing you there. Ben Kohn and Philip Wheeler, I quite simply adore you. You are curious, generous and genuine. You have tremendous personal and intellectual integrity, and I am delighted to have overlapped with you.

Derek Dalton, you live a gutsy life and do gutsy science. You push past your comfort zone, and I am in awe of that. It is so easy for me to keep my world small. But you show me that far more interesting places can be reached when you stop playing safe. Like the best scientists, you are always curious and always humble.

Tiff, Dar and J, you are my people. J-bear, I joined the Rovis group to be with you, and I graduated from the Rovis group thanks to you. You are wickedly smart, unrelentingly loyal and you see the best in people in a way I can only aspire to. I love you, girlie! Dar-bear, there were days when the only thing that got me through was the thought of Sunday crib-coff. You bake one hell of a crème brûlée. You make me laugh till I cry. You are a gem. Tiff, you once told me that you could never be friends with someone you don’t respect. Me neither. You are a force of nature. You are genuine, dogged, humble and smart. Tu es un monstre. We may have nothing in common, but I love you the more for it. You challenge me. You surprise me. You delight me. You are the French sister I never had.

TABLE OF CONTENTS

ABSTRACT	ii
ACKNOWLEDGMENTS.....	iii
GIVING IN	vii
CHAPTER ONE: Multicatalytic, Asymmetric Michael–Stetter Reaction of Salicylaldehydes and Activated Alkynes	1
1.1 Introduction	1
1.2 Results and discussion.....	3
1.2.1 Reaction optimization and salicylaldehyde scope.....	3
1.2.2 Investigations into reaction enantioselectivity	6
1.2.3 Unsymmetrical alkynes and electron-deficient terminal allenes as Michael acceptors.....	8
1.2.4 Side products and rationale for base selection	11
1.2.5 Substrate limitations.....	12
1.3 Summary	14
1.4 References	15
CHAPTER TWO: Rh(I)–Bisphosphine Catalyzed Asymmetric, Intermolecular Hydroheteroarylation of α -Substituted Acrylate Derivatives.....	18
2.1 Synopsis	18
2.2 Introduction	18
2.3 Results and discussion.....	21
2.3.1 Initial reaction optimization with [Rh(cod)OAc] ₂	21
2.3.2 Mechanistic investigations of achiral system.....	23
2.3.3 Optimization of the asymmetric hydroheteroarylation reaction with second generation ligands.....	26
2.3.4 Scope of the asymmetric hydroheteroarylation reaction.....	26
2.3.5 Mechanistic investigations into origin of enantioselectivity	28
2.4 Summary	34
2.5 References	35

APPENDIX ONE: Multicatalytic, Asymmetric Michael–Stetter Reaction of Salicylaldehydes and Activated Alkynes	41
APPENDIX TWO: Rh(I)–Bisphosphine Catalyzed Asymmetric, Intermolecular Hydroheteroarylation of α -Substituted Acrylate Derivatives.....	70

GIVING IN

At 1.4 million atmospheres
xenon, a gas, goes metallic.
Between squeezed single-bevel
diamond anvils jagged bits
of graphite shot with a YAG
laser form spherules. No one
has seen liquid carbon. Try
to imagine that dense world
between ungiving diamonds
as the pressure mounts, and
the latticework of a salt
gives, nucleating at defects
a shift to a tighter order.
Try to see graphite boil. Try
to imagine a hand, in a press,
in a cellar in Buenos Aires,
a low-tech press, easily
turned with one hand, easily
cracking a finger in another
man's hand, the jagged bone
coming through, to be crushed
again. No. Go back, up, up
like the deep diver with
a severed line, up, quickly,

to the orderly world of ruby
and hydrogen at 2.5 megabar,
the hydrogen coloring near
metallization, but you hear
the scream in the cellar, don't
you, and the diver rises too fast.

Roald Hoffman in *Verse and Universe: Poems about Science and Mathematics*; Brown, K., Ed.; Milkweed Editions:
Minneapolis, 1998

CHAPTER 1

Multicatalytic, Asymmetric Michael–Stetter Reaction of Salicylaldehydes and Activated Alkynes^[1]

1.1 Introduction

Cascade catalysis has garnered significant recent attention from the synthetic community as a means to swiftly assemble complex molecules from simple starting materials with minimal time, waste and manipulation of reaction intermediates.^[2] Especially powerful in its application to total synthesis, asymmetric tandem catalysis has enabled rapid access to enantioenriched products with high levels of selectivity.^[2b,2d–h,2i,2k] Although most examples exploit a single catalyst to promote multiple, sequential transformations,^[3] systems relying on two or more catalysts have been reported.^[2a,2c,2k,4] Inherent in any multiple catalyst system is the challenge of compatibility. Avoidance of mutual interference often obliges step-wise addition of catalysts or reagents and variation of reaction conditions over time.^[5] Nevertheless, cascades triggered by a single operation have been accomplished.^[4,6]

In 2012, we reported the development of a one-step, asymmetric Michael–benzoin reaction of β -ketoesters **1** and α,β -unsaturated aldehydes **2** mediated by compatible amine **3** and *N*-heterocyclic carbene (NHC, conjugate base of **4a**) catalysts (Figure 1.1).^[7] Importantly, the one-pot procedure was found to give elaborated cyclopentanone products **5** in higher yield and enantioselectivity than a step-wise protocol, wherein intermediate aldehyde **6** is isolated and subjected to the benzoin reaction in a subsequent step (Figure 1.1). This observation testifies to the power of cascade catalysis: by quickly relaying intermediates from one reaction to the next, catalysts can work synergistically to discourage undesired pathways.

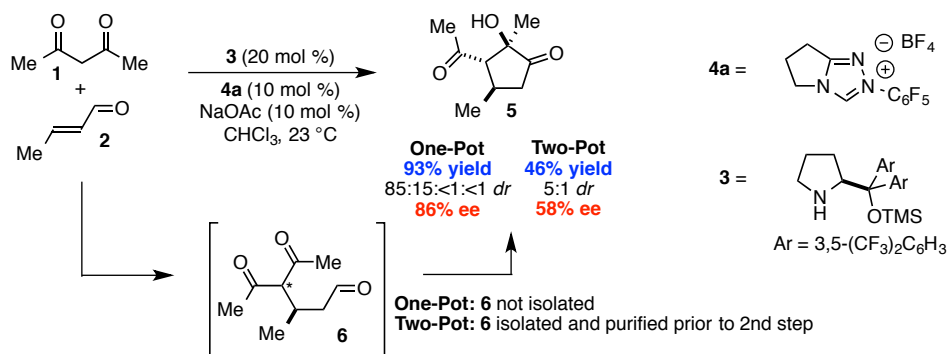
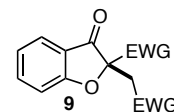


Figure 1.1 Lathrop and Rovis's Multicatalytic Michael–benzoin cascade^[7]

Encouraged by the discovery that NHCs could participate in cascade catalysis, we were inspired to use NHCs to mediate the cascade assembly of benzofuranone products **9** asymmetrically.^[8] A range of biological activities associated with 3(2H)-benzofuranones including antifungal,^[9] anti-psychotic^[10] and anti-cancer^[11] properties make these products attractive synthetic targets. Among recently-synthesized natural products containing a 2,2'-disubstituted benzofuranone core, rocaglamide demonstrates appreciable cytotoxicity in mice and human cells lines,^[12] vinigrol displays anti-hypertensive properties^[13] and Sch202596 shows promise in Alzheimers therapy.^[14]



Although a number of methods for the racemic assembly of benzofuranones containing C2 quaternary centers have been reported, many proceed from relatively advanced starting materials^[15] or suffer from competitive reaction pathways.^[16] More rare are enantioselective preparations of 2,2'-disubstituted benzofuranones. In 2008, Jørgensen and coworkers reported that 2-*tert*-butoxy carbonyl benzofuranone could be alkylated asymmetrically with tetraethyl ethylidene-bisphosphonate to give the corresponding 2,2'-disubstituted product in excellent enantioselectivity.^[17] In a different approach, we have shown that chiral triazolinylidene carbenes mediate the cyclization of aldehyde-tethered, β,β -disubstituted Michael acceptors related to **12** to give benzofuranone products in excellent enantioselectivities (Figure 1.2, **12** \rightarrow **9**).^[18]

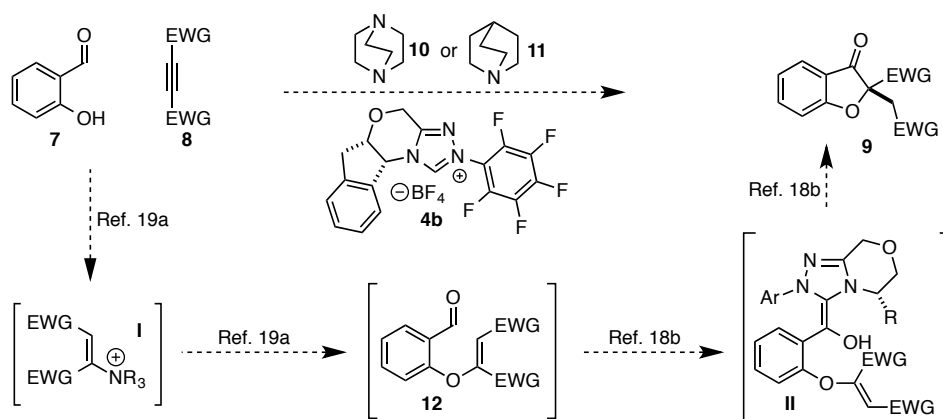


Figure 1.2 Envisioned multicatalytic Michael–Stetter cascade

Although the strategies described provide benzofuranone products in good yield and exceptional selectivities, both make use of substrates that require multiple steps to prepare.^[18b] We imagined that we could expedite the synthesis of benzofuranone products **9** by assembling intermediate aldehydes **12** *in situ* via a base-catalyzed conjugate addition reaction of salicylaldehydes **7** and electrophilic alkynes **8** (Figure 1.2, **7** \rightarrow **12**). Fan and

coworkers have shown that 1,4-diazabicyclo[2.2.2]octane (DABCO) (**10**) efficiently mediates the addition of amine and oxygen nucleophiles to dimethyl acetylenedicarboxylate (DMAD) (**8a**) and alkyl propiolates.^[19] In our envisioned sequence, a tertiary amine such as quinuclidine (**11**) or DABCO (**10**) activates alkyne **8** toward nucleophilic attack to give intermediate aldehyde **12** (Figure 1.2, **7** → **12**). Subsequent chiral carbene-promoted Stetter reaction sets a quaternary stereocenter and yields product **9** asymmetrically (Figure 1.2, **12** → **9**).

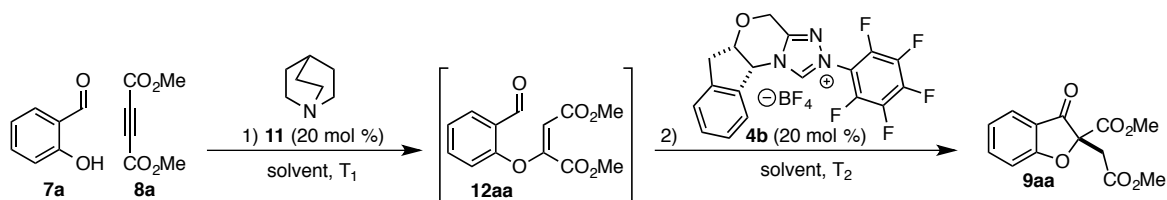
Crucial to the success of any catalytic cascade is a compatible catalyst system. For many Stetter systems, tertiary amines perform as optimal bases for carbene generation.^[18b,20] For this reason, we were encouraged that DABCO or quinuclidine would not only serve as nucleophilic “triggers”^[19a] to promote our imagined conjugate addition reaction but would also prove suitable bases to deprotonate triazolium salt precatalyst **4b** and generate the active carbene species.

1.2 Results and discussion

1.2.1 Reaction optimization and salicylaldehyde scope

We first examined whether our envisioned cascade could be performed in a one-pot, step-wise fashion. Carbenes have been shown capable of nucleophilic addition into DMAD and other activated alkynes.^[21] To circumvent this undesired reaction pathway, a mixture of salicylaldehyde (**7a**) and DMAD (**8a**) was treated first with quinuclidine **11** and then with triazolium salt **4b** in a second step. Benzofuranone product **9aa** was isolated from this

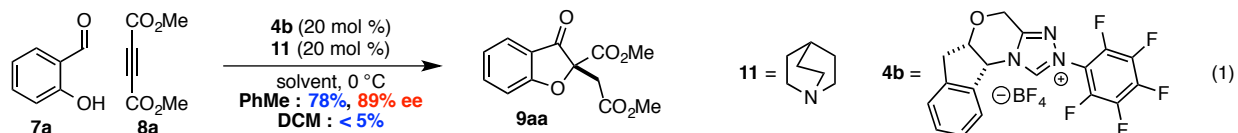
Table 1.1 Solvent and temperature screen



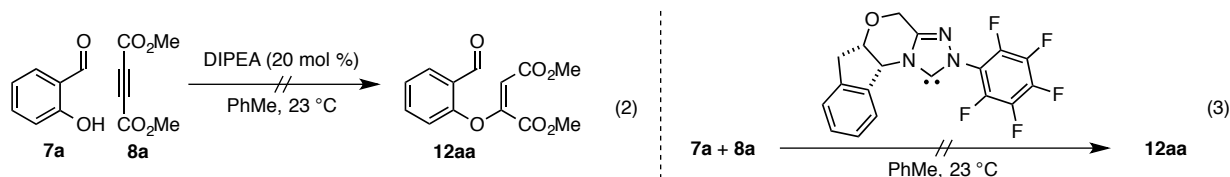
entry	solvent	T ₁ (°C)	T ₂ (°C)	yield (%)	ee (%)
1	DCM	23	0	85	81
2	THF	23	0	76	83
3	TAA	23	0	63	78
4	9:1 PhMe/TAA	23	0	87	86
5	PhMe	23	0	82	89
6	PhMe	23	23	75	86
7	PhMe	23	-10	60	90
8	PhMe	23	-40	64	92
9	PhMe	-40	NA	< 5%	NA

one-pot, two-step sequence in good overall yield and enantioselectivity (Table 1.1, entry 1). In a brief solvent screen, dichloromethane (DCM) and 9:1 toluene/*t*-amyl alcohol (PhMe/TAA) provided product **9aa** in similarly high yields (Table 1.1, entries 1 and 4), while toluene gave the highest level of enantioselectivity (Table 1.1, entries 1–5). Lowering temperatures of the Stetter reaction (step 2) improves enantioselectivity slightly but results in longer reaction times and lower product yields (Table 1.1, entries 6–8). No productive reaction is observed when the conjugate addition reaction is conducted at low temperature (Table 1.1, entry 9).

Although we had developed conditions to mediate two bond-forming events in one reaction vessel with high levels of asymmetric induction, we hoped to reduce the number of required synthetic manipulations to a single operation. To this end, we treated a mixture of **7a**, **8a** and **4b** with quinuclidine (**11**) at 0 °C in toluene. To our delight, the cascade proceeds smoothly to give **9aa** in undiminished yield and enantioselectivity (eq. 1). The one-step protocol was found to be scalable: on a 1 g scale, product **9aa** (1.48 g, 79% yield) is obtained in 88% ee. When the one-step reaction is performed in dichloromethane, however, only starting material and decomposition products are recovered; under these conditions, nucleophilic addition of **4b**-derived carbene into DMAD²¹ may interfere with the desired conjugate addition reaction (eq. 1).

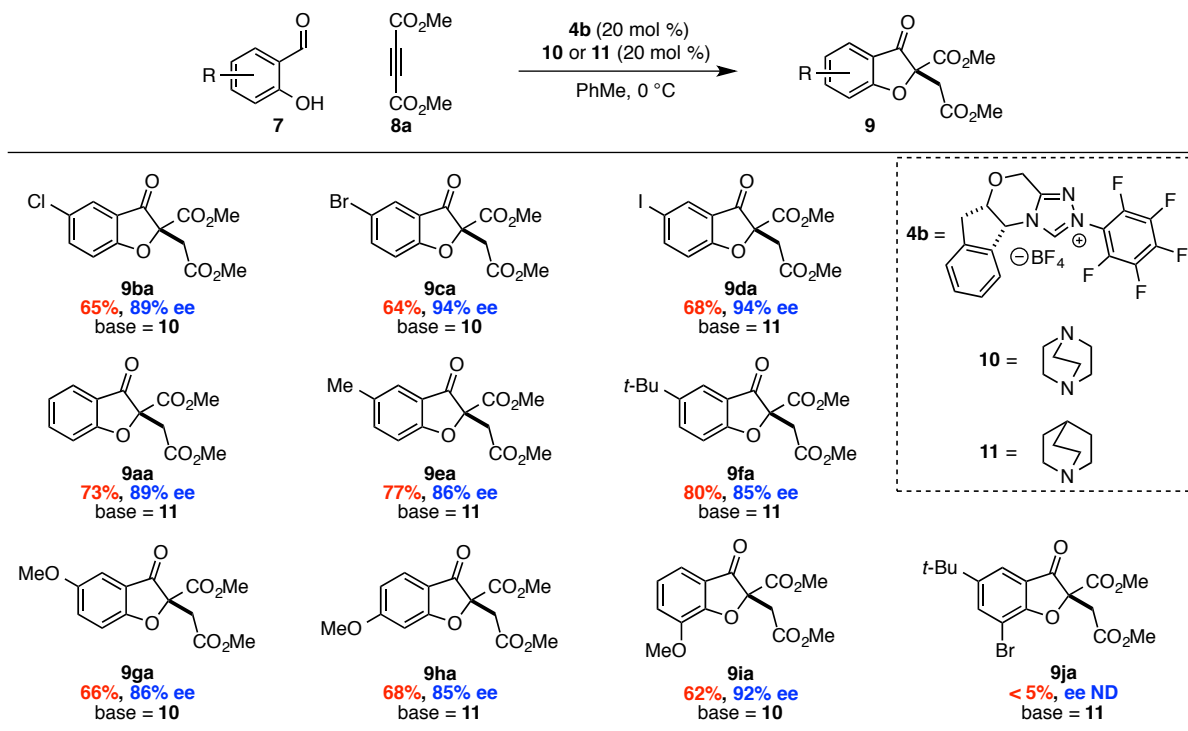


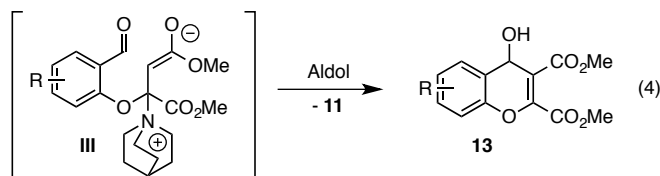
A series of control experiments were performed to probe the mechanism of the conjugate addition reaction. We had envisioned that Michael addition proceeds through nucleophilic activation of DMAD via intermediate **I** (Figure 1.2). However, an alternative pathway could be imagined in which quinuclidine deprotonates salicylaldehyde, which adds conjugately to DMAD. To examine the viability of a base-catalyzed pathway, we exchanged quinuclidine for diisopropylethylamine (DIPEA)— DIPEA should have similar basicity to quinuclidine (**11**), but since it is much bulkier than **11**, it should be much less nucleophilic. Treatment of salicylaldehyde and DMAD with this less competent nucleophile but similarly strong base resulted in complete recovery of starting material (eq. 2), suggesting that the proposed nucleophilic pathway is indeed at work in our developed conditions. Moreover, exposure of salicylaldehyde and DMAD to the free carbene derived from azolium salt **4b** gave no discernable product by ¹H NMR spectroscopy (eq. 3). Thus, it is highly probable that quinuclidine (**11**) rather than carbene-**4b** participates as the nucleophilic activator in our system.



With a productive one-step protocol in hand, we investigated the scope of the reaction with respect to salicylaldehyde 7. Indeed, both electron-rich and electron-deficient salicylaldehydes with various substitution patterns participate in the Michael–Stetter sequence to give products 9 in good yields and moderate to excellent enantioselectivities (Table 1.2). Electron-deficient salicylaldehydes give generally higher enantioselectivities but poorer yields than electron-rich salicylaldehydes. The lower yields observed for these substrates are attributed to competitive formation of chromene side-products 13 derived from intramolecular aldol of intermediate enolate **III** (eq. 4, *vide infra*, section 1.2.4). 3-Substituted salicylaldehydes give the lowest observed yields; steric bulk surrounding the phenoxide likely impedes nucleophilic addition into DMAD (Table 1.2, **9ia–9ja**). Indeed, when the 3-substituent is sufficiently large, no conjugate addition is observed (Table 1.2, **9ja**). Absolute configuration of products 9 was assigned by X-ray crystal structure of iodide **9da**. The others were assigned by analogy.

Table 1.2 Salicylaldehyde scope





1.2.2 Investigations into reaction enantioselectivity

We were intrigued by the variation of enantioselectivity across products **9** which appeared to be independent of steric or electronic factors. For example, 4- and 5-methoxy substrates **7h** and **7g** provide products with identical ees in spite of their differing electronic impact on both aldehyde and tethered alkene (Table 1.2, **9ga** vs. **9ha**). Furthermore, sterically similar substrates **7d** and **7e** give products with disparate ees (Table 1.2, **9da** vs. **9ea**, 94 and 86% ee respectively, corresponding to ~0.5 kcal/mol energy difference).

To probe the origin of ee variation, we performed a two-pot Michael–Stetter protocol wherein intermediate aldehyde **12** was isolated, purified and subjected to Stetter conditions in a second step (Table 1.3). Treatment of DMAD and salicylaldehydes **7f**, **7a**, and **7c** with base gives the corresponding intermediate aldehydes **12fa**, **12aa**, and **12ca** in good yields (Table 1.3). When intermediate aldehydes **12fa**, **12aa**, and **12ca** are exposed to precatalyst **4b** and base in the usual manner, however, products **9fa**, **9aa**, and **9ca** are obtained in appreciably lower and more uniform enantioselectivities than those observed in the one-pot procedure (Table 1.3).

Table 1.3 Ee erosion in a two-pot protocol

7

8a

1) base (20 mol %)
PhMe, 0 °C

12

2) **4b** (20 mol %)
PhMe, 0 °C

9

	7	base	9	Two-pot	One-pot
7f			<p>9fa</p>	90% 82% ee	80% 85% ee
7a			<p>9aa</p>	87% 84% ee	78% 89% ee
7c			<p>9ca</p>	86% 87% ee	64% 94% ee

4b =

Two-pot: 12 is isolated and purified prior to 2nd step.
Two-pot yields are over 2 steps

We speculated that a trace impurity present in or side-product derived from certain salicylaldehydes **7** might be crucial for the high enantioselectivities obtained in the one-pot protocol; removal of the species during isolation of intermediate **12** could result in a drop in enantioselectivity of the subsequent Stetter reaction. Indeed, when Stetter reactions of intermediate aldehydes **12ca** and **12fa** are conducted in the presence of an equivalent of exogenous salicylaldehyde **7c** (which gives product **9ca** in high ee in the one-pot protocol), the high enantioselectivities of products **9ca** and **9fa** are recovered (Table 1.4, entries 1 and 3).

Table 1.4 Additive effect on Stetter enantioselectivity

entry	9	base	additive	equiv	yield (%)	ee(%) w/o additive	ee(%) w/ additive
1		10	7c	1.05	78	86	93
2	9ca	10	14a	0.1	90	86	94
3		11	7c	1.05	63	83	89
4	9fa	11	14a	0.1	84	83	92

7c =

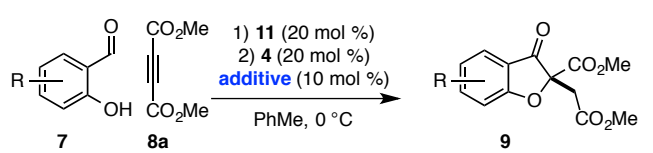
14a =

We aimed to identify the species present in exogenous salicylaldehydes **7** that might promote elevation of enantioselectivity. Strong H-bond donors such as catechols have been shown to improve yields and enantioselectivities of enamine-promoted Michael additions of aldehydes into enones.^[22] We hypothesized that trace catechol derived from Dakin oxidation^[23] of the salicylaldehyde might contribute to Stetter enantioselectivity. Consistent with this theory, addition of 10 mol % catechol **14a** to the Stetter reaction of intermediate aldehydes **12ca** and **12fa** improves product enantioselectivities to excellent 94% ee and 92% ee, respectively (Table 1.4, entries 2 and 4).

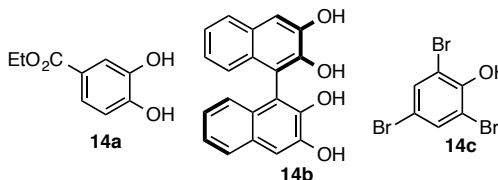
When catechol **14a** is added with precatalyst **4b** in the one-pot, two-step protocol, similar improvement in enantioselectivity is observed for a variety of substrates (Table 1.5, entries 1–3). On the other hand, addition of **14a** in the one-pot, one-step procedure provides virtually no change in selectivity (data not shown). Presumably, catechol **14a** adds conjugately to DMAD (**8a**) in these cases,^[19a] and the Stetter reaction proceeds with unimproved selectivity, since no free catechol exists in the reaction media at the time of the second step. Finally, an observed match–mismatch effect provides convincing support for catechol participation in the selectivity-determining step of

the Stetter reaction. When chiral, binaphthyl-derived catechol **14b** is used as an additive, enantioselectivity of product **9aa** improves from 89% ee to 95% ee with (*S,R*)-precatalyst **4b** but shows no change with (*R,S*) precatalyst **ent-4b** (Table 1.5, entries 4 and 5). Although the exact mechanism by which catechol improves enantioselectivities of products **9** is not fully understood, it appears that the 1,2-difunctionality of catechol rather than its low pKa is responsible for ee elevation: when catechol **14a** is replaced with acidic phenol **14c**, no improvement in enantioselectivity of products **9** is observed (Table 1.5, entry 6).^[24]

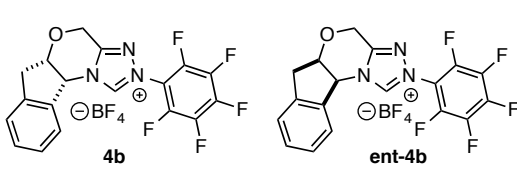
Table 1.5 Catechol effect on enantioselectivity in the one-pot, two-step Michael–Stetter reaction



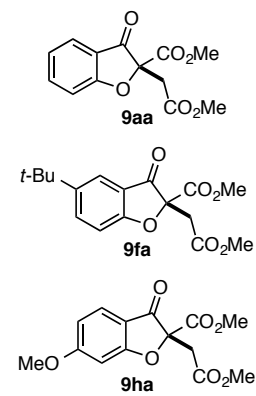
entry	additive	4	9	yield (%)	ee (%) w/o additive	ee (%) w/ additive
1	14a	4b	9aa	63	89	93
2	14a	4b	9fa	78	85	90
3	14a	4b	9ha	75	85	93
4	14b	4b	9aa	63	89	95
5	14b	ent-4b	9aa	73	-89	-89
6	14c (1 equiv)	4b	9aa	60	89	89



14a **14b** **14c**



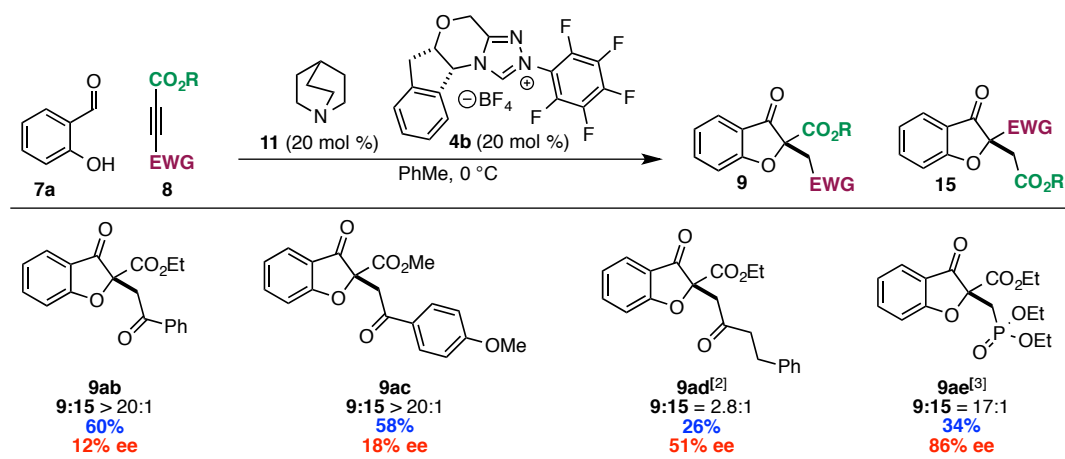
4b **ent-4b**



1.2.3 Unsymmetrical alkynes and electron-deficient terminal allenes as Michael acceptors

Having explored the scope and selectivity of our Michael–Stetter reaction between DMAD and a variety of salicylaldehydes, we focused on incorporation of unsymmetrical alkynes as Michael acceptors in this cascade. Ketoalkynoates **8b** and **8c** participate in the one-step reaction with salicylaldehyde (**7a**) to give moderate yields of products **9ab** and **9ac** regioselectively but with low enantioselectivity (Table 1.6). Attenuation of alkyne electrophilicity by substitution of the aryl ketone with phenethyl ketone improved the enantioselectivity of major product **9ad** but resulted in formation of a second regioisomer **15ad** in ~10% yield. Interestingly, minor regioisomer **15ad** is obtained in high enantioselectivity relative to major product **9ad** (Table 1.6, footnote 2). Finally, phosphonate ester **8e** reacts in a one-pot, two-step protocol to give **9ae** in fair yield and good enantioselectivity (Table 1.6, entry 4).

Table 1.6 Unsymmetric alkyne scope^[1]



^[1]Product ratio determined by ¹H NMR of the crude reaction mixture. ^[2]Minor regioisomer (**15ad**) isolated in 9% yield and 89% ee. ^[3]**9ae** was prepared in a one-pot, two-step sequence (see Appendix One).

Although we were pleased to find that a number of unsymmetrical alkynes were tolerated in our one-pot protocol, we were interested in identifying substrates that would participate with high levels of both regioselectivity and enantioselectivity. Intermediate aldehydes **16** containing a single electron-withdrawing substituent on the Michael acceptor have been shown to undergo the Stetter reaction with high enantioselectivity under conditions similar to these (eq. 5).^[18b] Our initial attempt to access related intermediate aldehyde **16** via the necessarily regioselective Michael addition of salicylaldehyde (**7a**) into singly activated alkynoate **17** resulted only in isolation of starting material and decomposition products (eq. 6).^[25] Nevertheless, we were encouraged to try other modes of entry to intermediates **16**. Shi and coworkers have shown that activated allenes behave as alkyne surrogates in a DABCO-catalyzed conjugate addition reaction with salicylaldehyde.^[25] Indeed, we were delighted to find that subjection of allenone **18a** and allenoate **18b** to our one-pot, two-step protocol in a variety of solvents gave benzofuranone products **19a** and **19b** in moderate yields and good to excellent enantioselectivities (Table 1.7).

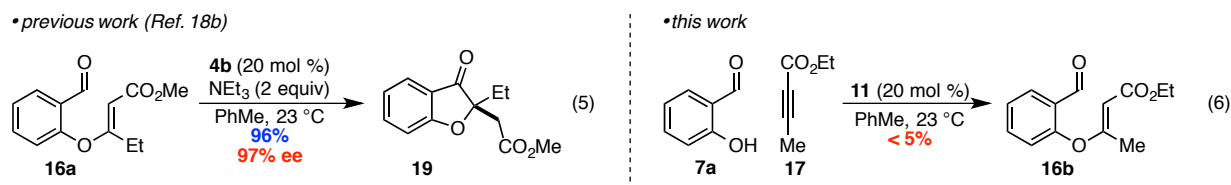
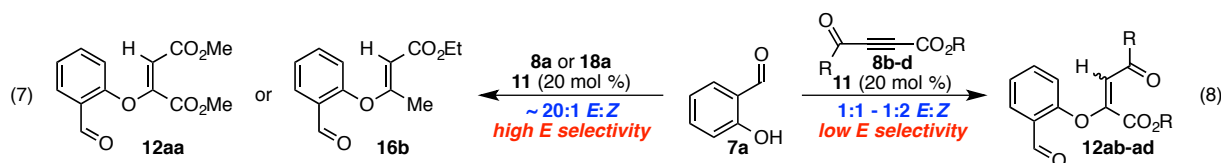


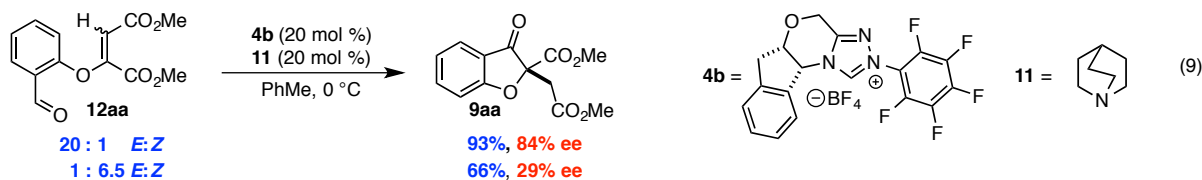
Table 1.7 One-pot, two-step Michael–Stetter reaction with activated allenes

entry	solvent	T ₁ (°C)	T ₂ (°C)	Product (19)	yield (%)	ee (%)
1	THF	23	0		60	78
2	PhMe	23	23		50	98
3	PhMe	110	110	19b	50	89
4	DCM	23	23	19b	59	96

We hoped to understand why certain substrates (DMAD, allenoate **18b**) react with much greater enantioselectivity than others (ketoalkynoates **8b** and **8c**). A factor that has been shown to influence Stetter enantioselectivity is olefin geometry.^[18a–b] While intermediate aldehydes **12aa** and **16b** (derived from DMAD and allenoate **18b**, respectively) form with near perfect *E*-selectivity under our conditions (eq. 7), intermediate aldehydes derived from ketoalkynoate substrates (**8b–d**) are observed as unselective mixtures of *E* and *Z* isomers (eq. 8).



For a number of Stetter scaffolds, the *E*-isomer has been shown to react in higher yield and with greater enantioselectivity than the corresponding *Z*-isomer.^[18a–b] To examine whether a relatively high *Z* to *E* ratio could contribute to the low enantioselectivities obtained for ketoalkynoate substrates **8a–c**, we subjected a 6.5:1 *Z* to *E* mixture^[26] of intermediate aldehyde **12aa** to our established Stetter conditions. Whereas *E*-**12aa** reacts to afford product **9aa** in 84% ee, *Z*-enriched **12aa** gives **9aa** in only 29% ee and in appreciably lower yield (eq. 9). The disparity in enantioselectivity across batches of intermediate aldehyde **12aa** suggests that striking differences in *E* to *Z* ratios of conjugate adducts **12aa** and **16b** on one hand, and **12ab–12ad** on the other, may contribute significantly to Stetter selectivity.

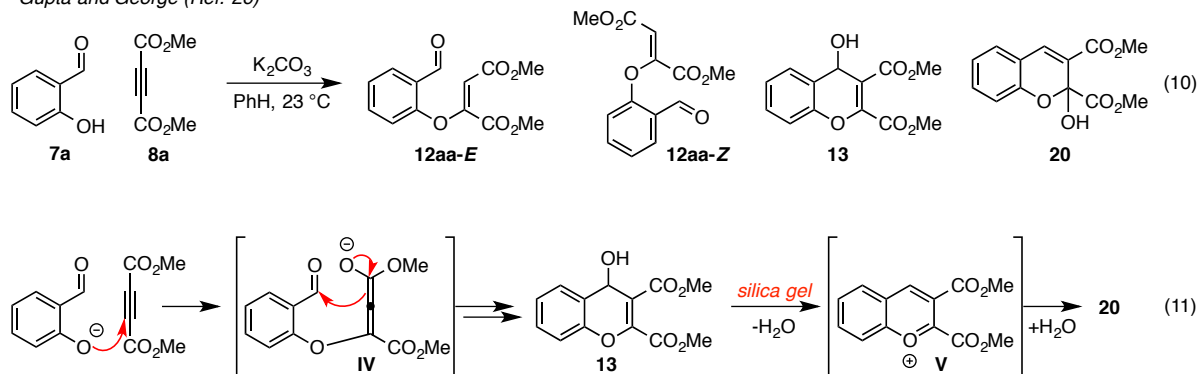


1.2.4 Side products and rationale for base selection

As described in the discussion of salicylaldehyde scope (Table 1.2), we found that electron-deficient salicylaldehydes **7** (i.e. **7b–d**, **7g** and **7i**) provided lower yields of product **9** than their electron-rich counterparts (**7a**, **7e–f**) (62–68% yield vs. 73–80% yield). This yield reduction was attributed to competitive formation of aldol adducts **13** from enolate intermediate **III** (eq. 4, *vide supra*). An elaboration of this hypothesis is provided below.

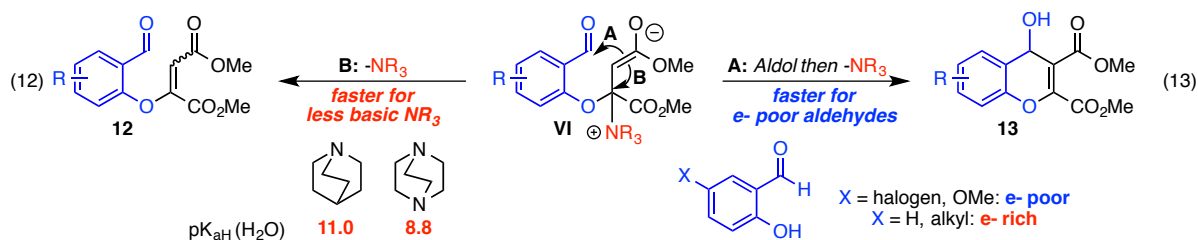
In 1975, Gupta and George reported that salicylaldehyde (**7a**) and DMAD (**8a**) react under basic conditions to provide a complex product mixture (eq. 10).^[26] In addition to the maleate and fumarate adducts **12aa-E** and **12aa-Z** (which are the intermediates exploited in our Michael–Stetter sequence—see, for instance, Figure 1.2 or Table 1.1), Gupta and George observe chromenol product **13** and its isomer **20**. The mechanism of formation of **13** and **20** presumably begins as for conjugate adducts **12aa-E** and **12aa-Z**: addition of the conjugate base of salicylaldehyde into DMAD provides allenolate **IV** (eq. 11). Whereas protonation of **IV** furnishes **12aa-E** and **12aa-Z** (path not shown), an intramolecular aldol reaction of allenolate **IV** onto the tethered aldehyde delivers chromenol **13**. Some **13** isomerizes to chromenol **20** on silica gel, presumably via benzopyrilium cation **V**.

•Gupta and George (Ref. 26)



If Gupta and George’s mechanism is correct, then product selectivity is controlled by relative rates of two competitive processes: reaction of allenolate **IV** with proton to give conjugate adducts **12aa**; or reaction of allenolate **IV** with tethered aldehyde to give aldol adduct **13**. We postulate that our mechanism may provide a similar opportunity for bifurcation (eq. 12 vs. 13). Tertiary amine-catalyzed addition of salicylaldehyde into DMAD

provides enolate intermediate **VI**, which resembles the allenolate intermediate **IV** invoked by Gupta and George. In our case, formation of products **12** does not proceed via protonation of enolate **VI** but by expulsion of the tertiary amine leaving group (path **B**, eq. 12). As in Gupta and George's case, however, enolate **VI** can undergo competitive cyclization, which, after loss of tertiary amine, provides aldol adduct **13** (path **A**, eq. 13).^[27] Notably, this mechanism is consistent with our previous observation that electron-deficient salicylaldehydes provide lower yields of Stetter product **9** in the one-pot protocol (Table 1.2); the undesired aldol reaction should be more competitive for adducts **VI** derived from electron-poor salicylaldehydes than for electron-rich or electron-neutral aldehydes, since electron-poor aldehyde adducts **VI** are better carbon electrophiles.

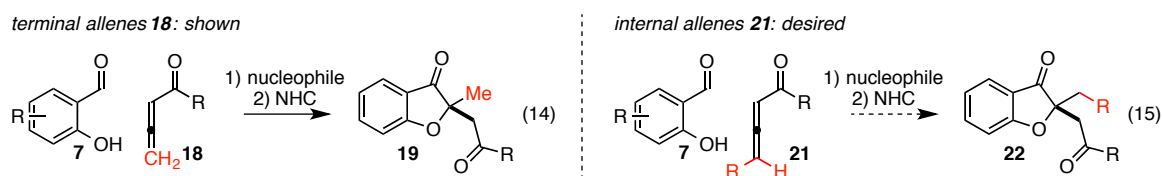


Finally, the invoked aldol pathway helps rationalize an observed yield-dependence on base identity. We found that choice of 3° amine catalyst exhibited a subtle but notable influence on reaction yield and purity. Specifically, reactions of electron-poor aldehydes **9b–c**, **9g** and **9i** appeared cleaner and slightly higher yielding when DABCO (**10**) was used in the place of quinuclidine (**11**). This observation is consistent with operation of the competitive paths shown in equations 12 and 13. Slightly less basic than quinuclidine, DABCO ($pK_{aH} = 8.8$ vs. 11)^[28] should be a better leaving group, and it should consequently be expelled more readily by enolate **VI** via path **B** (eq. 12). Use of DABCO in the place of more basic quinuclidine, then, mitigates some yield loss experienced in reactions of aldehydes **7b–c**, **7g** and **7i**, since it accelerates desired formation of conjugate adduct **12** relative to undesired intramolecular aldol addition via path **A** (eq. 13).

1.2.5 Substrate limitations

As discussed in the Chapter (Table 1.7), we found that activated terminal allenes **18** could participate in a one-pot, two-step Michael–Stetter reaction with salicylaldehydes **7** to provide benzofuranone product **19** in moderate yield and good to excellent enantioselectivity (eq. 14). We wondered, in light of this discovery, whether activated, internal allenes **21** could perform as competent substrates in the cascade reaction (eq. 15). Use of internal allenes would expand product scope considerably: when terminal allenes **18** are incorporated into benzofuranone products

19, substitution at the stereogenic carbon of **19** is limited to methyl (eq. 14). Use of internal allenes, on the other hand, would enable decoration of benzofuranone products **22** with diverse alkyl groups (eq. 15).



We began our investigations by testing just the conjugate addition reaction of salicylaldehyde **7a** with racemic internal allene ethyl 2,3-pentadienoate (**21a**) (Figure 1.3a, eq. 16). When quinuclidine (**11**) is used as the nucleophilic catalyst, no conjugate adduct **23aa** is obtained even at elevated temperatures. We wondered how ethyl 2,3-pentadienoate (**21a**) differed from terminal allenolate **18b** (Table 1.7). One hypothesis explains reluctant conjugate addition of **21a** in terms of allylic 1,3-strain (A[1,3]-strain) (Figure 1.3b). Because of the presence of the alkyl group (CH₃) in **21a**, development of A[1,3]-strain in intermediates **VII** or **VIII** derived from conjugate addition of quinuclidine (**11**) into ethyl 2,3-pentadienoate (**21a**) is inevitable. If quinuclidine (**11**) adds *cis* to the methyl group of **21** (path A, Figure 1.3b), the methyl group and **11** will experience allylic strain with each other in intermediate **VII** (Figure 1.3b). In what is presumably the more favorable approach, quinuclidine adds *trans* to the methyl group **21a** (path B, Figure 1.3b). This approach forces the methyl group and the enolate to adopt a *cis* relationship in intermediate **VIII**. While A[1,3]-strain exhibited by **VIII** is relatively mild, the barrier to formation of **VIII** is still higher than when the methyl group of **21a** is absent.

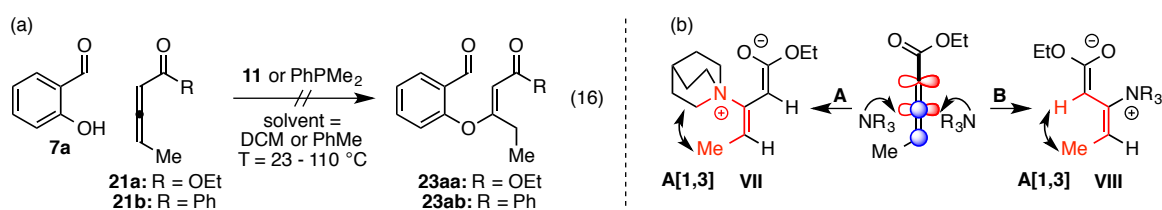


Figure 1.3 Internal allenes do not participate in the desired nucleophile-promoted conjugate addition reaction

We sought to overcome presumed high barriers to conjugate addition by increasing catalyst nucleophilicity or substrate electrophilicity. Unfortunately, reaction of salicylaldehyde **7a** with allenolate **21a** to give product **23aa** fails even in the presence of nucleophilic dimethylphenyl phosphine (PhPMe₂) catalyst; and quinuclidine-catalyzed reaction of **7a** with electrophilic allenone **21b** provides a mixture of products that does not include discernable amounts of **23ab** (Figure 1.3a, eq. 16).

1.3 Summary

In summary, we have described a novel and scalable one-pot procedure for the highly enantioselective preparation of benzofuranone products from simple starting materials. We have demonstrated that the one-pot Michael-Stetter protocol is superior to the two-step procedure with respect to enantioselectivity, and we have expanded on this observation to show that catechol additives improve enantioselectivity in the context of both two-pot and one-pot, two-step reactions. Moreover, we have identified olefin geometry as an important factor influencing Stetter enantioselectivity. Finally, we have illustrated that activated allenes behave as competent, *E*-selective Michael acceptors in our one-pot, two-step reaction to provide access to alkyl-substituted benzofuranones in moderate to excellent enantioselectivities.

REFERENCES

- [1] Text and figures for this chapter have been adapted with permission from Filloux, C. M.; Lathrop, S. P.; Rovis, T. *Proc. Natl. Acad. Sci. U. S. A.* **2010**, *107*, 20666 – 20671. Can be found online at: <http://www.pnas.org/content/107/48/20666.full?sid=9b0378a4-9ebd-44f5-88c0-0522c0239ce2>.
- [2] (a) Lee, J. M.; Na, Y.; Han, H.; Chang, S. *Chem. Soc. Rev.* **2004**, *33*, 302 – 312.
 (b) Ajamian, A.; Gleason, J. L. *Angew. Chem. Int. Ed.* **2004**, *43*, 3754 – 3760.
 (c) Wasilke, J. C.; Obrey, S. J.; Baker, R. T.; Bazan, G. C. *Chem. Rev.* **2005**, *105*, 1001 – 1020.
 (d) Chapman, C. J.; Frost, C. G. *Synthesis* **2007**, 1 – 21.
 (e) Walji, A. M.; MacMillan, D. W. C. *Synlett* **2007**, 1477 – 1489.
 (f) Enders, D.; Grondal, C.; Huttel, M. R. M. *Angew. Chem. Int. Ed.* **2007**, *46*, 1570 – 1581.
 (g) Yu, X.; Wang, W. *Org. Biomol. Chem.* **2008**, *6*, 2037 – 2046.
 (h) Alba, A. N.; Companyo, X.; Viciano, M.; Rios, R. *Curr. Org. Chem.* **2009**, *13*, 1432 – 1474 .
 (i) Bertelsen, S.; Jørgensen, K.A. *Chem. Soc. Rev.* **2009**, *38*, 2178 – 2189.
 (j) Jiang, H.; Elsner, P.; Jensen, K. L.; Falcicchio, A.; Marcos, V.; Jørgensen, K. A. *Angew. Chem. Int. Ed.* **2009**, *48*, 6844 – 6848.
 (k) Zhou, J. *Chem—Asian J.* **2010**, *5*, 422 – 434.
- [3] (a) Marigo, M.; Bertelsen, S.; Landa, A.; Jørgensen, K. A. *J. Am. Chem. Soc.* **2006**, *128*, 5475 – 5479.
 (b) Enders, D.; Huttel, M. R. M.; Grondal, C.; Raabe, G. *Nature* **2006**, *441*, 861 – 863.
 (c) Enders, D.; Narine, A. A.; Benninghaus, T. R.; Raabe, G. *Synlett* **2007**, 1667 – 1670.
 (d) Zu, L.; Li, H.; Xie, H.; Wang, J.; Jiang, W.; Tang, Y.; Wang, W. *Angew. Chem. Int. Ed.* **2007**, *46*, 3732 – 3734.
 (e) Wang, J.; Li, H.; Xie, H.; Zu, L.; Shen, X.; Wang, W. *Angew. Chem. Int. Ed.* **2007**, *46*, 9050 – 9053.
 (f) Hayashi, Y.; Toyoshima, M.; Gotoh, H.; Ishikawa, H. *Org. Lett.* **2008**, *11*, 45 – 48.
 (g) Zu, L.; Zhang, S.; Xie, H.; Wang, W. *Org. Lett.* **2009**, *11*, 1627 – 1630.
 (h) Ishikawa, H.; Suzuki, T.; Hayashi, Y. *Angew. Chem. Int. Ed.* **2009**, *48*, 1304 – 1307.
- [4] Cernak, T. A.; Lambert, T. H. *J. Am. Chem. Soc.* **2009**, *131*, 3124 – 3135.
- [5] (a) Licandro, E.; Maiorana, S.; Capella, L.; Manzotti, R.; Papagni, A.; Vandoni, B.; Albinati, A.; Chuang, S. H.; Hwu, J. *Organometallics* **2001**, *20*, 485 – 496.
 (b) Dijk, E. W.; Panella, L.; Pinho, P.; Naasz, R.; Meetsma, A.; Minnaard, A. J.; Feringa, B. L. *Tetrahedron* **2004**, *60*, 9687 – 9693.

- (c) Huang, Y.; Walji, A. M.; Larsen, C. H.; MacMillan, D. W. C. *J. Am. Chem. Soc.* **2005**, *127*, 15051 – 15053.
- (d) Shekhar, S.; Trantow, B.; Leitner, A.; Hartwig, J. F. *J. Am. Chem. Soc.* **2006**, *128*, 11770 – 11771.
- (e) Wang, Y. G.; Kumano, T.; Kano, T.; Maruoka, K. *Org. Lett.* **2009**, *11*, 2027 – 2029.
- (f) Simmons, B.; Walji, A. M.; MacMillan, D. W. C. *Angew. Chem. Int. Ed.* **2009**, *48*, 4349 – 4353.
- [6] (a) Zhou, J.; List, B. *J. Am. Chem. Soc.* **2007**, *129*, 7498 – 7499.
- (b) Scroggins, S. T.; Chi, Y.; Fréchet, J. M. J. *Angew. Chem. Int. Ed.* **2010**, *49*, 2393 – 2396.
- [7] Lathrop, S. P.; Rovis, T. *J. Am. Chem. Soc.* **2009**, *131*, 13628 – 13630.
- [8] Read de Alaniz, J.; Rovis, T. *Synlett* **2009**, 1189 – 1207.
- [9] (a) Pirrung, M. C.; Brown, W. L.; Rege, S.; Laughton, P. *J. Am. Chem. Soc.* **1991**, *113*, 8561 – 8562.
- (b) Karthikeyan, K.; Perumal, P. T. *Synlett* **2009**, 2366 – 2370.
- [10] Sheng, R.; Xu, Y.; Hu, C.; Zhang, J.; Lin, X.; Li, J.; Yang, B.; He, Q.; Hu, Y. *Eur. J. Med. Chem.* **2009**, *44*, 7 – 17.
- [11] (a) Awale, S.; Li, F.; Onozuka, H.; Esumi, H.; Tezuka, Y.; Kadota, S. *Bioorg. Med. Chem.* **2008**, *16*, 181 – 189.
- (b) Charrier, C.; Clarhaut, J.; Gesson, J.; Estiu, G.; Wiest, O.; Roche, J.; Bertrand, P. *J. Med. Chem.* **2009**, *52*, 3112 – 3115.
- (c) Rønne, M. H.; Rebacz, B.; Markworth, L.; Terp, A. H.; Larsen, T. O.; Krämer, A.; Clausen, M. H. *J. Med. Chem.* **2009**, *52*, 3342 – 3347.
- [12] Gerard, B.; Sangji, S.; O'Leary, D. J.; Porco, J. A. *J. Am. Chem. Soc.* **2006**, *128*, 7754 – 7755.
- [13] Morton, J. G. M.; Kwon, L. D.; Freeman, J. D.; Njardarson, J. T. *Tetrahedron Lett.* **2009**, *50*, 1684 – 1686.
- [14] Katoh, T.; Ohmori, O.; Iwasaki, K.; Inoue, M. *Tetrahedron* **2002**, *58*, 1289 – 1299.
- [15] (a) Patonay-Péli, E.; Litkei, G.; Patonay, T. *Synthesis* **1990**, 511 – 514.
- (b) He, J.; Zheng, J.; Liu, J.; She, X.; Pan, X. *Org. Lett.* **2006**, *8*, 4637 – 4640.
- [16] (a) Kokubo, K.; Matsumasa, K.; Nishinaka, Y.; Miura, M.; Nomura, M. *Bull. Chem. Soc. Jpn.* **1999**, *72*, 303 – 311.
- (b) Kadnikov, D. V.; Larock, R. C. *J. Org. Chem.* **2003**, *68*, 9423–9432.
- [17] Capuzzi, M.; Perdicchia, D.; Jørgensen, K. A. *Chem—Eur. J.* **2008**, *14*, 128 – 135.
- [18] (a) Kerr, M. S.; Rovis, T. *J. Am. Chem. Soc.* **2004**, *126*, 8876 – 8877.
- (b) Moore, J. L.; Kerr, M. S.; Rovis, T. *Tetrahedron* **2006**, *62*, 11477 – 11482.
- (c) Read de Alaniz, J.; Kerr, M. S.; Moore, J. L.; Rovis, T. *J. Org. Chem.* **2008**, *73*, 2033 – 2040.
- [19] (a) Fan, M. J.; Li, G. Q.; Li, L. H.; Yang, S. D.; Liang, Y. M. *Synthesis* **2006**, 2286 – 2292.

- (b) Fan, M. J.; Li, G. Q.; Liang, Y. M. *Tetrahedron* **2006**, *62*, 6782 – 6791.
- [20] (a) Liu, Q.; Perreault, S.; Rovis, T. *J. Am. Chem. Soc.* **2008**, *130*, 14066 – 14067.
- (b) DiRocco, D. A.; Oberg, K. M.; Dalton, D. M.; Rovis, T. *J. Am. Chem. Soc.* **2009**, *131*, 10872 – 10874.
- [21] (a) Nair, V.; Bindu, S.; Sreekumar, V.; Rath, N. P. *Org. Lett.* **2003**, *5*, 665 – 667.
- (b) Nair, V.; Sreekumar, V.; Bindu, S.; Suresh, E. *Org. Lett.* **2005**, *7*, 2297 – 2300.
- [22] (a) Peelen, T. J.; Chi, Y.; Gellman, S. H. *J. Am. Chem. Soc.* **2005**, *127*, 11598–11599.
- (b) Campbell, M. J.; Johnson, J. S. *J. Am. Chem. Soc.* **2009**, *131*, 10370 – 10371.
- (c) Chen, K.; Baran, P. S. *Nature* **2009**, *459*, 824 – 828.
- [23] (a) Dakin, H. D. *Am. Chem. J.* **1909**, *42*, 477 – 498.
- (b) Dakin, H. D. *Proc. Chem. Soc.* **1910**, *25*, 194.
- [24] Since publication of Ref. 1, Rovis and DiRocco reported that catechols dramatically accelerate the rate of an intermolecular Stetter reaction of nitroalkenes and enals: DiRocco, D. A.; Rovis, T. *J. Am. Chem. Soc.* **2011**, *133*, 10402 – 10405.
- [25] Shi, Y. L.; Shi, M. *Org. Lett.* **2005**, *7*, 3057 – 3060.
- [26] Gupta, R. K.; George, M. V. *Tetrahedron* **1975**, *31*, 1263 – 1275.
- [27] We observe some aldol adduct **13a** from reaction of **7a** and **8a** in the presence of a quinuclidine (**11**) catalyst.
- [28] Benoit, R. L.; Lefebvre, D.; Fréchette, M. *Can. J. Chem.* **1986**, *65*, 996 – 1001.

CHAPTER TWO

Rh(I)–Bisphosphine Catalyzed Asymmetric, Intermolecular Hydroheteroarylation of α -Substituted Acrylate Derivatives^[1]

2.1 Synopsis

Asymmetric hydroheteroarylation (HH) of alkenes represents a convenient entry to elaborated heterocyclic motifs. While chiral acids are known to mediate asymmetric addition of electron rich heteroarenes to Michael acceptors, very few methods exploit transition-metals to catalyze alkylation of heterocycles with olefins via a C–H activation, migratory insertion sequence. Herein, we describe the development of an asymmetric, intermolecular hydroheteroarylation reaction of α -substituted acrylates with benzoxazoles. The reaction provides 2-substituted benzoxazoles in moderate to excellent yields and good to excellent enantioselectivities. Notably, a series of mechanistic studies appears to contradict a pathway involving enantioselective protonation of a Rh(I)–enolate, despite the fact that such a mechanism is invoked almost unanimously in the related addition of aryl boronic acids to methacrylate derivatives. Evidence suggests instead that migratory insertion or β -hydride elimination is enantiodetermining and that isomerization of a Rh(I)–enolate to a Rh(I)–heterobenzyl species insulates the resultant α -stereocenter from epimerization. A bulky ligand, CTH-(*R*)-Xylyl-P-Phos is crucial for reactivity and enantioselectivity, as it likely discourages undesired ligation of benzoxazole substrates or intermediates to on- or off-cycle rhodium complexes and attenuates coordination-promoted product epimerization.

2.2 Introduction

Catalytic, enantioselective addition of a C–H bond of a heterocycle across an alkene represents a conceptually simple and atom economical method for the preparation of elaborated heterocyclic scaffolds. This concept has been implemented in a formal sense in the asymmetric Friedel–Crafts alkylation of electron rich heteroarenes, such as indoles, with Michael acceptors.^[2] Yet methods exploiting transition-metals to mediate asymmetric hydroheteroarylation of alkenes via a C–H activation, insertion sequence remain quite elusive.^[3–4] This deficiency is somewhat surprising given the diverse methods for asymmetric hydroarylation of olefins with activated arenes^[5] or with arenes containing directing groups for C–H functionalization.^[6] In the early 2000s, Bergman and Ellman pioneered the achiral, intramolecular HH of unactivated alkenes with a Rh(I)–phosphine catalyst.^[4a] This discovery was expanded in a great body of work to the intermolecular HH reaction of alkenes^[7] and to several discrete

asymmetric, intramolecular HH reactions.^[8] In 2012, Shibata provided an early example of an asymmetric intermolecular HH reaction mediated by a transition-metal (TM):^[9] an Ir(I)–SDP-catalyst promotes the branched-selective alkylation of N-benzoylindole and styrene in 42% ee (Figure 2.1, eq. 1). Notably, alkylation occurs at the indole 2-position, whereas functionalization typically proceeds at the 3-position under Friedel–Crafts conditions.^[2] Though only modestly selective, Shibata’s example foreshadows that TM-catalyzed HH may eventually serve as a selective and general complement to established methods using chiral acids. Indeed, Hartwig and Sevov described in short succession the asymmetric HH of norbornene with diverse heterocycles using a chiral Ir(I) catalyst (Figure 2.1, eq. 2).^[10] Most recently, Hou and coworkers reported the enantioselective alkylation of 2-substituted pyridines with unactivated, terminal alkenes using a chiral, half-sandwich scandium complex. (Figure 2.1, eq. 3).^[11]

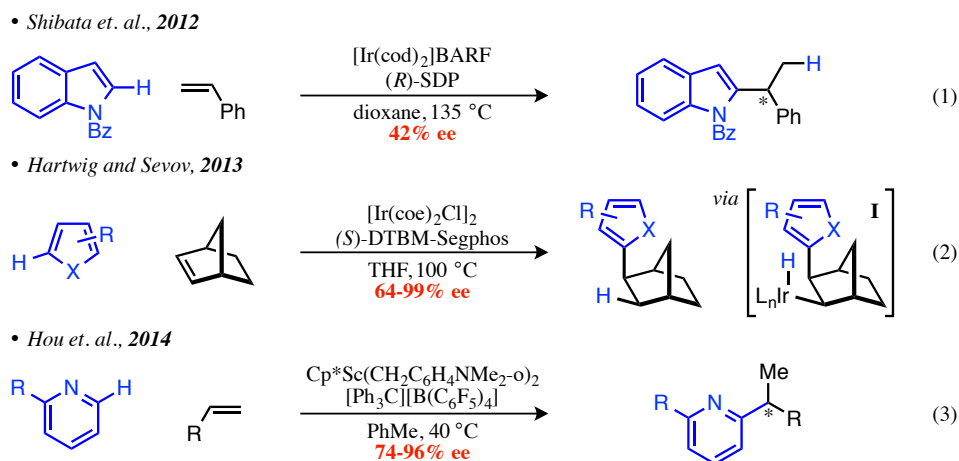


Figure 2.1 TM-catalyzed asymmetric intermolecular hydroheteroarylation reactions previously reported in the literature

While the work of Hartwig and Hou provides a powerful proof of concept, room for complementary asymmetric HH methods remain. Specifically, we sought to expand the scope of the olefin coupling partner. Hartwig’s HH reaction is demonstrated only with the strained cyclic alkene, norbornene,^[10] and Hou’s pyridine alkylation appears limited to relatively unfunctionalized, electron-neutral alkenes.^[11] Herein, we describe a Rh(I)-catalyzed asymmetric alkylation of benzoxazoles with acrylate derivatives (Figure 2.2, eq. 4). To our knowledge, this work represents the first example of an enantioselective, transition-metal-mediated, intermolecular HH of acyclic, electron-deficient alkenes. Moreover, the described reaction makes products of potential medicinal value; isosteres for purine bases and certain amino acids, 2-substituted benzoxazoles are known to exhibit tremendous biological activity.^[12]

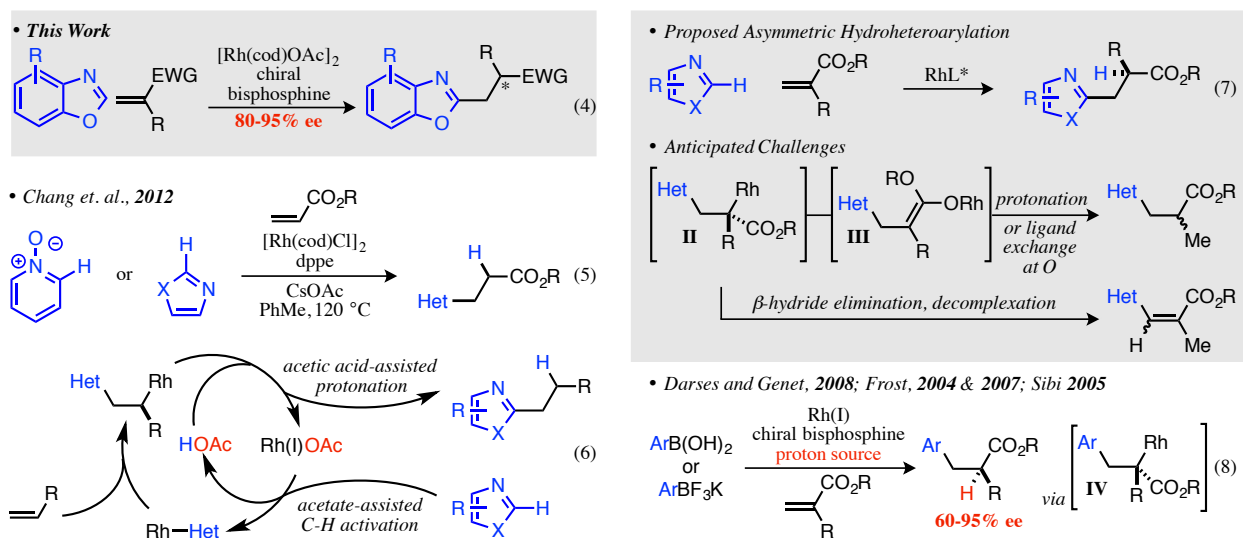


Figure 2.2 Our HH reaction of benzoxazoles and α -substituted acrylates and precedent inspiring its development

We found inspiration for the described HH reaction in chemistry developed by Chang et al.^[4j] This group reported the HH of acrylates and acrylate derivatives with benzheterocycles or pyridine oxides (Figure 2.2, eq. 5). Chang et al. invoke catalysis by a Rh(I)–acetate species: acetate counterion mediates C–H activation, while liberated acetic acid protonates an eventual C–Rh bond (Figure 2.2, eq. 6). We envisioned that use of a substituted acrylate in a system related to Chang’s would enable the asymmetric preparation of branched products (Figure 2.2, eq. 7). Notably, the Rh(I)–dppe system used by Chang lends itself to enantioselective modification: in contrast to relatively scarce chiral cyclopentadienyl ligands ubiquitous in Rh(III) catalysis,^[6d–e,6h] chiral bisphosphine ligands abound.^[13]

Despite the overt similarity between the known and proposed reactions, several complications could accompany the envisioned asymmetric method. The mechanism proposed by Chang invokes protonation of Rh–enolate **II** (Figure 2.2).^[4j] While protonation of C-bound **II** could provide enantioenriched products, protonation or ligand exchange of O-bound **III** at oxygen would give racemic product. Additionally, β -H elimination and dissociation of resultant conjugated alkene would furnish undesired Heck product.^[4j] Indeed, success of Hartwig’s and Hou’s chemistry may be understood in the light of these anticipated difficulties; the privileged nature of norbornene in eq. 2 (Figure 2.1) likely derives in part from the fact that presumed intermediate **I** cannot undergo β -H elimination. Hou’s pyridine alkylation is also presumably more insulated from β -H elimination than a Rh(I) system, since the enhanced thermodynamic stabilization of metal–hydrogen bonds over metal–carbon bonds is smaller for early TMs than for late ones.^[14]

While we were aware that the described pitfalls could plague our desired reaction with low stereo- or product-selectivity, work by Reetz, Genet and others offered hope that these obstacles would not be insurmountable.^[15] These groups report that a Rh(I)–chiral bisphosphine system mediates the asymmetric hydroarylation of α -substituted acrylates with boronic acid derivatives (Figure 2.2, eq. 8). Importantly, this reaction is presumed to intercept analogous Rh–enolate intermediate **IV**.^[15b-d] Similar opportunities for stereochemical scrambling or Heck reactivity exist for **IV** as for our presumed Rh–enolate **II**. Yet these pathways must not be competitive in the described systems, since saturated products are obtained in good to excellent enantioselectivities.^[15] These groups invoke asymmetric protonation of Rh–enolate **IV** or O-bound isomer to explain high product enantioselectivities,^[15-16] but aside from Genet et al.,^[15e] none provide rigorous mechanistic evidence in favor of this claim.

2.3 Results and discussion

2.3.1 Initial reaction optimization with $[\text{Rh}(\text{cod})\text{OAc}]_2$

Encouraged that our asymmetric HH could succeed, we decided to begin by investigating mechanistic aspects of the parent, achiral reaction (Figure 2.2, eq. 5). The first question we sought to address was the role of the CsOAc. If, as Chang and coworkers postulated, CsOAc serves to generate a Rh(I)–acetate catalyst *in situ*, then perhaps the same reactivity could be accomplished with a premade Rh(I)–acetate catalyst. Chatani and coworkers have indeed observed that $[\text{Rh}(\text{cod})\text{OAc}]_2$ can be used in the place of a KOAc– $[\text{Rh}(\text{cod})\text{Cl}]_2$ system in the directed hydroarylation of acrylates with 8-aminoquinoline-derived benzamides.^[17,18] We prepared $[\text{Rh}(\text{cod})\text{OAc}]_2$ by treating $[\text{Rh}(\text{cod})\text{Cl}]_2$ with KOAc in refluxing acetone according to a known procedure.^[19] Recrystallization from EtOAc provided X-Ray quality crystals of the air-stable, orange solid. These were characterized by X-Ray crystallography thanks to Dr. Kevin Martin Oberg to provide what we believe is the first reported crystal structure of the complex (Figure 2.3).^[20]

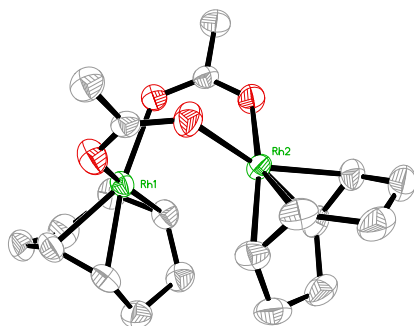
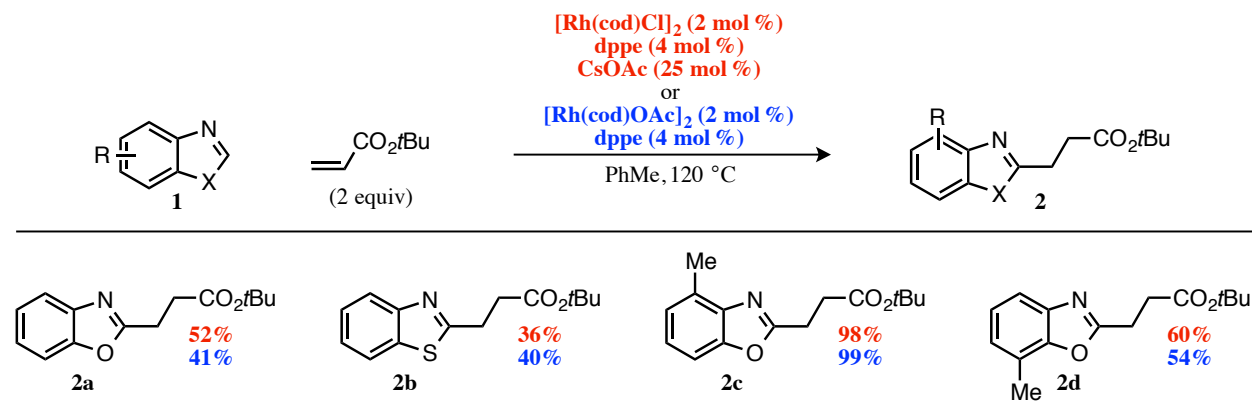


Figure 2.3 X-Ray crystal structure of $[\text{Rh}(\text{cod})\text{OAc}]_2$

As predicted, $[\text{Rh}(\text{cod})\text{OAc}]_2$ performs with equal efficiency as Chang's *in situ* generated catalyst in the HH of several benzheterocycles **1** with *tert*-butyl acrylate (Table 2.1). CsOAc thus appears to serve primarily as an acetate source in Chang's chemistry.

Table 2.1 HH using Chang's established conditions (red)^[Ref. 4j] or $[\text{Rh}(\text{cod})\text{OAc}]_2$ (blue)^[1-2]



^[1]To ensure uniformity for comparison, all reactions were performed by the first author. ^[2]Yields were determined with respect to 4,4'-di-*tert*-butylbiphenyl (DTBB) by ¹H NMR of the reaction mixture.

With $[\text{Rh}(\text{cod})\text{OAc}]_2$ in hand, we screened the asymmetric HH of ethyl methacrylate (**3a**) and 4-methylbenzoxazole (**1c**) (Table 2.2), since this heterocycle proved most reactive in the achiral reaction with *tert*-butyl acrylate (Table 2.1). Ligands resembling dppe were chosen at the outset. In PhMe at 120 °C, **1c** and **3a** react in the presence of a Rh(I)–prophos (**L1**) catalyst to deliver α -substituted product **4ca** in quantitative yields and 29% ee (Table 2.2, entry 1). Ees remain modest with Chiraphos (**L2**) and Me-Duphos (**L3**) (entries 2 and 3). Significant improvement in ee is achieved with Binap (**L4**), but yields of **4ca** suffer (entry 4). Since bite angle is known to have a pronounced effect on reaction selectivity and efficiency,^[21] we examined Binap derivatives, Synphos (**L5**, entry 5) and Segphos (**L6**, entry 6), whose bite angles we hoped would compare more favorably to dppe.^[22-23] Gratifyingly, a Rh(I)–Segphos system delivers product **4ca** in acceptable 56% yield, and good selectivity (85% ee, entry 6). A two-fold increase in acrylate concentration further increases reactivity, providing comparable yields in 24 h to what is obtained in 60 h with lower acrylate concentrations (entries 6-9). Concurrently, a solvent and temperature screen (entries 9-17) revealed acetonitrile (CH_3CN) to be optimal for selectivity (95% ee, entry 11). Combining results, execution of the HH reaction in CH_3CN with 8 equivalents of acrylate **3a** and 5 mol % $[\text{Rh}(\text{cod})\text{OAc}]_2$ provides satisfactory yields of **4ca** in excellent enantioselectivity (entry 18).

Table 2.2 Initial reaction optimization

entry	ligand	solvent	equiv 3a	T (°C)	time (h)	4ca (%) ^[1]	ee (%) ^[2]
1	L1	PhMe	4	120	60	100	29
2	L2	PhMe	4	120	60	95	-47
3	L3	PhMe	4	120	60	39	57
4	L4	PhMe	4	120	60	9	-78
5	L5	PhMe	4	120	60	20	84
6	L6	PhMe	4	120	60	56	85
7	L6	PhMe	4	120	24	19	89
8	L6	PhMe	6	120	24	29	85
9	L6	PhMe	8	120	24	58	77
10	L6	PhMe	4	100	24	17	88
11	L6	CH ₃ CN	4	100	24	15	95
12	L6	TFE	4	100	24	< 5	16
13	L6	DCE	4	100	24	< 5	95
14	L6	DME	4	100	24	6	91
15	L6	DMF	4	100	24	22	88
16	L6	PhCF ₃	4	100	24	10	95
17	L6	<i>o</i> -DCB	4	160	24	7	17
18^[3]	L6	CH ₃ CN	8	100	24	58	95

L1

L2

L3

L4

L5

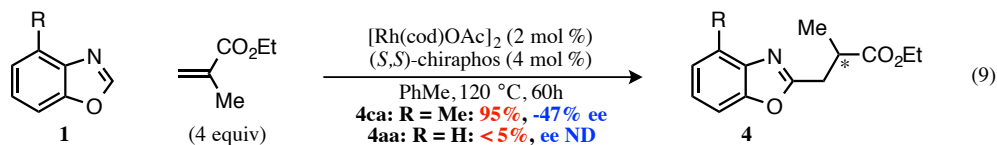
L6

^[1]Determined with respect to DTBB by LC analysis of the crude reaction mixture on a chiral stationary phase.

^[2]Determined at the same time as percent yield by LC analysis of the crude reaction mixture on a chiral stationary phase. ^[3]Reaction conducted with 5 mol % [Rh(cod)OAc]₂ and 10 mol % **L6**.

2.3.2 Mechanistic investigations of achiral system

Although we were pleased with this result, we anticipated that reaction efficiency would need to be further improved in order to extend the substrate scope to less reactive heterocycles. For instance, when benzoxazole **1a** is reacted under the conditions shown in entry 2 of Table 1 (which provide nearly quantitative yields of **4ca**), no discernable product **4aa** is obtained (eq. 9). Before refining our conditions, we sought to understand what made 4-methylbenzoxazole (**1c**) so much more reactive than its unsubstituted- or 6-substituted counterparts (Table 2.1, **1a**–**1b** and **1d**). Yields displayed in Table 2.1 fail to adequately capture this striking reactivity difference—while reaction of **1c** is complete in 3h, reaction of **1a**, **1b** and **1d** stall at about 50% after 60 h. To gain insight into this disparate reactivity, we performed two competition experiments—one between **1b**-D and **1c**-H (eq. 10 and Figure 2.4),^[24] and one between **1b**-H and **1c**-H (eq. 11).



From the former, the following significant observations are made: (a) crossover substrates **1b-H** and **1c-D** are observed by ^1H and ^2H NMR (Figure 2.4a) (b) deuterium is incorporated into the alkyl backbone of both products **2b** and **2c** (eq. 10) and (c) deuterium is incorporated predominantly at the β -position of both products (eq. 10). From this data, we propose a mechanistic cycle similar to that offered by Chang et al. (Figure 2.5b).^[4j,25] A Rh(I)-acetate catalyst mediates reversible C–H activation of heteroarene **1** (observation a) to provide Rh–heteroaryl complex **V**. Migratory insertion (MI) across the terminal acrylate ($\text{R} = \text{H}$) furnishes Rh–enolate **VI**, which isomerizes via a β -H elimination, hydorrhodation sequence to heterobenzyl-Rh **VIII** (observation c). Protonation appears to occur predominantly from **VIII** (or the N-bound isomer, see **XIV**, Figure 2.8). Protonation likely proceeds via an outer sphere mechanism (observation b), but an inner sphere mechanism after D–H exchange cannot be ruled out.

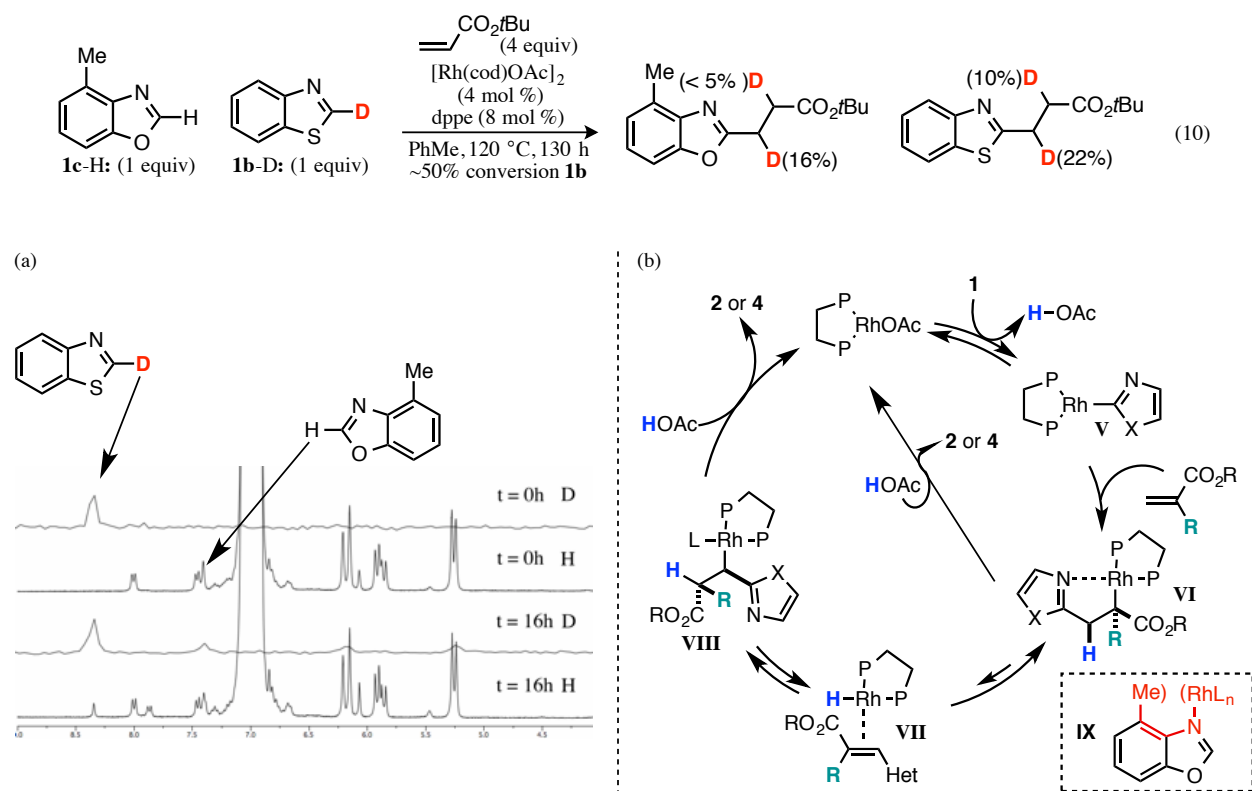
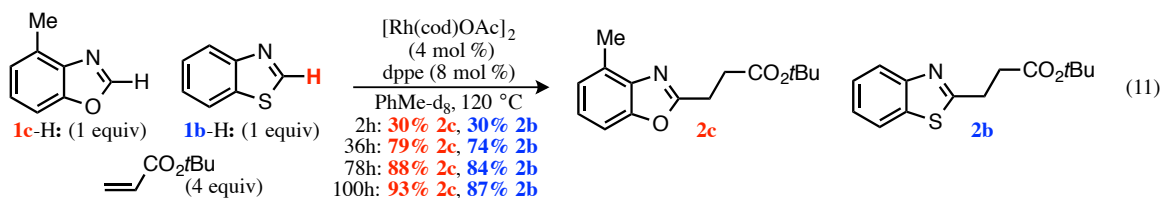


Figure 2.4 (a) ^1H and ^2H NMR of competition experiment between **1c-H** and **1b-D** (eq. 10) implicates reversible C–H activation. (b) Proposed mechanistic cycle for the HH of terminal ($\text{R} = \text{H}$) or α -substituted ($\text{R} \neq \text{H}$) acrylates.



Competition between **1b**-H and **1c**-H provides further mechanistic insights (eq. 11). When reactive **1c** and sluggish **1b** (Chart 1) are subjected to the standard conditions, products **2b** and **2c** form in roughly equal rates (eq. 11). We rationalize the identical rates of formation of **2b** and **2c** in one of two ways, both of which invoke the different ligating abilities of **1b** and **1c**. Given that C–H activation is reversible, one explanation assumes that there exists one or more irreversible steps before the turnover-limiting step (TLS) of sluggish substrate **1b**.^[26] In the context of the mechanism shown in Figure 2.4, we assume that MI is irreversible, and therefore product determining, and that protonation of **1b**-derived intermediates **VI** or **VIII** is turnover limiting. Sluggish protonation of **1b**-derived **VI** or **VIII** is understood by invoking coordination of the heterocycle to rhodium in **1b**-derived intermediate **VI**. Ligation blocks a free coordination site necessary for either protonation of **VI** or isomerization to **VIII** via β -H elimination. While unhindered azoles such as **1b**, **1a** and **1d** can presumably bind in the fashion described, A[1,3]-strain would disfavor analogous coordination of **1c**-derived **IX**, accelerating the reactivity of **1c** relative to its unsubstituted counterparts. Indeed, ^{15}N NMR studies suggest that bulky substitution adjacent to the coordinating nitrogen of various oxazoles impedes their coordination to Rh(II)-complexes.^[27] To sum up, then, so long as the C–H activation, MI sequence proceeds at roughly equal rates for both substrates, products **2b** and **2c** will form in a one-to-one ratio, since all catalyst will eventually funnel to **1b**-derived **VI**.

In perhaps a more simple explanation, strongly coordinating **1b** (and **1a** and **1d**) but not weakly coordinating **1c** acts as a competitive ligand toward important intermediates on or off the catalytic cycle, slowing catalysis of both **1b** and **1c**.

Although it would be difficult to discriminate between these two explanations—one invoking an intramolecular coordination event and one invoking an intermolecular coordination event—both suggest similar avenues for reaction optimization. Specifically, if deleterious coordination of the heteroarene were responsible for low reactivity of **1a–1b** and **1d**, then perhaps coordination could be discouraged by increasing the bulk of the bisphosphine ligand. We were optimistic that increasing ligand bulk might offer additional advantages. A congested coordination environment could also encourage a difficult MI event for steric reasons, since MI necessarily reduces the metal coordination number by one.^[28]

2.3.3 Optimization of the asymmetric hydroheteroarylation reaction with second generation ligands

To this end, we sought to further optimize the reaction of ethyl methacrylate (**3a**) and **1c** by screening bulky Segphos derivatives (Table 2). While DTBM-Segphos (**L8**) is fairly unreactive (entry 3), DM-Segphos (**L7**) improves yields by about 20% relative to Segphos (Table 2, entries 1 vs. 2). With the arene held constant, exploration of the phosphine backbone revealed CTH-(*R*)-Xylyl-P-Phos (**L11**) to be a superior ligand.^[29] It provides quantitative yield of product **4ca** in excellent enantioselectivity after 24 h (entry 6). A control reaction confirms that the acetate counterion is crucial for reactivity—no product is obtained under optimal conditions when [Rh(cod)Cl]₂ is used.^[30]

Table 2.3 Reaction optimization with second generation, bulky bisphosphine ligands

entry	ligand	Ar	4ca (%) ^[1]	ee (%) ^[2]
1	L6	Ph	58	95
2	L7	<i>m</i> -xylyl	79	93
3 ^[3]	L8	DTBM	23	57
4	L9	<i>m</i> -xylyl	33	93
5	L10	<i>m</i> -xylyl	29	92
6	L11	<i>m</i> -xylyl	> 98	95

L6: Ar = Ph

L9: R = H X = CH

m-xylyl

DTBM

L7: Ar = *m*-xylyl

L8: Ar = DTBM

L10: R = OMe X = CH

L11: R = OMe X = N

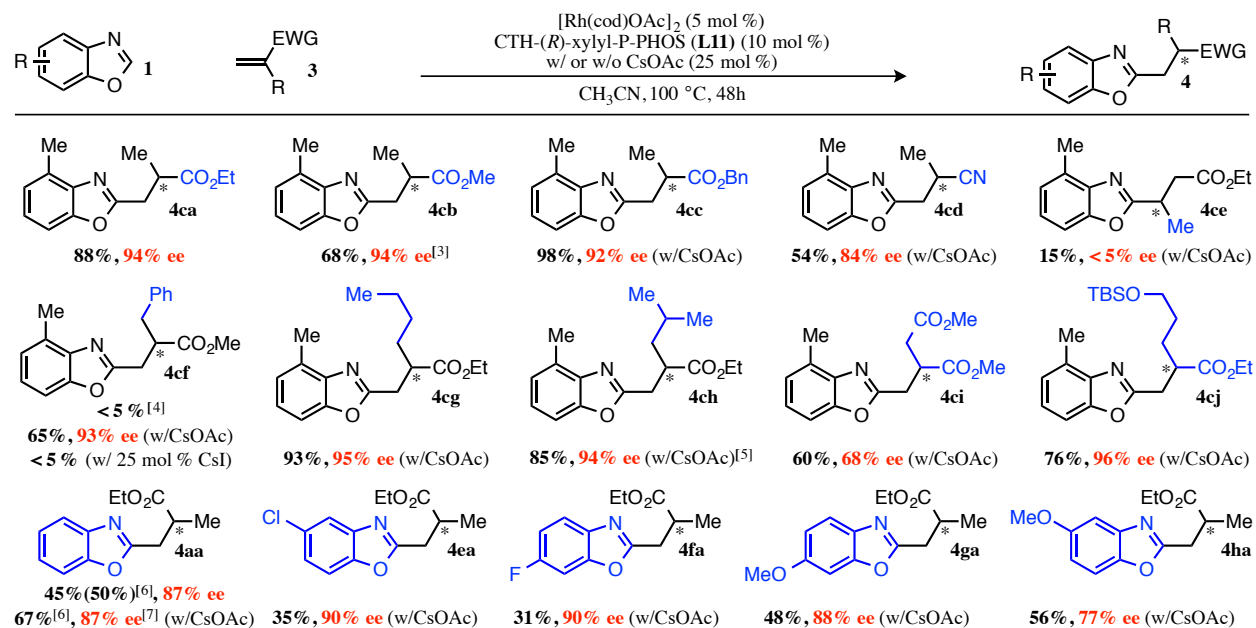
^[1]–^[2]See footnotes for Table 2.2. ^[3]With 2 mol % [Rh(cod)OAc]₂, 4 mol % **L8**, 4 equiv **3a** in PhMe at 120 °C for 60 h: these conditions give **4ca** in 56% yield and 85% ee when **L6** is used as a ligand.

2.3.4 Scope of the asymmetric hydroheteroarylation reaction

With these second generation conditions in hand, we sought to examine the substrate scope of our HH reaction (Table 2.4).^[31] Variation of the ester group provides products **4ca–4cc** in excellent yields and selectivities. Methacrylonitrile (**3d**) participates in moderate yield and good enantioselectivity. The HH reaction is also tolerant of diverse acrylate backbones, although α -substitution appears crucial—racemic product **4ce** is obtained in low yield from the reaction of **1c** and ethyl crotonate (**3e**). Acrylates with benzyl, *n*-butyl and sterically bulky isobutyl substituents at the α -position react in good yield to give products **4cf–4ch** in very high enantioselectivities despite

the opportunity for β -H elimination into the alkyl backbone. Dimethyl itaconate (**3i**) provides good yields of functionalized product **4ci** albeit in modest enantioselectivity. Acrylate **3j** containing a protected alcohol reacts without difficulty to give silyl ether **4cj** in excellent enantioselectivity.

Table 2.4 Scope of the Rh(I)-xylyl-P-Phos-catalyzed HH of benzoxazoles and methacrylate derivatives^[1-2]



^[1]Isolated yields after column chromatography on silica gel. ^[2]Ees of isolated products determined by LC analysis on chiral stationary phase. ^[3]Reaction run for 24 h. ^[4]Yield determined with respect to DTBB by LC analysis of the crude reaction mixture on a chiral stationary phase. ^[5]Reaction run for 80 h. ^[6]Yield determined with respect to DTBB by ¹H NMR of the crude reaction mixture. ^[7]Ee determined by LC analysis of the crude reaction mixture on a chiral stationary phase.

Notably, it was found that addition of 25 mol % CsOAc is necessary to promote reactivity for these more hindered acrylates—indeed, no product is obtained from the reaction of benzyl-substituted **3f** in its absence (Table 2.4).^[32] While the beneficial effect of CsOAc is not fully understood, acetate rather than cesium ion appears to be responsible for the yield improvement, since no product is obtained from the reaction of **3f** and **1c** when CsI is used in the place of CsOAc.

Finally, and much to our gratification, variation of the benzoxazole backbone is possible with bulky P-Phos ligand **L11**. Unsubstituted benzoxazole **1a** reacts smoothly; chloro and fluoro products **4ea–4fa** are assembled in high ees albeit in diminished yields. Isomeric methoxy products **4ga–4ha** are obtained in moderate yield and moderate to high enantioselectivities. While addition of 25 mol % CsOAc also appears to accelerate reactions with these benzoxazole substrates, its effect is less pronounced (**4aa**, 50% vs. 67%).

The HH reaction is not without limitations. Acrylates substituted with secondary alkyl (**3k**) or aryl (**3l**) groups do not participate effectively, nor do α,β -disubstituted acrylates (**3o** and **3p**) or acrylates containing β -leaving groups (**3m** and **3n**) (Figure 2.5). Amide **3q**, acetamidoacrylates **3r** and **3s**, 3-methyl-3-buten-2-one (**3t**) and thioester **3u** either do not react under conditions using CTH-(*R*)-xylyl-P-Phos (**L11**) or DM-segphos (**L7**) or react to give products **4** in poor yields (Figure 2.5). Exploration of heteroarene coupling partner reveals very electron-deficient benzoxazole **2i** to be a poor substrate in the HH reaction with ethyl methacrylate (Figure 2.6). Benzothiazole **2j** provides product in low yields despite 4-methyl substitution. Oxazoles **2k** and **2l**, which bear bulky substituents at the 4-position to discourage undesired coordination, also react sluggishly. Finally, electron-deficient oxazole **2m** provides product **4** only in low yields. Although the relative reactivity of benzoxazoles **2** is not entirely understood, substrate pK_a and steric environment at nitrogen appear to contribute.

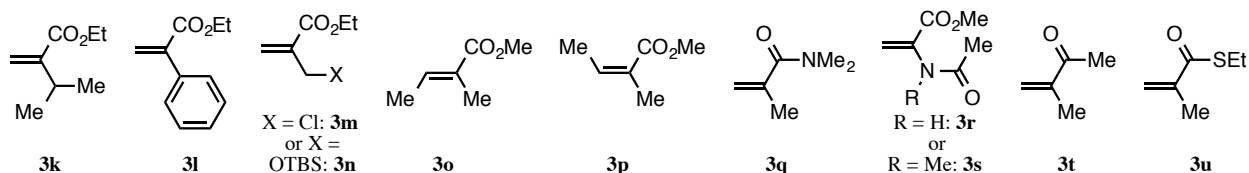


Figure 2.5 Acrylate derivatives that do not provide significant product in the HH reaction with benzoxazoles using CTH-(*R*)-xylyl-P-Phos (**L11**) or DM-segphos (**L7**)

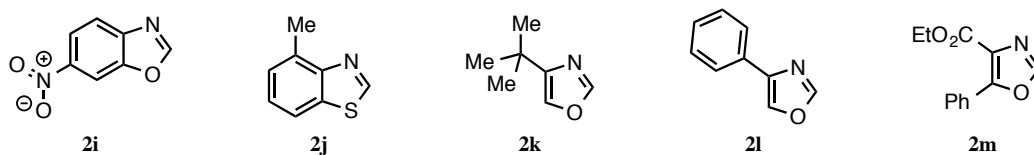


Figure 2.6 Benzoxazoles and oxazoles do not provide significant product in the HH reaction with ethyl methacrylate CTH-(*R*)-xylyl-P-Phos (**L11**) or DM-segphos (**L7**)

2.3.5 Mechanistic investigations into origin of enantioselectivity

At this point in our studies, we wanted to better understand the origin of enantioselectivity of our HH reaction. Asymmetric protonation of a rhodium enolate (e.g. **IV** or O-bound isomer, eq. 8, Figure 2.2) is classically invoked as the enantiodetermining step of the Rh(I)-bisphosphine mediated addition of boronic acids to α -substituted acrylates, although mechanistic evidence is sparse.^[15] We chose to test plausibility of this enantiodetermining step with a labeling study using deuterated **1c** (**1c-D**) (Figure 2.7, eq. 12). Were our HH mechanism to proceed via protonation of a rhodium-enolate (e.g. **II** or **III**, Figure 2.2; or **VI**, Figure 2.4b), then we should see ^2H -incorporation at the α -position of product **4ca**, since **1c** is the terminal proton source. Contrary to this expectation, reaction of **1c-D** with **3a** to 42 % conversion under standard conditions provides product **4ca**, in which ^2H is

incorporated exclusively at the β -position (eq. 12). **1c** is recovered with 33% H incorporation, consistent with a reversible C–H activation event. The proton source responsible for formation of **1c**-H in eq. 12 is presumably solvent: indeed, when the experiment is repeated in CD_3CN , virtually no H–D exchange in **1c**-D is observed (eq. 13). All ^2H from **1c**-D is accounted for in product **4ca**, since CH_3CN cannot compete as a proton source (eq. 13). β -deuterium incorporation in **4ca** does not likely arise from *in situ* generation and subsequent preferential reaction of β -deutero-**3a**, since reciprocal reaction of **1c**-H and **3b**-d8 gives **4ba** with ^1H -incorporation at the β -position exclusively (eq. 14).

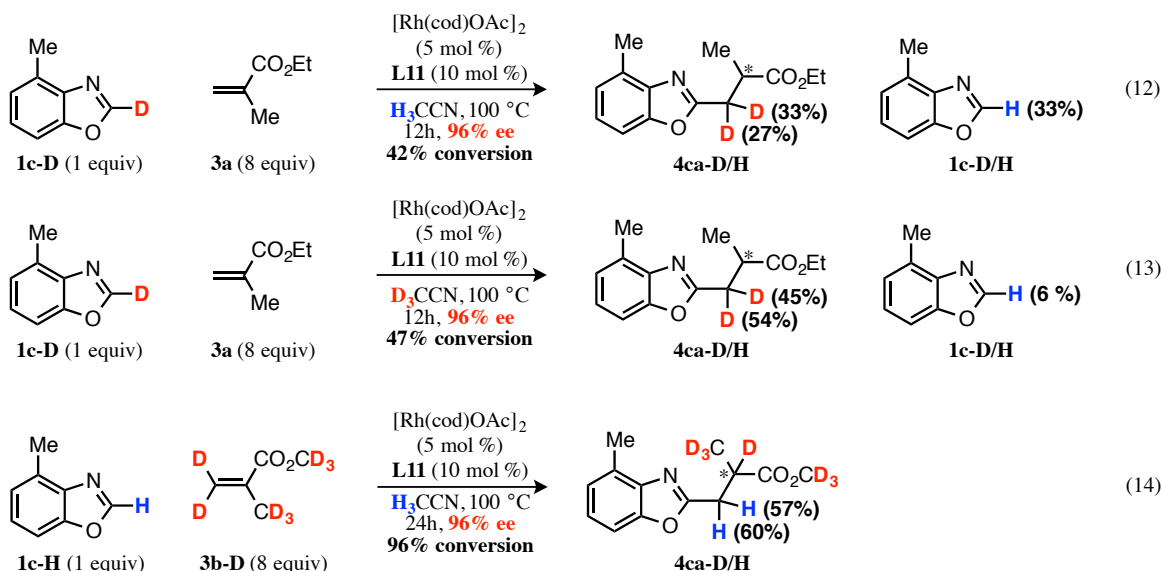


Figure 2.7 Labeling studies suggest that enolate protonation is *not* enantiodetermining

These labeling studies provide considerable insight into the reaction mechanism. First, they give grounds for dismissal of several possible elementary steps. For instance, protonation of a rhodium enolate cannot be enantiodetermining, as protonation takes place predominantly at the β - rather than the α -position.

The labeling study also seems to contradict a mechanism involving migratory insertion of a Rh(III)–heteroarene (in a 3,2 sense) or a Rh(III)–hydride (in a 2,3 sense) across acrylate **3** followed by reductive elimination to form a C–H or C–C bond respectively—this mechanism, too, would deliver products deuterated at the α - not the β -position.^[33] To account for the results of our labeling experiment, then, we propose a mechanism analogous to that proffered by Chang and coworkers for the hydroheteroarylation of terminal acrylates (Figure 2.4, $\text{R} \neq \text{H}$).^[4j] Reversible C–H activation liberates a molecule of acetic acid and gives a Rh–heteroaryl complex **V**, which

undergoes MI across the acrylate. At this point, a β -H elimination, hydorrhodation sequence isomerizes resultant Rh-enolate **VI** to alkyl-Rh **VIII**, which is protonated by acetic acid, regenerating a rhodium-acetate complex.

We believe that the proposed isomerization event is crucial for the high enantioselectivities obtained in our reaction. In our preferred mechanism, enantiodetermining MI delivers C-bound Rh-enolate **X** in a stereodefined fashion (Figure 2.8). One might imagine that C-bound **X** could equilibrate with O-bound rhodium isomer **XI**. Protonation or ligand exchange of **XI** on oxygen would deliver racemic product, and ees would suffer to the extent that this path is operative. Isomerization of Rh-enolate **X** to isomer **XII**, then, insulates the α -stereocenter from epimerization, so long as isomerization is stereospecific. Stereospecificity is guaranteed if the β -H elimination, hydorrhodation steps take place from the same face of alkene **XIII**, or said another way, if Rh-H intermediate **XIII** stays bound to the alkene in a sigma fashion. Indeed, β -H-elimination, hydrometalation sequences mediated by late transition-metals have been shown to preserve with high fidelity the stereochemistry set by MI events.^[5m]

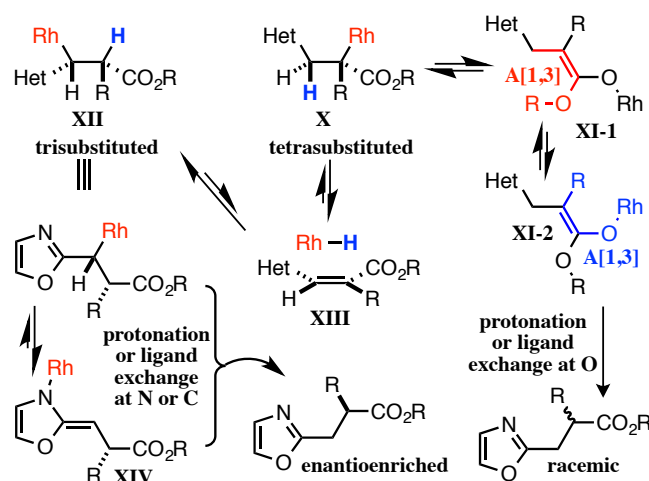


Figure 2.8 Rationale for isomerization of a rhodium enolate intermediate

This mechanism may also help explain why α -substituted acrylates are privileged substrates for our HH reaction and perhaps even for the Rh(I)-bisphosphine mediated asymmetric hydroarylation reported by Darses and others.^[15] When an α -substituted acrylate is used, C-bound Rh-enolate **X** is tetrasubstituted (Figure 2.8), and O-bound isomer **XI** experiences significant allylic strain, either between the ester OR group and the heterobenzylic carbon (red, **XI-1**) or between rhodium and the α -R substituent (blue, **XI-2**). Sterics may thus discourage formation of **XI** and promote isomerization to less-hindered, trisubstituted, alkyl-rhodium **XII**. Trisubstituted **XII** is further stabilized as

the heterobenzyl complex. Protonation or ligand exchange may be facilitated by isomerization to Rh–enamido complex **XIV**.^[34]

Final evidence for our proposed mechanism is provided by epimerization studies (Figure 2.9). We wanted to know why the reaction of **1c** appeared significantly more selective than the reaction of other benzoxazole substrates, particularly **1h**. We speculated that epimerization over the long reaction time might be partially responsible, but we struggled to rationalize why **4ha** would epimerize more quickly than other products: the most simple racemization pathway that can be imagined is deprotonation-reprotonation of the α -stereocenter by an acetate–acetic acid couple. Yet electronics of the benzoxazole backbone should not affect acidity of the remote stereocenter. Nevertheless, we resubjected low (**4ha**)-, intermediate (**4ga**)- and high (**4ca**)-ee products to the reaction of **1c** and an appropriate acrylate (eq. 15-17). When low ee-product **4ha** is resubjected to the reaction of **1c** and **3a** under standard conditions, it is indeed found to epimerize to 50% ee (eq. 15). In contrast, the ee of product **4ca** drops to only 93 % ee when it is resubjected to the reaction of **1c** and benzyl methacrylate **3c** under identical conditions (eq. 17).^[35] Yet epimerization does not appear solely responsible for the low ees of **4ha**, since intermediate-ee product **4ga** also shows significant stereochemical scrambling under the reaction conditions (eq. 16).

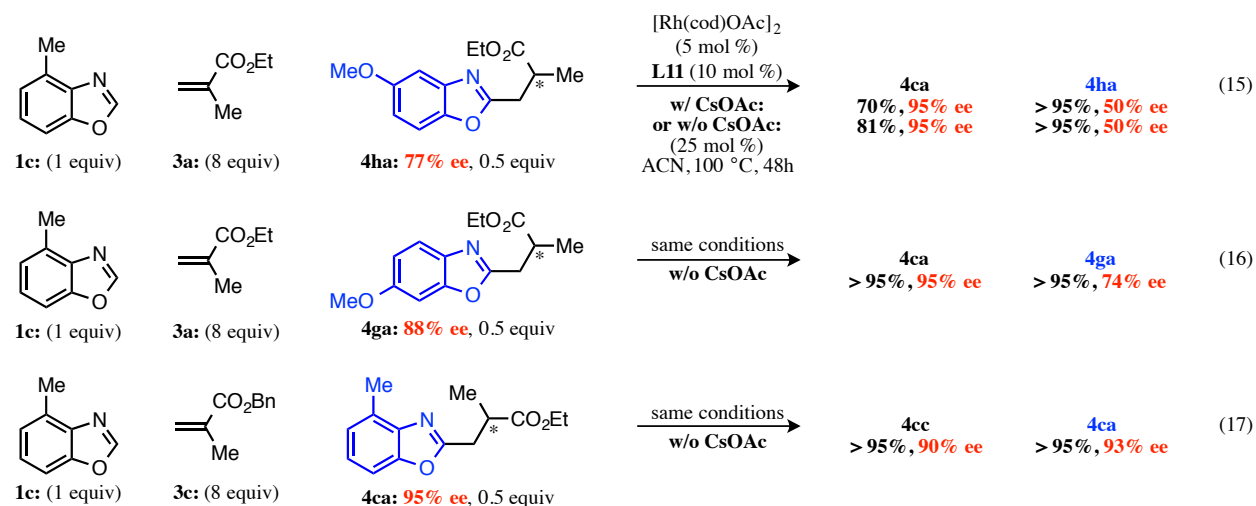


Figure 2.9 Epimerization experiments of **4ha**, **4ga** and **4ca**

That rates of epimerization of product **4** depend crucially on the benzoxazole backbone challenge an epimerization mechanism via traditional, base-assisted deprotonation of the α -stereocenter. Tenuousness of this racemization pathway is reinforced by the fact that product **4ha** epimerizes at the same rate in the presence or

absence of added base (eq. 15)^[36] and that CsOAc alone fails to epimerize product **4ha** even after prolonged heating (data not shown).

In light of insights gained from labeling studies in eq. 12-14, we wondered whether epimerization takes place by the microscopic reverse of the mechanism proposed in Figure 2.8: coordination of the benzoxazole nitrogen to rhodium acidifies the heterobenzylic hydrogen of product **4**, which is abstracted by acetate (Figure 2.10, step 1).^[37] Resultant Rh–enamido complex **XVI**, which is in equilibrium with C-bound **XVII** (step 2), isomerizes back into the acrylate backbone via a series of β -H-elimination, hydorrhodation events (steps 3-5) to eventually give O-bound Rh–enolate **XX**. Enolate **XX** is shown as, but need not exist as, the rhodacycle. Protonation or ligand exchange of **XX** at oxygen epimerizes the α -stereocenter of product **4** (step 6).^[38] While intermediate **XVII** is shown with a specific stereochemistry at the carbon bearing rhodium, this is only intended to illustrate that no stereochemical scrambling of the α -stereocenter occurs prior to formation of O-bound **XX** if alkene **XVIII** remains coordinated to rhodium (i.e. the stereochemistry of the starting material is relayed to the stereochemistry of C-bound **XIX**).

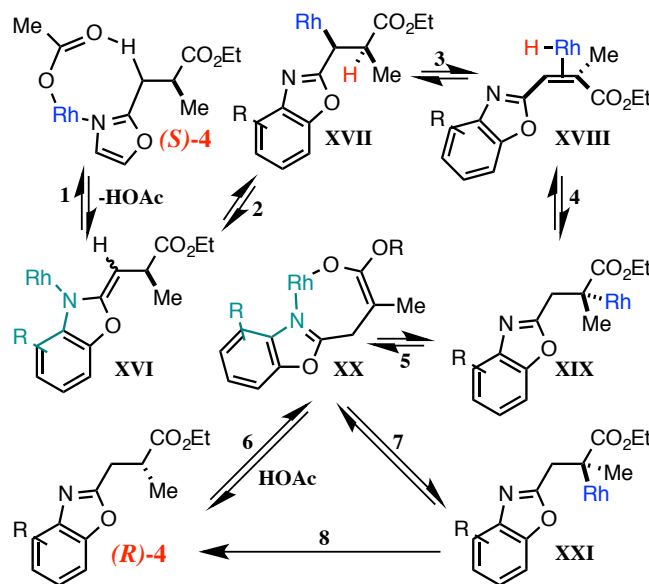


Figure 2.10 Proposed epimerization mechanism

We tested credence of this mechanism by treating product **4ha** (75% ee) with [Rh(cod)OAc]₂ and CTH-(*R*)-xylyl-P-Phos in CD₃CN (Figure 2.11, eq. 18), since we knew CD₃CN to be a competent proton source (Figure 2.7, eq. 12). If epimerization were occurring via a typical deprotonation-reprotonation sequence at the α -carbon, then we should see deuterium incorporation at the α -position of product **4ha**. On the other hand, if epimerization mechanism depicted in Figure 2.10 were operative, we would see deuterium incorporation at both β - and α -positions of product.

In accord with our hypothesis, **4ha** is isolated from the reaction in eq. 18 in 20 % ee with significant deuterium incorporation at the α -position and predominant deuterium incorporation at the β -position (Figure 2.11, eq. 18).

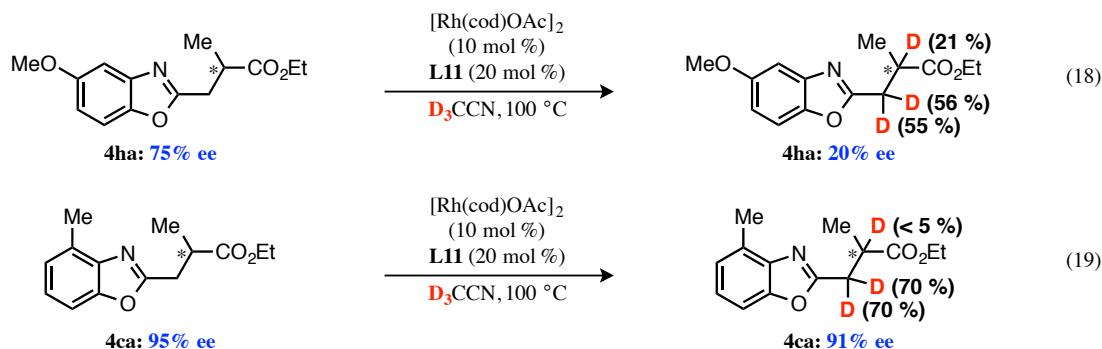


Figure 2.11 Epimerization-labeling studies

While this data cannot unequivocally debunk a mechanism by which deuteration at the α - and β -positions occur by independent deprotonation-reprotonation events at vicinal carbons, the level of deuterium incorporation at the α -position of product **4ca** strongly suggests that the two incorporation events are coupled by a common intermediate. Specifically, 22% deuterium at the α -position of **4ca** does not nearly account for a 55% loss in ee of **4ca** (Scheme 2.11, eq. 18).^[39] Thus, **4ca** must epimerize by at least one other mechanism besides protonation. We propose that Rh–enolate intermediate **XX** has two opportunities to scramble α -stereochemistry (Figure 2.10). It can, as already discussed, protonate or undergo ligand exchange on oxygen to give enantiomeric product (Figure 2.10, step 6). Yet protonation is not necessary for epimerization to occur. To the extent that the α -stereochemistry of C-bound **XIX** is lost in O-bound **XX**, then isomerization back to the C-bound isomer should be able to deliver diastereomeric complex **XXI** in which α -stereochemistry is inverted (Figure 2.10, step 7). A reverse sequence of elimination and addition events relays **XXI** to enantiomeric product (Figure 2.10, step 8).

We wondered how the epimerization mechanism depicted in Figure 2.10 could account for the very different fates of low-ee product **4ha** and high-ee product **4ca** when they are resubjected to our Rh–bisphosphine system. Interestingly, when highly enantioenriched product **4ca** (95% ee) is treated with rhodium and ligand under conditions identical to those described for **4ha**, **4ca** also deuterates considerably at the β -position (Figure 2.11, eq. 19). In contrast to **4ha**, however, product **4ca** epimerizes quite slowly (to 91%) even at high dimer loading, and it shows no discernable ^2H incorporation at the α -position. We provide two possible explanations to account for the data in eq. 18-19, but alternatives are possible. As illustrated in Figure 2.10, C–H activation of **4** gives Rh–enamido complex **XVI**. It is possible that A[1,3]-strain between the axial methyl of **4ca** and rhodium shortens the lifetime of

XVI such that a rapid backward reaction—protonation of **XVI**—outcompetes isomerization into the acrylate backbone.

An alternative explanation invokes differential stability of **4ha** and **4ca** Rh–enolate complexes **XX** (Figure 2.10). Whereas coordination of the heterocyclic nitrogen to rhodium could stabilize **4ha**-derived Rh–enolate **XX**, A[1,3]-strain would prevent analogous stabilization of **4ca**-derived **XX**. In either case, relative coordinating abilities of **4ca** and other benzoxazoles appear to crucially influence product epimerization rates. If this is true, then our bulky P-Phos ligand may serve an additional service: it may discourage ligation-promoted racemization pathways.

2.4 Summary

In summary, mechanistic insights gained from a known reaction of heterocycles and *tert*-butyl acrylate^[4] enabled development of an asymmetric, hydroheteroarylation reaction of benzoxazoles and α -substituted acrylates. The reaction is mediated by a rhodium–acetate precatalyst and bulky bisphosphine ligand, CTH-(*R*)-xylyl-P-Phos, and it delivers diverse elaborated benzoxazole products in moderate to excellent yields and good to excellent enantioselectivities. Mechanistically, the reaction is thought to proceed via a C–H activation, MI and protonation sequence in which acetate serves as a proton shuttle. Labeling studies implicate MI as a possible enantiodetermining step, after which stereospecific isomerization to a Rh–heterobenzyl complex insulates the newly formed stereocenter from epimerization. Products that are good ligands for rhodium can epimerize by a reverse sequence: coordination and subsequent C–H activation at the heterobenzyl position provides a Rh–enamido complex. A series of β -H elimination-hydrorhodation events relays the enamido complex to an O-bound rhodium enolate, in which α -stereochemistry is lost. Our proposed mechanism differs importantly from those implicated in studies describing the related Rh(I)–bisphosphine-mediated hydroarylation of α -substituted acrylates with boronic acids.^[15] These studies invoke protonation of a rhodium enolate as the enantiodetermining step of the reaction. Since little mechanistic evidence is provided in these studies, it is conceivable that an isomerization pathway such as ours is operative in these systems. Finally, a bulky bisphosphine ligand is found to be crucial for reactivity and selectivity in our HH reaction, as it likely discourages deleterious coordination of benzoxazole substrates to on- or off-cycle intermediates, accelerates a difficult MI step and discourages coordination-initiated epimerization. In short, careful mechanistic analysis has enabled the development of an efficient and highly selective catalytic, asymmetric HH of readily accessible reagents to produce chiral compounds of high biological importance.

REFERENCES

- [1] Text and figures for this chapter have been adapted with permission from Filloux, C. M.; Rovis, T. *J. Am. Chem. Soc.* **2015**, *137*, 508 – 517. Can be found online at: <http://pubs.acs.org/doi/abs/10.1021/ja511445x>.
- [2] For selected reviews and examples of catalytic, asymmetric alkylation of heteroarenes mediated by chiral acids, see:
- (a) Bandini, M.; Melloni, A.; Umani-Ronchi, A. *Angew. Chem., Int. Ed.* **2004**, *43*, 550 – 556.
 - (b) Bandini, M.; Melloni, A.; Tommasi, S.; Umani-Ronchi, A. *Synlett* **2005**, 1199 – 1222.
 - (c) Evans, D. A.; Fandrick, K. R.; Song, H. J.; Scheidt, K. A.; Xu, R. *J. Am. Chem. Soc.* **2007**, *129*, 10029 – 10041.
 - (d) Alexakis, A.; Bäckvall, J. E.; Krause, N.; Pàmies, O.; Diéguez, M. *Chem. Rev.* **2008**, *108*, 2796 – 2823.
 - (e) You, S. L.; Cai, Q.; Zeng, M. *Chem. Soc. Rev.* **2009**, *38*, 2190 – 2201.
 - (f) Boersma, A. J.; Feringa, B. L.; Roelfes, G. *Angew. Chem. Int. Ed.* **2009**, *48*, 3346 – 3348.
 - (g) Terrasson, V.; Marcia de Figueiredo, R.; Campagne, J. M. *Eur. J. Org. Chem.* **2010**, 2635 – 2655.
 - (h) Duan, S.; An, J.; Chen, J.; Xiao, W. *Org. Lett.* **2011**, *13*, 2290 – 2293.
 - (i) Chauhan, P.; Chimni, S. S. *RSC. Adv.* **2012**, *2*, 6117 – 6134.
 - (j) Huo, H.; Fu, C.; Harms, K.; Meggers, E. *J. Am. Chem. Soc.* **2014**, *136*, 2990 – 2993.
- [3] For reviews of transition-metal-catalyzed hydroheteroarylation, see:
- (a) Lewis, J. C.; Bergman, R. G.; Ellman, J. A. *Acc. Chem. Res.* **2008**, *41*, 1013 – 1025.
 - (b) Colby, D. A.; Bergman, R. G.; Ellman, J. A. *Chem. Rev.* **2010**, *110*, 624 – 655.
- [4] For selected examples of non-asymmetric, transition-metal-catalyzed hydroheteroarylation, see:
- (a) Tan, K. L.; Bergman, R. G.; Ellman, J. A. *J. Am. Chem. Soc.* **2001**, *123*, 2685 – 2686.
 - (b) Tan, K. L.; Bergman, R. G.; Ellman, J. A. *J. Am. Chem. Soc.* **2002**, *124*, 3202 – 3203.
 - (c) Tan, K. L.; Bergman, R. G.; Ellman, J. A. *J. Am. Chem. Soc.* **2002**, *124*, 13964 – 13965.
 - (d) Baran, P. S.; Guerrero, C. A.; Corey, E. J. *J. Am. Chem. Soc.* **2003**, *125*, 5628 – 5629.
 - (e) Ferreira, E. M.; Stoltz, B. M. *J. Am. Chem. Soc.* **2003**, *125*, 9578 – 9579.
 - (f) Liu, C.; Han, X.; Wang, X.; Widenhoefer, R. A. *J. Am. Chem. Soc.* **2004**, *126*, 3700 – 3701.
 - (g) Nakao, Y.; Kashiwara, N.; Kanyiva, K. S. Hiyama, T. *Angew. Chem. Int. Ed.* **2010**, *122*, 4553 – 4454.
 - (h) Nakao, Y.; Yamada, Y.; Kashiwara, N.; Hiyama, T. *J. Am. Chem. Soc.* **2010**, *132*, 13666 – 13668.
 - (i) Jiao, L.; Herdtweck, E.; Bach, T. *J. Am. Chem. Soc.* **2012**, *134*, 14563 – 14572.

- (j) Ryu, J.; Cho, S. H.; Chang, S. *Angew. Chem. Int. Ed.* **2012**, *51*, 3677 – 3681.
- [5] For selected reviews and examples of asymmetric, transition-metal-catalyzed hydroarylation of olefins with activated arenes, see:
- (a) Hayashi, T.; Ueyama, K.; Tokunaga, N.; Yoshida, K. *J. Am. Chem. Soc.* **2003**, *125*, 11508 – 11509.
- (b) Shintani, R.; Ueyama, K.; Yamada, I.; Hayashi, T. *Org. Lett.* **2004**, *6*, 3425 – 3427.
- (c) Tietze, L. F.; Ila, H.; Bell, H. P. *Chem. Rev.* **2004**, *104*, 3453 – 3561.
- (d) Hayashi, T.; Tokunaga, N.; Okamoto, K.; Shintani, R. *Chem. Lett.* **2005**, *34*, 1480 – 1481.
- (e) Nakao, Y.; Chen, J.; Imanaka, H.; Hiyama, T.; Ichikawa, Y.; Duan, W.; Shintani, R.; Hayashi, T. *J. Am. Chem. Soc.* **2007**, *129*, 9137 – 9143.
- (f) Edwards, H. J.; Hargrave, J. D.; Penrose, S. D.; Frost, C. G. *Chem. Soc. Rev.* **2010**, *39*, 2093 – 2105.
- (g) Menard, F.; Perez, D.; Roman, D. S.; Chapman, T. M.; Lautens, M. *J. Org. Chem.* **2010**, *75*, 4056 – 4068.
- (h) Nishimura, T.; Wang, J.; Nagaosa, M.; Okamoto, K.; Shintani, R.; Kwong, F.; Yu, W.; Chan, A. S. C.; Hayashi, T. *J. Am. Chem. Soc.* **2010**, *132*, 464 – 465.
- (i) Tian, P.; Dong, H.; Lin, G. *ACS Catal.* **2012**, *2*, 95 – 119.
- (j) Howell, G. P. *Org. Process Res. Dev.* **2012**, *16*, 1258 – 1272.
- (k) Brawn, R. A.; Guimarães, C. R. W.; McClure, K. F.; Liras, S. *Org. Lett.* **2013**, *15*, 3424 – 3427.
- (l) Liu, S.; Zhou, J. *Chem. Commun.* **2013**, *49*, 11758 – 11760.
- (m) Mei, T.; Werner, E. W.; Burckle, A. J.; Sigman, M. S. *J. Am. Chem. Soc.* **2013**, *135*, 6830 – 6833 (functionally an asymmetric hydroarylation reaction).
- (n) So, C. M.; Kume, S.; Hayashi, T. *J. Am. Chem. Soc.* **2013**, *135*, 10990 – 10993.
- [6] For selected reviews and examples of transition-metal-catalyzed, asymmetric hydroarylation of olefins via directed C–H activation, see:
- (a) Aufdenblatten, R.; Diezi, S.; Togni, A. *Monatsh. Chem.* **2000**, *131*, 1345 – 1350.
- (b) Thalji, R. K.; Ellman, J. A.; Bergman, R. G. *J. Am. Chem. Soc.* **2004**, *126*, 7192 – 7193.
- (c) Tsuchikama, K.; Kasagawa, M.; Hashimoto, Y.; Endo, K.; Shibata, T. *J. Organomet. Chem.* **2008**, *693*, 3939 – 3942.
- (d) Hyster, T. K.; Knörr, L.; Ward, T. R.; Rovis, T. *Science* **2012**, *338*, 500 – 503.
- (e) Ye, B.; Cramer, N. *Science* **2012**, *338*, 504 – 506.
- (f) Pan, S.; Shibata, T. *ACS Catal.* **2013**, *3*, 704 – 712.
- (g) Zheng, C.; You, S. *RSC Adv.* **2014**, *4*, 6173 – 6214.
- (h) Ye, B.; Donets, P. A.; Cramer, N. *Angew. Chem. Int. Ed.* **2014**, *53*, 507 – 511.

- [7] Wiedemann, S. H.; Lewis, J. C.; Ellman, J. A.; Bergman, R. G. *J. Am. Chem. Soc.* **2006**, *128*, 2452 – 2462.
- [8] (a) Wilson, R. M.; Thalji, R. K.; Bergman, R. G.; Ellman, J. A. *Org. Lett.* **2006**, *8*, 1745 – 1747.
- (b) Rech, J. C.; Yato, M.; Duckett, D.; Ember, B.; LoGrasso, P. V.; Bergman, R. G.; Ellman, J. A. *J. Am. Chem. Soc.* **2007**, *129*, 490 – 491.
- (c) Tsai, A. S.; Wilson, R. M.; Harada, H.; Bergman, R. G.; Ellman, J. A. *Chem. Commun.* **2009**, 3910 – 3912.
- [9] Pan, S.; Ryu, N.; Shibata, T. *J. Am. Chem. Soc.* **2012**, *134*, 17474 – 17477.
- [10] Sevov, C. S.; Hartwig, J. F. *J. Am. Chem. Soc.* **2013**, *135*, 2116 – 2119.
- [11] Song, G.; O, W. W. N.; Hou, Z. *J. Am. Chem. Soc.* **2014**, *136*, 12209 – 12212.
- [12] (a) Razavi, H.; Palaninathan, S. K.; Powers, E. T.; Wiseman, R. L.; Purkey, H. E.; Mohamedmohaideen, N. N.; Deechongkit, S.; Chiang, K. P.; Dendle, M. T. A.; Sacchettini, J. C.; Kelly, J. W. *Angew. Chem. Int. Ed.* **2003**, *42*, 2758 – 2761.
- (b) Plemper, R. K.; Erlandson, K. J.; Lakdawala, A. S.; Sun, A.; Prussia, A.; Boonsombat, J.; Aki-Sener, E.; Yalcin, I.; Yildiz, I.; Temiz-Arpaci, O.; Tekiner, B.; Liotta, D. C.; Snyder, J. P.; Compans, R. W. *Proc. Natl. Acad. Sci. U.S.A.* **2004**, *101*, 5628 – 5633.
- (c) McKee, M. L. Ph.D. Dissertation, University of Texas at Austin, Austin, 2007.
- (d) McKee, M. L.; Kerwin, S. M. *Bioorg. Med. Chem.* **2008**, *16*, 1775 – 1783.
- (e) Sommer, P. S. M.; Almeida, R. C.; Schneider, K.; Beil, W.; Süßmuth, R. D.; Fiedler, H. *J. Antibiot.* **2008**, *61*, 683 – 686.
- (f) Gautam, M. K.; Sonal; Sharma, N. K.; Priyanka; Jha, K. K. *Int. J. ChemTech. Res.* **2012**, *4*, 640 – 650.
- [13] *Phosphorous Ligands in Asymmetric Catalysis: Synthesis and Applications*, Börner, A., Ed.; Wiley-VCH: Weinheim, 2008.
- [14] Hartwig, J. *Organotransition Metal Chemistry*; University Science Books: Sausalito, 2010.
- [15] (a) Reetz, M. T.; Moulin, D.; Gosberg, A. *Org. Lett.* **2001**, *3*, 4083 – 4085.
- (b) Moss, R. J.; Wadsworth, K. J.; Chapman, C. J.; Frost, C. G. *Chem. Commun.* **2004**, 1984 – 1985.
- (c) Sibi, M. P.; Tatamidani, H.; Patil, K. *Org. Lett.* **2005**, *7*, 2571 – 2573.
- (d) Frost, C. G.; Penrose, S. D.; Lambshead, K.; Raithby, P. R.; Warren, J. E.; Gleave, R. *Org. Lett.* **2007**, *9*, 2119 – 2122.
- (e) Navarre, L.; Martinez, R.; Genet, J.; Darses, S. *J. Am. Chem. Soc.* **2008**, *130*, 6159 – 6169.
- [16] For established or alleged enantioselective protonation of transition metal enolates, see:
- (a) Ref. 15b–e.
- (b) Bergens, S. H.; Bosnich, B. *J. Am. Chem. Soc.* **1991**, *113*, 958 – 967.
- (c) Hamashima, Y.; Somei, H.; Shimura, Y.; Tamura, T.; Sodeoka, M. *Org. Lett.* **2004**, *6*, 1861 – 1864.

- (d) Mohr, J. T.; Hong, A. Y.; Stoltz, B. M. *Nat. Chem.* **2009**, *1*, 359 – 369.
- (e) Hamashima, Y.; Tamura, T.; Suzuki, S.; Sodeoka, M. *Synlett* **2009**, 1631 – 1634.
- (f) Hamashima, Y.; Suzuki, S.; Tamura, T.; Somei, H.; Sodeoka, M. *Chemistry—Asian J.* **2011**, *6*, 658 – 668.
- [17] Shibata, K.; Chatani, N. *Org. Lett.* **2014**, *16*, 5148 – 5151.
- [18] [Rh(cod)OAc]₂ as a hydroformylation precatalyst:
- (a) Burke, S. D.; Cobb, J. E. *Tetrahedron Lett.* **1986**, *27*, 4237 – 4240.
- (b) Burke, S. D.; Cobb, J. E.; Takeuchi, K. *J. Org. Chem.* **1990**, *55*, 2138 – 2151.
- (c) da Silva, A. C.; de Oliveira, K. C. B.; Gusevskaya, E. V.; dos Santos, E. N. J. *Mol. Catal. A: Chem.* **2002**, *179*, 133 – 141.
- (d) Barros, H. J. V.; Ospina, M. L.; Arguello, E.; Rocha, W. R.; Gusevskaya, E. V.; dos Santos, E. N. J. *Organomet. Chem.* **2003**, *671*, 150 – 157.
- (e) Barros, H. J. V.; Guimarães, C. C.; dos Santos, E. N.; Gusevskaya, E. V. *Organometallics* **2007**, *26*, 2211 – 2218.
- (f) Barros, H. J. V.; Guimarães, C. C.; dos Santos, E. N.; Gusevskaya, E. V. *Catal. Commun.* **2007**, *8*, 747 – 750.
- (g) Barros, H. J. V.; da Silva, J. G.; Guimarães, C. C.; dos Santos, E. N.; Gusevskaya, E. V. *Organometallics* **2008**, *27*, 4523 – 4531.
- As a hydrogenation precatalyst: (h) Nagy-Magos, Z.; Vastag, S.; Heil, B.; Markó, L. *J. Organomet. Chem.* **1979**, *171*, 97 – 102.
- As a hydroboration precatalyst: (i) Endo, K.; Hirokami, M.; Shibata, T. *Organometallics* **2008**, *27*, 5390 – 5393.
- As a precatalyst for cine substitution of vinyl acetates and boronic acids:
- (j) Yu, J.; Shimizu, R.; Kuwano, R. *Angew. Chem. Int. Ed.* **2010**, *49*, 6396 – 6399.
- (k) Kuwano, R. *J. Syn. Org. Chem. Jpn.* **2011**, *69*, 1263 – 1270.
- [19] Chatt, J.; Venanzi, L. M. *J. Chem. Soc.* **1957**, 4735 – 4741.
- [20] We deposited the crystal structure of [Rh(cod)OAc]₂ to the Cambridge Crystallographic Data Centre: CCDC 936197
- [21] (a) van Leeuwen, P. W. N. M.; Kamer, P. C. J.; Reek, J. N. H. *Pure Appl. Chem.* **1999**, *71*, 1443 – 1452.
- (b) van Leeuwen, P. W. N. M.; Kamer, P. C. J.; Reek, J. N. H.; Dierkes, P. *Chem. Rev.* **2000**, *100*, 2741 – 2770.
- (c) Kamer, P. C. J.; van Leeuwen, P. W. N. M.; Reek, J. N. H. *Acc. Chem. Res.* **2001**, *34*, 895 – 904.
- (d) Birkholz, M.; Freixab, Z.; van Leeuwen, P. W. N. M. *Chem. Soc. Rev.* **2009**, *38*, 1099 – 1118.
- (e) Shen, Z.; Dornan, P. K.; Khan, H. A.; Woo, T. K.; Dong, V. M. *J. Am. Chem. Soc.* **2009**, *131*, 1077 – 1091.

- (f) Ito, S.; Itoh, T.; Nakamura, M. *Angew. Chem. Int. Ed.* **2011**, *50*, 454 – 457.
- [22] Dppe has a natural bite angle of 86° vs. 93°
- For Binap, see: Ref. 21d.
- [23] Segphos is known to have a smaller dihedral angle than Binap: Jeulin, S.; de Paule, S. D.; Ratovelomanana-Vidal, V.; Genêt, J.; Champion, N.; Dellis, P. *Proc. Natl. Acad. Sci. U. S. A.* **2004**, *101*, 5799 – 5804.
- For a demonstration of the correlation between dihedral angle and natural bite angle, see: Raebiger, J. W.; Miedaner, A.; Curtis, C. J.; Miller, S. M.; Anderson, O. P.; DuBois, D. L. *J. Am. Chem. Soc.* **2004**, *126*, 5502 – 5514.
- [24] Substrate **1b** (vs. **1a**) was chosen for the experiment, since the C–H resonance of the azole is easily resolved from that of **1c**.
- [25] Chang et al. also see deuterium scrambling in the products of a reaction between ethyl acrylate and a mixture of proteo- and deuterio-pyridine oxides (Ref. 4j).
- [26] There could also exist irreversible steps prior to the TLS of reactive substrate **1c**, but such an assumption is not required.
- [27] Bocian, W.; Jazwiński, J.; Sadlej, A. *Magn. Reson. Chem.* **2008**, *46*, 156 – 165.
- [28] We provide no rigorous evidence that MI is turnover limiting. Yet turnover-limiting MI is consistent with the positive dependence of product yield on acrylate concentration (Table 2.2) as well as with the observation that bulky acrylates react more sluggishly than less hindered ones (Table 2.4).
- [29] For the development of P-Phos ligands and selected examples of catalytic, asymmetric reactions that use CTH-Xylyl-P-Phos, see:
- (a) Ref. 5i.
- (b) Chan, A. S. C.; Pai, C. U.S. Patent 5,886,182, 1999.
- (c) Pai, C.; Lin, C.; Lin, C.; Chen, C.; Chan, A. S. C.; Wong, W. T. *J. Am. Chem. Soc.* **2000**, *122*, 11513 – 11514.
- (d) Wu, J.; Chen, X.; Guo, R.; Yeung, C.; Chan, A. S. C. *J. Org. Chem.* **2003**, *68*, 2490 – 2493.
- (e) Grasa, G. A.; Zanotti-Gerosa, A.; Medlock, J. A.; Hems, W. P. *Org. Lett.* **2005**, *7*, 1449 – 1451.
- (f) Chan, S. H.; Lam, K. H.; Li, Y.; Xu, L.; Tang, W.; Lam, F. L.; Lo, W. H.; Yu, W. Y.; Fan, Q.; Chan, A. S. C. *Tetrahedron: Asymmetry* **2007**, *18*, 2625 – 2631.
- (g) Zhang, X.; Wu, Y.; Yu, F.; Wu, F.; Wu, J.; Chan, A. S. C. *Chem. Eur. J.* **2009**, *15*, 5888 – 5891.
- [30] In the absence of CsOAc, [Rh(cod)Cl]₂ is also an ineffective precatalyst in the chemistry of Chang et al. (Ref. 4j).
- [31] Absolute configuration was not determined. Thus, product stereocenters are indicated with an asterisk.
- [32] When 25 mol % CsOAc is used, [Rh(cod)Cl]₂ is a competent precatalyst (see Ref. 4j).
- [33] Hawkes, K. J.; Cavell, K. J.; Yates, B. F. *Organometallics* **2008**, *27*, 4758 – 4771.

- [34] For a benzheterocycle-derived Rh(I)–enamido complex, see: Julius, G. R.; Cronje, S.; Neveling, A.; Esterhuysen, C.; Raubenheimer, H. G. *Helv. Chim. Acta* **2002**, *85*, 3737 – 3747.
- [35] 93% ee likely overestimates the degree of epimerization of **4ca** under the described conditions: a minor impurity coelutes with the minor enantiomer, and **4ca** does not epimerize in the absence of added substrates **1** and **3** even in the presence of higher catalyst concentrations (Figure 2.11, eq. 19).
- [36] The higher yield of **4ca** obtained in the reaction with CsOAc is consistent with the accelerating effect of CsOAc reported earlier (see Table 2.4 and discussion).
- [37] For reversible formation of a Rh(I)–enamido complex from an imine precursor, see: Zhao, P.; Krug, C.; Hartwig, J. F. *J. Am. Chem. Soc.* **2005**, *127*, 12066 – 12073.
- [38] For simplicity, this figure shows only formation of (*R*)-product from O-bound **XX** (Figure 2.10, step 6), yet (*S*)-product is presumably also formed.
- [39] Since the amount of deuterium in CD₃CN presumably overwhelms the amount of H⁺ liberated from product **4**, we approximate that one percent deuterium will incorporate into the α -position for each protonation event. Each (*R*) \rightarrow (*S*) conversion contributes 2% ee, which means we would need (75% starting ee - 20% final ee)/2 \sim 28 protonation events *if all were selective for the minor enantiomer*. In reality, protonation should give both enantiomers of product. A significant excess of protonation events is needed, then, to account for the observed 50% ee difference. The deuterium incorporation in **4ca** should reflect this excess.

APPENDIX ONE

Multicatalytic, Asymmetric Michael–Stetter Reaction of Salicylaldehydes and Activated Alkynes^[1]

A.1.1 Materials and methods.....	42
A.1.2 General procedure for the one-pot, one-step multicatalytic Michael–Stetter reaction (Chapter 1, eq. 1 and Table 1.2)	43
A.1.3 General procedure for the one-pot, two-step Michael–Stetter reaction of salicylaldehydes 7 and DMAD (8a) in the presence or absence of catechol (Chapter 1, Table 1.5)	43
A.1.4 Procedure for the preparation of 9aa on 7.0 mmol scale	43
A.1.5 Characterization data for products 9 and 15 (Chapter 1, Table 1.2 and Table 1.6)	44
A.1.6 Preparation and characterization data for product 19a (Chapter 1, Table 1.7)	48
A.1.7 Preparation and characterization data for product 19b (Chapter 1, Table 1.7)	48
A.1.8 General procedure for the preparation of conjugate adducts 12aa , 12ca and 12fa with 1,4-diazabicyclo[2.2.2]octane (DABCO, 10) or quinuclidine (11) (Chapter 1, Table 1.3–1.4 and eq. 7)	49
A.1.9 Characterization data for conjugate adducts 12ca and 12fa	49
A.1.10 Preparation of <i>Z</i> -enriched 12aa (Chapter 1, eq. 8).....	50
A.1.11 Preparation of <i>E</i> -enriched 12aa (Chapter 1, Table 1.3–1.4 and eq. 7).....	50
A.1.12 General procedure for the asymmetric Stetter reaction of conjugate adducts 12 (i.e. 12 → 9) (Chapter 1, Table 1.3 and eq. 9)	50
A.1.13 Preparation and characterization of ketoalkynoates 8b–d (Chapter 1, Table 1.6)	51
A.1.14 ¹ H and ¹³ C NMR spectra for compounds 9 and 15	54

[1] This appendix has been adapted with permission from supporting information for Filloux, C. M.; Lathrop, S. P.; Rovis, T. *Proc. Natl. Acad. Sci. U. S. A.* **2010**, *107*, 20666 – 20671. Can be found online at: <http://www.pnas.org/content/107/48/20666.full?tab=ds>.

A.1.1 Materials and methods

Unless noted, all reactions were performed in flame-dried glassware and carried out under an atmosphere of argon with magnetic stirring. HPLC grade chloroform preserved with pentane was purchased from Fisher Scientific. Tetrahydrofuran (THF), diethyl ether (Et₂O), and dichloromethane (DCM) were degassed with argon and passed through two columns of neutral alumina. Toluene was degassed with argon and passed through one column of neutral alumina and one column of Q5 reagent. Column chromatography was performed on SiliCycle® SilicaFlash® P60, 40 – 63 µm 60 Å and in general were performed according to the guidelines reported by Still et al.^[2] Thin-layer chromatography was performed on SiliCycle® 250 µm 60 Å plates. Visualization was accomplished with UV light or KMnO₄ stain followed by heating.

¹H NMR spectra were recorded on Varian 300 or 400 MHz spectrometers at ambient temperature unless otherwise stated. Data are reported as follows: chemical shift in parts per million (δ, ppm) from CDCl₃ (7.26 ppm), toluene-d₈ (7.09, 7.0, 6.98, 2.09 ppm), or benzene-d₆ (7.16 ppm) multiplicity (s, singlet; bs, broad singlet; d, doublet; t, triplet; q, quartet; and m, multiplet), coupling constants (Hz). ¹³C NMR was recorded on Varian 300 or 400 MHz spectrometers (at 75 or 100 MHz) at ambient temperature. Chemical shifts are reported in ppm from CDCl₃ (77.2 ppm) or toluene-d₈ (137.86 (1), 129.4 (3), 128.33 (3), 125.49 (3), 20.4 (5) ppm). High-resolution mass spectra (electrospray ionization (ESI)) were obtained by Donald Dick of Colorado State University.

Salicylaldehydes **7a–c**, **7e**, and **7g–j**, dimethyl acetylenedicarboxylate (DMAD) (**8a**), and catechol **14a** were purchased from Aldrich or Acros and used without subsequent purification. Salicylaldehydes **7d**^[3] and **7f**^[4] phosphonate ester **8e**^[5] allenes **19a**^[6] and **19b**^[7] and triazolium precatalysts^[8] **4b** and **ent-4b** were prepared according to literature procedures.

-
- [2] Still, W. C.; Kahn, M.; Mitra, A. *J. Org. Chem.* **1978**, *43*, 2923 – 2925.
[3] Knight, P. D.; O'Shaughnessy, P. N.; Munslow, I. J.; Kimberley, B. S.; Scott, P. *J. Organomet. Chem.* **2003**, *683*, 103 – 113.
[4] Toumi, M.; Couty, F.; Evano, G. *Angew. Chem. Int. Ed.* **2007**, *46*, 572 – 575.
[5] (a) Hall, R. G.; Trippett, S. *Tetrahedron Lett.* **1982**, *23*, 2603 – 2604.
(b) Myers, A. G.; Alauddin, M. M.; Fuhry, M. M.; Dragovich, P. S.; Finney, N. S.; Harrington, P. M. *Tetrahedron Lett.* **1989**, *30*, 6997 – 7000.
[6] Buono, G. *Synthesis* **1981**, 872 – 872.
[7] Lang, R. W.; Hansen, H. J. *Helv. Chim. Acta* **1980**, *63*, 438 – 455.
[8] Kerr, M. S.; Read de Alaniz, J.; Rovis, T. *J. Org. Chem.* **2005**, *70*, 5725 – 5728.

A.1.2 General procedure for the one-pot, one-step multicatalytic Michael–Stetter reaction (Chapter 1, eq. 1 and Table 1.2)

A 1-dram vial was equipped with a magnetic stir bar under argon and charged sequentially with DMAD (**8a**) or activated alkyne **8b–d** (0.15 mmol), salicylaldehyde **7** (0.16 mmol), and triazolium salt **4b** (14 mg, 0.030 mmol). Toluene (1.5 mL) was added, and the mixture was cooled to 0 °C. Quinuclidine (**11**) (3.0 mg, 0.030 mmol) or 1,4-diazabicyclo[2.2.2]octane (DABCO) (**10**) (3.0 mg, 0.030 mmol) was added in one portion, and the reaction was monitored by TLC (Hex:Acetone). *Note: many benzofuranone products 9 coelute with intermediate conjugate adducts 12 in Hex:EtOAc solvent systems. Resolution was typically accomplished with a Hex:Acetone system.* When the reaction was observed to be complete, the mixture was quenched with glacial acetic acid (1–2 drops), filtered through a plug of silica with Et₂O (~ 40 mL), and concentrated in vacuo. The resulting crude product **9** was purified via flash column chromatography on silica gel.

A.1.3 General procedure for the one-pot, two-step Michael–Stetter reaction of salicylaldehydes 7 and DMAD (8a) in the presence or absence of catechol (Chapter 1, Table 1.5)

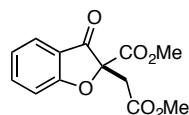
A 1-dram vial was equipped with a magnetic stir bar under argon and charged with DMAD (**8a**) (21 mg, 0.15 mmol) and salicylaldehyde **7** (0.16 mmol). Toluene (1.5 mL) was added, and the mixture was cooled to 0 °C. Quinuclidine (**11**) (3.0 mg, 0.030 mmol) or DABCO (**10**) (3.0 mg, 0.030 mmol) was added in one portion, and the reaction was monitored by TLC (EtOAc:Hex) until consumption of **8a** was observed to be complete. Catechol (if used) (0.015 mmol) was added to the reaction followed by triazolium salt precatalyst **4b** (14 mg, 0.030 mmol). The reaction was again monitored by TLC (Hex:Acetone) until conversion of intermediate aldehyde **12** to product **9** was complete. At this time, the reaction mixture was quenched with glacial acetic acid (1–2 drops), filtered through a plug of silica with Et₂O (~ 40 mL), and concentrated in vacuo. The resulting crude product **9** was purified by flash column chromatography on silica gel.

A.1.4 Procedure for the preparation of 9aa on 7.0 mmol scale

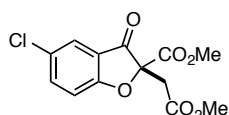
A 250 mL, flame-dried, round-bottom flask was charged with triazolium salt **4b** (164 mg, 0.350 mmol) and evacuated for 3 min, then filled with argon. After the evacuation procedure was repeated an additional two times, DMAD (**8a**) (1.01 g, 7.12 mmol), salicylaldehyde (**7a**) (933 mg, 7.64 mmol), and toluene (72 mL) were added sequentially, and the reaction mixture was cooled to 0 °C. Quinuclidine (**11**) (156 mg, 1.40 mmol) was added portionwise to the reaction mixture. After stirring at 0 °C for 9 h, the reaction was quenched with glacial acetic acid

(150 μ L) and poured directly onto a silica gel column (5:1 \rightarrow 1:1 Hex:EtOAc) to give 1.48 g (79% yield) **9aa** as a clear, amorphous solid.

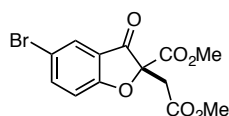
A.1.5 Characterization data for products 9 and 15 (Chapter 1, Table 1.2 and Table 1.6)



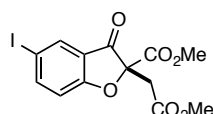
9aa. R_f = 0.24 (3:1 Hex:EtOAc); $[\alpha]_D^{25}$ = +99.1° (c = 1.56 g/100 mL, CHCl_3); HPLC analysis – Chiracel IC column, 60:40 Hex:*i*PrOH, 0.7 mL/min, major enantiomer: 14.9 min, minor enantiomer: 27.0 min, 89% ee; ^1H NMR (400 MHz, CDCl_3) δ 7.66 (m, 2H), 7.22 (d, 1H, J = 8.4 Hz), 7.14 (t, 1H, J = 7.5 Hz), 3.76 (s, 3H), 3.64 (s, 3H), 3.47 (d, 1H, J = 17.5 Hz), 3.10 (d, 1H, J = 17.5); ^{13}C NMR (100 MHz, CDCl_3) δ 194.6, 172.3, 169.0, 165.6, 138.7, 125.1, 123.1, 119.5, 113.7, 88.0, 53.8, 52.4, 38.5; IR (Thin Film/NaCl) 2950, 1747, 1727, 1614, 1465, 1214 cm^{-1} ; HRMS (ESI) m/z $[\text{C}_{13}\text{H}_{13}\text{O}_6]^+$ calcd ($[\text{M}+\text{H}]^+$) 265.0707, found 265.0710.



9ba. R_f = 0.26 (3:1 Hex:EtOAc); $[\alpha]_D^{25}$ = +56.6° (c = 1.46 g/100 mL, CHCl_3); HPLC analysis – Chiracel IC column, 50:50 Hex:*i*PrOH, 0.7 mL/min, major enantiomer: 13.7 min, minor enantiomer: 20.7 min, 89% ee; ^1H NMR (400 MHz, CDCl_3) δ 7.65 (d, 1H, J = 2.3 Hz), 7.60 (dd, 1H, J = 8.8, 2.3 Hz), 7.17 (d, 1H, J = 8.8 Hz), 3.77 (s, 3H), 3.65 (s, 3H), 3.45 (d, 1H, J = 17.6 Hz), 3.21 (d, 1H, J = 17.6); ^{13}C NMR (100 MHz, CDCl_3) δ 193.6, 170.7, 168.8, 165.2, 138.4, 128.7, 124.4, 121.0, 115.0, 88.9, 53.9, 52.5, 38.4; IR (Thin Film/NaCl) 2956, 1756, 1735, 1606, 1463, 1212 cm^{-1} ; HRMS (ESI) m/z $[\text{C}_{13}\text{H}_{11}\text{ClNaO}_6]^+$ ($[\text{M}+\text{H}]^+$) calcd 321.0136, found 321.0137.

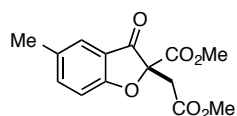


9ca. R_f = 0.25 (7:2 Hex:EtOAc); $[\alpha]_D^{25}$ = +56.7° (c = 1.60 g/100 mL, CHCl_3); HPLC analysis – Chiracel IC column, 50:50 Hex:*i*PrOH, 0.7 mL/min, major enantiomer: 14.2 min, minor enantiomer: 20.5 min, 94% ee; ^1H NMR (400 MHz, CDCl_3) δ 7.79 (d, 1H, J = 1.6 Hz), 7.72 (dd, 1H, J = 8.8, 1.6 Hz), 7.12 (d, 1H, J = 8.8 Hz), 3.75 (s, 3H), 3.63 (s, 3H), 3.43 (d, 1H, J = 17.6 Hz), 3.20 (d, 1H, J = 17.6); ^{13}C NMR (100 MHz, CDCl_3) δ 193.4, 171.0, 168.8, 165.2, 141.1, 127.5, 121.5, 115.6, 115.3, 88.7, 53.9, 52.5, 38.4; IR (Thin Film/NaCl) 2950, 1757, 1737, 1609, 1460, 1440, 1214 cm^{-1} ; HRMS (ESI) m/z $[\text{C}_{13}\text{H}_{11}\text{BrNaO}_6]^+$ ($[\text{M}+\text{H}]^+$) calcd 364.9631, found 364.9637.

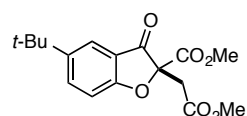


9da. R_f = 0.28 (3:1 Hex:EtOAc); $[\alpha]_D^{25}$ = +54.6° (c = 2.19 g/100 mL, CHCl_3); HPLC analysis – Chiracel IC column, 60:40 Hex:*i*PrOH, 0.7 mL/min, major enantiomer: 16.5 min, minor enantiomer: 22.4 min, 94% ee; ^1H NMR (400 MHz, CDCl_3) δ 7.98 (s, 1H), 7.88 (d, 1H, J = 8.7 Hz), 7.02 (d, 1H, J = 8.7 Hz), 3.75 (s, 3H), 3.64 (s, 3H), 3.43 (d, 1H, J = 17.6), 3.20 (d, 1H, J = 17.6 Hz); ^{13}C NMR (100 MHz, CDCl_3) δ

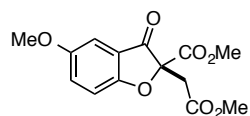
193.1, 171.7, 168.8, 165.1, 146.6, 133.6, 122.1, 115.8, 88.3, 85.3, 53.9, 52.4, 38.4; IR (Thin Film/NaCl) 2955, 1756, 1737, 1603, 1455, 1434, 1209 cm^{-1} ; HRMS (ESI) m/z $[\text{C}_{13}\text{H}_{11}\text{INaO}_6]^+$ ($[\text{M}+\text{H}]^+$) calcd 412.9493, found 412.9497.



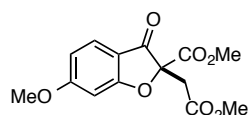
9ea. R_f = 0.23 (3:1 Hex:EtOAc); $[\alpha]_D^{25}$ = +78.0° (c = 1.60 g/100 mL, CHCl_3); HPLC analysis – Chiracel IC column, 60:40 Hex:*i*PrOH, 0.7 mL/min, major enantiomer: 15.6 min, minor enantiomer: 19.7 min, 86% ee; ^1H NMR (400 MHz, CDCl_3) δ 7.47 (m, 2H), 7.12 (m, 1H), 3.76 (s, 3H), 3.65 (s, 3H), 3.46 (d, 1H, J = 17.4 Hz), 3.09 (d, 1H, J = 17.4 Hz), 2.35 (s, 3H); ^{13}C NMR (100 MHz, CDCl_3) δ 194.7, 170.9, 169.0, 165.8, 140.0, 132.8, 124.5, 119.4, 113.3, 88.3, 53.7, 52.4, 38.6, 20.7; IR (Thin Film/NaCl) 2953, 1747, 1721, 1619, 1490, 1440, 1209 cm^{-1} ; HRMS (ESI) m/z $[\text{C}_{13}\text{H}_{15}\text{O}_6]^+$ ($[\text{M}+\text{H}]^+$) calcd 279.0863, found 279.0865.



9fa. R_f = 0.26 (4:1 Hex:EtOAc); $[\alpha]_D^{25}$ = +87.3° (c = 1.95 g/100 mL, CHCl_3); HPLC analysis – Chiracel IC column, 90:10 Hex:*i*PrOH, 0.7 mL/min, major enantiomer: 20.8 min, minor enantiomer: 16.4 min, 85% ee; ^1H NMR (400 MHz, CDCl_3) δ 7.73 (dd, 1H, J = 8.8, 2.0 Hz), 7.65 (d, 1H, J = 1.7 Hz), 7.16 (d, 1H, J = 8.8 Hz), 3.76 (s, 3H), 3.66 (s, 3H), 3.48 (d, 1H, J = 17.4 Hz), 3.04 (d, 1H, J = 17.4 Hz), 1.31 (s, 9H); ^{13}C NMR (100 MHz, CDCl_3) δ 194.8, 170.8, 169.1, 165.8, 146.4, 137.0, 121.0, 118.8, 113.1, 88.5, 53.7, 52.4, 38.6, 34.7, 31.4; IR (Thin Film/NaCl) 2960, 2905, 1747, 1726, 1619, 1491, 1210 cm^{-1} ; HRMS (ESI) m/z $[\text{C}_{17}\text{H}_{21}\text{O}_6]^+$ ($[\text{M}+\text{H}]^+$) calcd 321.1333, found 321.1337.

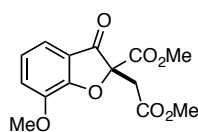


9ga. R_f = 0.26 (2:1 Hex:EtOAc); $[\alpha]_D^{25}$ = +73.6° (c = 1.48 g/100 mL, CHCl_3); HPLC analysis – Chiracel IC column, 50:50 Hex:*i*PrOH, 0.7 mL/min, major enantiomer: 19.9 min, minor enantiomer: 14.5 min, 86% ee; ^1H NMR (400 MHz, CDCl_3) δ 7.29 (dd, 1H, J = 9.0, 2.8 Hz), 7.16 (d, 1H, J = 9.0 Hz), 7.07 (d, 1H, J = 2.8 Hz), 3.81 (s, 3H), 3.78 (s, 3H), 3.67 (s, 3H), 3.47 (d, 1H, J = 17.4 Hz), 3.11 (d, 1H, J = 17.4); ^{13}C NMR (100 MHz, CDCl_3) δ 194.8, 169.0, 167.8, 165.8, 155.8, 128.7, 119.5, 114.6, 104.8, 88.8, 56.0, 53.8, 52.4, 38.6; IR (Thin Film/NaCl) 2955, 1747, 1716, 1491, 1440, 1209 cm^{-1} ; HRMS (ESI) m/z $[\text{C}_{14}\text{H}_{15}\text{O}_7]^+$ ($[\text{M}+\text{H}]^+$) calcd 295.0812, found 295.0809.



9ha. R_f = 0.22 (2:1 Hex:EtOAc); $[\alpha]_D^{25}$ = +171.3° (c = 1.71 g/100 mL, CHCl_3); HPLC analysis – Chiracel IC column, 50:50 Hex:*i*PrOH, 1.0 mL/min, major enantiomer: 40.7 min, minor enantiomer: 24.5 min, 85% ee; ^1H NMR (400 MHz, CDCl_3) δ 7.56 (d, 1H, J = 8.6 Hz), 6.68 (m, 2H), 3.88 (s, 3H), 3.77 (s, 3H), 3.67 (s, 3H), 3.48 (d, 1H, J = 17.4 Hz), 3.00 (d, 1H, J = 17.4 Hz); ^{13}C NMR (100 MHz, CDCl_3) δ 192.0, 175.0, 169.2, 169.0, 165.9, 126.2, 112.9, 112.2, 96.6, 88.9, 56.1, 53.7, 52.4, 38.5; IR (Thin

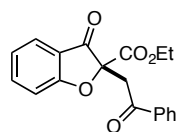
Film/NaCl) 2950, 1747, 1711, 1614, 1440, 1286 cm^{-1} ; HRMS (ESI) m/z $[\text{C}_{14}\text{H}_{15}\text{O}_7]^+$ ($[\text{M}+\text{H}]^+$) calcd 295.0812, found 295.0812.



9ia. $R_f = 0.29$ (3:2 Hex:EtOAc); $[\alpha]_D^{25} = +70.1^\circ$ ($c = 0.850$ g/100 mL, CHCl_3); HPLC analysis

– Chiracel IC column, 60:40 Hex:*i*PrOH, 0.7 mL/min, major enantiomer: 19.9 min, minor enantiomer: 33.5 min, 92% ee; ^1H NMR (400 MHz, CDCl_3) δ 7.28 (dd, 1H, $J = 7.7, 1.2$ Hz),

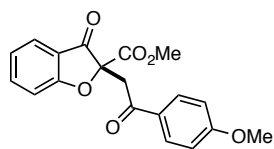
7.16 (dd, 1H, $J = 7.9, 1.1$ Hz), 7.09 (t, 1H, $J = 7.8$ Hz), 3.96 (s, 3H), 3.75 (s, 3H), 3.63 (s, 3H), 3.46 (d, 1H, $J = 17.6$ Hz), 3.30 (d, 1H, $J = 17.6$ Hz); ^{13}C NMR (100 MHz, CDCl_3) δ 195.0, 168.8, 165.6, 162.4, 146.5, 123.6, 121.1, 119.3, 116.0, 88.3, 56.4, 53.9, 52.4, 38.4; IR (ATR) 2956, 1723, 1617, 1504, 1438, 1206 cm^{-1} ; HRMS (ESI) m/z $[\text{C}_{14}\text{H}_{14}\text{NaO}_7]^+$ ($[\text{M}+\text{Na}]^+$) calcd 317.0632, found 317.0637.



9ab. $R_f = 0.30$ (3:1 Hex:EtOAc); $[\alpha]_D^{25} = +15.4^\circ$ ($c = 1.05$ g/100 mL, CHCl_3); HPLC analysis –

Chiracel IC column, 90:10 Hex:*i*PrOH, 0.7 mL/min, major enantiomer: 21.8 min, minor enantiomer: 18.6 min, 12% ee; ^1H NMR (400 MHz, CDCl_3) δ 7.93 (m, 2H), 7.65 (m, 3H), 7.46

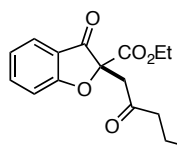
(m, 2H), 7.19 (m, 2H), 4.24 (m, 3H), 3.69 (d, 1H, $J = 18.2$ Hz), 1.24 (t, 3H, $J = 7.1$ Hz); ^{13}C NMR (100 MHz, CDCl_3) δ 195.7, 194.2, 172.5, 165.6, 138.6, 135.9, 133.9, 128.9, 128.3, 125.0, 122.9, 119.7, 113.8, 88.4, 63.0, 43.4, 14.1; IR (Thin Film/NaCl) 2978, 1747, 1726, 1690, 1614, 1460, 1224 cm^{-1} ; HRMS (ESI) m/z $[\text{C}_{19}\text{H}_{17}\text{O}_5]^+$ ($[\text{M}+\text{H}]^+$) calcd 325.1071, found 325.1078.



9ac. $R_f = 0.26$ (2:1 Hex:EtOAc); $[\alpha]_D^{25} = +24.2^\circ$ ($c = 1.36$ g/100 mL, CHCl_3); HPLC

analysis – Chiracel IC column, 85:15 Hex:*i*PrOH, 0.7 mL/min, major enantiomer: 38.3 min, minor enantiomer: 42.5 min, 18% ee; ^1H NMR (400 MHz, CDCl_3) δ 7.91 (d, 2H, J

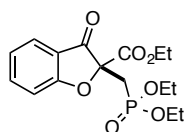
$= 8.9$ Hz), 7.73 (d, 1H, $J = 7.7$ Hz), 7.66 (m, 1H), 7.23 (d, 1H, $J = 8.4$ Hz), 7.16 (t, 1H, $J = 7.5$ Hz), 6.92 (d, 2H, $J = 8.9$ Hz), 4.19 (d, 1H, $J = 18.1$ Hz), 3.86 (s, 3H), 3.79 (s, 3H), 3.67 (d, 1H, $J = 18.1$ Hz); ^{13}C NMR (100 MHz, CDCl_3) δ 195.6, 192.6, 172.3, 166.3, 164.1, 138.6, 130.7, 128.9, 125.0, 122.9, 119.7, 114.0, 113.8, 88.5, 55.6, 53.7, 43.2; IR (Thin Film/NaCl) 2955, 1753, 1722, 1679, 1600, 1462, 1264, 1233 cm^{-1} ; HRMS (ESI) m/z $[\text{C}_{19}\text{H}_{16}\text{NaO}_6]^+$ ($[\text{M}+\text{Na}]^+$) calcd 363.0839, found 363.0845.



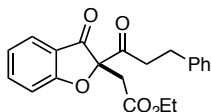
9ad. $R_f = 0.21$ (2:1 pentane:Et₂O); $[\alpha]_D^{25} = +35.9^\circ$ ($c = 0.370$ g/100 mL, CHCl_3); HPLC

analysis – Chiracel IC column, 90:10 Hex:*i*PrOH, 0.7 mL/min, major enantiomer: 47.0 min, minor enantiomer: 39.6 min, 51% ee; ^1H NMR (400 MHz, CDCl_3) δ 7.66 (m, 2H), 7.20 (m,

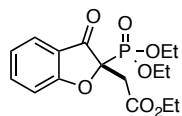
7H), 4.22 (dq, 1H, $J = 10.8, 7.1$ Hz), 4.19 (dq, 1H, $J = 10.8, 7.1$ Hz), 3.61 (d, 1H, $J = 18.2$ Hz), 3.13 (d, 1H, $J = 18.2$ Hz), 2.78 (m, 2H), 2.75 (m, 2H), 1.22 (t, 3H, $J = 7.1$ Hz); ^{13}C NMR (100 MHz, CDCl_3) δ 204.0, 195.3, 172.4, 165.4, 140.6, 138.6, 128.7, 128.4, 126.4, 125.0, 122.9, 119.6, 113.7, 88.2, 63.0, 46.7, 44.3, 29.5, 14.0; IR (Thin Film/NaCl) 2981, 1751, 1722, 1612, 1462, 1247 cm^{-1} ; HRMS (ESI) m/z $[\text{C}_{21}\text{H}_{20}\text{NaO}_5]^+$ ($[\text{M}+\text{Na}]^+$) calcd 375.1203, found 375.1199.



9ae. A 1-dram vial equipped with a magnetic stir bar under argon was charged with phosphonate **8e** (51 mg, 0.22 mmol), salicylaldehyde (**7a**) (28 mg, 0.23 mmol), and toluene (2.2 mL). Quinuclidine (**11**) (5.0 mg, 0.040 mmol) was added in one portion, and the reaction mixture was stirred for 25 h at 23 °C. At this point, the reaction mixture was cooled to 0 °C, and triazolium salt **4b** (20 mg, 0.040 mmol) was added. After an additional 75 minutes of stirring, the mixture was quenched with glacial acetic acid (2 drops), filtered through a plug of silica with Et_2O (~40 mL), and concentrated *in vacuo*. Flash column chromatography on silica gel yielded 28 mg (36% yield) of partially purified **9ae**, which was contaminated with about 20% chromene impurity which coeluted in a variety of solvent systems. $R_f = 0.35$ (95:5 DCM:MeOH); $[\alpha]_D^{25} = +32.4^\circ$ ($c = 0.230$ g/100 mL, CHCl_3); HPLC analysis – Chiracel ASH column, 85:15 Hex:*i*PrOH, 1.0 mL/min, major enantiomer: 10.0 min, minor enantiomer: 8.2 min, 86% ee; ^1H NMR (400 MHz, CDCl_3) δ 7.67 (m, 2H), 7.26 (m, 1H), 7.15 (m, 1H), 4.23 (q, 2H, $J = 7.1$ Hz), 4.00–4.07 (m, 4H), 2.98 (dd, 1H, $J = 16.9, 15.9$ Hz), 2.62 (dd, 1H, $J = 18.1, 15.8$ Hz), 1.23 (m, 9H); ^{13}C NMR (100 MHz, CDCl_3) δ 195.1 (d, $J = 7.3$ Hz), 172.3, 165.4 (d, $J = 12.8$ Hz), 138.7, 125.2, 123.0, 119.4, 113.7, 87.4 (d, $J = 7.4$ Hz), 63.2, 62.3 (d, $J = 5.6$ Hz), 62.1 (d, $J = 6.8$ Hz), 30.7 (d, $J = 145.0$ Hz), 16.4 (d, $J = 6.9$ Hz), 14.1; ^{31}P NMR (121 MHz, CDCl_3) δ 24.0 (s); IR (Thin Film/NaCl) 2984, 2930, 1753, 1729, 1613, 1463, 1247, 1026 cm^{-1} ; HRMS (ESI) m/z $[\text{C}_{16}\text{H}_{22}\text{O}_7\text{P}]^+$ ($[\text{M}+\text{H}]^+$) calcd 357.1098, found 357.1099.

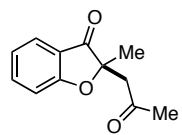


15ad. $R_f = 0.29$ (2:1 pentane: Et_2O); HPLC analysis – Chiracel IC column, 90:10 Hex:*i*PrOH, 0.7 mL/min, major enantiomer: 19.2 min, minor enantiomer: 60.5 min, 89% ee; ^1H NMR (400 MHz, CDCl_3) δ 7.68 (m, 2H), 7.08–7.26 (m, 7H), 4.09 (q, 2H, $J = 7.2$ Hz), 3.52 (d, 1H, $J = 17.2$ Hz), 3.21 (ddd, 1H, $J = 18.5, 9.9, 5.6$ Hz), 2.96 (d, 1H, $J = 17.2$ Hz), 2.89 (ddd, 1H, $J = 14.6, 9.6, 5.4$ Hz), 2.80 (ddd, 1H, $J = 14.6, 10.0, 5.3$ Hz), 2.52 (ddd, 1H, $J = 18.5, 9.8, 5.6$ Hz), 1.16 (t, 3H, $J = 7.2$ Hz); IR (Thin Film/NaCl) 2981, 1739, 1711, 1611, 1462, 1205 cm^{-1} ; HRMS (ESI) m/z $[\text{C}_{21}\text{H}_{20}\text{NaO}_5]^+$ ($[\text{M}+\text{Na}]^+$) calcd 375.1203, found 375.1211.



15ae. ^1H NMR (400 MHz, CDCl_3) δ 7.73 (m, 1H), 7.61 (m, 1H), 7.16, (m, 2H), 4.21 (m, 4H), 3.94 (m, 2H), 3.51 (dd, 1H, $J = 17.1, 3.1$ Hz), 3.34 (dd, 1H, $J = 17.1, 9.2$ Hz), 1.32 (t, 3H, $J = 7.1$ Hz), 1.22 (t, 3H, $J = 7.1$ Hz), 0.96 (t, 3H, $J = 7.2$ Hz).

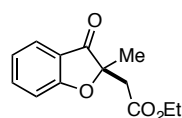
A.1.6 Preparation and characterization data for product 19a (Chapter 1, Table 1.7)



19a. A 1-dram vial was equipped with a magnetic stir bar under argon and charged with allenone **18a** (27 mg, 0.33 mmol), salicylaldehyde (**7a**) (37 mg, 0.30 mmol), and THF (1.5 mL). Quinuclidine (**11**) (6.7 mg, 0.060 mmol) was added in one portion, and the reaction mixture was

stirred at 23 °C until consumption of **7a** was observed to be complete by TLC (Hex:EtOAc). At this point, the reaction mixture was cooled to 0 °C, triazolium salt **4b** (28 mg, 0.060 mmol) was added, and the reaction was again monitored by TLC (Hex:Acetone). When the reaction was observed to be complete, the mixture was quenched with glacial acetic acid (2 drops), filtered through a plug of silica with Et_2O (~ 40 mL), and concentrated in vacuo. Flash column chromatography on silica gel yielded 37 mg (60% yield) of **19a**. $R_f = 0.22$ (3:1 Hex:EtOAc); $[\alpha]_D^{25} = -5.6^\circ$ ($c = 1.84$ g/100 mL, CHCl_3); HPLC analysis – Chiracel ADH column, 97:3 Hex:*i*PrOH, 1.0 mL/min, major enantiomer: 14.4 min, minor enantiomer: 16.5 min, 78% ee; ^1H NMR (400 MHz, CDCl_3) δ 7.70 (ddd, 1H, $J = 7.7, 1.4, 0.6$ Hz), 7.59 (ddd, 1H, $J = 8.5, 7.3, 1.5$ Hz), 7.07 (m, 2H), 3.15 (d, 1H, $J = 17.3$ Hz), 3.09 (d, 1H, $J = 17.2$ Hz), 2.11 (s, 3H), 1.42 (s, 3H); ^{13}C NMR (100 MHz, CDCl_3) δ 203.4, 203.1, 170.8, 137.7, 124.7, 122.0, 120.8, 113.3, 86.4, 50.1, 30.4, 22.5; IR (Thin Film/NaCl) 2359, 1712, 1610, 1462, 1367 cm^{-1} ; HRMS (ESI) m/z $[\text{C}_{12}\text{H}_{13}\text{O}_3]^+$ ($[\text{M}+\text{H}]^+$) calcd 205.0859, found 205.0863.

A.1.7 Preparation and characterization data for product 19b (Chapter 1, Table 1.7)



19b. A 1-dram vial was equipped with a magnetic stir bar under argon and charged with allenolate **18b** (47 mg, 0.42 mmol), salicylaldehyde (**7a**) (46 mg, 0.38 mmol) and solvent (1.5 mL). Quinuclidine (**11**) (8.4 mg, 0.076 mmol) was added in one portion, and the reaction

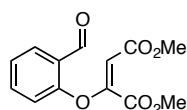
mixture was stirred at 23 °C until consumption of **7a** was observed to be complete by TLC (DCM:EtOAc). At this point, triazolium salt **4b** (35 mg, 0.076 mmol) was added, and the reaction was again monitored by TLC (Hex:Acetone). When the reaction was observed to be complete, the mixture was quenched with glacial acetic acid (2 drops), filtered through a plug of silica with Et_2O (~ 40 mL), and concentrated in vacuo. Flash column chromatography on silica gel yielded 52 mg (59% yield) of **19b**. $R_f = 0.27$ (4:1 Hex:EtOAc); $[\alpha]_D^{25} = -11.3^\circ$ ($c = 0.920$ g/100 mL, CHCl_3); HPLC analysis – Chiracel IC column, 50:50 Hex:*i*PrOH, 0.7 mL/min, major enantiomer:

44.0 min, minor enantiomer: 25.9 min, 96% ee; ^1H NMR (400 MHz, CDCl_3) δ 7.70 (m, 1H), 7.60 (m, 1H), 7.09 (m, 2H), 3.99 (dq, 1H, J = 10.8, 7.1 Hz), 3.93 (dq, 1H, J = 10.8, 7.1 Hz), 3.05 (d, 1H, J = 16.3 Hz), 2.92 (d, 1H, J = 16.3 Hz), 1.46 (s, 3H), 0.98 (t, 3H, J = 7.1 Hz); ^{13}C NMR (100 MHz, CDCl_3) δ 202.8, 171.1, 168.6, 137.9, 124.7, 122.0, 120.7, 113.4, 86.5, 61.0, 41.8, 22.7, 13.8; IR (Thin Film/NaCl) 2980, 1721, 1612, 1464, 1213 cm^{-1} ; HRMS (ESI) m/z $[\text{C}_{13}\text{H}_{15}\text{O}_4]^+$ ($[\text{M}+\text{H}]^+$) calcd 235.0965, found 235.0967.

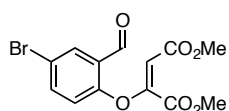
A.1.8 General procedure for the preparation of conjugate adducts **12aa**, **12ca** and **12fa** with DABCO (**10**) or quinuclidine (**11**) (Chapter 1, Table 1.3–1.4 and eq. 7)

A flame-dried, 50 mL round-bottom flask was charged with DMAD (**8a**) (2.0 mmol), salicylaldehyde (**7a**) (2.1 mmol), and toluene (20 mL) under argon. The mixture was cooled to 0 °C, and quinuclidine (**11**) or DABCO (**10**) (0.40 mmol) was added in one portion. After stirring for 30 – 60 min, the reaction mixture was concentrated *in vacuo*, and the resulting crude product **12** was purified by flash column chromatography on silica gel.

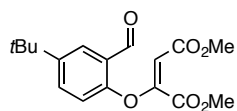
A.1.9 Characterization data for conjugate adducts **12aa**, **12ca** and **12fa**



12aa. Characterization data for **12aa** matched that reported in the literature.^[9] **12aa** was isolated as a > 20:1 mixture of *E*:*Z* isomers (*E* = **5a** in Ref. 8; *Z* = **4a** in Ref. 8). The vinylic resonance of *E*-**12aa** appears at 5.40 ppm, and the vinylic resonance of *Z*-**12aa** appears at 6.87 ppm.



12ca. **12ca** was obtained as a 16:1 *E*:*Z* mixture. ^1H and ^{13}C data is for *E* isomer only. R_f = 0.24 (3:1 Hex:EtOAc); ^1H NMR (400 MHz, CDCl_3) δ 10.21 (s, 1H), 8.06 (d, 1H, J = 2.5 Hz), 7.75 (dd, 1H, J = 8.7, 2.5 Hz), 7.10 (d, 1H, J = 8.7 Hz), 5.32 (s, 1H), 3.91 (s, 3H), 3.71 (s, 3H); ^{13}C NMR (100 MHz, CDCl_3) δ 186.4, 165.0, 162.3, 158.8, 154.3, 138.8, 132.1, 129.1, 123.3, 120.3, 103.4, 53.5, 52.2; IR (ATR) 2953, 1747, 1712, 1687, 1645, 1627, 1360, 1126 cm^{-1} ; HRMS (ESI) m/z $[\text{C}_{13}\text{H}_{11}\text{BrNaO}_6]^+$ ($[\text{M}+\text{Na}]^+$) calcd 364.9631, found 364.9631.



12fa. **12fa** was obtained as a > 20:1 *E*:*Z* mixture. ^1H and ^{13}C data is for *E* isomer only. R_f = 0.24 (4:1 Hex:EtOAc); ^1H NMR (400 MHz, CDCl_3) δ 10.25 (s, 1H), 7.96 (d, 1H, J = 2.6 Hz), 7.68 (dd, 1H, J = 8.6, 2.6 Hz), 7.12 (d, 1H, J = 8.6 Hz), 5.18 (s, 1H), 3.93 (s, 3H), 3.68 (s, 3H), 1.34 (s, 9H); ^{13}C NMR (100 MHz, CDCl_3) δ 188.1, 165.4, 162.8, 160.7, 153.0, 150.5, 133.4, 127.2, 125.9, 121.5, 100.9, 53.4,

[9] Gupta, R. K.; George, M. V. *Tetrahedron* **1975**, *31*, 1263 – 1275.

52.1, 35.0, 31.3; IR (Thin Film/NaCl) 2958, 2870, 1754, 1726, 1695, 1639, 1365, 1133 cm^{-1} ; HRMS (ESI) m/z $[\text{C}_{17}\text{H}_{21}\text{NaO}_6]^+$ ($[\text{M}+\text{Na}]^+$) calcd 343.1152, found 343.1153.

A.1.10 Preparation of *Z*-enriched **12aa** (Chapter 1, eq. 8)

Z-enriched **12aa** was prepared according to the method of Gupta and George.^[9] A mixture of salicylaldehyde (**7ab**) (702 mg, 5.8 mmol, 1.0 equiv), DMAD (**8a**) (817 mg, 5.8 mmol, 1.0 equiv) and K_2CO_3 (802 mg, 5.8 mmol, 1.0 equiv) in benzene (7.2 mL) was heated to reflux under argon. An additional 802 mg (1.0 equiv) K_2CO_3 was added 2h later, and the reaction was heated at reflux again until it was deemed complete by TLC (9:4 Hex:EtOAc). At this point, the brown reaction mixture was cooled to room temperature and purified by flash column chromatography on silica gel (9:4 Hex:EtOAc). Purest fractions were combined to give **12aa** (108 mg, 7%) as a ~ 6.9:1 (*Z*:*E*) mixture of stereoisomers (Figure A.1.1).

A.1.11 Preparation of *E*-enriched **12aa** (Chapter 1, Table 1.3–1.4 and eq. 7)

E-enriched **12aa** (Figure A.1.1) was prepared according to the general procedure (A.1.8).

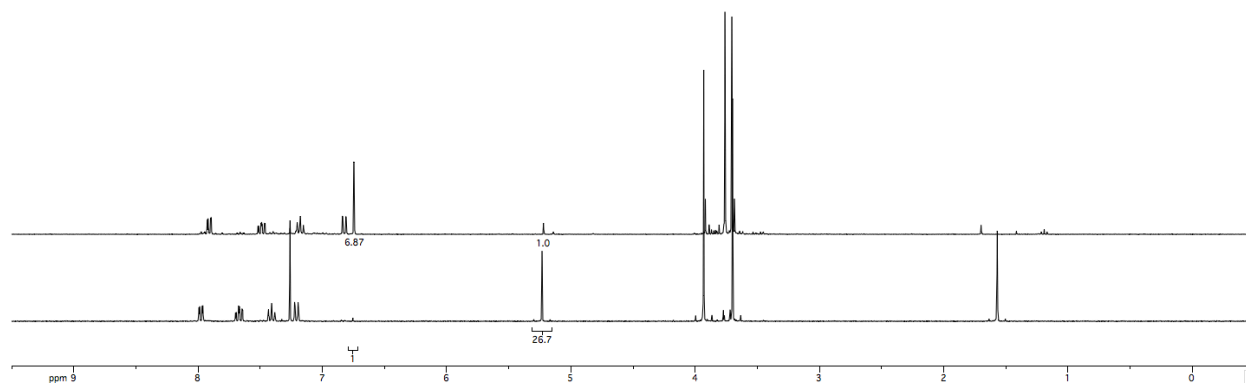


Figure A.1.1 ^1H NMR spectra for *Z*-enriched **12aa** (top) and *E*-enriched **12aa** (bottom). The vinylic resonance of *E*-**12aa** appears at 5.40 ppm, and the vinylic resonance of *Z*-**12aa** appears at 6.87 ppm.

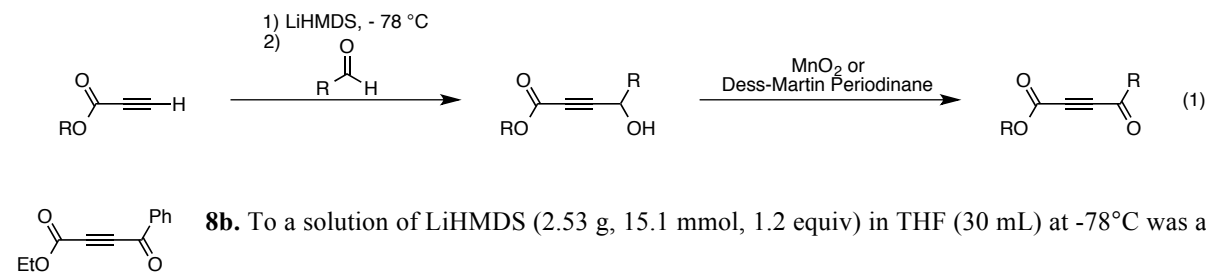
A.1.12 General procedure for the asymmetric Stetter reaction of conjugate adducts **12** (i.e. **12** \rightarrow **9**) (Chapter 1, Table 1.3 and eq. 9)

To a solution of **12aa** (34.6 mg, 0.31 mmol, 1.0 equiv) in toluene (1.3 mL) was added triazolium salt **4b** (12.4 mg, 0.20 equiv), and the reaction mixture was cooled to 0 $^\circ\text{C}$. Quinuclidine (**11**) (2.7 mg, 0.20 equiv) or DABCO (**10**) (2.9 mg, 0.20 equiv) was added at this time, and the reaction was stirred at 0 $^\circ\text{C}$ until it was observed to be complete by TLC (Hex:Acetone). The reaction mixture was quenched with glacial acetic acid (1–2 drops), filtered

through a plug of silica with Et₂O (~ 40 mL), and concentrated in vacuo. The resulting crude product **9** was purified by flash column chromatography on silica gel.

A.1.13 Preparation and characterization of ketoalkynoates **8b–d** (Chapter 1, Table 1.6)

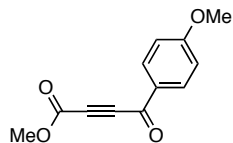
Ketoalkynoates were oxidized from the corresponding propargylic alcohols, which were prepared according to a modified literature procedure (eq. 1).^[10]



The resultant mixture was stirred for 30 minutes, at which point a solution of benzaldehyde (1.34 g, 12.6 mmol, 1.0 equiv) in THF (6.0 mL) was added via syringe pump over 30 minutes. After an additional 45 minutes of stirring, the reaction mixture was quenched with saturated NH₄Cl and allowed to warm to room temperature. The organic layer was diluted with Et₂O, washed with NH₄Cl, H₂O and brine and dried over MgSO₄. Concentration and flash column chromatography on silica gel gave 1.77 g (69% yield) of crude propargylic alcohol.

To a solution of the crude alcohol (494 mg, 2.42 mmol) in DCM (2.4 mL) at 0 °C was added dropwise a solution of MnO₂ (1.48 g, 17.0 mmol) in DCM (1.2 mL). The ice bath was removed, and the reaction mixture was allowed to stir at 23 °C for 4 h. Filtration through celite and purification by flash column chromatography on silica gel gave 260 mg of **8b** (36% yield over two steps) as a light yellow oil. R_f = 0.35 (5:1 Hex:EtOAc); ¹H NMR (400 MHz, CDCl₃) δ 8.12 (dd, 2H, *J* = 8.0, 0.4 Hz), 7.67 (t, 1H, *J* = 7.2 Hz), 7.52 (t, 2H, *J* = 8.0 Hz), 4.35 (q, 2H, *J* = 7.2 Hz), 1.37 (t, 3H, *J* = 7.2 Hz); ¹³C NMR (100 MHz, CDCl₃) δ 176.3, 152.4, 135.7, 135.3, 129.9, 129.0, 80.6, 79.9, 63.2, 14.1; IR (Thin Film/NaCl) 2986, 1719, 1653, 1450, 1262 cm⁻¹; LRMS (GC) *m/z* [C₁₂H₁₀O₃] ([M]⁺) calcd 202, found 202.

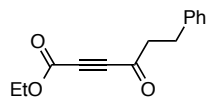
[10] Crimmins, M. T.; Nantermet, P. G.; Trotter, B. W.; Vallin, I. M.; Watson, P. S.; McKerlie, L. A.; Reinhold, T. L.; Cheung, A. W. H.; Stetson, K. A. *J. Org. Chem.* **1993**, 58, 1038 – 1047.



8c. To a solution of LiHMDS (836 mg, 5.00 mmol, 1.2 equiv) in THF (10 mL) at -78 °C was added methyl propiolate (386 mg, 4.59 mmol, 1.1 equiv) in THF (4.2 mL) over 30 minutes via syringe pump. The resultant mixture was stirred for 30 minutes, at which point a

solution of *p*-anisaldehyde (566 mg, 4.16 mmol, 1.0 equiv) in THF (2.0 mL) was added via syringe pump over 20 minutes. After an additional 45 minutes of stirring, the reaction mixture was quenched with saturated NH₄Cl and allowed to warm to room temperature. The organic layer was diluted with Et₂O, washed with NH₄Cl, H₂O and brine and dried over MgSO₄. Concentration and flash column chromatography on silica gel gave 744 mg (81% yield) of crude propargylic alcohol.

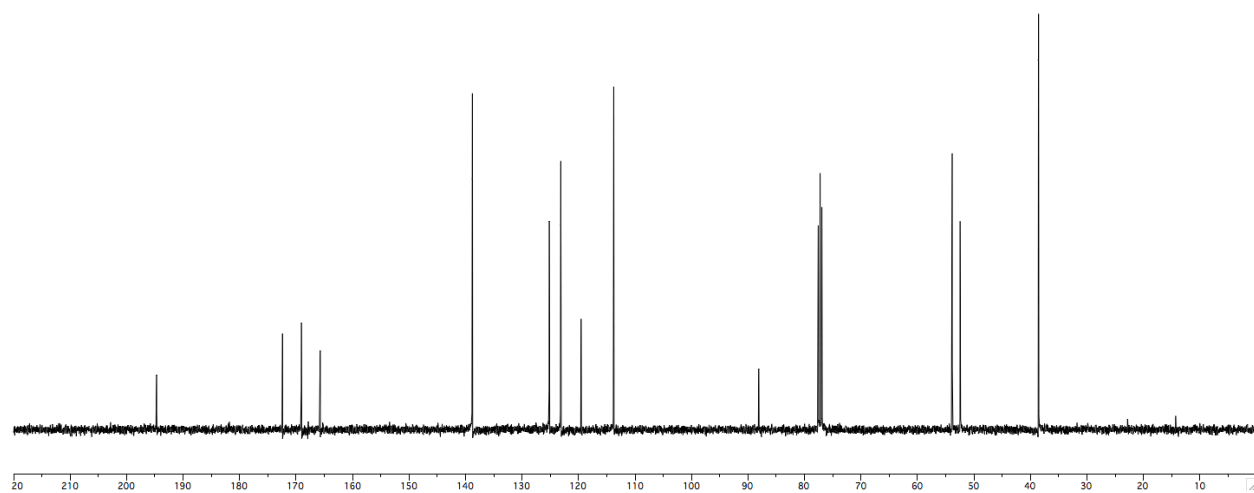
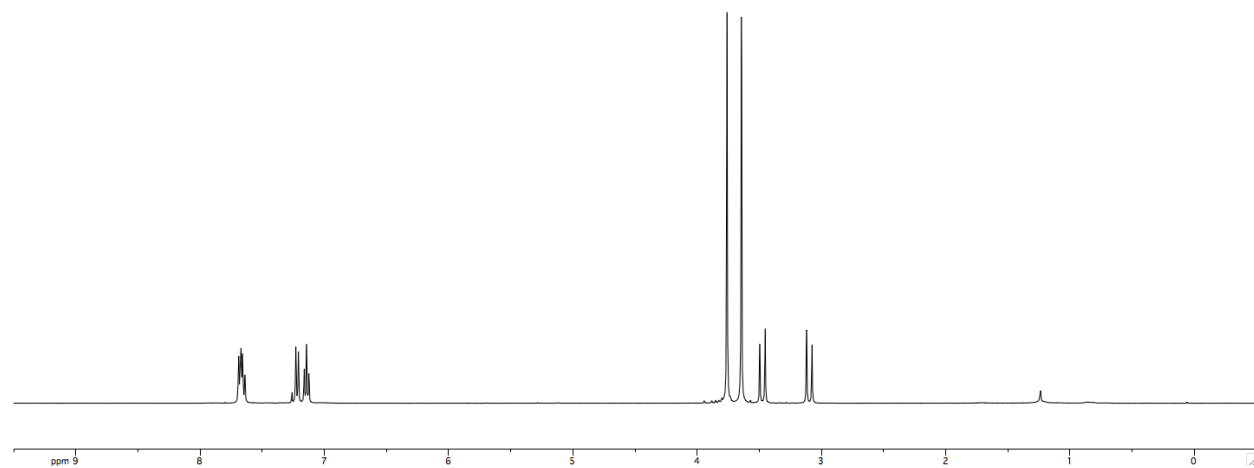
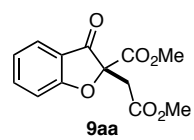
To a solution of the crude alcohol (473 mg, 2.15 mmol, 1.0 equiv) in DCM (11 mL) at 0 °C was added Dess–Martin Periodinane (DMP) (1.01 g, 2.38 mmol, 1.1 equiv) portion-wise. After stirring for 90 minutes at 0 °C and another 2 h at 23 °C, the reaction mixture was again cooled to 0 °C and another portion of DMP (275 mg, 0.650 mmol) was added. The reaction was placed in the fridge (-5 °C) overnight and then quenched with a 1:1 mixture of Na₂S₂O₃:NaHCO₃ (12 mL). The biphasic mixture was stirred until both layers cleared, at which point the organic layer was diluted with Et₂O, washed with H₂O and brine and dried over MgSO₄. Concentration and purification by flash column chromatography on silica gel gave 154 mg of **8c** (26% yield over two steps) as a white powder. *R*_f = 0.26 (7:2 Hex:EtOAc); ¹H NMR (400 MHz, CDCl₃) δ 8.08 (d, 2H, *J* = 9.0 Hz), 6.97 (d, 2H, *J* = 9.0 Hz), 3.90 (s, 3H), 3.88 (s, 3H); ¹³C NMR (100 MHz, CDCl₃) δ 174.6, 165.5, 153.0, 132.4, 129.2, 114.4, 80.5, 79.7, 55.9, 53.5; IR (Thin Film/NaCl) 2959, 1712, 1638, 1596, 1254 cm⁻¹; HRMS (ESI) *m/z* [C₁₂H₁₁O₄]⁺ ([M+H]⁺) calcd 219.0652, found 219.0653.

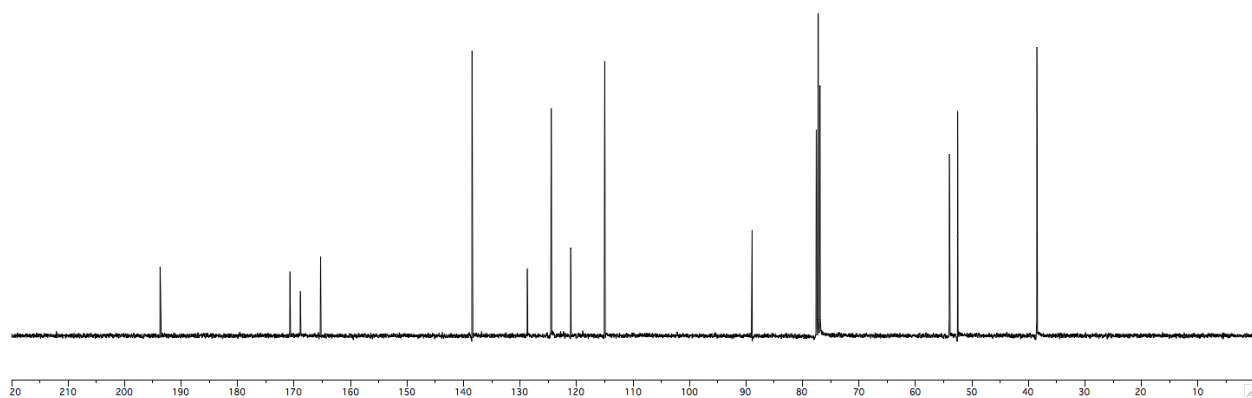
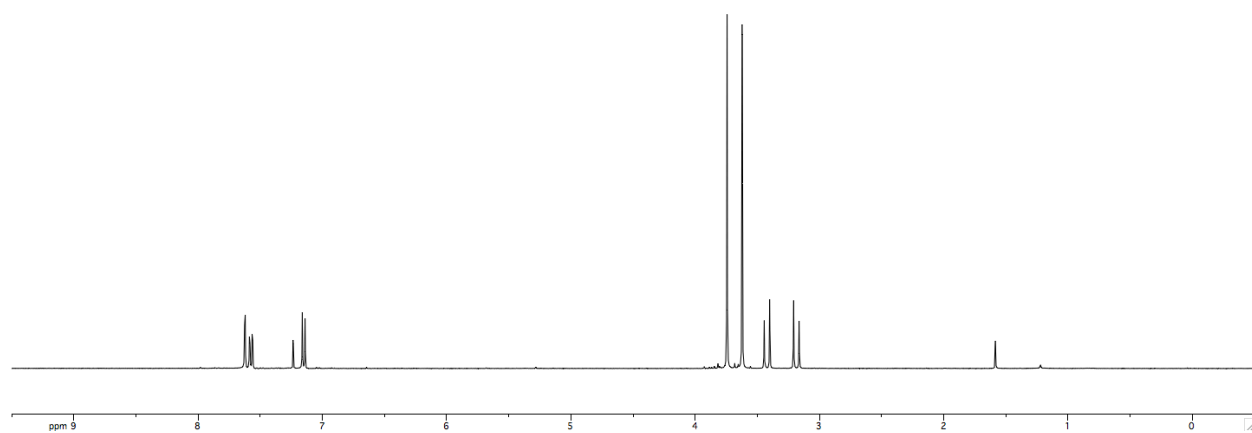
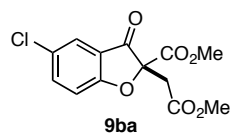


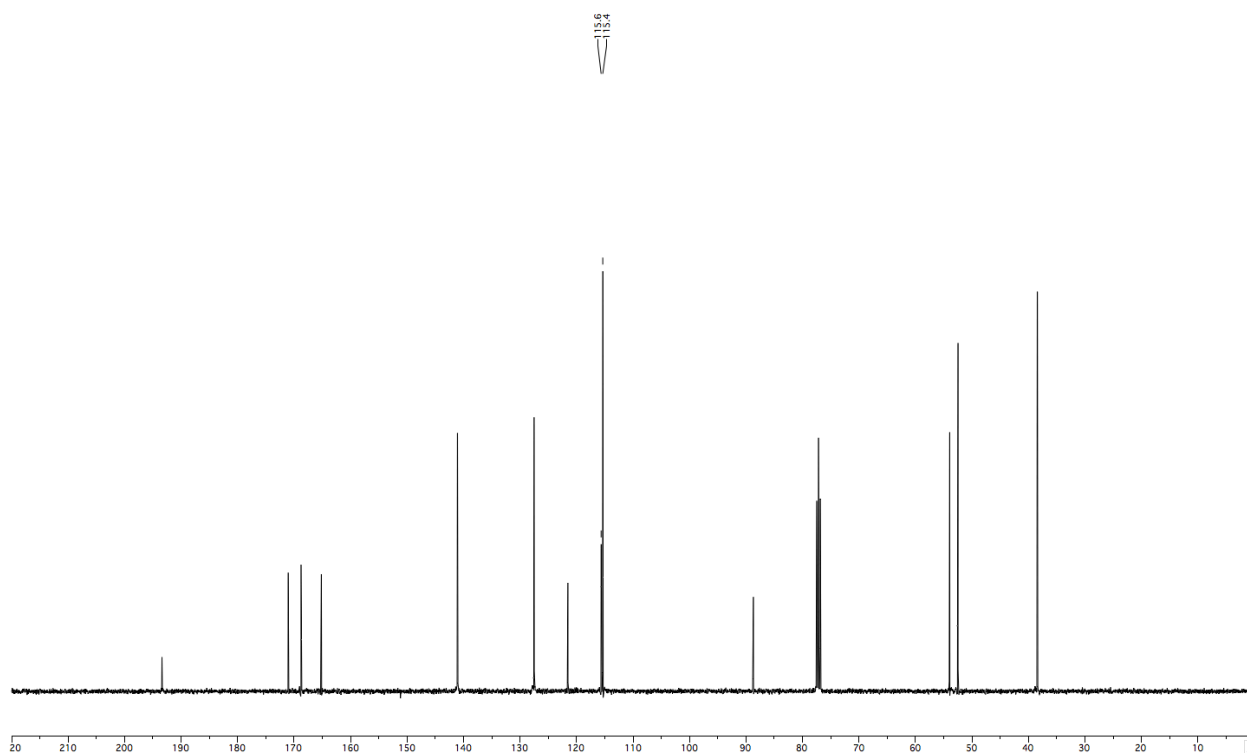
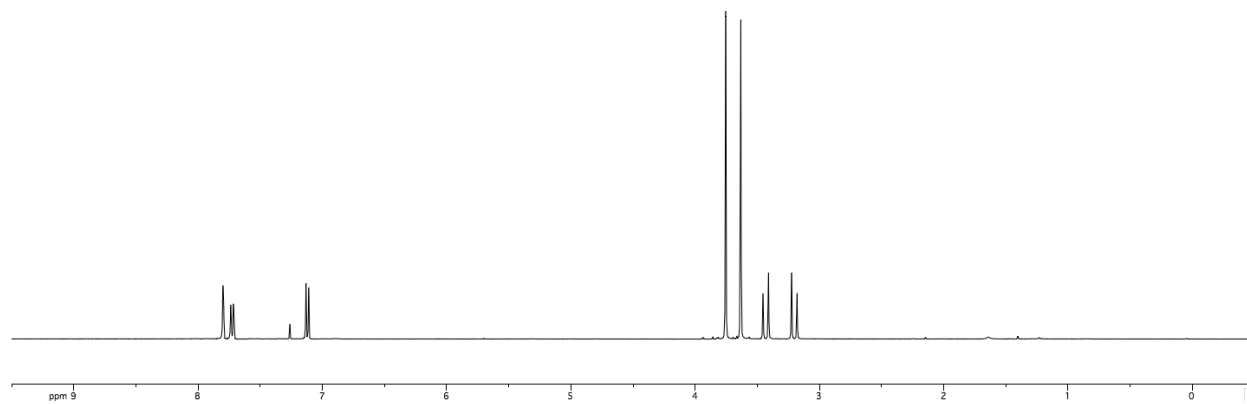
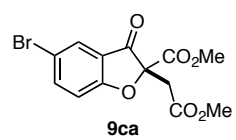
8d. To a solution of LiHMDS (2.55 g, 15.2 mmol, 1.2 equiv) in THF (30 mL) at -78°C was added ethyl propiolate (1.37 g, 13.9 mmol, 1.1 equiv) in THF (13 mL) over 30 minutes via

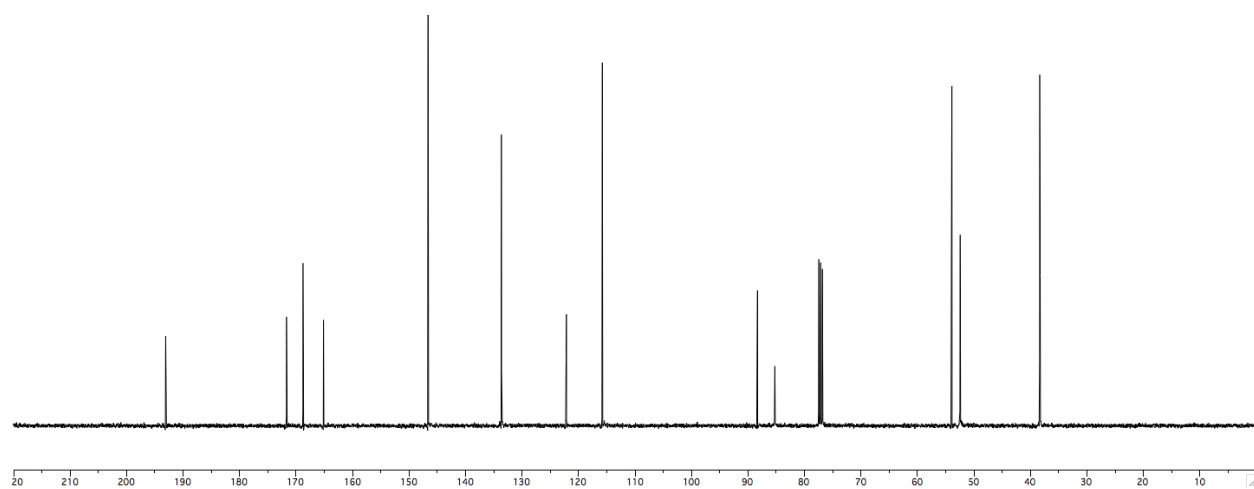
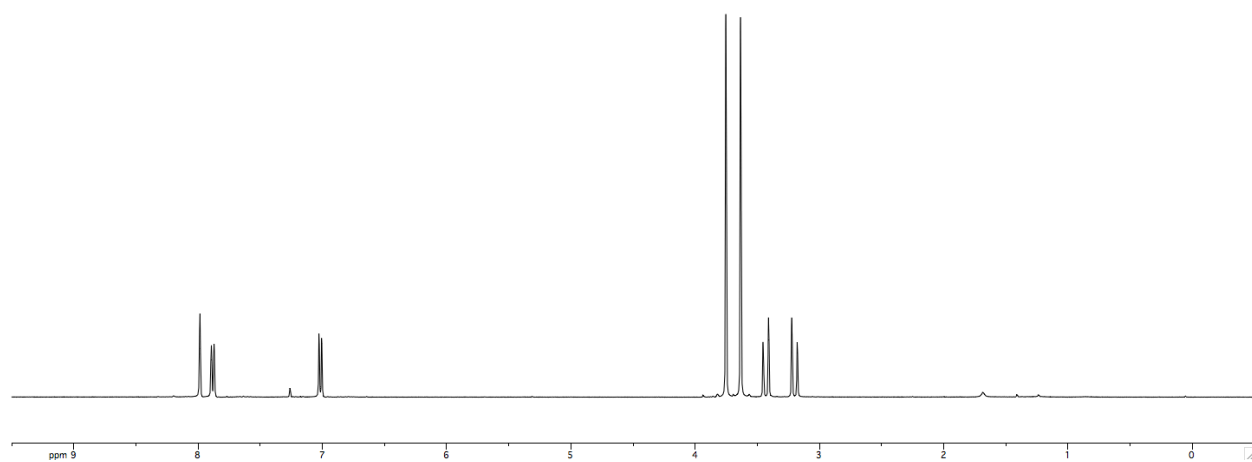
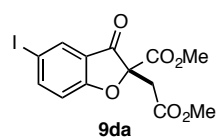
syringe pump. The resultant mixture was stirred for 30 minutes, at which point a solution of hydrocinnamaldehyde (1.70 g, 12.7 mmol, 1.0 equiv) in THF (6.0 mL) was added via syringe pump over 20 minutes. After an additional 45 minutes of stirring, the reaction mixture was quenched with saturated NH₄Cl and allowed to warm to room temperature. The organic layer was diluted with Et₂O, washed with NH₄Cl, H₂O and brine and dried over MgSO₄. Concentration and flash column chromatography on silica gel gave 1.81 g (62% yield) of the crude propargylic alcohol.

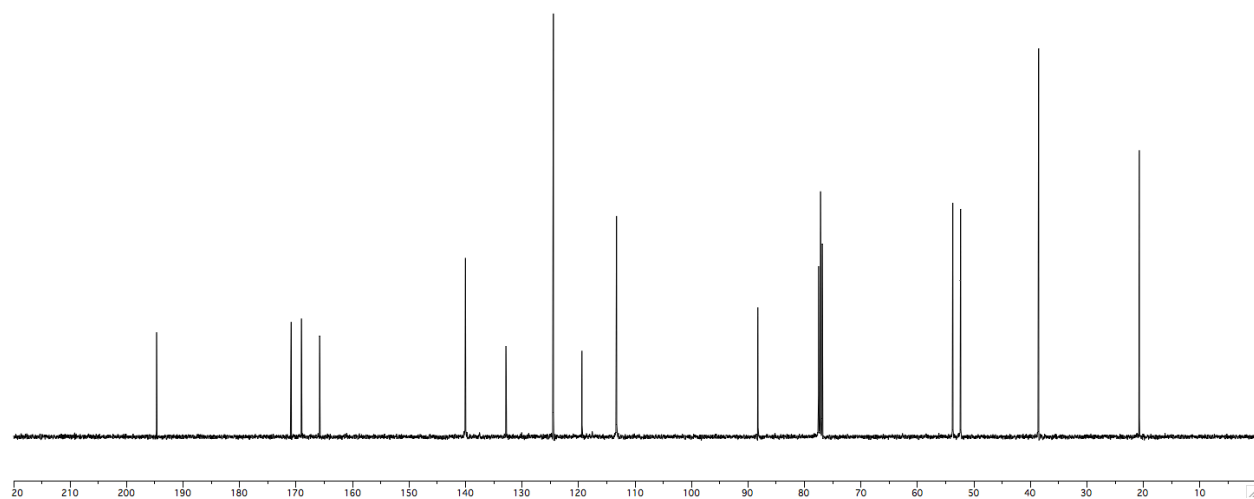
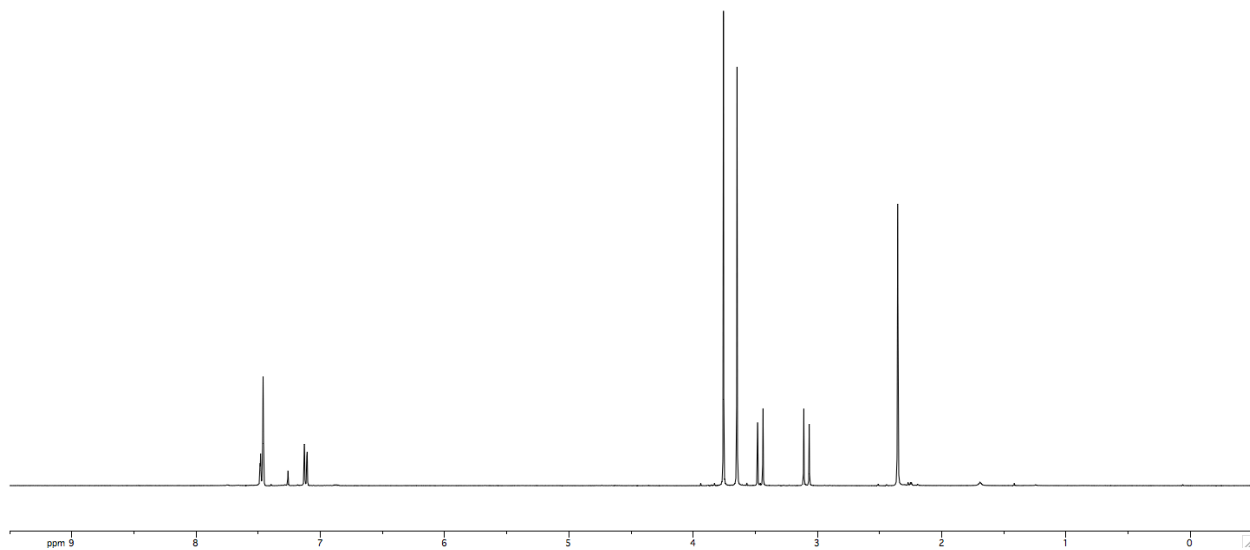
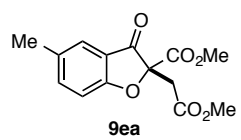
To a solution of the crude alcohol (465 mg, 2.00 mmol, 1.0 equiv) in DCM (10 mL) at 0 °C was added Dess–Martin Periodinane (DMP) (938 mg, 2.21 mmol, 1.1 equiv) portion-wise. The reaction was stirred for 3 h at 23 °C and then placed in the fridge (-5 °C) overnight. Another portion of DMP (155 mg, 0.365 mmol) was added at this point, and the reaction was allowed to stir for an additional 4 h at 23 °C before it was quenched with a 1:1 mixture of Na₂S₂O₃:NaHCO₃ (13 mL). The biphasic mixture was stirred until both layers cleared, at which point the organic layer was diluted with Et₂O, washed with H₂O and brine and dried over MgSO₄. Concentration and purification by flash column chromatography on silica gel gave 373 mg of **8d** (50% yield over two steps) as a clear oil. *R*_f = 0.48 (4:1 Hex:EtOAc); ¹H NMR (400 MHz, CDCl₃) δ 7.30 (m, 2H), 7.21 (m, 3H), 4.31 (q, 2H, *J* = 7.2 Hz), 2.99 (m, 4H), 1.34 (t, 3H, *J* = 7.2 Hz); ¹³C NMR (100 MHz, CDCl₃) δ 184.9, 152.2, 139.6, 128.7, 128.4, 126.6, 80.5, 78.6, 63.1, 46.8, 29.3, 14.0; IR (Thin Film/NaCl) 3029, 2985, 1721, 1689, 1496, 1244 cm⁻¹; LRMS (GC) *m/z* [C₁₄H₁₄O₃] ([M]⁺) calcd 230, found 230.

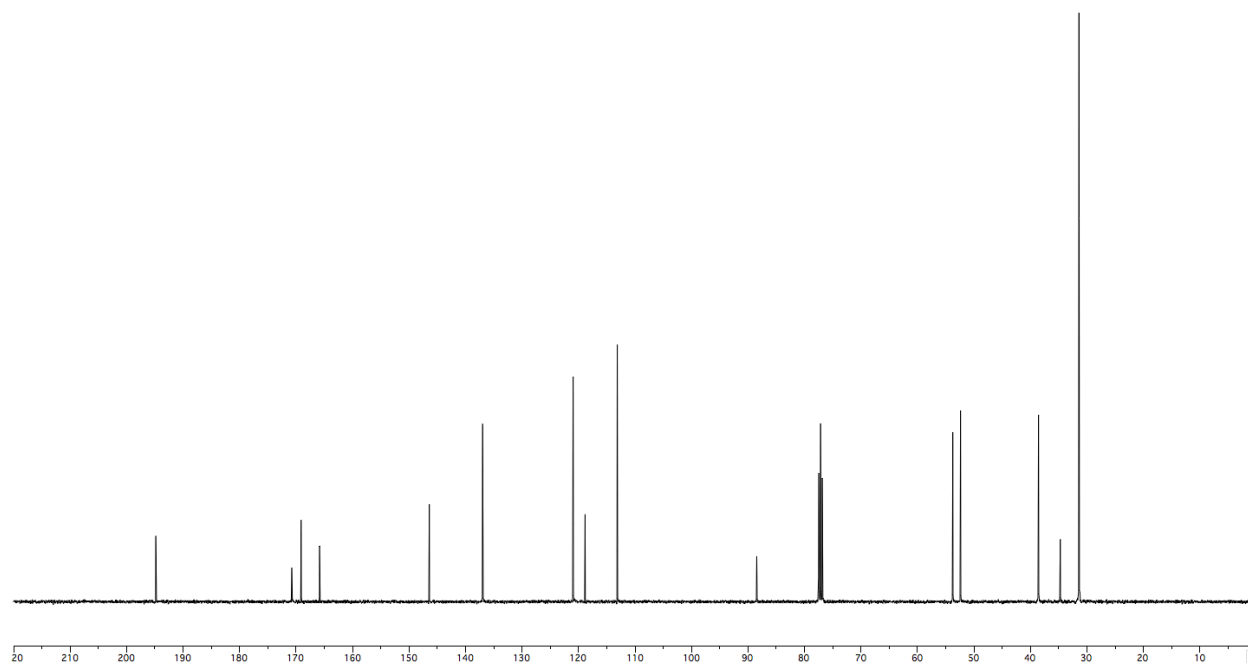
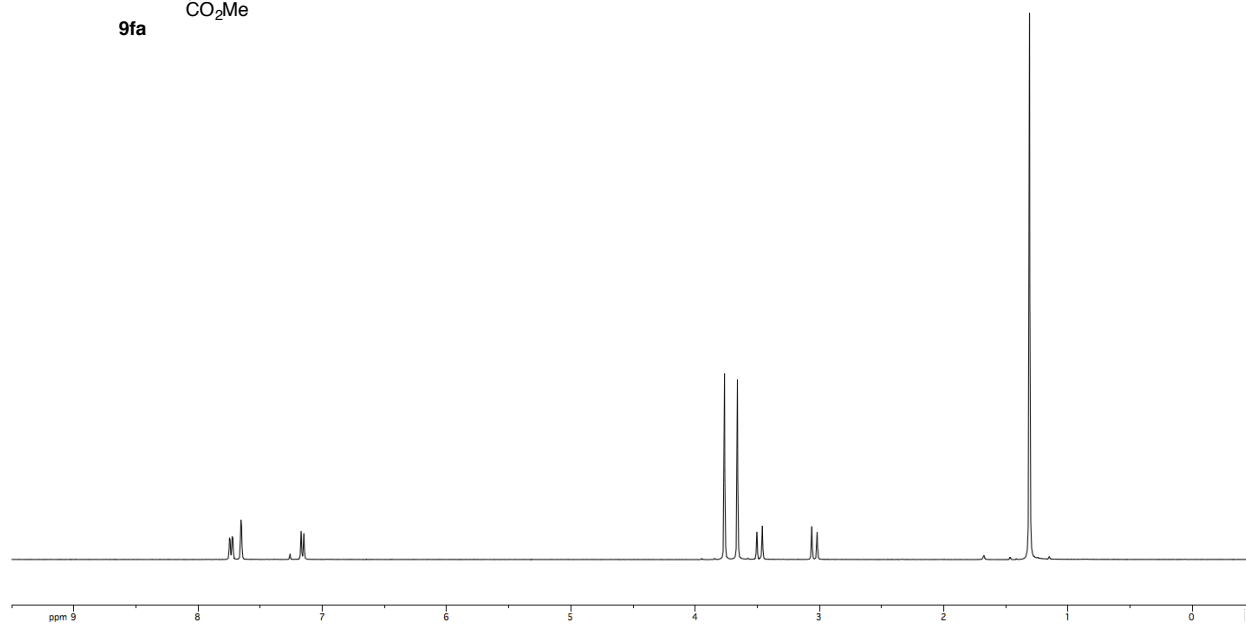
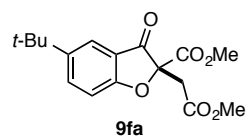


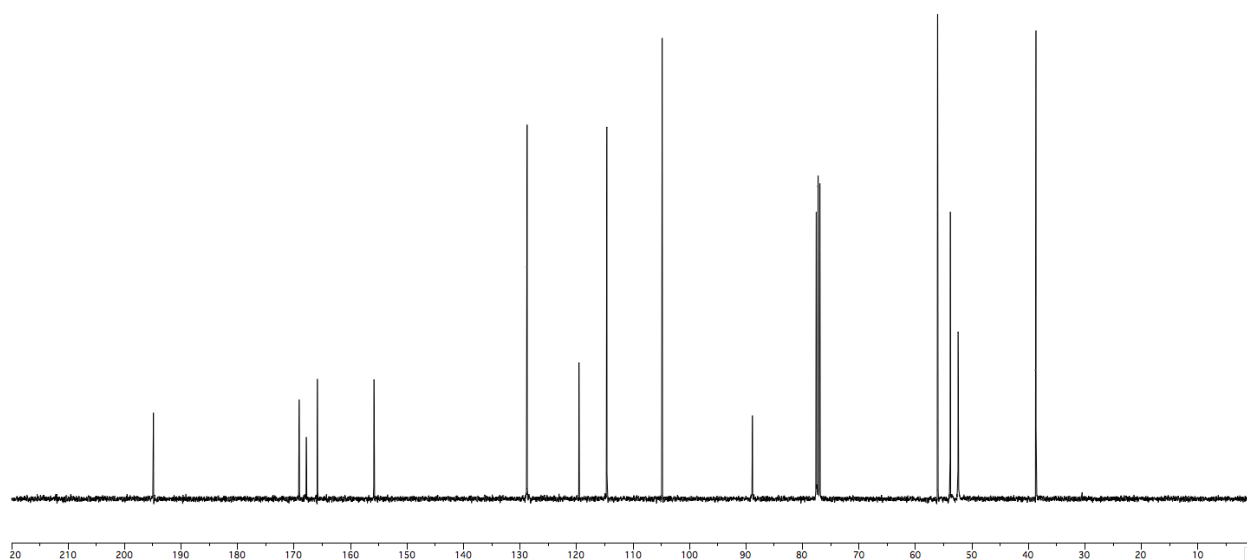
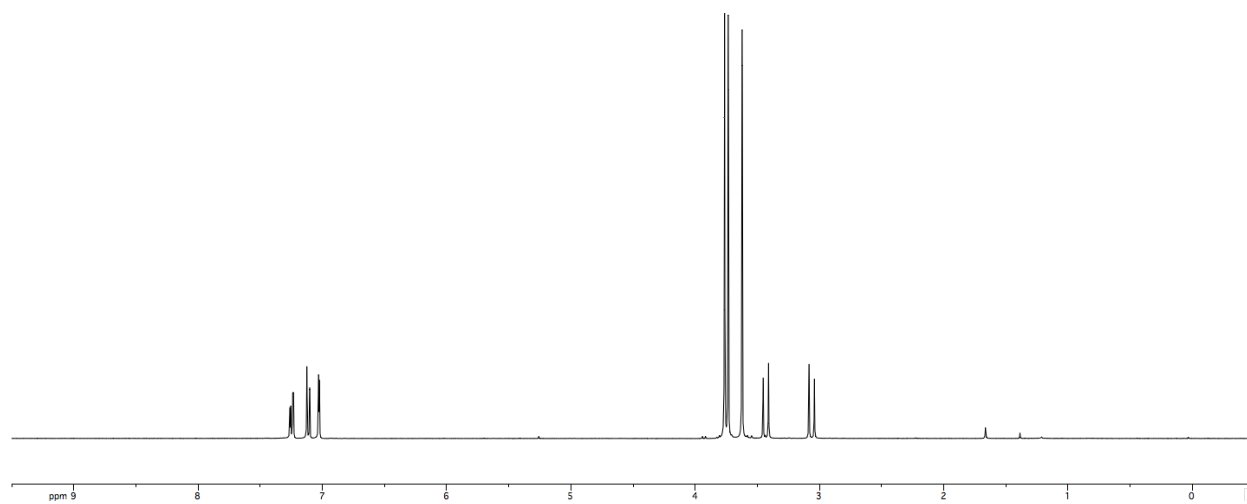
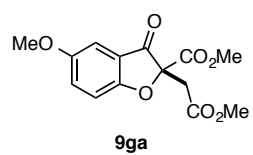


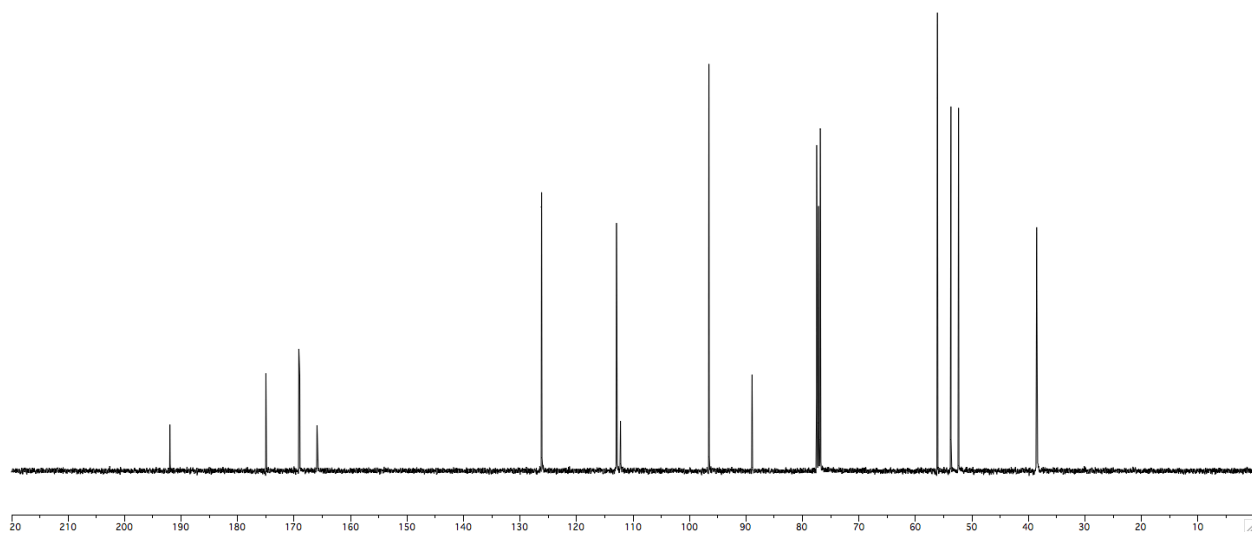
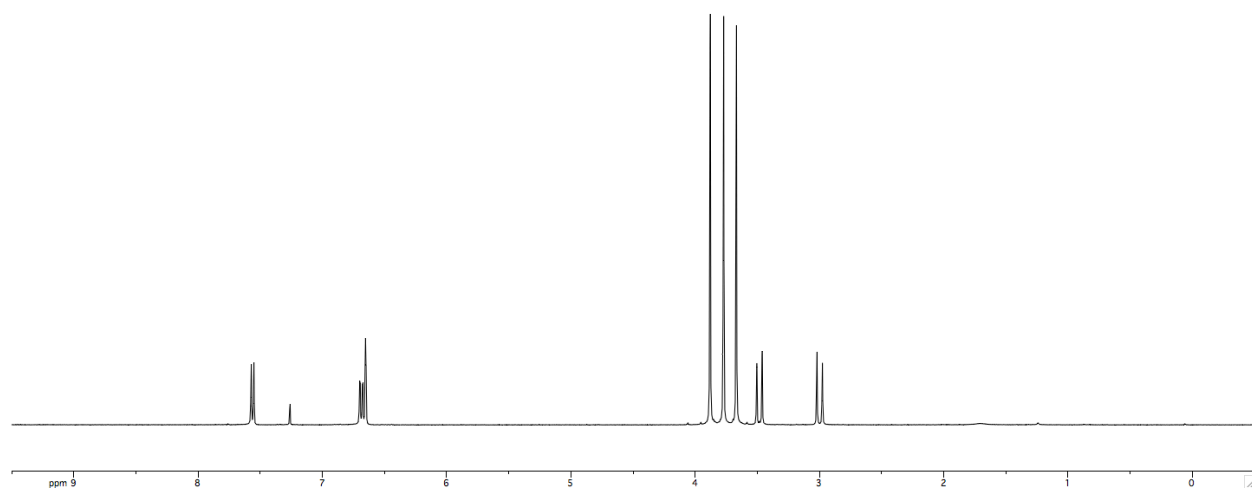
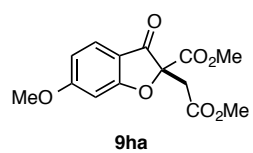


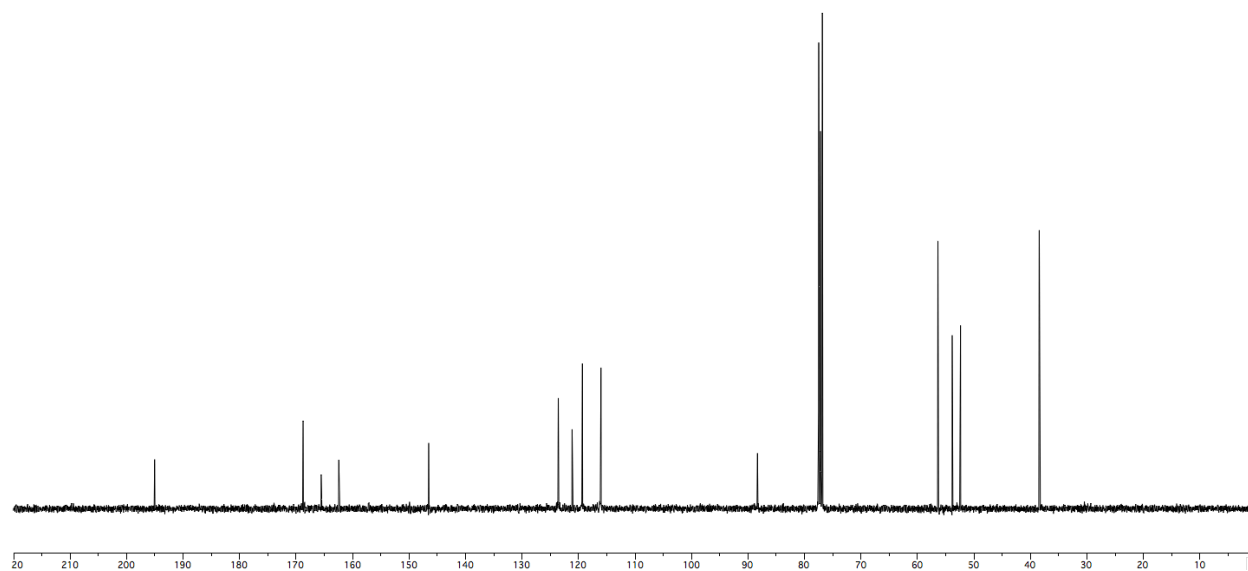
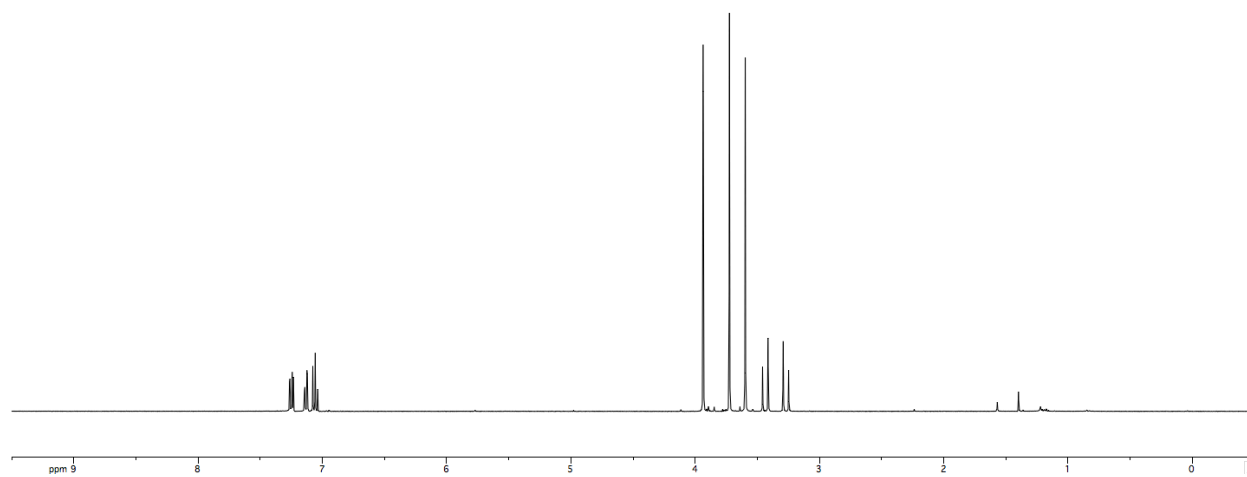
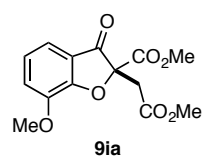


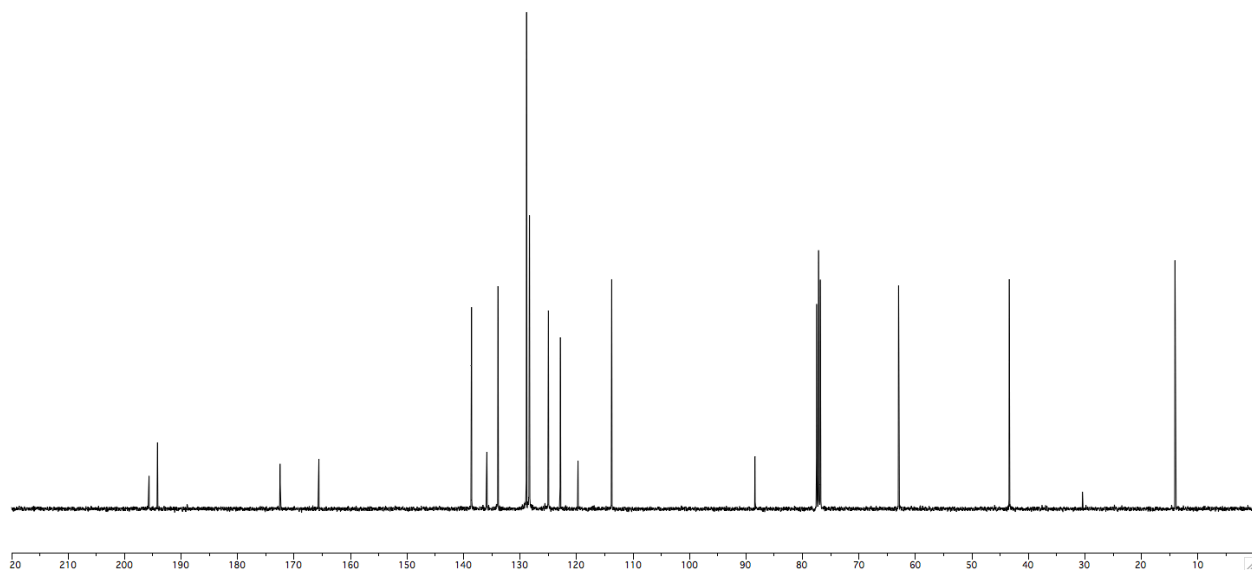
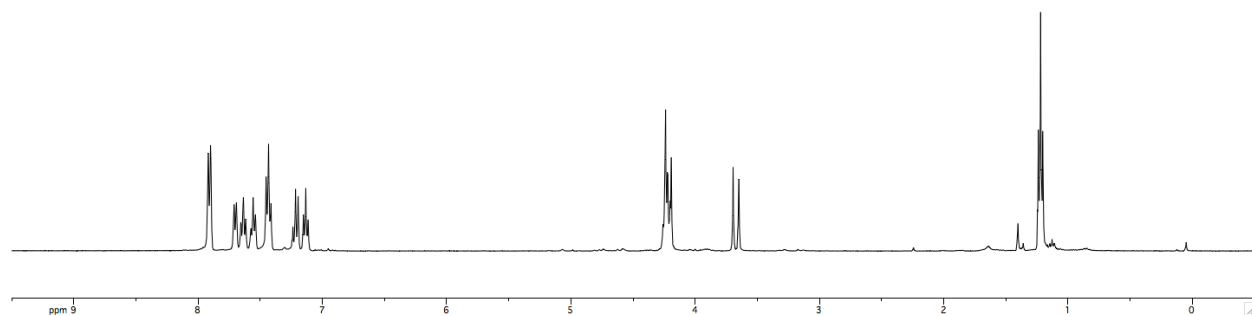
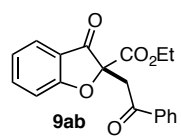


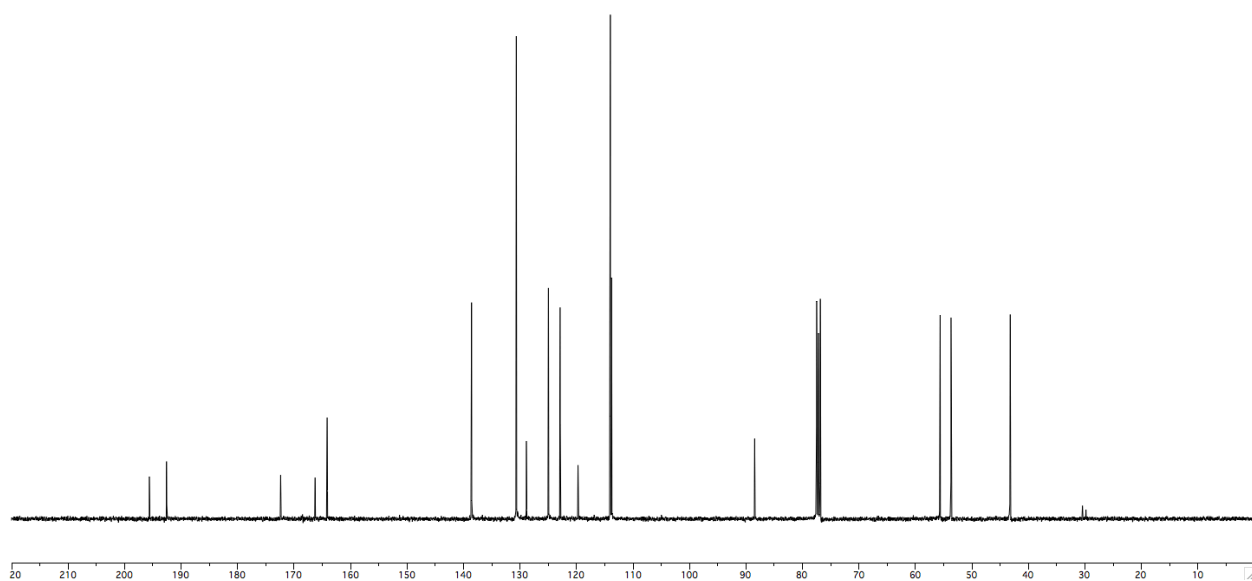
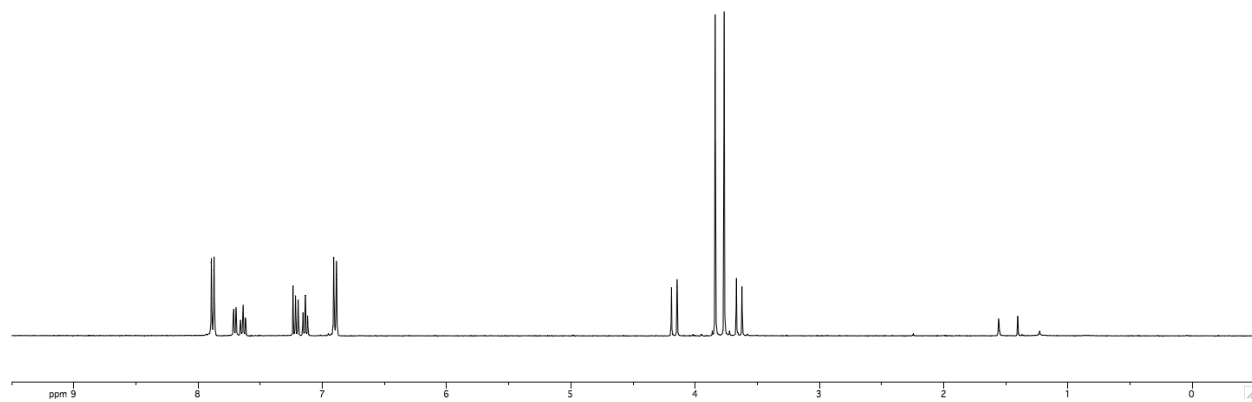
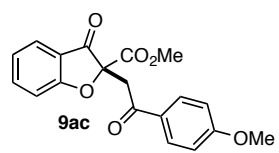


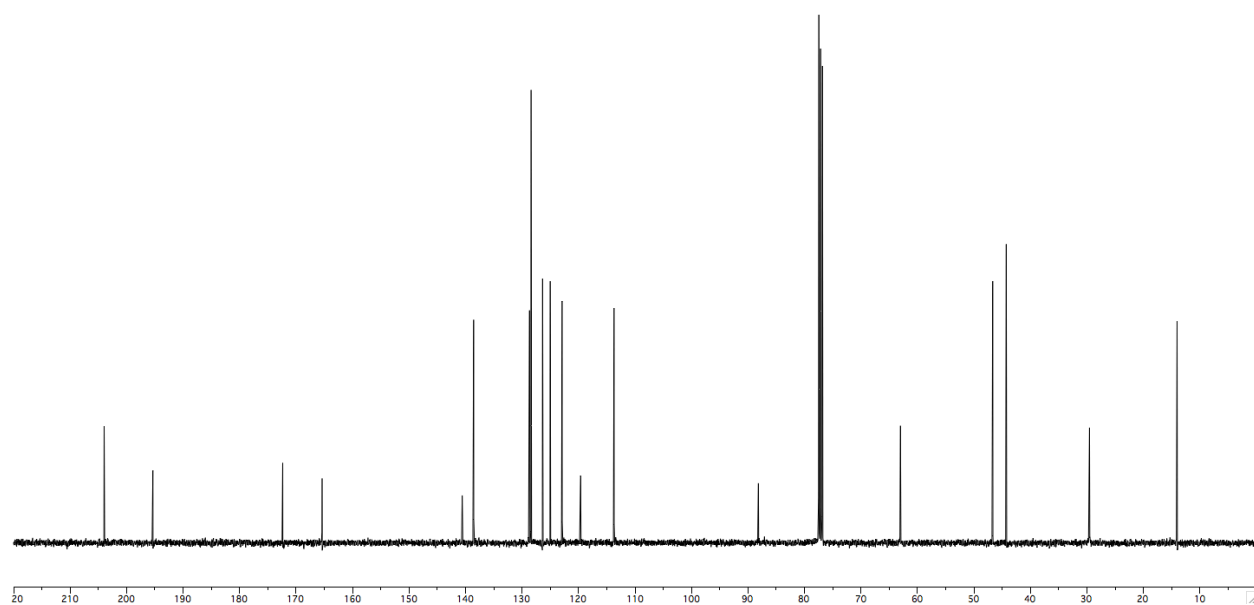
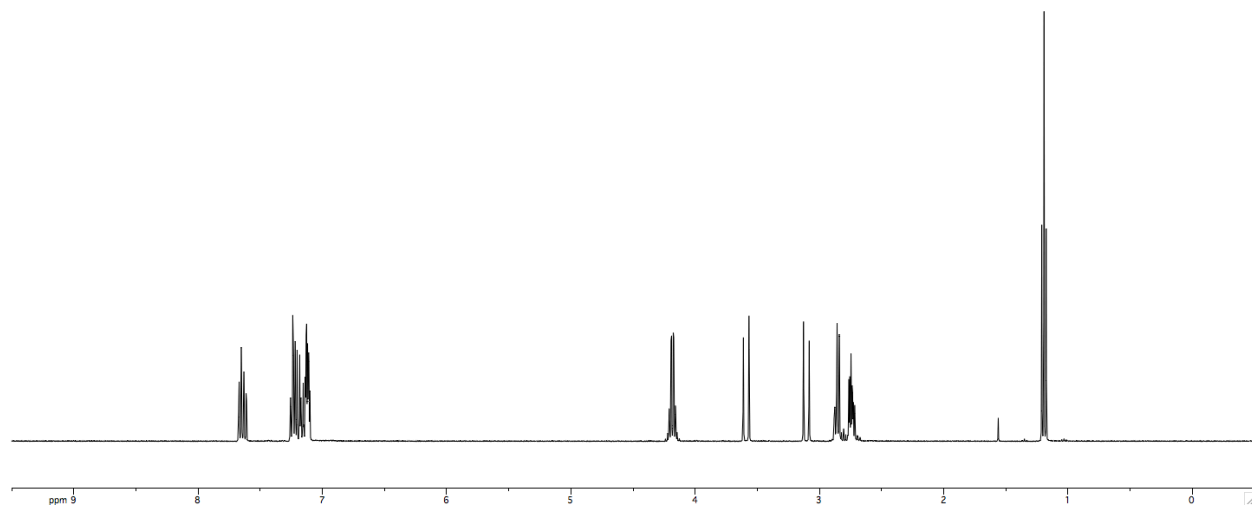
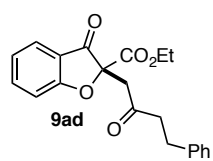


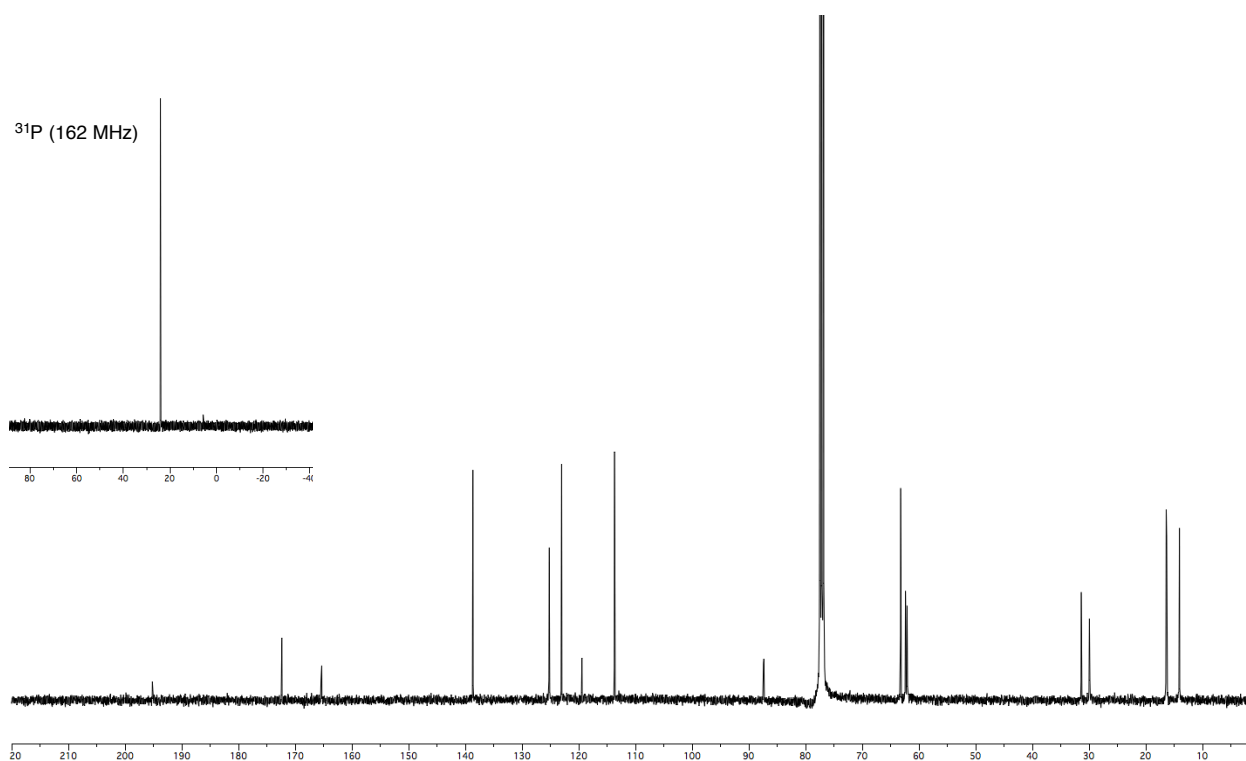
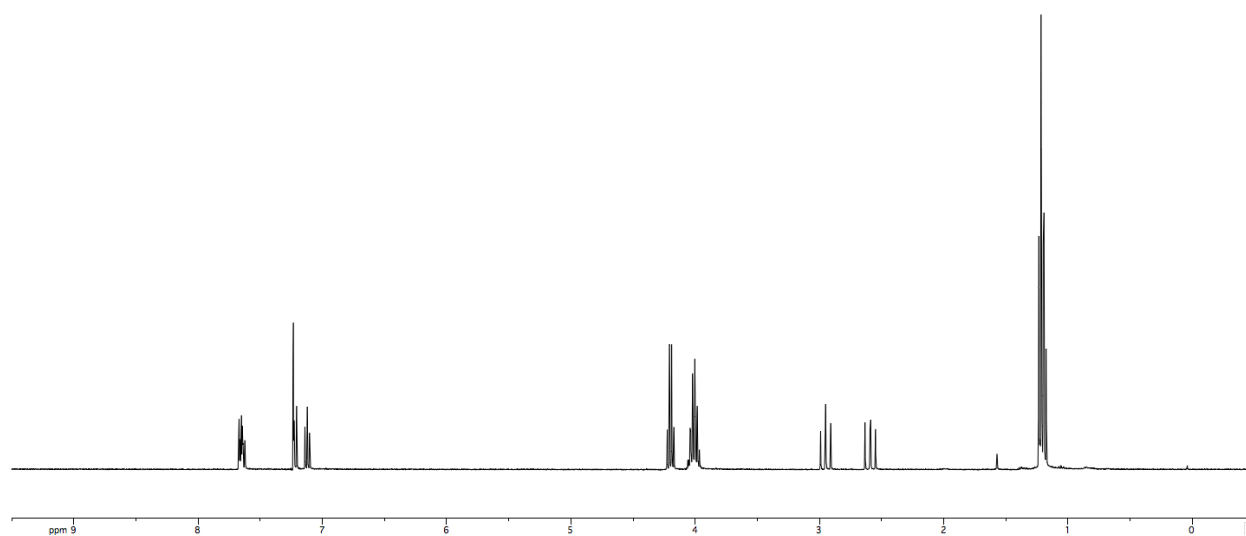
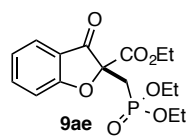


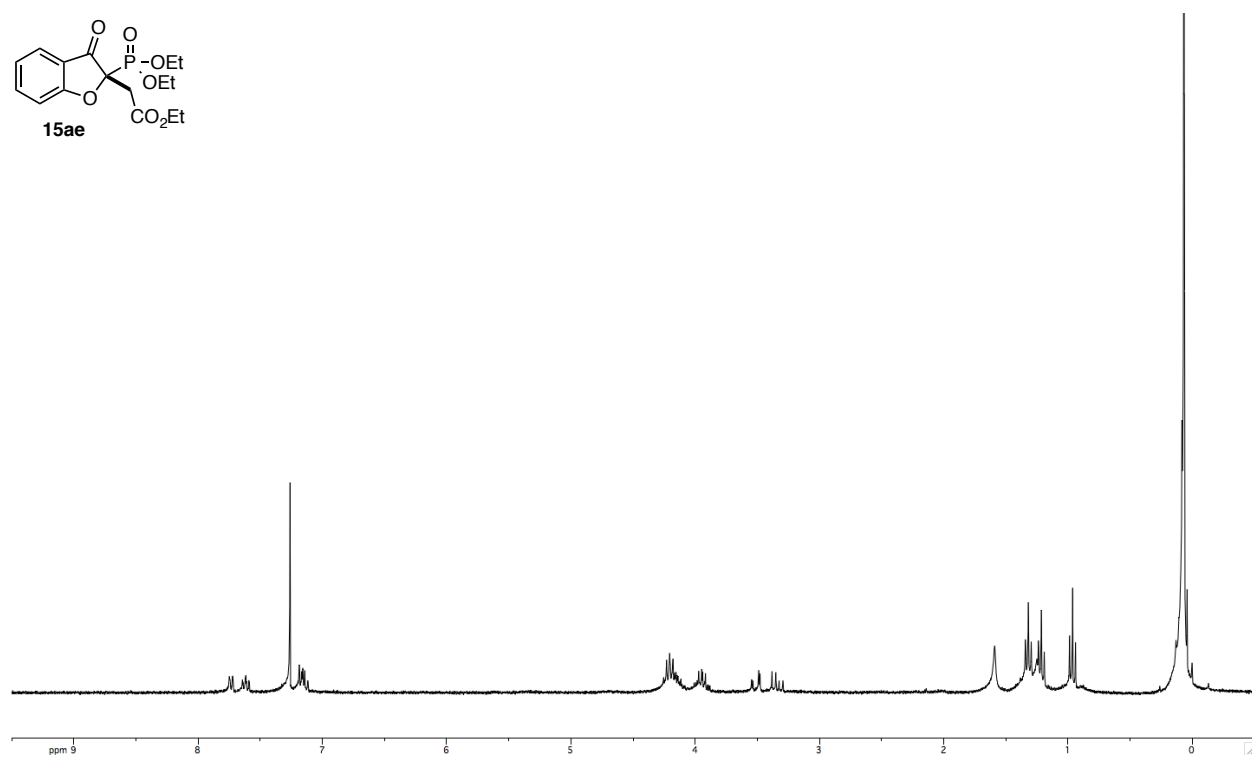
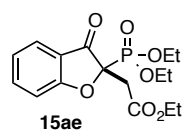
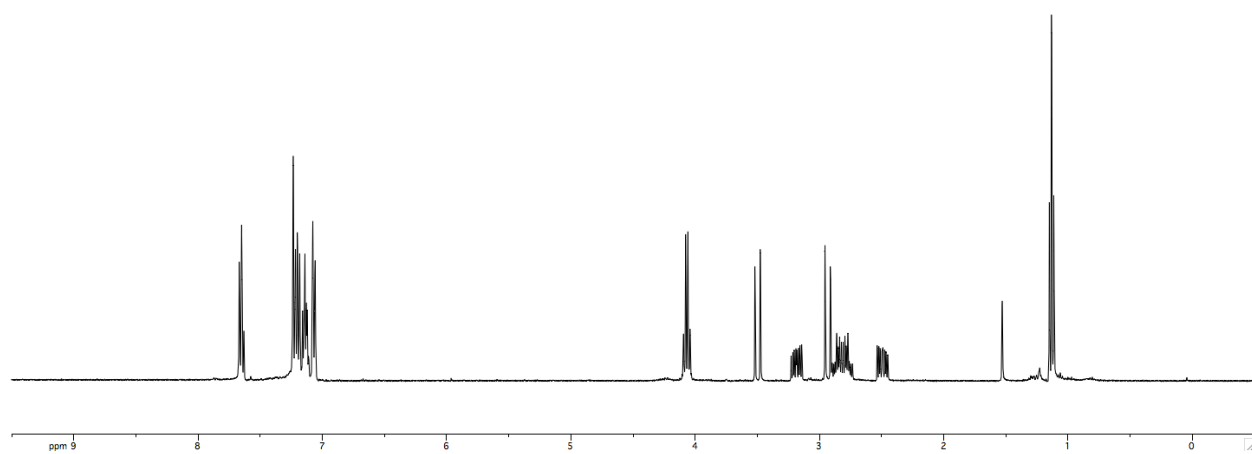
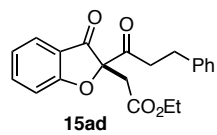


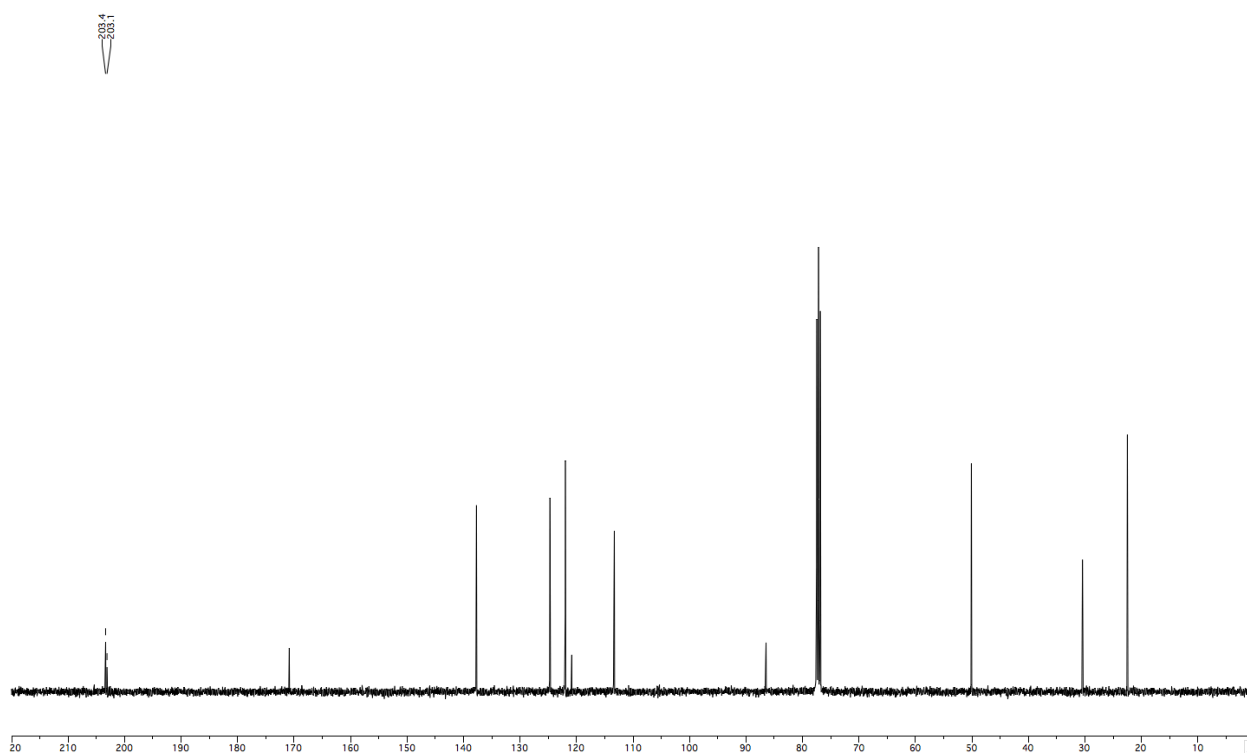
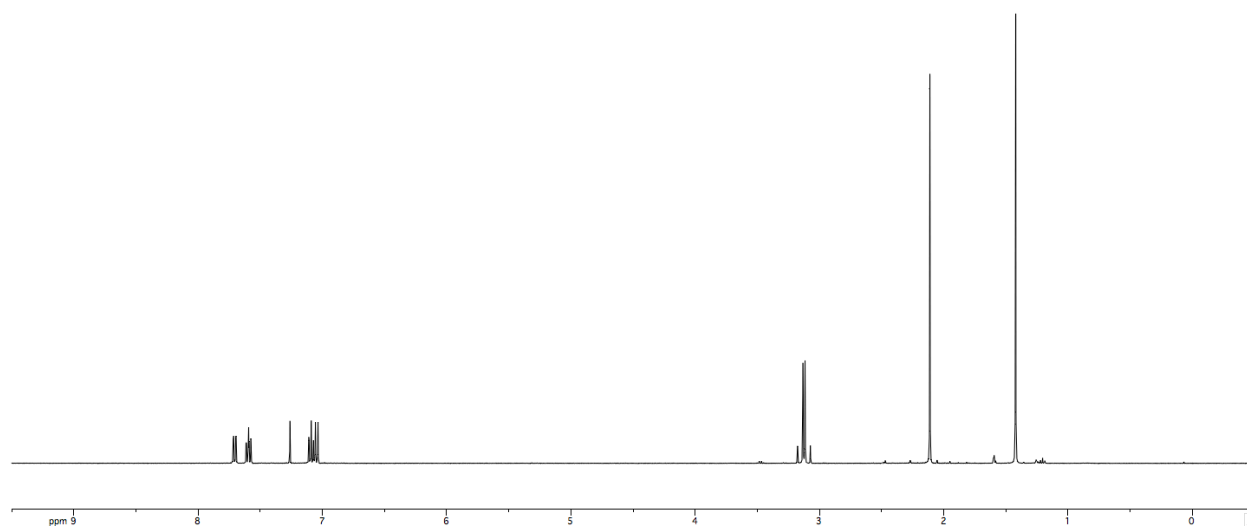
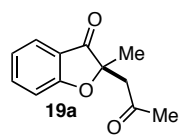


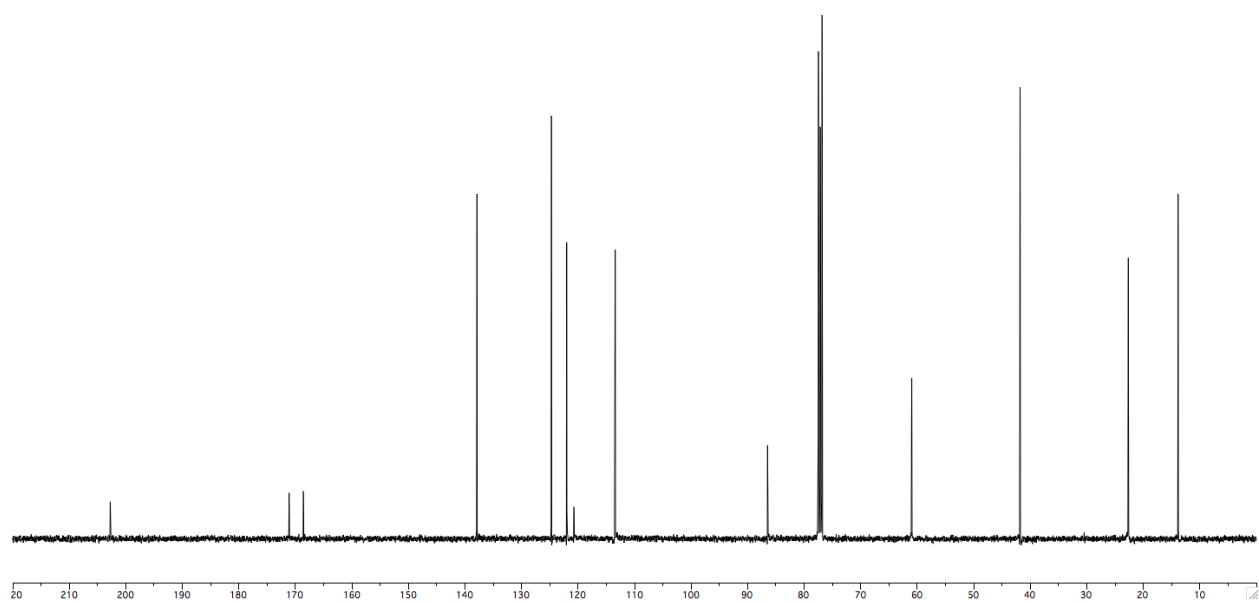
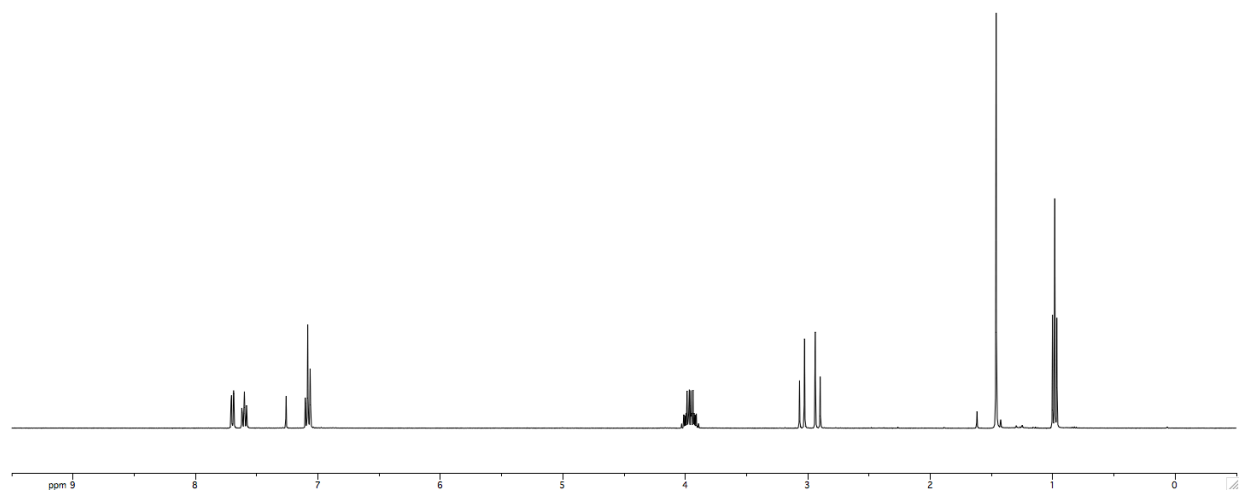
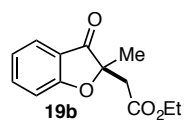












APPENDIX TWO

Rh(I)–Bisphosphine Catalyzed Asymmetric, Intermolecular Hydroheteroarylation of α -Substituted Acrylate Derivatives^[1]

A.2.1 Materials and Methods	72
A.2.2 Synthesis of [Rh(cod)OAc] ₂	73
A.2.3 Hydroheteroarylation (HH) of <i>tert</i> -butyl acrylate with azoles using [Rh(cod)OAc] ₂ (Chapter 2, Table 2.1, blue conditions).....	73
A.2.4 HH of <i>tert</i> -butyl acrylate with azoles using [Rh(cod)Cl] ₂ and CsOAc (Chapter 2, Table 2.1, red conditions)	74
A.2.5 HH yield determination by ¹ H NMR spectroscopy (Chapter 2, Table 2.1)	74
A.2.6 Characterization data for products 2a–2d (Chapter 2, Table 2.1).....	74
A.2.7 Synthesis of 1b-D (Chapter 2, eq. 10 and Figure 2.4a).....	75
A.2.8 C–H reversibility experiment between 1c and 1b-D (Chapter 2, eq. 10 and Figure 2.4a).....	76
A.2.8.1 Reaction set-up.....	76
A.2.8.2 Determination of percent conversion of 1b-D	76
A.2.8.3 Determination of percent ² H incorporation in products 2b and 2c	76
A.2.9 General procedure for the synthesis of benzoxazoles 1c–1d and 1f–1h	77
A.2.10 Characterization data for benzoxazoles 1c–1d and 1f–1h	78
A.2.11 Preparation of α -substituted acrylates 3g , 3h and 3j	79
A.2.12 Initial optimization of the asymmetric HH reaction of 4-methyl benzoxazole (1c) and ethyl methacrylate (3a) (Chapter 2, Table 2.2)	82
A.2.12.1 Reaction set-up.....	82
A.2.12.2 Analysis of the HH reaction of 4-methylbenzoxazole (1c) and ethyl methacrylate (3a) by chiral HPLC.	82

[1] This appendix has been adapted with permission from supporting information for Filloux, C. M.; Rovis, T. *J. Am. Chem. Soc.* **2015**, *137*, 508 – 517. Can be found online at: <http://pubs.acs.org/doi/suppl/10.1021/ja511445x>.

A.2.13 General procedure for second generation optimization of the asymmetric HH reaction of 4-methyl benzoxazole (1c) and ethyl methacrylate (3a) (Chapter 2, Table 2.3).....	84
A.2.14 General procedure for the asymmetric HH of methacrylate derivatives (3) with benzoxazoles (1) (Chapter 2, Table 2.4)	84
A.2.15 Comparison of reaction efficiency in presence or absence of CsOAc (Chapter 2, Table 2.4, 4cf and 4aa).....	85
A.2.16 Characterization data for products 4	85
A.2.17 Mechanistic experiments	90
A.2.17.1 Synthesis of 1c-D	90
A.2.17.2 Reaction of 1c-D and 3a in CH ₃ CN (Chapter 2, Figure 2.7, eq. 12)	91
A.2.17.3 Reaction of 1c-D and 3a in CD ₃ CN (Chapter 2, Figure 2.7, eq. 13)	92
A.2.17.4 Reaction of 1c and 3b-d₈ in CH ₃ CN (Chapter 2, Figure 2.7, eq. 14).....	93
A.2.17.5 Epimerization experiments (Chapter 2, Figure 2.9, eq. 15–17).....	94
A.2.17.5.1 General procedure	94
A.2.17.5.2 A note on HPLC retention times.....	95
A.2.17.5.3 A note on HPLC analysis of racemic mixtures.....	95
A.2.17.5.4 Reaction of 1c , 3a and 4ha (77% ee) (Chapter 2, Figure 2.9, eq. 15)	95
A.2.17.5.5 Reaction of 1c , 3a and 4ga (88% ee) (Chapter 2, Figure 2.9, eq. 16)	97
A.2.17.5.6 Reaction of 1c , 3c and 4ca (95% ee) (Chapter 2, Figure 2.9, eq. 17).....	99
A.2.17.6 Epimerization–labeling experiments of 4ha and 4ca in CD ₃ CN (Chapter 2, Figure 2.11, eq. 18–19).....	101
A.2.18 ¹ H NMR and ¹³ C NMR spectra of products 2 and 4	104
A.2.19 HPLC data for products 4 (see also A.2.17.5.2 and A.2.17.5.3).....	121
A.2.20 X-Ray crystal structure data for [Rh(cod)OAc] ₂	136

A.2.1 Materials and methods

Unless noted, all reactions were performed in flame-dried glassware and carried out under an atmosphere of argon with magnetic stirring. Tetrahydrofuran (THF), diethylether (Et₂O), and dichloromethane (DCM) were degassed with argon and passed through two columns of neutral alumina. Toluene was degassed with argon and passed through one column of neutral alumina and one column of Q5 reagent. Anhydrous acetonitrile was purchased in the Sure Seal® from Aldrich Chemical Company. Column chromatography was performed on SiliCycle® SilicaFlash® P60, 40-63 µm 60 Å and in general were performed according to the guidelines reported by Still et al.^[2] Thin layer chromatography was performed on SiliCycle® 250 µm 60 Å plates. Preparative thin layer chromatography was performed on SiliCycle® 2000 µm 60 Å plates. Visualization was accomplished with UV light or KMnO₄ stain followed by heating.

¹H NMR spectra were recorded on Varian 300 or 400 MHz spectrometers at ambient temperature unless otherwise stated. Data is reported as follows: chemical shift in parts per million (ppm) from CDCl₃ (7.26 ppm), toluene-d₈ (7.09, 7.0, 6.98, 2.09 ppm), multiplicity (s = singlet, bs = broad singlet, d = doublet, t = triplet, q = quartet, and m = multiplet), coupling constants (Hz). ¹³C NMR was recorded on Varian 300 or 400 MHz spectrometers (at 75 or 100 MHz) at ambient temperature. Chemical shifts are reported in ppm from CDCl₃ (77.2 ppm) or toluene-d₈ (137.86 (1), 129.4 (3), 128.33 (3), 125.49 (3), 20.4 (5) ppm). High-resolution mass spectra (ESI) were obtained by Donald Dick of Colorado State University.

[Rh(cod)Cl]₂ was purchased from Pressure Chemical Company. **L1–L11** were purchased from Strem Chemicals. CsOAc was purchased from commercial sources and dried at 60 °C over P₂O₅ under high vacuum overnight. *Tert*-butyl acrylate, **1a**, **1b**, **3a–3e** and **3i** were purchased from commercial sources, distilled off of stabilizers and stored over 3 Å molecular sieves. **3b–d₈** was purchased from Aldrich Chemical Company, distilled off of stabilizers and stored over 3 Å molecular sieves. 5-chlorobenzoxazole (**1e**) was purchased from AK Scientific. CD₃CN was purchased from Cambridge Isotope Laboratories and stored over 3 Å molecular sieves. 2-amino phenol starting materials for the synthesis of benzoxazoles **1c–1d**, **1f** and **1h** were purchased from AK Scientific. 2-amino-5-methoxyphenol hydrochloride (for the synthesis of **1g**) was purchased from Accela Chembio Inc. via Fisher Scientific. Teflon-lined screw caps were purchased from Fisher Scientific (03-340-14F).

[2] Still, W. C.; Kahn, M.; Mitra, A. *J. Org. Chem.* **1978**, *43*, 2923 – 2925.

A.2.2 Synthesis of $[\text{Rh}(\text{cod})\text{OAc}]_2$ ^[3]

$[\text{Rh}(\text{cod})\text{OAc}]_2$ was synthesized according to a procedure adapted from Chatt and Venanzi.^[3] A flame-dried 100 mL round-bottom flask was charged with $[\text{Rh}(\text{cod})\text{Cl}]_2$ (1.04 g, 2.11 mmol, 1 equiv) and KOAc (1.04 g, 10.6 mmol, 5.03 equiv), evaporated and backfilled with argon. Acetone (65 mL, freshly distilled over CaSO_4) was added and the reaction was heated at reflux for 6 h, at which point near complete conversion was observed by TLC (1:1 Hex:EtOAc, R_f $[\text{Rh}(\text{cod})\text{Cl}]_2$ = 0.60; R_f $[\text{Rh}(\text{cod})\text{OAc}]_2$ = 0.05, spots observed by UV and KMnO_4). An additional 1.03 g (4.98 equiv) KOAc was added, and the reaction was allowed to reflux overnight. At this point, the reaction was filtered through celite and rinsed with HPLC grade dichloromethane until all traces of orange had been washed from the celite. After concentration by rotary evaporation, the orange residue was recrystallized from HPLC grade EtOAc (~15 mL) to give $[\text{Rh}(\text{cod})\text{OAc}]_2$ as red orange plates (750 mg, 66% yield). The melting point was collected under air, and product decomposition was observed beginning at 182 °C (reported MP = 197–198 °C).^[3] The mother liquor was concentrated to a brown residue which was further recrystallized from HPLC grade EtOAc to give a second crop of $[\text{Rh}(\text{cod})\text{OAc}]_2$ (269 mg, 24%). R_f = 0.05 (1:1 Hex:EtOAc); IR (Thin Film/NaCl) 2998, 2984, 2945, 2867, 2838, 1573 (s), 1412 (s).

A.2.3 Hydroheteroarylation (HH) of *tert*-butyl acrylate with azoles using $[\text{Rh}(\text{cod})\text{OAc}]_2$ (Chapter 2, Table 2.1, *blue conditions*)

In a glove box, a 1-dram vial was equipped with a magnetic stirring bar and charged with $[\text{Rh}(\text{cod})\text{OAc}]_2$ (2.7 mg, 0.005 mmol, 2.0 mol %) and dppe (4.0 mg, 0.010 mmol, 4.0 mol %). To this was added a solution of heterocycle **1** (0.25 mmol, 1.0 equiv), *tert*-butyl acrylate (0.50 mmol, 2.0 equiv) and 1,3,5-trimethoxybenzene (4.2 mmol, 0.025 mmol, 0.10 equiv) in PhMe (Aldrich 244511, 500 μL). The vial containing the resultant yellow suspension was then sealed with a Teflon-lined screw cap, removed from the glove box and heated to 120 °C in an aluminum heating block. After several minutes at 120 °C, reactions turned a homogeneous orange or dark red (with **1b**). After 24 hours, the reactions were cooled to room temperature, concentrated, dissolved in CDCl_3 and analyzed by ^1H NMR spectroscopy (see section A.2.5).

[3] Chatt, J.; Venanzi, L. M. *J. Chem. Soc.* **1957**, 4735 – 4741.

A.2.4 Hydroheteroarylation (HH) of *tert*-butyl acrylate with azoles using [Rh(cod)Cl]₂ and CsOAc (Chapter 2,

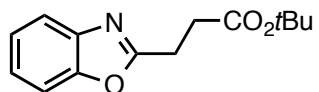
Table 2.1, red conditions)^[4]

In a glove box, a 1-dram vial was equipped with a magnetic stirring bar and charged with [Rh(cod)Cl]₂ (2.5 mg, 0.005 mmol, 2 mol %), dppe (4 mg, 0.010 mmol, 4 mol %) and CsOAc (12 mg, 0.06 mmol, 25 mol %). To this, was added a solution of heterocycle **1** (0.25 mmol, 1.0 equiv), *tert*-butyl acrylate (0.50 mmol, 2.0 equiv) and 1,3,5-trimethoxybenzene (4.20 mg, 0.025 mmol, 0.10 equiv) in PhMe (Aldrich 244511, 500 μ L). The vial containing the resultant yellow suspension was then sealed with a teflon-lined screw cap, removed from the glove box and heated to 120 °C in an aluminum heating block. After several minutes at 120 °C, the reactions turned a heterogeneous orange or dark red (with **1b**). After 24 hours, the reactions were cooled to room temperature, concentrated, dissolved in CDCl₃ and analyzed by ¹H NMR spectroscopy (see section A.2.5). Particularly heterogeneous reactions were filtered through celite into the NMR tube prior to analysis.

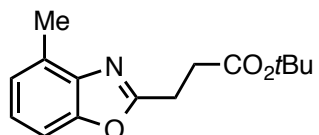
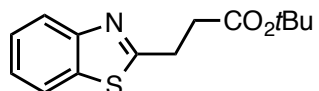
A.2.5 Hydroheteroarylation yield determination by ¹H NMR spectroscopy (Chapter 2, Table 2.1)

For accurate integration, 4 scans were collected, and d₁ was set to 45 seconds to ensure complete relaxation of aryl resonances. All yields were determined relative to the H₃CO-resonance of 1,3,5-trimethoxybenzene at 3.77 ppm.

A.2.6 Characterization data for products 2a–2d (Chapter 2, Table 2.1)



2a. For characterization, two representative reactions were combined and purified by preparative thin layer chromatography (3:1 Hex:Acetone) to give **2a** as a colorless oil. R_f = 0.50 (3:1 Hex:Acetone); ¹H NMR (300 MHz, CDCl₃) δ 7.62-7.68 (m, 1H), 7.43-7.50 (m, 1H), 7.26-7.31 (m, 2H), 3.20 (t, 2H, *J* = 7.5 Hz), 2.84 (t, 2H, *J* = 7.5 Hz), 1.42 (s, 9H); ¹³C NMR (75 MHz, CDCl₃) δ 171.1, 165.9, 150.9, 141.3, 124.7, 124.2, 119.7, 110.4, 81.1, 32.1, 28.1, 24.2; IR (Thin Film/NaCl) 2979, 2933, 1731, 1616, 1574 cm⁻¹; LRMS (EI) *m/z* [C₁₄H₁₇NO₃] ([M]⁺) calcd 247, found 247.

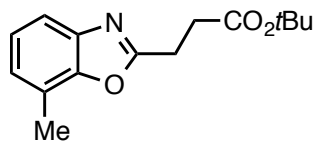


2b. Characterization data for **2b** match that reported in the literature.^[4]

2c. Flash column chromatography on silica gel (10:1 Hex:EtOAc) gave **2c** as a colorless oil (87%). R_f = 0.26 (10:1 Hex:EtOAc); ¹H NMR (400 MHz, CDCl₃) δ 7.29

[4] Ryu, J.; Cho, S. H.; Chang, S. *Angew. Chem. Int. Ed.* **2012**, 51, 3677 – 3681.

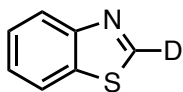
(d, 1H, $J = 8.0$ Hz), 7.17 (t, 1H, $J = 8.0$ Hz), 7.09 (d, 1H, $J = 7.2$ Hz), 3.21 (t, 2H, $J = 7.4$ Hz), 2.83 (t, 2H, $J = 7.4$ Hz), 2.58 (s, 3H), 1.45 (s, 9H); ^{13}C NMR (100 MHz, CDCl_3) δ 171.2, 165.0, 150.7, 140.6, 130.1, 124.8, 124.3, 107.7, 81.1, 32.4, 28.2, 24.4, 16.6; IR (Thin Film/NaCl) 2978, 1731, 1150 cm^{-1} ; LRMS (EI) m/z [$\text{C}_{15}\text{H}_{19}\text{NO}_3$] ($[\text{M}]^+$) calcd 261, found 261.



2d. For characterization, two representative reactions were combined and purified by preparative thin layer chromatography (2% EtOAc in DCM) to give **3d** as a colorless oil. This was found to be the best purification method on small scale as the product is

difficult to separate from residual starting material. $R_f = 0.35$ (98:2 DCM:EtOAc); ^1H NMR (400 MHz, CDCl_3) δ 7.47 (d, 1H, $J = 7.6$ Hz), 7.18 (t, 1H, $J = 7.6$ Hz), 7.08 (d, 1H, $J = 7.6$ Hz), 3.21 (t, 2H, $J = 7.6$ Hz), 2.85 (t, 2H, $J = 7.6$ Hz), 2.50 (s, 3H), 1.44 (s, 9H); ^{13}C NMR (100 MHz, CDCl_3) δ 171.2, 165.6, 150.2, 141.0, 125.7, 124.2, 121.0, 117.0, 81.1, 32.2, 28.2, 24.3, 15.3; IR (ATR) 2978, 2929, 1729, 1612, 1574, 1141 cm^{-1} ; LRMS (ESI+APCI) m/z [$\text{C}_{15}\text{H}_{20}\text{NO}_3$] $^+$ ($[\text{M}+\text{H}]^+$) calcd 262.0, found 262.1.

A.2.7 Synthesis of **1b-D** (Chapter 2, eq. 10 and Figure 2.4a)



1b-D. To a solution of benzothiazole (**1b**) (250 mg, 1.85 mmol, 1.0 equiv) in THF (15 mL) at -78 $^\circ\text{C}$ was added *tert*-butyl lithium (2.0 mL, 1.4 M in pentane, 2.8 mmol, 1.5 equiv) via syringe pump over 1 hour. An instantaneous color change from clear to yellow was observed. The reaction mixture was stirred for an additional 30 minutes at -78 $^\circ\text{C}$, and then MeOH-d_4 (1.5 mL) was added dropwise at -78 $^\circ\text{C}$. The reaction mixture was adsorbed onto silica gel and purified by flash column chromatography (7:1 Hex:EtOAc) to give 42 mg (0.31 mmol, 16%) **1b-D** as a light yellow oil: $R_f = 0.22$ (5:1 Hex:EtOAc); ^1H NMR (300 MHz, CDCl_3) δ 8.13-8.16 (m, 1H), 7.95-7.98 (m, 1H), 7.42-7.55 (m, 2H) (Less than 1% ^1H observed at δ 9.00) (Figure A.2.1); ^2H NMR (300 MHz, PhMe-d_8) δ 8.23 (s) (see Chapter 2, Figure 2.4a). *Note: the azole C-H resonance appears at $\delta = 9.00$ ppm in CDCl_3 and at $\delta = 8.23$ ppm in PhMe-d_8 .*

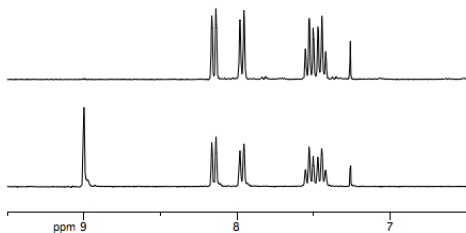


Figure A.2.1 ^1H NMR of **1b-D** (top) and **1b** (bottom) in CDCl_3

A.2.8 C–H reversibility experiment between **1c** and **1b-D** (Chapter 2, eq. 10 and Figure 2.4a)

A.2.8.1 Reaction set-up

[Rh(cod)OAc]₂ (3.2 mg, 0.006 mmol, 4.0 mol %) and dppe (4.8 mg, 0.012 mmol, 8.0 mol %) were weighed into a J. Young tube in the glove box. To this was added a solution of **1c** (20 mg, 0.15 mmol, 1.0 equiv) and *tert*-butyl acrylate (88 μ L, 0.60 mmol, 4.0 equiv) in 480 μ L PhMe and 120 μ L of a solution of **1b-D** (42 mg, 0.31 mmol) and 1,3,5-trimethoxybenzene (8.2 mg, 0.05 mmol) in 200 μ L PhMe. The J. Young tube was sealed and removed from the box. ¹H NMR analysis (300 MHz) of the reaction mixture prior to heating showed no ¹H resonance at δ = 8.36 ppm, and ²H NMR showed a corresponding single ²H resonance at δ = 8.23 ppm. The NMR tube was suspended in a 120 °C oil bath, and the reaction was removed periodically for ¹H and ²H NMR analysis (300 MHz). Crossover peaks for **1b-H** and **1c-D** began to populate the ¹H and ²H spectra over time (see Chapter 2, Figure 2.4a).

A.2.8.2 Determination of percent conversion of **1b-D**

Percent conversion of **1b-D** was approximated by comparing the integration values in the ¹H NMR for the aromatic resonance of starting material **1b-D** at δ = 8.00 (J = 8.1 Hz) with the corresponding aromatic resonance of product **2b** at δ = 7.87 (J = 8.7 Hz) (Figure A.2.2).

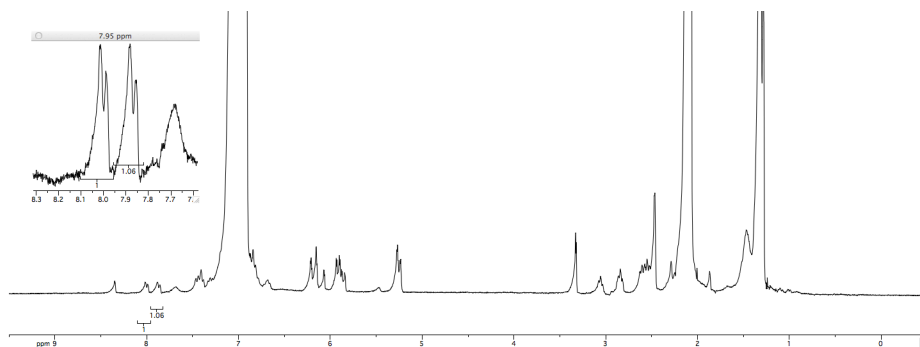


Figure A.2.2 ¹H NMR of eq. 10 (Chapter 2) after 130 h at 120 °C. Percent conversion of **1b-D** was determined by comparison of integration values for starting material **1b-D** at δ = 8.00 (J = 8.1 Hz) with the corresponding aromatic resonance of product **2b** at δ = 7.87 (J = 8.7 Hz)

A.2.8.3 Determination of percent ²H incorporation in products **2b** and **2c**

The crude reaction mixture from the reversibility experiment was concentrated, dissolved in dichloromethane and pipetted onto a preparative TLC. Preparative TLC (2 x 13:1 Hex:Acetone) allowed fairly clean separation of **2b** (contaminated with **1b**) and **2c** (contaminated with some **2b**). ²H incorporation was determined by ¹H NMR analysis of fairly pure **2b** and **2c** (Figure A.2.3 and A.2.4).

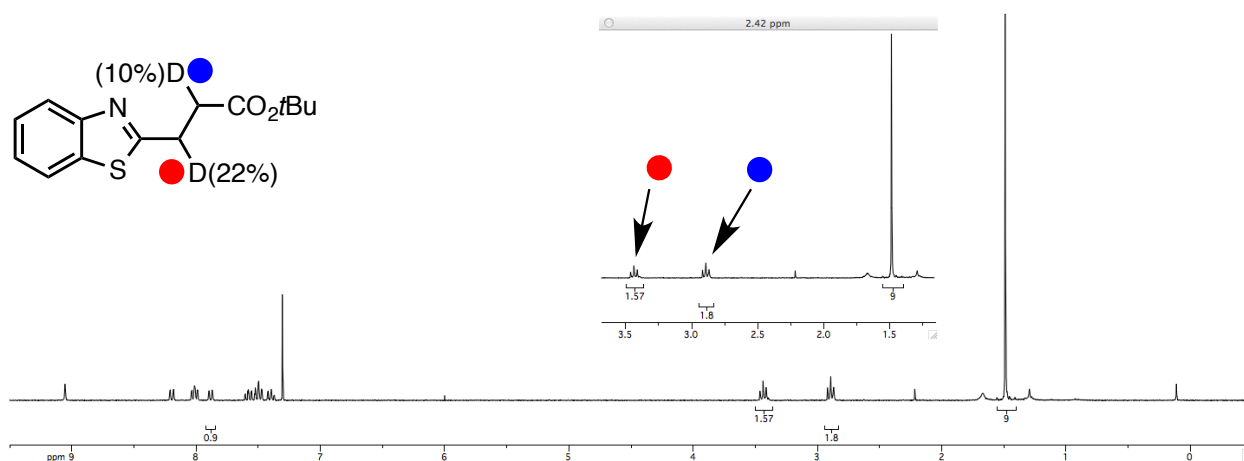


Figure A.2.3 ^1H NMR spectrum of **2b** (contaminated with some **1b**)

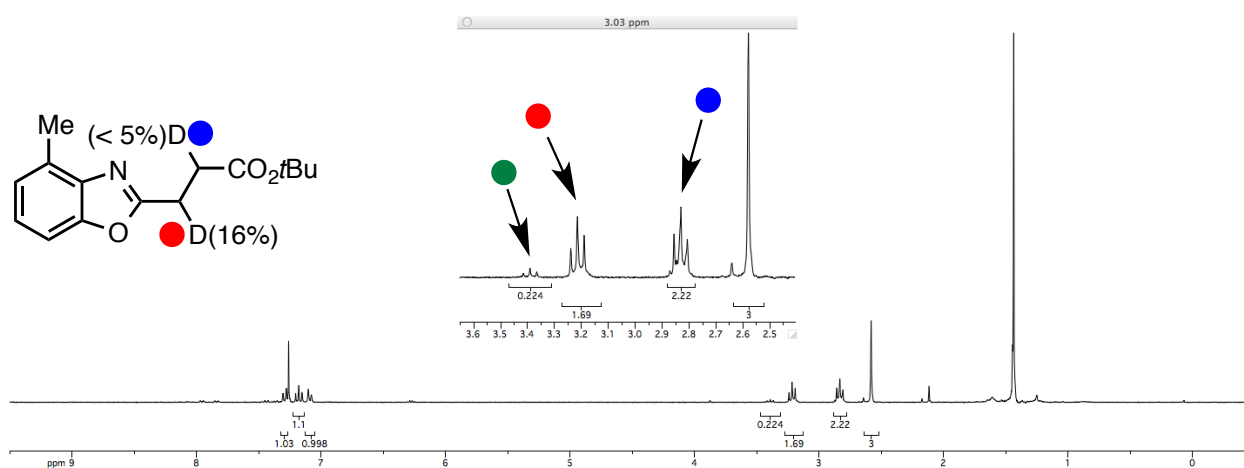


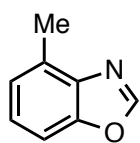
Figure A.2.4 ^1H NMR spectrum of **2c** (contaminated with about 10 % **2b** (green dot)). A corresponding amount (0.22) is subtracted from blue integral of **2c** (i.e. $2.22 - 0.22$), since the other methylene resonance of **2b** underlies it.

A.2.9 General procedure for the synthesis of benzoxazoles **1c–1d** and **1f–1h**

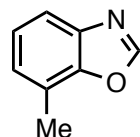
Benzoxazoles **1c–1d** and **1f–1h** were prepared from the corresponding 2-amino phenols according to a modified known procedure.^[5] To a flame-dried, round-bottom flask equipped with reflux condenser was charged the appropriate 2-amino phenol derivative (1.0 equiv) and trimethyl orthoformate (Aldrich 108456, 12 equiv). The dark red reaction mixture was heated to 110 °C overnight. After cooling to room temperature, trimethylorthoformate was removed by rotary evaporation, and the crude residue was purified by column chromatography, distillation or a combination of both.

[5] Cho, S. H.; Kim, J. Y.; Lee, S. Y.; Chang, S. *Angew. Chem. Int. Ed.* **2009**, 48, 9127 – 9130.

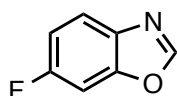
A.2.10 Characterization data for benzoxazoles 1c–1d and 1f–1h



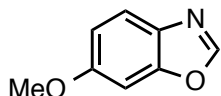
1c.^[5–6] Flash column chromatography on silica gel (2 x 7:1 Hex:EtOAc) followed by repeated (2x) kugelrohr distillation under reduced pressure yielded a colorless liquid (55%). $R_f = 0.24$ (10:1 Hex:EtOAc); IR (thin film/NaCl) 3062, 3105, 3063, 3032, 2924, 1623, 1519, 1242, 1071 cm^{-1} ; LRMS (EI) m/z $[\text{C}_8\text{H}_7\text{NO}]^+$ ($[\text{M}]^+$) calcd 133, found 133. ^1H and ^{13}C NMR spectra match those reported in the literature.^[5–6] Full characterization data available in Ref. 6a.



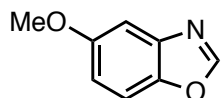
1d. Kugelrohr distillation followed by flash column chromatography on silica gel (8:1 Hex:EtOAc) provided **1d** as a white solid (61%). $R_f = 0.22$ (10:1 hexanes:EtOAc); ^1H NMR (400 MHz, CDCl_3) δ 8.08 (s, 1H), 7.61 (d, 1H, $J = 8.0$ Hz), 7.27 (t, 1H, $J = 7.6$ Hz), 7.18 (d, 1H, $J = 7.2$ Hz), 2.55 (s, 3H); ^{13}C NMR (100 MHz, CDCl_3) δ 152.4, 149.4, 139.7, 126.6, 124.6, 121.7, 118.0, 15.3; IR (ATR) 3085, 2922, 1511, 1489 cm^{-1} ; LRMS (ESI+APCI) m/z $[\text{C}_8\text{H}_8\text{NO}]^+$ ($[\text{M}+\text{H}]^+$) calcd 134.1, found 134.0.



1f.^[6a] Flash column chromatography on silica gel (4:1 \rightarrow 3:1 Hex:Et₂O) followed by kugelrohr distillation yielded a white solid (17%) *Note: this compound is quite volatile, and a good portion was lost while drying under high vacuum after the chromatography step.* $R_f = 0.31$ (3:1 Hex:Et₂O); ^{19}F NMR (376 MHz, CDCl_3) δ -114.7 (m). All other characterization data (^1H NMR, ^{13}C NMR, IR and MS) match those reported in the literature.^[6a]



1g.^[6a,6c] Prepared with 2-amino-5-methoxyphenol hydrochloride according to the general procedure but with additional 1.1 equiv NEt_3 to liberate the HCl salt. Flash column chromatography on silica gel (2:1 \rightarrow 1:1 Hex:Et₂O) yielded a white solid (90%). Full characterization data available in Ref. 6a.



1h.^[6] Flash column chromatography on silica gel (3:1 Hex:EtOAc) followed by kugelrohr distillation under reduced pressure yielded a white solid (35%). $R_f = 0.25$ (3:1 Hex:EtOAc); IR (ATR) 3123, 3013, 2977, 2944, 2888, 2835, 1612, 1515 cm^{-1} ; LRMS (ESI + APCI) m/z $[\text{C}_8\text{H}_8\text{NO}_2]^+$ ($[\text{M}+\text{H}]^+$) calcd 150.1, found 150.1; ^1H NMR and ^{13}C NMR spectra match those reported in the literature.^[6] Full characterization data available in Ref. 6a.

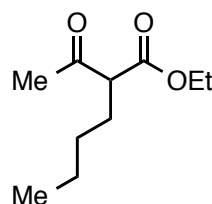
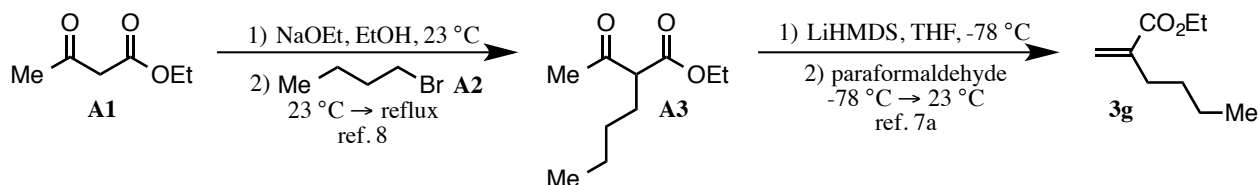
[6] (a) Lee, J. J.; Kim, J.; Jun, Y. M.; Lee, B. M.; Kim, B. H. *Tetrahedron* **2009**, 65, 8821 – 8831.
 (b) Guo, S.; Qian, B.; Xie, Y.; Xia, C.; Huang, H. *Org. Lett.* **2011**, 13, 522 – 525.
 (c) Wertz, S.; Kodama, S.; Studer, A. *Angew. Chem. Int. Ed.* **2011**, 50, 11511 – 11515.

A.2.11 Preparation of α -substituted acrylates **3g**, **3h** and **3j**

3a-e and **3i** were purchased from commercial sources, and **3f** was prepared according to a known procedure.^[7]

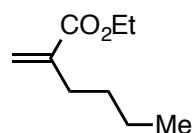
Full characterization data for **3f** is found in Ref. 7b.

3g was prepared according to the two-step sequence below:



A3 was prepared according to a procedure described by Gani et al.^[8] To a solution of NaOEt (126.5 mmol, 1.1 equiv, prepared by addition of Na(0) to EtOH) in EtOH (45 mL) was added ethyl acetoacetate (**A1**) (15.0 g, 115 mmol, 1.0 equiv) over about 1 minute. To the resultant yellow solution was then slowly added butyl bromide (**A2**) (16.0 mL, 149.5 mmol, 1.3 equiv,

washed with NaHCO₃ and distilled before use). The reaction was heated to reflux for 24h at which point it was cooled and partitioned between Et₂O and water in a separatory funnel. The aqueous layer was extracted with Et₂O two times more, and the combined organic extracts were washed with brine and dried (MgSO₄). Distillation under reduced pressure yielded 9.19g (43%) of crude product (contaminated with about 10% dialkylated product), which was taken to the next step without further purification.



3g was prepared from **A3** according to a procedure modified from one described by Gellman et al.^[7a] To a solution of LiHMDS (7.43 g, 44.4 mmol, 1.1 equiv) in THF (250 mL) at -78 °C was added a solution of **A3** (7.53 g, 40.4 mmol, 1.0 equiv) in THF (45 mL) via addition funnel. The

reaction was stirred for an additional 75 minutes at -78 °C, and then paraformaldehyde (5.70 g, excess) was added in one portion. The ice bath was removed, and the reaction was allowed to stir at room temperature for an additional 4 h. At this point, the reaction was filtered through celite to remove excess paraformaldehyde and concentrated by rotary evaporation. The crude reaction mixture was purified by flash column chromatography on silica gel (30:1 → 10:1 Hex:EtOAc), and the purest fractions were combined to give **3g** as a clear liquid (2.41 g, 15.4 mmol, 12% over 2 steps): R_f = 0.20 (40:1 Hex:EtOAc); ¹H NMR (400 MHz, CDCl₃) δ 6.11 (m, 1H), 5.49 (m, 1H), 4.19 (q, 2H, *J* = 7.2

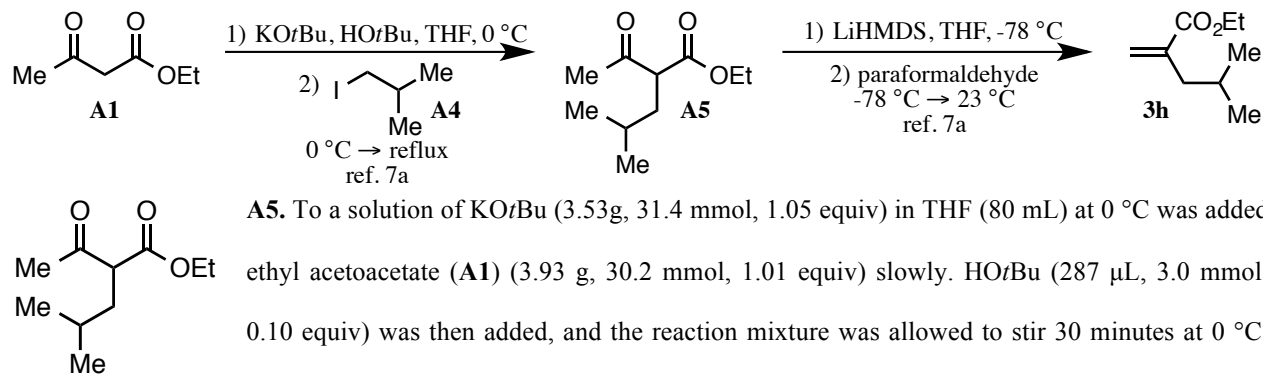
[7] (a) Lee, H.; Park, J.; Kim, B. M.; Gellman, S. H. *J. Org. Chem.* **2003**, 68, 1575 – 1578.

(b) Biju, A. T.; Padmanaban, M.; Wurz, N. E.; Glorius, F. *Angew. Chem. Int. Ed.* **2011**, 50, 8412 – 8415.

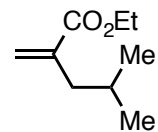
[8] Akhtar, M.; Botting, N. P.; Cohen, M. A.; Gani, D. *Tetrahedron* **1987**, 43, 5899 – 5908.

Hz), 2.29 (m, 2H), 1.40-1.48 (m, 2H), 1.29-1.37 (m, 2H), 1.29 (t, 3H, $J = 7.2$ Hz), 0.90 (t, 3H, $J = 7.2$ Hz); ^{13}C NMR (100 MHz, CDCl_3) δ 167.5, 141.2, 124.2, 60.6, 31.7, 30.7, 22.4, 14.3, 14.0; IR (ATR) 2958, 2931, 2873, 1716, 1631, 1153 cm^{-1} ; LRMS (EI) m/z $[\text{C}_9\text{H}_{16}\text{O}_2]^+$ ($[\text{M}]^+$) calcd 156, found 156.

3h was prepared according to the two-step procedure of Gellman et al.:^[7a]

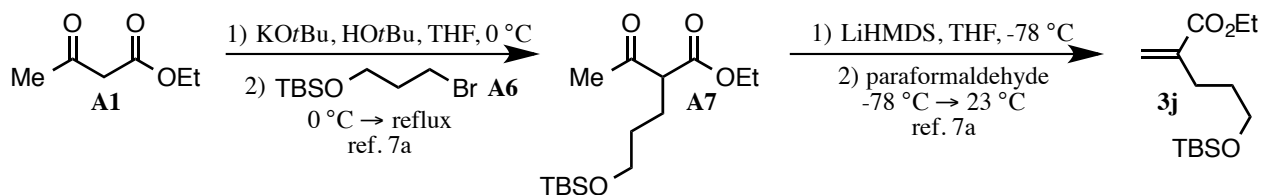


Iodide **A4** (5.52 g, 30.0 mmol, 1.0 equiv, distilled before use) was added in one portion, and the ice bath was removed. The reaction was heated to reflux for 24 h and then cooled to room temperature. After removal of THF by rotary evaporator, the reaction mixture was partitioned between Et_2O and saturated NaHCO_3 . The aqueous layer was extracted with Et_2O two times more, and the combined organic layers were washed with brine and dried (MgSO_4). Flash column chromatography on silica gel (8% EtOAc in Hex) yielded 3.18 g of crude product, which was taken to the next step without further purification.



3h. To a solution of **A5** (3.18 g, 17.1 mmol, 1.0 equiv) in THF (110 mL) at -78 °C was added a solution of LiHMDS (3.15 g, 18.7 mmol, 1.1 equiv) in THF (20 mL). The reaction mixture was allowed to stir for 30 minutes at -78 °C, and then paraformaldehyde (2.40 g, excess) was added as a solid in one portion. The ice bath was removed, and the reaction was allowed to stir at room temperature overnight. At this point, the reaction was filtered through celite to remove excess paraformaldehyde and concentrated by rotary evaporation. The crude reaction mixture was purified by flash column chromatography on silica gel (Hex \rightarrow 2% \rightarrow 4% \rightarrow 8% \rightarrow 15% EtOAc in Hex) to give **3h** as a clear liquid (1.76 g, 11.3 mmol, 37% over two steps): $R_f = 0.32$ (4% EtOAc in Hex); ^1H NMR (400 MHz, CDCl_3) δ 6.15 (d, 1H, $J = 1.6$ Hz), 5.47 (m, 1H), 4.19 (q, 2H, $J = 7.2$ Hz), 2.18 (dd, 1H, $J = 7.2, 1.2$ Hz), 1.79 (m, 1H), 1.30 (t, 3H, $J = 7.2$ Hz), 0.89 (d, 6H, $J = 6.8$ Hz); ^{13}C NMR (100 MHz, CDCl_3) δ 167.7, 140.1, 125.6, 60.7, 41.5, 27.4, 22.4, 14.4; IR (ATR) 2957, 2934, 2870, 1715, 1630 cm^{-1} ; LRMS (EI) m/z $[\text{C}_9\text{H}_{16}\text{O}_2]^+$ ($[\text{M}]^+$) calcd 156, found 156.

3j was prepared according to the two-step procedure of Gellman et al.:^[7a]



A7. To a solution of KOtBu (3.70 g, 33.0 mmol, 1.10 equiv) in THF (80 mL) at 0 °C was added ethyl acetoacetate (**A1**) (3.88 g, 29.8 mmol, 1.01 equiv) slowly. HOtBu (287 μ L, 3.0 mmol, 0.10 equiv) was then added, and the reaction mixture was allowed to stir 30 minutes at 0 °C. Bromide **A6** (7.50 g, 29.6 mmol, 1.0 equiv, prepared from 3-bromo-1-propanol according to a known procedure)^[9] was added in one portion, and the ice bath was removed. The reaction was heated to reflux for 36 h and then cooled to room temperature. After removal of THF by rotary evaporator, the reaction mixture was partitioned between Et₂O and H₂O. The aqueous layer was extracted with Et₂O two times more, and the combined organic layers were washed with brine and dried (MgSO₄). Flash column chromatography on silica gel (Hex → 5% → 8% → 10% → 15% EtOAc in Hex) yielded 4.89 g of crude product, which was taken to the next step without further purification.

3j. To a solution of **A7** (4.89 g, 16.2 mmol, 1.0 equiv) in THF (110 mL) at -78 °C was added a solution of LiHMDS (2.97 g, 17.8 mmol, 1.1 equiv) in THF (20 mL). The reaction mixture was allowed to stir for 30 minutes at -78 °C, and then paraformaldehyde (2.30 g, excess) was added as a solid in one portion. The ice bath was removed, and the reaction was allowed to stir at room temperature overnight. At this point, the reaction was filtered through celite to remove excess paraformaldehyde and concentrated by rotary evaporation. The crude reaction mixture was purified by flash column chromatography on silica gel (Hex → 2% → 4% → 6% → 10% EtOAc in Hex) to yield **3j** as a clear liquid (3.59 g, 44% over two steps). Characterization data for **3j** match that reported in the literature.^[10]

[9] Trapella, C.; Fischetti, C.; Pela, M.; Lazzari, I.; Guerrini, R.; Calo, G.; Rizzi, A.; Camarda, V.; Lambert, D. G.; McDonald, J.; Regoli, D.; Salvadori, S. *Bioorg. Med. Chem.* **2009**, 17, 5080 – 5095.

[10] Wang, X.; Buchwald, S. L. *J. Am. Chem. Soc.* **2011**, 133, 19080 – 19083.

A.2.12 Initial optimization of the asymmetric HH reaction of 4-methyl benzoxazole (1c) and ethyl methacrylate (3a) (Chapter 2, Table 2.2)

A.2.12.1 Reaction set-up

In a glove box, a 1 dram vial equipped with magnetic stirring bar was charged [Rh(cod)OAc]₂ (1.4 mg, 2.6 μmol, 2 mol %) and ligand (5.2 μmol, 4 mol %). To this was added a solution of 4-methylbenzoxazole (**1c**) (16.6 mg, 14.7 μL, 0.125 mmol, 1 equiv) and 4,4'-di-*tert*-butylbiphenyl (3.3 mg, 12.5 μmol, 0.10 equiv) in 250 μL of the appropriate solvent. Ethyl methacrylate (**3a**) (62 μL, 4 equiv up to 124 μL, 8.0 equiv) was then added, and the vial was sealed with a Teflon-lined screw cap. At this point, the vial was removed from the glove box and placed in an aluminum block set to the indicated temperature. After the reaction was heated for the indicated amount of time, it was cooled to room temperature. A 15 μL aliquot of the crude reaction mixture was removed and diluted with 500 μL 1:1 Hex:*i*PrOH. *Note: in the case that solid precipitated at this point—acrylate polymerized under some conditions listed in Table 1—the sample was filtered prior to analysis.* Percent yield and percent ee of **4ca** was determined with respect to 4,4'-di-*tert*-butylbiphenyl by LC analysis on a chiral stationary phase as described below.

A.2.12.2 Analysis of the HH reaction of 4-methylbenzoxazole (1c) and ethyl methacrylate (3a) by chiral HPLC

HPLC Method: 4,4'-di-*tert*-butylbiphenyl (DTBB), ethyl methacrylate (**3a**), 4-methylbenzoxazole (**1c**) and both enantiomers of product **4ca** are separated by the following method: Chiracel IB column, 94:6 Hex:10% *i*PrOH in Hex, 1 mL/min. *Note: See section A.2.19 for HPLC traces of racemic and enantioenriched 4ca.*

DTBB: 3.5 min

Ethyl methacrylate (**3a**): 3.9 min (**3a** has a very low absorbance)

4-methylbenzoxazole (**1c**): 6.0 min

First enantiomer **4ca**: 7.3 min

Second enantiomer **4ca**: 8.1 min

Response factor calculation for 4ca: Using stock solutions of appropriate concentrations of 4,4'-di-*tert*-butylbiphenyl (DTBB) and racemic **4ca**, each of five HPLC vials was charged with DTBB (2.0 mg, 7.5 μmol), increasing amounts of racemic **4ca** (to mimic 5, 10, 20, 40 and 80 percent yield **4ca** assuming 20 percent loading of DTBB) and enough 1:1 Hex:*i*PrOH to make a total volume of 1000 μL:

Vial 1: 0.46 mg, 1.87 μmol **4ca**

Vial 2: 0.93 mg, 3.75 μmol **4ca**

Vial 3: 1.86 mg, 7.51 μmol **4ca**

Vial 4: 3.71 mg, 15.0 μmol **4ca**

Vial 5: 7.43 mg, 30.0 μmol **4ca**

Each of these five samples was analyzed by chiral HPLC according to the method above. The areas of both enantiomers of **4ca** were summed together to give the total area of product **4ca**. The ratio (Area **4ca**:Area **DTBB**) (Y-axis) was plotted against the ratio **[4ca]:[DTBB]** (X-axis) for various wavelengths (DAD A–D) to give a response factor curve (Figure A.2.5). The response factor curve was found to be highly linear for all wavelengths in the region analyzed, and the slope of each line gave the response factor, R_f **4ca** for a given wavelength (Figure A.2.5):

R_f **4ca** DAD A (254 nm): 0.17

R_f **4ca** DAD B (254 nm): 0.20

R_f **4ca** DAD C (210 nm): 0.69

R_f **4ca** DAD D (230 nm): 1.18

Percent yield 4ca: Yields of **4ca** were either reported as averages from those determined at each of these four wavelengths or from the wavelength that provided the cleanest spectrum.

Percent ee 4ca: Percent ee of **4ca** was determined simply by subtraction of the areas of **4ca** enantiomers.

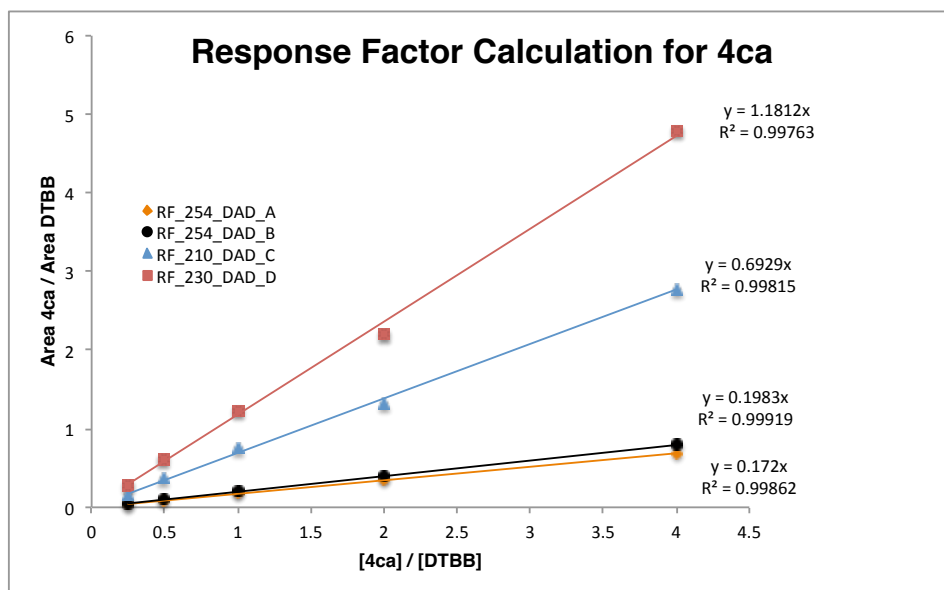


Figure A.2.5 Response factor curves for **4ac** at various wavelengths

A.2.13 General procedure for second generation optimization of the asymmetric HH reaction of 4-methyl benzoxazole (1c) and ethyl methacrylate (3a) (Chapter 2, Table 2.3)

In a glove box, a 1.5 dram vial equipped with magnetic stirring bar was charged $[\text{Rh}(\text{cod})\text{OAc}]_2$ (6.8 mg, 12.6 μmol , 5 mol %) and ligand (25.2 μmol , 10 mol %). To this was added a solution of 4-methylbenzoxazole (**1c**) (33.3 mg, 29.5 μL , 0.25 mmol, 1.0 equiv), 4,4'-di-*tert*-butylbiphenyl (6.6 mg, 25.0 μmol , 0.10 equiv) and ethyl methacrylate (**3a**) (228 mg, 250 μL , 2.0 mmol, 8.0 equiv) in CH_3CN (500 μL). The vial was sealed with a Teflon-lined screw cap and removed from the glove box. The reaction was heated at 100 $^\circ\text{C}$ in an aluminum block for 24 h. After cooling to room temperature, a 15 μL aliquot of the crude reaction mixture was removed and diluted with 500 μL 1:1 Hex:*i*PrOH. Percent yield and percent ee were determined as described above for the initial reaction optimization (section A.2.12.2).

Note: It was found that small changes in $[\text{Rh}(\text{cod})\text{OAc}]_2$ to ligand ratio can influence the rate of formation of 4ca rather dramatically. For acceptable reproducibility, it was necessary to double the scale from 0.125 mmol 1c (initial reaction optimization, section A.2.12.1) to 0.25 mmol 1c.

A.2.14 General procedure for the asymmetric HH of methacrylate derivatives 3 with benzoxazoles 1 (Chapter 2, Table 2.4)

In a glove box, a 1.5 dram vial equipped with magnetic stirring bar was charged $[\text{Rh}(\text{cod})\text{OAc}]_2$ (6.8 mg, 12.6 μmol , 0.05 equiv), CTH-(*R*)-xylyl-P-Phos (18.9 mg, 25.2 μmol , 0.10 equiv) and CsOAc (12.0 mg, 62.5 μmol , 0.025 equiv) where applicable. To this was added a solution of benzoxazole **1** (0.25 mmol, 1.0 equiv), 4,4'-di-*tert*-butylbiphenyl (6.6 mg, 25.0 μmol , 0.10 equiv) and acrylate derivative (**3a**) (2.0 mmol, 8.0 equiv) in CH_3CN (500 μL). The vial was sealed with a Teflon-lined screw cap and removed from the glove box. The reaction was heated at 100 $^\circ\text{C}$ in an aluminum block for 48 h unless otherwise indicated. After cooling to room temperature, the reaction mixture was either concentrated directly (without CsOAc) or filtered through celite prior to concentration (with CsOAc). Crude reaction mixtures were analyzed by ^1H NMR spectroscopy if desired. Crude reaction mixtures were then adsorbed onto silica and purified by flash column chromatography on silica gel to give the corresponding products **4**.

*Note 1: Racemic products were prepared in the same fashion but with 9.8 mg (12.6 μmol , 0.05 equiv) CTH-(*R*)-xylyl-P-Phos and 9.8 mg (12.6 μmol , 0.05 equiv) CTH-(*S*)-xylyl-P-Phos.*

Note 2: Whereas most reactions were performed by placing the 1.5 dram vial in the bottom of the aluminum block, it was found that slight improvements in ee for epimerizable or lower ee products (4cc–4cd, 4aa and 4ea–4ha)

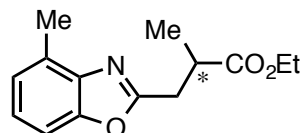
could be achieved by filling the aluminum well with sand to such a level that the reaction solvent reached the top of the aluminum well.

A.2.15 Comparison of reaction efficiency in presence or absence of CsOAc (Chapter 2, Table 2.4, 4cf and 4aa)

Because subtle changes in rhodium to ligand ratio is known to influence reaction efficiency (*vide supra*), comparison of reactions with and without CsOAc were performed with the same stock solution of [Rh(cod)OAc]₂, CTH-(R)-xylyl-P-Phos, DTBB, benzoxazole **1** and acrylate **3**. For instance, for the comparison of the reaction of benzoxazole (**1a**) and (**3a**), the following procedure was used:

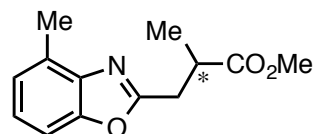
15.5 mg (0.05 equiv) [Rh(cod)OAc]₂, 43.5 mg (0.10 equiv) CTH-(R)-xylyl-P-Phos, 68 mg (58 μ L, 1.0 equiv) **1a**, 15.4 mg (0.10 equiv) DTBB, 526 mg (574 μ L, 8.0 equiv) **3a** were dissolved in 1150 μ L CH₃CN. 807 μ L of the resultant solution was added to either an empty 1.5 dram vial or a 1.5 dram vial containing 12.0 mg (62.5 μ mol, 0.25 equiv) CsOAc. Both vials were sealed with a Teflon-lined screw cap, removed from the box and heated to 100 °C in an aluminum block for 48 h. A 15 μ L aliquot was removed from each reaction and subjected to chiral HPLC analysis (Chiracel IC column, 80:20 Hex:*i*PrOH, 1.0 mL/min, see characterization data for **4aa** in section A.2.16 and HPLC data for **4aa** in section A.2.19) to determine percent ee of **4aa**. The reaction without CsOAc was then concentrated directly, whereas the reaction with CsOAc was filtered through celite prior to concentration. Percent yield of **4aa** was determined with respect to DTBB by ¹H NMR analysis of the crude reaction mixture.

A.2.16 Characterization data for products 4



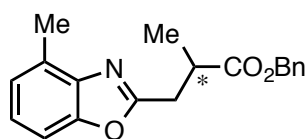
4ca. Flash column chromatography on silica gel (7:1 Hex:EtOAc) yielded a colorless oil (88%). R_f = 0.20 (7:1 Hex:EtOAc); HPLC analysis – Chiracel IB column, 94:6 Hex:10% *i*PrOH in Hex, 1.0 mL/min, major enantiomer: 8.1 min, minor enantiomer:

7.3 min, 94% ee; [α]_D²⁵ = +13.7° (c = 0.995 g/100 mL, EtOAc); ¹H NMR (400 MHz, CDCl₃) δ 7.26 (d, 1H, *J* = 8.0 Hz), 7.15 (m, 1H), 7.07 (d, 1H, *J* = 7.6 Hz), 4.08-4.20 (m, 2H), 3.32 (dd, 1H, *J* = 15.2, 6.8 Hz), 3.12 (m, 1H), 3.01 (dd, 1H, *J* = 15.2, 7.2 Hz), 2.56 (s, 3H), 1.28 (d, 3H, *J* = 7.2 Hz), 1.20 (t, 3H, 7.2 Hz); ¹³C NMR (100 MHz, CDCl₃) δ 175.0, 164.2, 150.7, 140.6, 130.2, 124.8, 124.4, 107.8, 60.9, 37.9, 32.4, 17.2, 16.6, 14.2; IR (ATR) 2979, 2937, 1732, 1610 cm⁻¹; LRMS (ESI + APCI) *m/z* [C₁₄H₁₈NO₃]⁺ ([M+H]⁺) calcd 248.1, found 248.1.



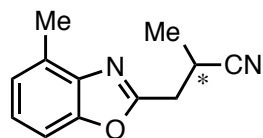
4cb. Flash column chromatography on silica gel (7:1 → 5:1 Hex:EtOAc) yielded a colorless oil (68%). R_f = 0.17 (7:2 Hex:Et₂O); HPLC analysis – Chiracel IB column, 94:6 Hex:10% *i*PrOH in Hex, 1.0 mL/min, major enantiomer: 9.5 min, minor

enantiomer: 8.6 min, 94% ee; $[\alpha]_D^{25} = +12.4^\circ$ ($c = 1.835$ g/100 mL, CDCl_3); ^1H NMR (400 MHz, CDCl_3) δ 7.29 (d, 1H, $J = 8.0$ Hz), 7.18 (m, 1H), 7.09 (d, 1H, $J = 7.6$ Hz), 3.71 (s, 3H), 3.35 (dd, 1H, $J = 15.2, 6.8$ Hz), 3.17 (m, 1H), 3.04 (dd, 1H, $J = 15.2, 7.6$ Hz), 2.59 (s, 3H), 1.31 (d, 3H, $J = 7.2$ Hz); ^{13}C NMR (100 MHz, CDCl_3) δ 175.5, 164.1, 150.7, 140.6, 130.2, 124.9, 124.4, 107.8, 52.2, 37.8, 32.4, 17.2, 16.6; IR (ATR) 2976, 2952, 2923, 1736, 1625 cm^{-1} ; LRMS (ESI + APCI) m/z $[\text{C}_{13}\text{H}_{16}\text{NO}_3]^+$ ($[\text{M}+\text{H}]^+$) calcd 234.1, found 234.1.



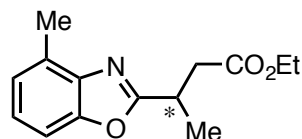
4cc. Flash column chromatography on silica gel (4:1 \rightarrow 3:1 Hex:Et₂O) yielded a colorless oil (98%). $R_f = 0.22$ (4:1 Hex:Et₂O); HPLC analysis – Chiracel IB column, 90:10 Hex:*i*PrOH, 1.0 mL/min, major enantiomer: 5.3 min, minor enantiomer: 4.9

min, 92% ee; $[\alpha]_D^{25} = +6.2^\circ$ ($c = 3.560$ g/100 mL, CDCl_3); ^1H NMR (400 MHz, CDCl_3) δ 7.26-7.30 (m, 6H), 7.18 (t, 1H, $J = 7.6$ Hz), 7.09 (d, 1H, $J = 7.6$ Hz), 5.15 (s, 2H), 3.37 (dd, 1H, $J = 15.6, 7.2$ Hz), 3.23 (m, 1H), 3.06 (dd, 1H, $J = 15.6, 7.2$ Hz), 2.58 (s, 3H), 1.34 (d, 3H, $J = 7.2$ Hz); ^{13}C NMR (100 MHz, CDCl_3) δ 174.8, 164.0, 150.7, 140.6, 135.9, 130.2, 128.6, 128.3, 128.2, 124.9, 124.4, 107.8, 66.7, 37.9, 32.4, 17.2, 16.6; IR (ATR) 3063, 3033, 2975, 2938, 1734 cm^{-1} ; LRMS (ESI + APCI) m/z $[\text{C}_{19}\text{H}_{20}\text{NO}_3]^+$ ($[\text{M}+\text{H}]^+$) calcd 310.1, found 310.2.



4cd. Flash column chromatography on silica gel (1:1 Hex:Et₂O) yielded a colorless oil (54%). $R_f = 0.20$ (3:1 Hex:EtOAc); HPLC analysis – Chiracel IB column, 98:2 Hex:*i*PrOH, 1.0 mL/min, major enantiomer: 13.4 min, minor enantiomer: 12.3 min, 84%

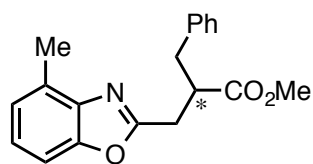
ee; $[\alpha]_D^{25} = +29.7^\circ$ ($c = 1.105$ g/100 mL, CDCl_3); ^1H NMR (400 MHz, CDCl_3) δ 7.33 (d, 1H, $J = 8.0$ Hz), 7.23 (m, 1H), 7.13 (d, 1H, $J = 7.2$ Hz), 3.32-3.40 (m, 2H), 3.13-3.20 (m, 1H), 2.60 (s, 3H), 1.48 (d, 3H, $J = 6.8$ Hz); ^{13}C NMR (100 MHz, CDCl_3) δ 161.4, 150.8, 140.4, 130.7, 125.2, 125.0, 121.6, 108.0, 33.2, 23.9, 18.0, 16.6; IR (ATR) 3062, 3033, 2984, 2942, 2244, 1610 cm^{-1} ; LRMS (ESI + APCI) m/z $[\text{C}_{12}\text{H}_{13}\text{N}_2\text{O}]^+$ ($[\text{M}+\text{H}]^+$) calcd 201.1, found 201.1.



4ce. Flash column chromatography on silica gel (2 x 5:1 pentane:Et₂O) yielded a light yellow oil (15%, *Note: ^1H NMR with respect to DTBB shows that 4ce is formed in 41% yield, but it is difficult to separate from starting material 1c*). $R_f = 0.17$ (5:1

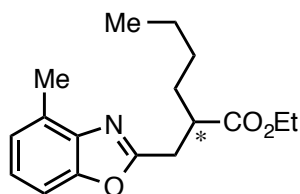
pentane:Et₂O); HPLC analysis – Chiracel IC column, 90:10 Hex:*i*PrOH, 0.7 mL/min, 1st enantiomer: 7.8 min, 2nd enantiomer: 8.3 min, < 5 % ee; ^1H NMR (300 MHz, CDCl_3) δ 7.29 (d, 1H, $J = 8.1$ Hz), 7.17 (m, 1H), 7.08 (d, 1H, $J = 7.5$ Hz), 4.14 (q, 2H, $J = 7.2$ Hz), 3.65 (m, 1H), 3.03 (dd, 1H, $J = 16.2, 6.9$ Hz), 2.68 (dd, 1H, $J = 16.2, 7.5$ Hz), 2.59 (s, 3H), 1.48 (d, 3H, $J = 6.9$ Hz), 1.22 (t, 3H, $J = 7.2$ Hz); ^{13}C NMR (75 MHz, CDCl_3) δ 171.6, 168.2, 150.6, 140.6,

130.3, 124.8, 124.3, 107.8, 60.8, 39.2, 31.0, 18.6, 16.6, 14.3; IR (ATR) 2979, 2935, 1734, 1625, 1608 cm^{-1} ; LRMS (ESI + APCI) m/z $[\text{C}_{14}\text{H}_{18}\text{NO}_3]^+$ ($[\text{M}+\text{H}]^+$) calcd 248.1, found 248.1.



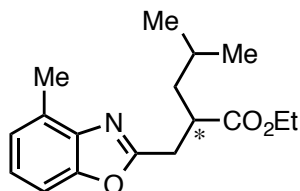
4cf. Flash column chromatography on silica gel (16:3 \rightarrow 4:1 \rightarrow 2:1 Hex:Et₂O) yielded a light golden oil (65%). R_f = 0.18 (16:3 Hex:Et₂O); HPLC analysis – Chiracel IB column, 94:6 Hex:10% *i*PrOH in Hex, 1.0 mL/min, major enantiomer:

13.8 min, minor enantiomer: 17.1 min, 93% ee; $[\alpha]_{\text{D}}^{25} = -2.89^\circ$ ($c = 2.395 \text{ g}/100 \text{ mL}$, CDCl_3);^[11] ^1H NMR (400 MHz, CDCl_3) δ 7.26-7.30 (m, 3H), 7.15-7.22 (m, 4H), 7.08 (d, 1H, $J = 7.2 \text{ Hz}$), 3.64 (s, 3H), 3.36-3.45 (m, 1H), 3.25-3.31 (m, 1H), 3.06-3.15 (m, 2H), 2.93 (dd, 1H, $J = 13.6, 7.2 \text{ Hz}$), 2.56 (s, 3H); ^{13}C NMR (100 MHz, CDCl_3) δ 174.4, 163.9, 150.7, 140.6, 138.2, 130.3, 129.2, 128.7, 126.8, 124.9, 124.4, 107.8, 52.1, 45.1, 38.1, 30.3, 16.6; IR (ATR) 3062, 3028, 2950, 2923, 2856, 1736, 1624 cm^{-1} ; LRMS (ESI + APCI) m/z $[\text{C}_{19}\text{H}_{20}\text{NO}_3]^+$ ($[\text{M}+\text{H}]^+$) calcd 310.1, found 310.1.



4cg. Flash column chromatography on silica gel (10:1 Hex:EtOAc) yielded a colorless oil (93%). R_f = 0.22 (DCM); HPLC analysis – Chiracel IC column, 98:2 Hex:*i*PrOH, 1.0 mL/min, major enantiomer: 9.9 min, minor enantiomer: 8.9 min, 95% ee; $[\alpha]_{\text{D}}^{25} = +4.4^\circ$ ($c = 2.595 \text{ g}/100 \text{ mL}$, CDCl_3); ^1H NMR (400 MHz, CDCl_3) δ 7.28 (d, 1H, $J =$

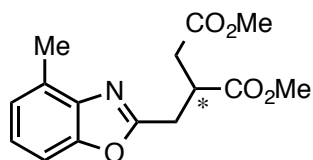
8.0 Hz), 7.17 (m, 1H), 7.08 (d, 1H, $J = 7.6 \text{ Hz}$), 4.09-4.21 (m, 2H), 3.24-3.31 (m, 1H), 3.00-3.10 (m, 2H), 2.58 (s, 3H), 1.71-1.77 (m, 1H), 1.59-1.64 (m, 1H), 1.28-1.35 (m, 4H), 1.20 (t, 3H, $J = 7.2 \text{ Hz}$), 0.86-0.90 (m, 3H); ^{13}C NMR (100 MHz, CDCl_3) δ 174.5, 164.1, 150.5, 140.4, 130.0, 124.7, 124.2, 107.6, 60.6, 43.3, 31.8, 30.9, 29.0, 22.4, 16.4, 14.1, 13.8; IR (ATR) 2957, 2931, 2861, 1732 cm^{-1} ; LRMS (ESI + APCI) m/z $[\text{C}_{17}\text{H}_{24}\text{NO}_3]^+$ ($[\text{M}+\text{H}]^+$) calcd 290.2, found 290.1.



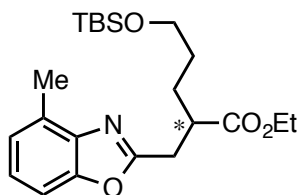
4ch. The crude reaction mixture was dried under high vacuum overnight to remove residual benzoxazole **1c**, since it coelutes with **4ch**. Flash column chromatography on silica gel (7:1 \rightarrow 6:1 Hex:Et₂O) yielded a clear oil (85%). R_f = 0.32 (5:1 Hex:Et₂O);

[11] Compounds **4cf** and **4cj** have low negative specific rotations, whereas all other products **4** (made with same antipode of chiral ligand) have low to moderate positive specific rotations. It is not clear whether the observed negative specific rotations of **4cf** and **4cj** reflect a true, negative specific rotation or whether the observed negative specific rotation arises simply because the magnitude of specific rotation for these products is small relative to experimental error. In terms of HPLC data, **4cj** is consistent with that of other compounds: the major enantiomer elutes second. **4cf** is different than other compounds: the major enantiomer elutes first.

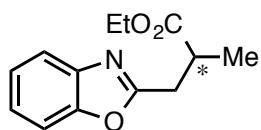
HPLC analysis – Chiracel IC column, 98:2 Hex:*i*PrOH, 1.0 mL/min, major enantiomer: 10.2 min, minor enantiomer: 9.4 min, 94% ee; $[\alpha]_D^{25} = +5.6^\circ$ ($c = 3.070$ g/100 mL, CDCl_3); ^1H NMR (400 MHz, CDCl_3) δ 7.28 (d, 1H, $J = 8.0$ Hz), 7.17 (m, 1H), 7.08 (d, 1H, $J = 7.6$ Hz), 4.09-4.21 (m, 2H), 3.19-3.30 (m, 1H), 3.03-3.14 (m, 2H), 2.58 (s, 3H), 1.59-1.77 (m, 2H), 1.34-1.41 (m, 1H), 1.20 (t, 3H, $J = 7.2$ Hz), 0.90-0.94 (m, 6H); ^{13}C NMR (100 MHz, CDCl_3) δ 175.0, 164.1, 150.7, 140.5, 130.2, 124.8, 124.4, 107.8, 60.7, 41.8, 41.6, 31.7, 26.1, 23.0, 22.1, 16.6, 14.3; IR (ATR) 3061, 2957, 2930, 2871, 1732, 1624 cm^{-1} ; LRMS (ESI + APCI) m/z $[\text{C}_{17}\text{H}_{24}\text{NO}_3]^+$ ($[\text{M}+\text{H}]^+$) calcd 290.2, found 290.2.



4ci. Flash column chromatography on silica gel (DCM \rightarrow 6% \rightarrow 12% EtOAc in DCM) yielded a colorless oil (60%). $R_f = 0.23$ (6% EtOAc in DCM); HPLC analysis – Chiracel IC column, 80:20 Hex:*i*PrOH, 1.0 mL/min, major enantiomer: 11.6 min, minor enantiomer: 10.8 min, 69% ee; $[\alpha]_D^{25} = +7.2^\circ$ ($c = 2.030$ g/100 mL, CDCl_3); ^1H NMR (400 MHz, CDCl_3) δ 7.29 (d, 1H, $J = 7.6$ Hz), 7.19 (t, 1H, $J = 7.6$ Hz), 7.10 (d, 1H, $J = 7.6$ Hz), 3.73 (s, 3H), 3.66 (s, 3H), 3.48-3.54 (m, 1H), 3.40 (dd, 1H, $J = 15.6, 6.0$ Hz), 3.21 (dd, 1H, 15.6, 8.0 Hz), 2.87 (dd, 1H, $J = 16.8, 8.0$ Hz), 2.71 (dd, 1H, $J = 16.8, 5.6$ Hz), 2.58 (s, 3H); ^{13}C NMR (100 MHz, CDCl_3) δ 173.5, 171.9, 163.1, 150.7, 140.5, 130.4, 125.0, 124.6, 107.8, 52.5, 52.0, 39.2, 35.0, 30.3, 16.6; IR (ATR) 3027, 2998, 2953, 2850, 1735 cm^{-1} ; LRMS (ESI + APCI) m/z $[\text{C}_{15}\text{H}_{18}\text{NO}_5]^+$ ($[\text{M}+\text{H}]^+$) calcd 292.1, found 292.1.

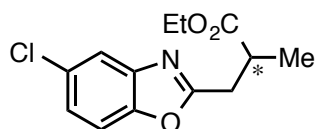


4cj. Flash column chromatography on silica gel (2 x 5% \rightarrow 10% EtOAc in Hex) yielded a very light brown oil (76%). $R_f = 0.26$ (10% EtOAc in Hex); HPLC analysis – Chiracel IC column, 98:2 Hex:*i*PrOH, 1.0 mL/min, major enantiomer: 8.3 min, minor enantiomer: 7.5 min, 96% ee; $[\alpha]_D^{25} = -2.1^\circ$ ($c = 3.590$ g/100 mL, CDCl_3); ^1H NMR (400 MHz, CDCl_3) δ 7.28 (d, 1H, $J = 8.0$ Hz), 7.17 (m, 1H), 7.08 (d, 1H, $J = 7.6$ Hz), 4.10-4.21 (m, 2H), 3.56-3.65 (m, 2H), 3.26-3.33 (m, 1H), 3.04-3.11 (m, 2H), 2.57 (s, 3H), 1.49-1.84 (m, 4H), 1.21 (t, 3H, $J = 7.2$ Hz), 0.85 (s, 9H), 0.02 (s, 6H); ^{13}C NMR (100 MHz, CDCl_3) δ 174.5, 164.2, 150.7, 140.6, 130.2, 124.8, 124.4, 107.8, 62.7, 60.8, 43.2, 31.1, 30.2, 28.6, 26.0, 18.4, 16.6, 14.3, -5.2; IR (ATR) 2953, 2928, 2856, 1733, 1610 cm^{-1} ; LRMS (ESI + APCI) m/z $[\text{C}_{22}\text{H}_{36}\text{NO}_4\text{Si}]^+$ ($[\text{M}+\text{H}]^+$) calcd 406.2, found 406.3.



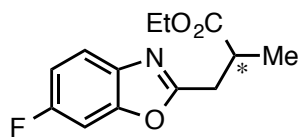
4aa. Flash column chromatography on silica gel (50:44:6 Hex:DCM:Et₂O) yielded a colorless oil (45%). $R_f = 0.13$ (50:44:6 Hex:DCM:Et₂O); HPLC analysis – Chiracel IC

column, 80:20 Hex:*i*PrOH, 1.0 mL/min, major enantiomer: 6.8 min, minor enantiomer: 6.4 min, 87% ee; $[\alpha]_{\text{D}}^{25} = +3.09^{\circ}$ ($c = 1.080$ g/100 mL, CDCl_3); ^1H NMR (400 MHz, CDCl_3) δ 7.65-7.69 (m, 1H), 7.45-7.50 (m, 1H), 7.28-7.32 (m, 2H), 4.16 (q, 2H, $J = 7.2$ Hz), 3.35 (dd, 1H, $J = 15.6, 7.2$ Hz), 3.16 (m, 1H), 3.03 (dd, 1H, $J = 15.6, 7.2$ Hz), 1.32 (d, 3H, $J = 7.2$ Hz), 1.22 (t, 3H, $J = 7.2$ Hz); ^{13}C NMR (100 MHz, CDCl_3) δ 175.0, 165.1, 150.9, 141.4, 124.8, 124.3, 119.8, 110.5, 61.0, 37.7, 32.3, 17.3, 14.3; IR (ATR) 2979, 2928, 1731, 1615, 1572 cm^{-1} ; LRMS (ESI + APCI) m/z $[\text{C}_{13}\text{H}_{16}\text{NO}_3]^+$ ($[\text{M}+\text{H}]^+$) calcd 234.1, found 234.1.



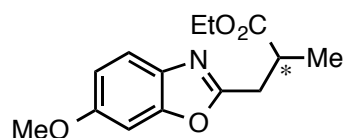
4ea. Flash column chromatography on silica gel (DCM \rightarrow 2% \rightarrow 5% \rightarrow 10% Et_2O in DCM) yielded a colorless oil (35%). $R_f = 0.30$ (8:1 Hex:Acetone); HPLC analysis – Chiracel IB column, 94:6 Hex:10% *i*PrOH in Hex, 1.0 mL/min, major enantiomer:

9.1 min, minor enantiomer: 8.4 min, 90% ee; $[\alpha]_{\text{D}}^{25} = +8.9^{\circ}$ ($c = 1.155$ g/100 mL, CDCl_3); ^1H NMR (400 MHz, CDCl_3) δ 7.65 (d, 1H, $J = 2.0$ Hz), 7.39 (d, 1H, $J = 8.8$ Hz), 7.27 (dd, 1H, $J = 8.8, 2.0$ Hz), 4.16 (q, 2H, $J = 7.2$ Hz), 3.34 (dd, 1H, $J = 15.6, 7.2$ Hz), 3.10-3.10 (m, 1H), 3.03 (dd, 1H, $J = 15.6, 7.2$ Hz), 1.32 (d, 3H, $J = 7.2$ Hz), 1.22 (t, 3H, $J = 7.2$ Hz); ^{13}C NMR (100 MHz, CDCl_3) δ 174.6, 166.4, 149.3, 142.4, 129.7, 124.9, 119.7, 111.0, 60.8, 37.4, 32.1, 17.1, 14.1; IR (ATR) 3096, 2980, 2938, 1732, 1568, 1451 cm^{-1} ; LRMS (ESI + APCI) m/z $[\text{C}_{13}\text{H}_{15}\text{ClNO}_3]^+$ ($[\text{M}+\text{H}]^+$) calcd 268.1, found 268.0.

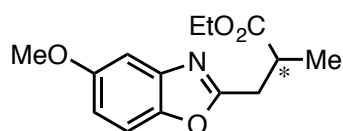


4fa. The crude reaction mixture was dried under high vacuum overnight to remove residual benzoxazole **1f**, since it coelutes with **4fa**. Flash column chromatography on silica gel (5:2 Hex: Et_2O) yielded a light yellow oil (31%). $R_f = 0.26$ (5:2 Hex: Et_2O);

HPLC analysis – Chiracel IC column, 94:6 Hex:10% *i*PrOH in Hex, 1.0 mL/min, major enantiomer: 9.1 min, minor enantiomer: 8.4 min, 90% ee; $[\alpha]_{\text{D}}^{25} = +3.0^{\circ}$ ($c = 0.970$ g/100 mL, CDCl_3); ^1H NMR (400 MHz, CDCl_3) δ 7.58 (dd, 1H, $J = 8.8, 4.8$ Hz), 7.20 (dd, 1H, $J = 8.0, 2.8$ Hz), 7.04 (ddd, 1H, $J = 9.2, 8.8, 2.8$ Hz), 4.15 (q, 2H, $J = 7.2$ Hz), 3.32 (dd, 1H, $J = 15.6, 7.2$ Hz), 3.13 (m, 1H), 3.00 (dd, 1H, $J = 15.6, 6.8$ Hz), 1.31 (d, 3H, $J = 6.8$ Hz), 1.22 (t, 3H); ^{13}C NMR (100 MHz, CDCl_3) δ 174.8, 165.6 (d, $J = 3.1$ Hz), 160.5 (d, $J = 242$ Hz), 150.8 (d, $J = 14.6$ Hz), 137.7, 120.0 (d, $J = 9.9$ Hz), 112.2 (d, $J = 24.4$), 98.6 (d, $J = 28.1$ Hz), 61.0, 37.6, 32.3, 17.3, 14.3; ^{19}F NMR (376 MHz, CDCl_3) δ -116.1 (ddd, $J = 9.2, 8.8, 4.8$ Hz); IR (ATR) 3081, 2980, 2939, 2909, 1730, 1623 cm^{-1} ; LRMS (ESI + APCI) m/z $[\text{C}_{13}\text{H}_{15}\text{FNO}_3]^+$ ($[\text{M}+\text{H}]^+$) calcd 252.1, found 252.1.



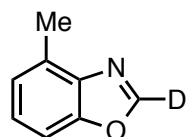
4ga. Flash column chromatography on silica gel (DCM \rightarrow 1% \rightarrow 2% \rightarrow 4% \rightarrow 10% \rightarrow 30% EtOAc in DCM) yielded a light golden oil (48%). R_f = 0.24 (4% EtOAc in DCM); HPLC analysis – Chiracel IC column, 90:10 Hex:*i*PrOH, 1.0 mL/min, major enantiomer: 14.7 min, minor enantiomer: 13.5 min, 88% ee; $[\alpha]_D^{25}$ = +3.1° (c = 1.580 g/100 mL, $CDCl_3$); 1H NMR (400 MHz, $CDCl_3$) δ 7.52 (d, 1H, J = 8.8 Hz), 7.00 (d, 1H, J = 2.4 Hz), 6.89 (dd, 1H, J = 8.8, 2.4 Hz), 4.15 (q, 2H, J = 7.2 Hz), 3.84 (s, 3H), 3.30 (dd, 1H, J = 15.2, 6.8 Hz), 3.12 (m, 1H), 2.98 (dd, 1H, J = 15.2, 7.2 Hz), 1.30 (d, 3H, J = 7.2 Hz), 1.22 (t, 3H, J = 7.2 Hz); ^{13}C NMR (100 MHz, $CDCl_3$) δ 175.0, 164.0, 158.0, 151.7, 135.1, 119.7, 112.3, 95.5, 60.9, 56.1, 37.7, 32.3, 17.2, 14.3; IR (ATR) 2978, 2939, 2907, 2836, 1729, 1615 cm^{-1} ; LRMS (ESI + APCI) m/z $[C_{14}H_{18}NO_4]^+$ ($[M+H]^+$) calcd 264.1, found 264.1.



4ha. Flash column chromatography on silica gel (1% \rightarrow 2% \rightarrow 4% \rightarrow 10% \rightarrow 30% EtOAc in DCM) yielded a colorless oil (56%). R_f = 0.15 (2% EtOAc in DCM); HPLC analysis – Chiracel IB column, 93:7 Hex:10% *i*PrOH in Hex, 1.0 mL/min, major enantiomer: 17.1 min, minor enantiomer: 15.8 min, 77% ee; $[\alpha]_D^{25}$ = +7.4° (c = 1.830 g/100 mL, $CDCl_3$); 1H NMR (400 MHz, $CDCl_3$) δ 7.34 (d, 1H, J = 9.2 Hz), 7.16 (d, 1H, J = 2.4 Hz), 6.89 (dd, 1H, J = 9.2, 2.4 Hz), 4.15 (q, 2H, J = 7.2 Hz), 3.84 (s, 3H), 3.31 (dd, 1H, J = 15.6, 7.2 Hz), 3.13 (m, 1H), 2.99 (dd, J = 15.6, 7.6 Hz), 1.31 (d, 3H, J = 6.8 Hz), 1.22 (t, 3H, J = 7.2 Hz); ^{13}C NMR (100 MHz, $CDCl_3$) δ 174.9, 165.9, 157.2, 145.5, 142.2, 113.2, 110.6, 103.0, 60.9, 56.1, 37.7, 32.4, 17.2, 14.3; IR (ATR) 2979, 2938, 2907, 2835, 1730, 1571 cm^{-1} ; LRMS (ESI + APCI) m/z $[C_{14}H_{18}NO_4]^+$ ($[M+H]^+$) calcd 264.1, found 264.1.

A.2.17 Mechanistic experiments

A.2.17.1 Synthesis of 1c-D



1c-D. In the glove box, a 1.5 dram vial was charged with $[Rh(cod)OAc]_2$ (27.5 mg, 0.05 mmol, 2 mol %) and dppe (40.5 mg, 0.10 mmol, 4 mol %). To this was added a solution of **1c** (339 mg, 300 μ L, 2.55 mmol, 1.0 equiv) in PhMe (2000 μ L). MeOH- d_4 (910 μ L) was added, and the vial was sealed with a Teflon-lined stir cap. The reaction was removed from the glove box and heated to 120 °C in an aluminum heating block for 24 h. At this point, the crude reaction mixture was adsorbed onto silica gel and purified by flash column chromatography (7:1 Hex:EtOAc). The obtained product **1c-H/D** was subjected to the same reaction, purification sequence 3 times more until < 95% azole 1H was observed by 1H NMR spectroscopy (Figure A.2.6).

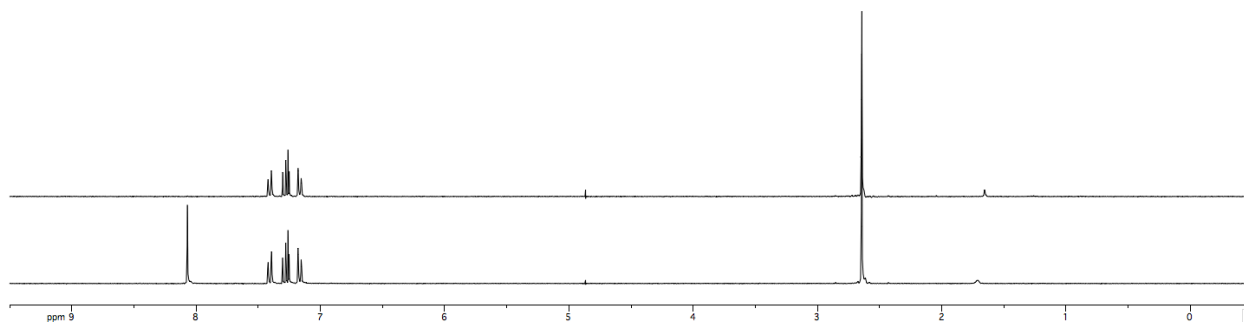


Figure A.2.6 ^1H NMR spectrum of **1c-D** (top) and **1c** (bottom) in CDCl_3

A.2.17.2 Reaction of **1c-D** and **3a** in CH_3CN (Chapter 2, Figure 2.7, eq. 12)

Reaction set-up: In the glove box, a 1.5 dram vial containing $[\text{Rh}(\text{cod})\text{OAc}]_2$ (6.8 mg, 12.6 μmol , 5 mol %) and CTH-(*R*)-xylyl-P-Phos (18.9 mg, 25.2 μmol , 10 mol %) was charged with a solution of **1c-D** (32.6 mg, 0.25 mmol, 1.0 equiv) and DTBB (6.6 mg, 25.0 μmol , 0.10 equiv) in 500 μL CH_3CN . Ethyl methacrylate (**3a**) (228 mg, 250 μL , 2.0 mmol, 8.0 equiv) was added, and the vial was sealed with a Teflon-lined stir cap. The reaction was removed from the glove box and heated to 100 $^\circ\text{C}$ in an aluminum block for 12 h.

Percent yield and percent ee determination: Percent yield and percent ee of **4ca** was determined by LC analysis of the crude reaction mixture on a chiral stationary phase as described above for initial reaction optimization (A.2.12.2). **4ca**: 42%, 96% ee

Determination of percent ^1H incorporation in **1c:** Percent ^1H incorporation in **1c** was determined by ^1H NMR analysis of the crude reaction mixture (Figure A.2.7).

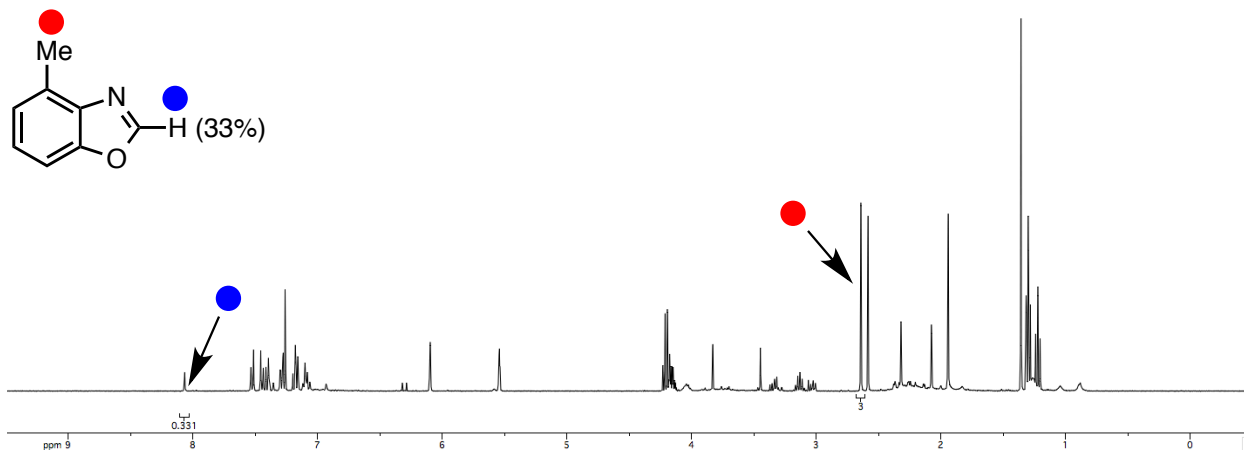


Figure A.2.7 Percent ^1H incorporation in **1c** determined by ^1H NMR analysis of crude reaction mixture (Chapter 2, Figure 2.7, eq. 12)

Determination of percent deuterium incorporation in 4ca: Percent ^2H incorporation in product **4ca** was determined by ^1H NMR analysis of pure **4ca** obtained by flash column chromatography on silica gel (2 x 7:1 Hex:EtOAc) (Figure A.2.8).

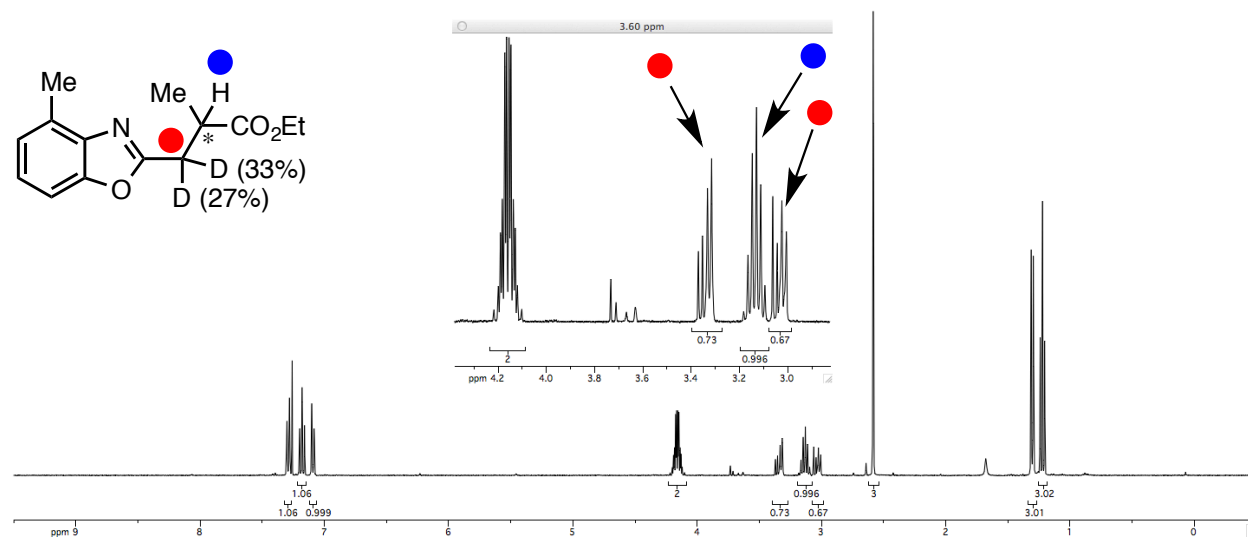


Figure A.2.8 Percent ^2H incorporation in **4ca** determined by ^1H NMR analysis of pure **4ca** (Chapter 2, Figure 2.7, eq. 12)

A.2.17.3 Reaction of **1c-D** and **3a** in CD_3CN (Chapter 2, Figure 2.7, eq. 13)

Reaction set-up: In the glove box, a 1.5 dram vial containing $[\text{Rh}(\text{cod})\text{OAc}]_2$ (6.8 mg, 12.6 μmol , 5 mol %) and CTH-(*R*)-xylyl-P-Phos (18.9 mg, 25.2 μmol , 10 mol %) was charged with a solution of **1c-D** (32.6 mg, 0.25 mmol, 1.0 equiv) and DTBB (6.6 mg, 25.0 μmol , 0.10 equiv) in 500 μL CD_3CN . Ethyl methacrylate (**3a**) (228 mg, 250 μL , 2.0 mmol, 8.0 equiv) was added, and the vial was sealed with a Teflon-lined stir cap. The reaction was removed from the glove box and heated to 100 $^\circ\text{C}$ in an aluminum block for 12 h.

Percent yield and percent ee determination: Percent yield and percent ee of **4ca** was determined by LC analysis of the crude reaction mixture on a chiral stationary phase as described above for initial reaction optimization (A.2.12.2). **4ca**: 47%, 96% ee

Determination of percent ^1H incorporation in 1c: Percent ^1H incorporation in **1c** was determined by ^1H NMR analysis of the crude reaction mixture (Figure A.2.9).

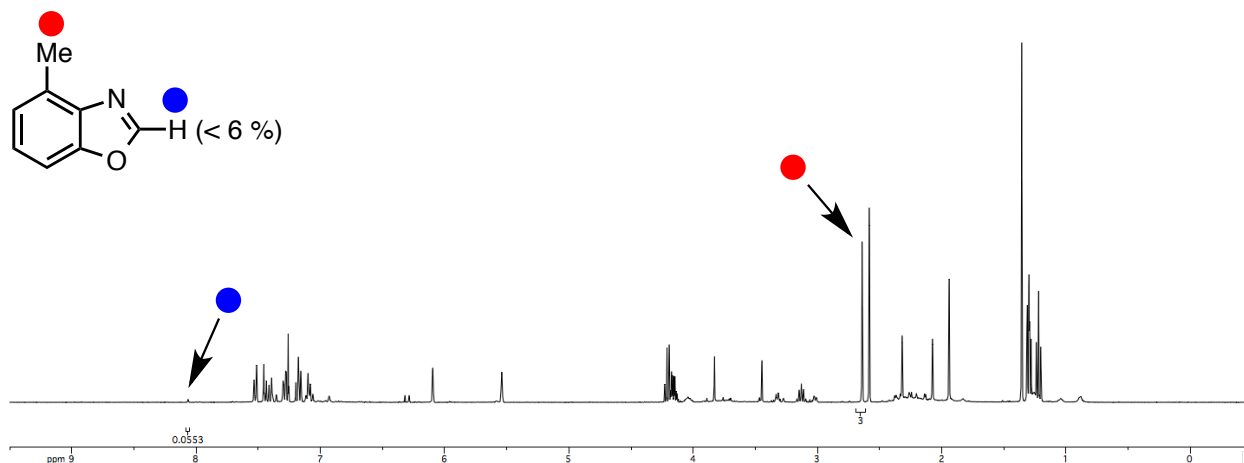


Figure A.2.9 Percent ^1H incorporation in **1c** determined by ^1H NMR analysis of crude reaction mixture (Chapter 2, Figure 2.7, eq. 13)

Determination of percent deuterium incorporation in 4ca: Percent ^2H incorporation in product **4ca** was determined by ^1H NMR analysis of pure **4ca** obtained by flash column chromatography on silica gel (2 x 7:1 Hex:EtOAc) (Figure A.2.10).

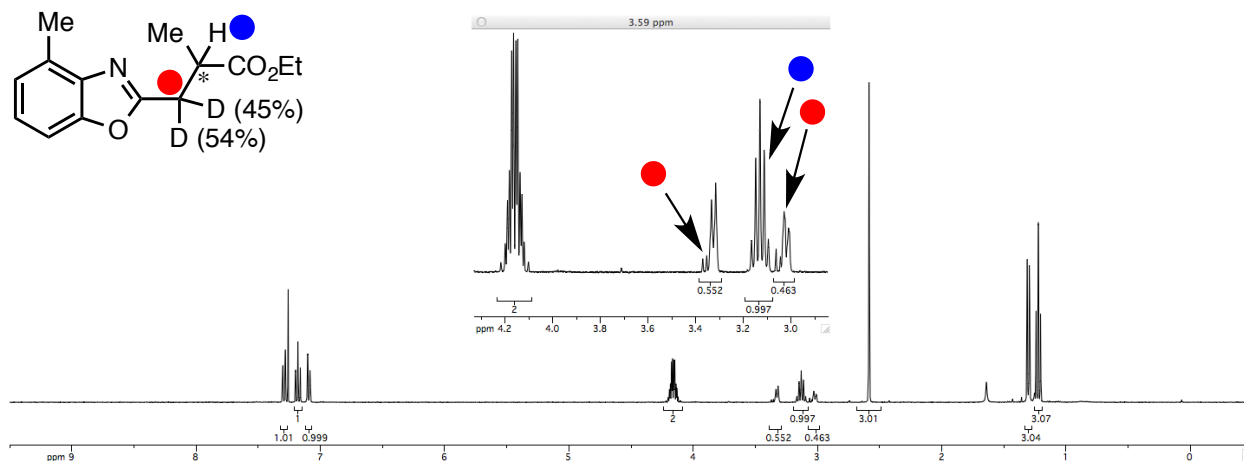


Figure A.2.10 Percent ^2H incorporation in **4ca** determined by ^1H NMR analysis of pure **4ca** (Chapter 2, Figure 2.7, eq. 13)

A.2.17.4 Reaction of **1c** and **3b-d₈** in CH_3CN (Chapter 2, Figure 2.7, eq. 14)

Reaction set-up: In the glove box, a 1.5 dram vial containing $[\text{Rh}(\text{cod})\text{OAc}]_2$ (6.8 mg, 12.6 μmol , 5 mol %) and CTH-(*R*)-xylyl-P-Phos (18.9 mg, 25.2 μmol , 10 mol %) was charged with a solution of **1c** (32.0 mg, 0.25 mmol, 1.0 equiv) and DTBB (6.6 mg, 25.0 μmol , 0.10 equiv) in 500 μL CH_3CN . Ethyl methacrylate (**3b-d₈**) (216 mg, 214 μL , 2.0 mmol, 8.0 equiv) was added, and the vial was sealed with a Teflon-lined stir cap. The reaction was removed from the glove box and heated to 100 $^\circ\text{C}$ in an aluminum block for 26 h.

Percent yield and percent ee determination: Percent ee of **4cb** was determined by LC analysis on a chiral stationary phase as described above for initial reaction optimization (A.2.12.2). Percent yield of **4cb** was determined with respect to DTBB by ^1H NMR analysis of the crude reaction mixture.

Determination of percent ^1H incorporation in **4ca:** Percent ^1H incorporation in product **4cb** was determined by ^1H NMR analysis of pure **4cb** obtained by flash column chromatography on silica gel (7:1 Hex:EtOAc) (Figure A.2.11).

*Note: The total percent ^1H incorporation in **4cb** exceeds the one hundred percent that would be expected were **1c** the only ^1H source. We account for greater than one hundred percent ^1H incorporation by invoking reversible C–H activation at the β -position of product **4cb** and protonation with CH_3CN (vide infra, section A.2.17.6).*

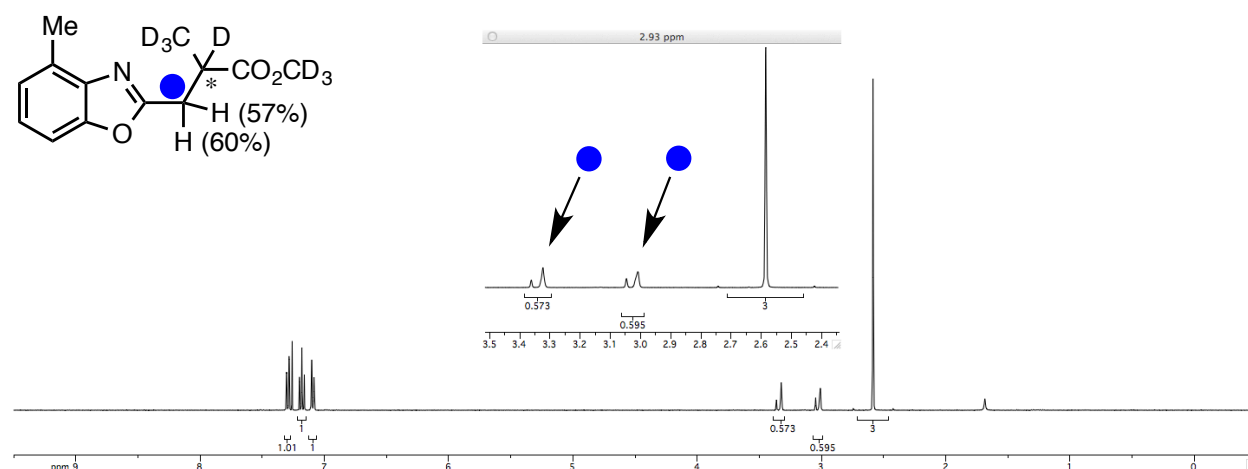


Figure A.2.11 Percent ^1H incorporation in **4cb** determined by ^1H NMR analysis of pure **4cb** (Chapter 2, Figure 2.7, eq. 14)

A.2.17.5 Epimerization experiments (Chapter 2, Figure 2.9, eq. 15–17)

A.2.17.5.1 General procedure

In the glove box, a 1.5 dram vial containing $[\text{Rh}(\text{cod})\text{OAc}]_2$ (3.4 mg, 6.3 μmol , 5 mol %), CTH-(*R*)-xylyl-P-Phos (9.5 mg, 12.6 μmol , 10 mol %) was charged with a solution of **1c** (16.6 mg, 15.0 μL , 0.125 mmol, 1.0 equiv), DTBB (3.3 mg, 12.5 μmol , 0.10 equiv) and **4** (0.063 mmol, 0.5 equiv) in 250 μL CH_3CN . The appropriate acrylate **3** (1.0 mmol, 8.0 equiv) was added, and the vial was sealed with a Teflon-lined stir cap. The reaction was removed from the glove box and heated to 100 $^\circ\text{C}$ in an aluminum block for 48 h. Percent yield and percent ee of products **4** were determined from the crude reaction mixture as described below.

A.2.17.5.2 A note on HPLC retention times

Slight variation in retention time across products **4** is sometimes observed. We attribute this at least in part to the very low polarity of typical column conditions. We use a premade solution of 10 % iPrOH in Hex as the polar component. The concentration of this mixture can vary from batch to batch. Moreover, polar solvents such as CD₃CN or CDCl₃ introduced from the crude reaction or from NMR samples can discernably modify retention times.

A.2.17.5.3 A note on HPLC analysis of racemic mixtures (see also section A.2.19)

We make racemic CTH-xylyl-P-Phos (*rac*-**L11**) *in situ* by mixing small (< 10 mg) quantities of (*R*)- and (*S*)-**L11**. Racemic samples prepared in this way can have ees up to three percent. In general, the major enantiomer prepared from *in situ rac*-**L11** is the same as that when (*R*) catalyst is used. This pattern may simply be random, or it could arise from differences in purity or physical properties between catalysts (while the *R*-catalyst is a fine, free-flowing white power that is easily weighed, the *S* catalyst is a clumpy yellow solid that is difficult to weigh).

A.2.17.5.4 Reaction of **1c**, **3a** and **4ha** (77% ee) (Chapter 2, Figure 2.9, eq. 15)

DTBB, **1c**, **3a**, both enantiomers of **4ha** and both enantiomers of **4ca** are all separable on Chiracel IB column, 94:6 Hex:10% iPrOH in Hex, 1 mL/min:

DTBB: 3.4 min

Ethyl methacrylate (**3a**): 3.9 min (**3a** has a very low absorbance)

4-methylbenzoxazole (**1c**): 6.2 min

First enantiomer **4ca**: 7.6 min (minor)

Second enantiomer **4ca**: 8.5 min (major)

First enantiomer **4ha**: 17.5 min (minor)

Second enantiomer **4ha**: 19.0 min (major)

Percent ee of **4ca** and **4ha** were determined by HPLC analysis (see HPLC data on next page, Figure A.2.12).

Percent yield 4ca was determined by HPLC analysis with respect to DTBB as described in initial reaction optimization (A.2.12.2).

Percent yield 4ha was determined with respect to DTBB by ¹H NMR.

Results:

w/o CsOAc—**4ca**: 70%, 95% ee; **4ha**: > 95%, 50% ee

w/ 25 mol % CsOAc—**4ca**: 81%, 95% ee; **4ha**: > 95%, 50% ee

Injection Date : 10/1/2014 10:18:37 AM Seq. Line : 2
 Sample Name : 5-9-CF_pure Location : Vial 51
 Acq. Operator : Inj : 1
 Acq. Instrument : Instrument 1 Inj Volume : 10 µl
 Different Inj Volume from Sequence ! Actual Inj Volume : 2 µl
 Acq. Method : C:\CHEM32\1\METHODS\ODH 93-7 HEX-10-1-HEX-IPA 15 MIN.M
 Last changed : 10/1/2014 10:08:22 AM
 (modified after loading)
 Analysis Method : C:\CHEM32\1\METHODS\IC 80-20 1ML-1UL 40MIN.M
 Last changed : 12/2/2014 7:06:11 AM
 (modified after loading)

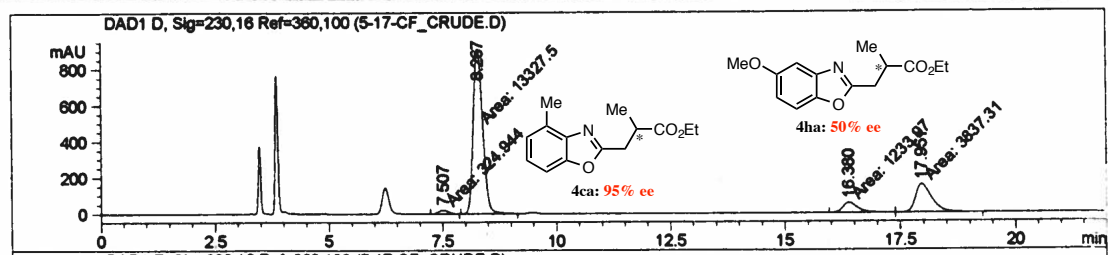
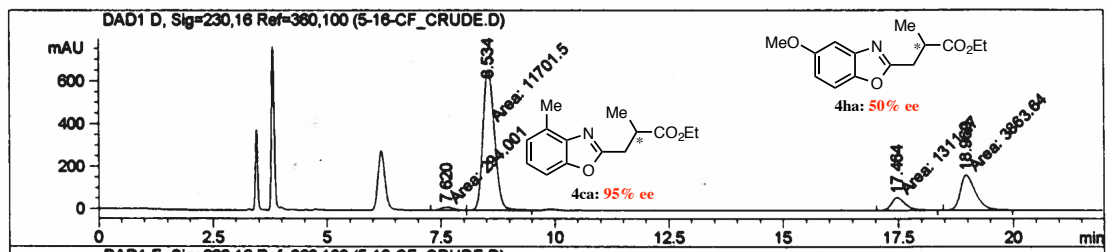
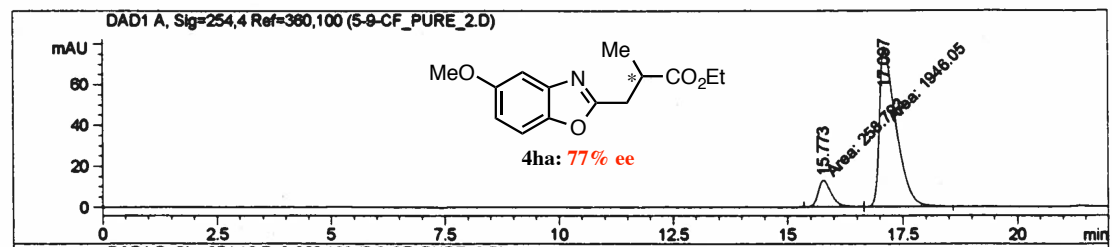


Figure A.2.12 HPLC data from epimerization study of **4ha** in presence of **1c** and **3a** (Chapter 2, Figure 2.9, eq. 15).
 Top: pure **4ha** (77% ee); Middle: reaction mixture w/o CsOAc; Bottom: reaction mixture w/ CsOAc

A.2.17.5.5 Reaction of 1c, 3a and 4ga (88% ee) (Chapter 2, Figure 2.9, eq. 16)

Percent yield and percent ee **4ca** were determined as for the reaction of **1c**, **3a** and **4ha** above (A.2.17.5.4 and A.2.12.2). Note: Both enantiomers of **4ga** elute after 20 min using Chiracel IB column, 94:6 Hex:10% iPrOH in Hex, 1 mL/min.

For ee analysis of **4ca**, see Figure A.2.13 below.

Percent ee **4ga** was determined by HPLC analysis: Chiracel IC column, 90:10 Hex:iPrOH, 1 mL/min:

First enantiomer **4ga**: 13.8 min (minor)

Second enantiomer **4ga**: 14.8 min (major)

DTBB, **1c**, **3a** and **4ca** elute before 7.5 min.

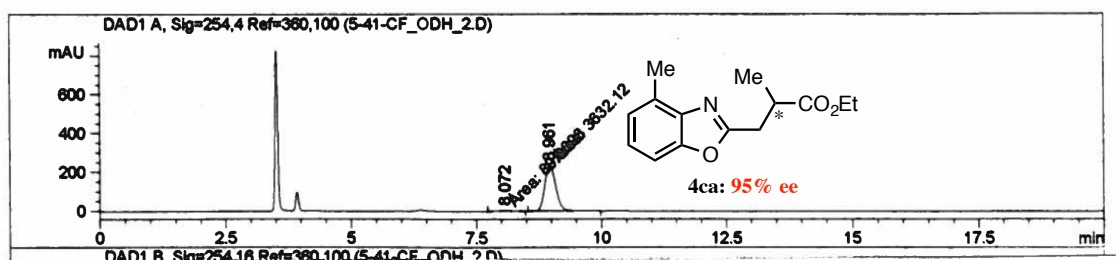
For ee analysis of **4ga**, see Figure A.2.14 on next page.

Percent yield **4ga** was determined with respect to DTBB by ^1H NMR.

Results: **4ca**: > 95%, 95% ee; **4ga**: > 95%, 74% ee

Data File C:\CHEM32\1\DATA\5-41-CF_ODH_2.D
Sample Name: 5-41-CF

```
=====
Injection Date : 10/27/2014 8:01:53 PM      Seq. Line : 3
Sample Name    : 5-41-CF                  Location  : Vial 2
Acq. Operator  :                          Inj      : 1
Acq. Instrument : Instrument 1             Inj Volume: 10 µl
Different Inj Volume from Sequence !      Actual Inj Volume : 2 µl
Acq. Method    : C:\CHEM32\1\METHODS\ODH 94-6 HEX-10-1-HEX-IPA 25 MIN.M
Last changed   : 10/23/2014 8:24:54 PM
Analysis Method : C:\CHEM32\1\METHODS\IC 80-20 1ML-1UL 40MIN.M
Last changed   : 12/2/2014 7:43:31 AM
                  (modified after loading)
=====
```

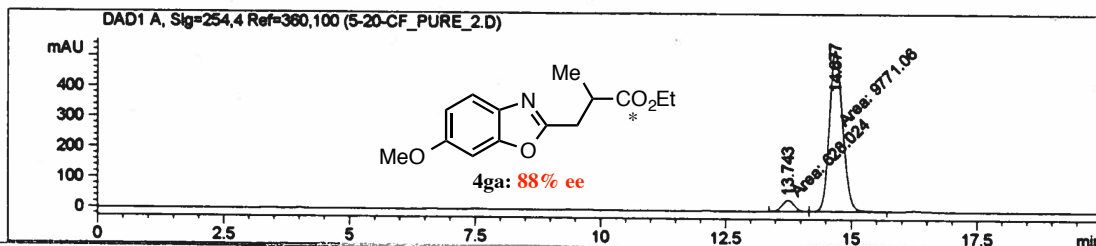


Peak #	RetTime [min]	Type	Width [min]	Area [mAU*s]	Height [mAU]	Area %
1	8.072	MM	0.2903	89.00981	5.11051	2.3920
2	8.961	MM	0.2588	3632.11841	233.94763	97.6080

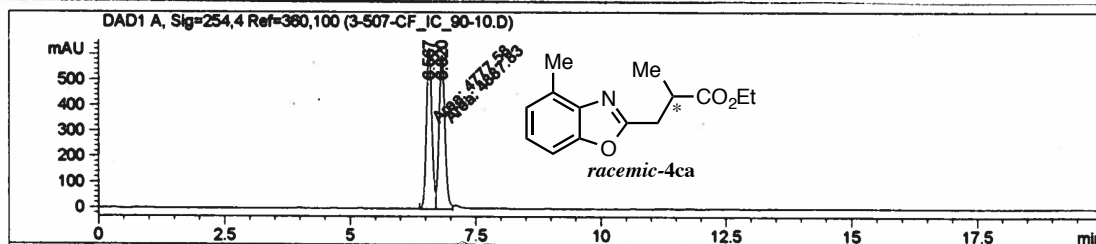
Figure A.2.13 HPLC data from epimerization study of **4ga** in the presence of **1c** and **3a** (Chapter 2, Figure 2.9, eq. 16). Crude reaction mixture under conditions that separate enantiomers of **4ca**. Note: Both enantiomers of **4ga** elute after 20 min under these column conditions

Data File C:\CHEM32\1\DATA\5-20-CF_PURE_2.D
 Sample Name: 5-20-CF_pure

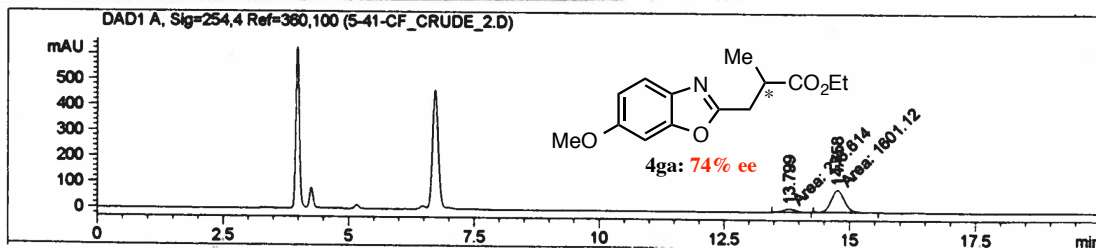
```
=====
Injection Date : 10/17/2014 2:25:27 PM      Seq. Line :    5
Sample Name    : 5-20-CF_pure                Location  : Vial 4
Acq. Operator  :                             Inj       :    1
Acq. Instrument: Instrument 1                 Inj Volume: 1 µl
Different Inj Volume from Sequence !         Actual Inj Volume: 2 µl
Acq. Method    : C:\CHEM32\1\METHODS\IC 90-10 1ML-1UL 20MIN.M
Last changed   : 8/21/2014 7:51:32 AM
Analysis Method: C:\CHEM32\1\METHODS\IC 80-20 1ML-1UL 40MIN.M
Last changed   : 12/2/2014 7:43:31 AM
                    (modified after loading)
=====
```



Peak #	RetTime [min]	Type	Width [min]	Area [mAU*s]	Height [mAU]	Area %
1	13.743	MM	0.2794	628.02368	37.46505	6.0392
2	14.677	MM	0.3080	9771.06152	528.75690	93.9608



Peak #	RetTime [min]	Type	Width [min]	Area [mAU*s]	Height [mAU]	Area %
1	6.567	MM	0.1259	4777.57715	632.45520	49.4296
2	6.820	MM	0.1343	4887.83496	606.73096	50.5704



Peak #	RetTime [min]	Type	Width [min]	Area [mAU*s]	Height [mAU]	Area %
1	13.799	MM	0.2934	238.61444	13.55513	12.9700
2	14.758	MM	0.3106	1601.12207	85.91681	87.0300

Figure A.2.14 HPLC data from epimerization study of **4ga** in the presence of **1c** and **3a** (Chapter 2, Figure 2.9, eq. 16). Top: pure **4ga** (88% ee); Middle: racemic **4ca**; Bottom: crude reaction mixture. Note: ee data for **4ca** was obtained under conditions that give better separation for **4ca** (see Figure A.2.13 above)

A.2.17.5.6 Reaction of 1c, 3c and 4ca (95% ee) (Chapter 2, Figure 2.9, eq. 17)

Relevant species are all separable under column conditions used for initial reaction optimization (A.2.12.2):

DTBB: 3.4 min

3c: 4.8 min

4-methylbenzoxazole (**1c**): 6.2 min

First enantiomer **4ca**: 7.6 min (minor)

Second enantiomer **4ca**: 8.5 min (major)

First enantiomer **4cc**: 13.6 min (minor)

Second enantiomer **4cc**: 19.1 min (major)

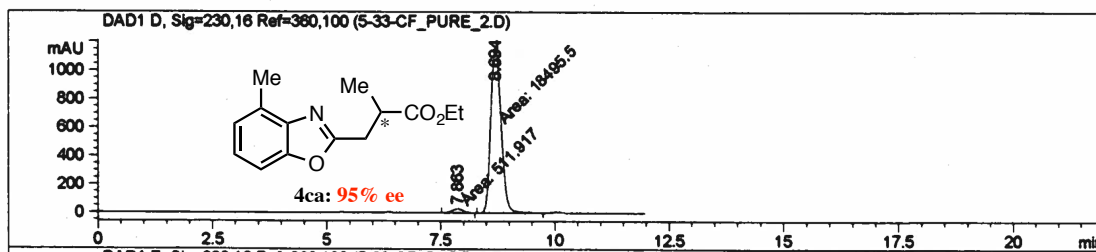
Percent yield and percent ee 4ca were determined as for the reaction of **1c**, **3a** and **4ha** above (A.2.17.5.4 and A.2.12.2) (see Figure A.2.15 on next page).

Percent ee 4cc was determined by HPLC analysis (see Figure A.2.15 on next page), and **percent yield 4cc** was determined with respect to DTBB by ¹H NMR.

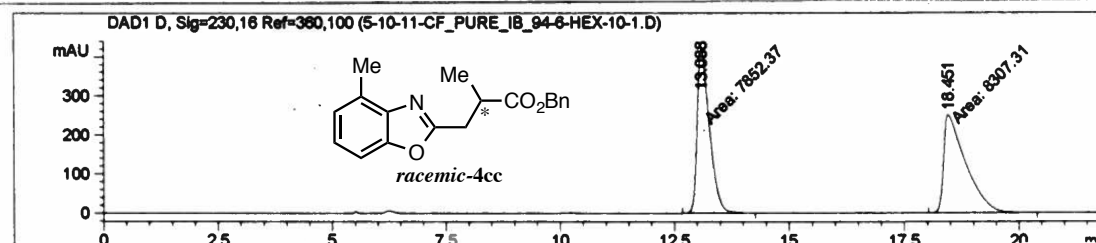
Results: 4cc: > 95%, 90% ee; **4ca**: > 95%, 93% ee

Data File C:\CHEM32\1\DATA\5-33-CF_PURE_2.D
Sample Name: 5-33-CF_pure

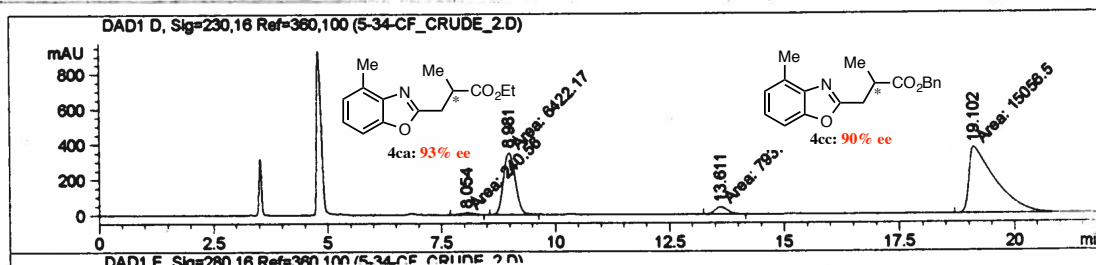
```
=====
Injection Date : 10/20/2014 12:28:28 PM      Seq. Line :    6
Sample Name    : 5-33-CF_pure                Location  : Vial 3
Acq. Operator  :                             Inj      :    1
Acq. Instrument: Instrument 1                 Inj Volume: 10 µl
Different Inj Volume from Sequence !         Actual Inj Volume: 2 µl
Acq. Method    : C:\CHEM32\1\METHODS\ODH 94-6 HEX-10-1-HEX-IPA 12 MIN.M
Last changed   : 5/27/2014 11:31:49 AM by TAD
Analysis Method: C:\CHEM32\1\METHODS\IC 80-20 1ML-1UL 40MIN.M
Last changed   : 12/2/2014 7:06:11 AM
                    (modified after loading)
=====
```



Peak #	RetTime [min]	Type	Width [min]	Area [mAU*s]	Height [mAU]	Area %
1	7.863	MM	0.2989	511.91733	28.54807	2.6933
2	8.694	MM	0.2666	1.84955e4	1156.09485	97.3067



Peak #	RetTime [min]	Type	Width [min]	Area [mAU*s]	Height [mAU]	Area %
1	13.088	MM	0.3125	7852.37402	418.76968	48.5924
2	18.451	MM	0.5530	8307.30664	250.35989	51.4076



Peak #	RetTime [min]	Type	Width [min]	Area [mAU*s]	Height [mAU]	Area %
1	8.054	MM	0.3580	240.56030	11.20030	1.0685
2	8.981	MM	0.3070	6422.17188	348.69690	28.5263
3	13.611	MM	0.3204	793.90314	41.30356	3.5264
4	19.102	MM	0.6728	1.50565e4	372.95621	66.8787

Figure A.2.15 HPLC data from epimerization study of 4ca in the presence of 1c and 3c (Chapter 2, Figure 2.9, eq. 17). Top: pure 4ca (95% ee); Middle: racemic 4cc; Bottom: crude reaction mixture

A.2.17.6 Epimerization-labeling experiments of **4ha** and **4ca** in CD₃CN (Chapter 2, Figure 2.11, eq. 18–19)

In the glove box, a 1.5 dram vial containing [Rh(cod)OAc]₂ (3.4 mg, 6.3 μmol, 13 mol %), CTH-(*R*)-xylyl-P-Phos (9.5 mg, 12.6 μmol, 26 mol %) was charged with a solution of **4ha** (75% ee) or **4ca** (95% ee) (0.05 mmol, 1.0 equiv) in 105 μL CD₃CN. The vial was sealed with a Teflon-lined screw cap, removed from the glove box and heated to 100 °C in an aluminum block for 48 h. The crude reaction mixture was adsorbed onto silica gel and purified by flash column chromatography—**4ha**: 3:1 Hex:EtOAc and **4ca**: 7:1 Hex:EtOAc. Percent ²H incorporation was determined by ¹H NMR analysis of the pure products (Figure A.2.16–A.2.17). Percent ee **4ha** and **4ca** determined by LC analysis of crude or purified reaction (Figure A.2.18–A.2.19, next page).

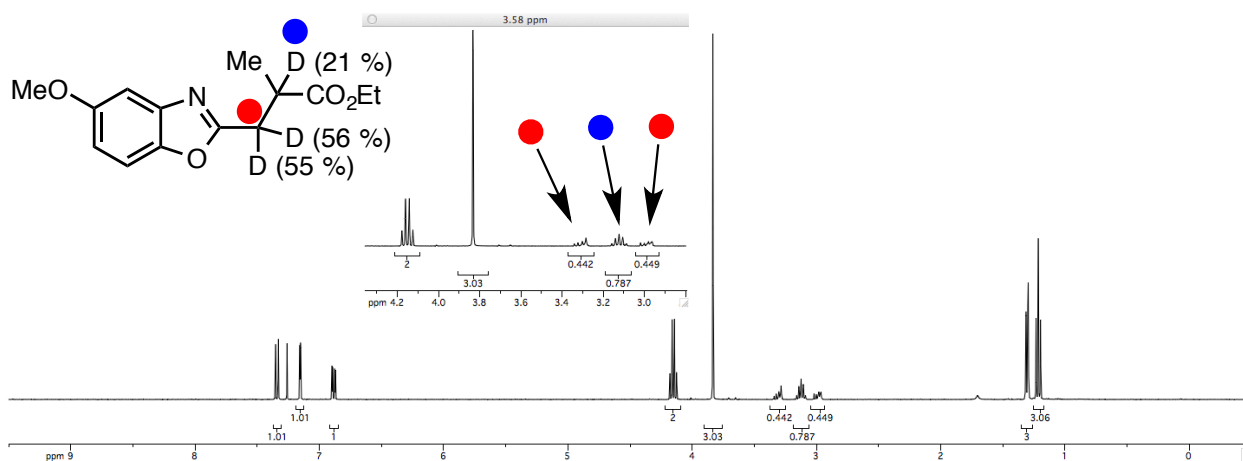


Figure A.2.16 ¹H NMR spectrum of pure **4ha** in CDCl₃ (Chapter 2, Figure 2.11, eq. 18)

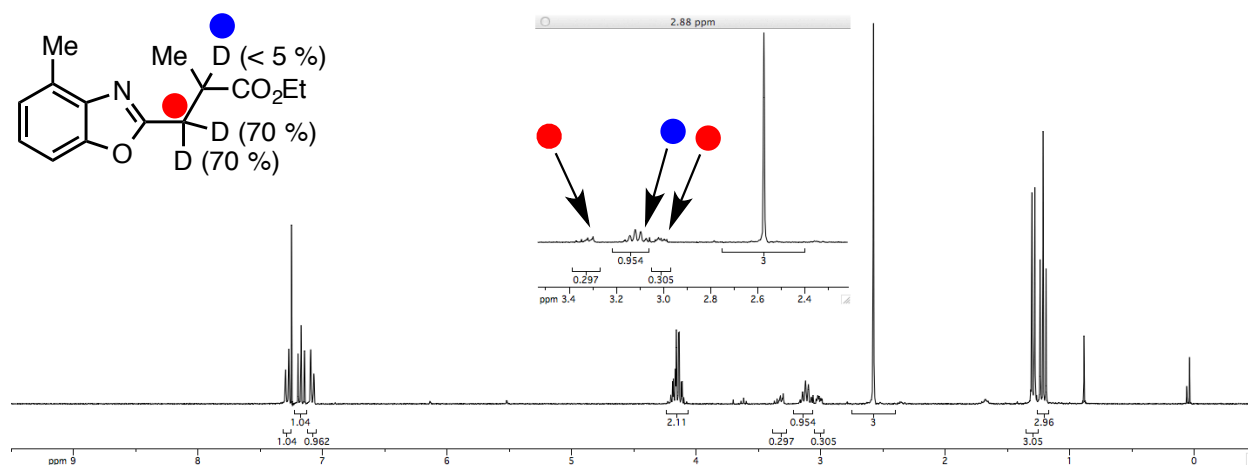
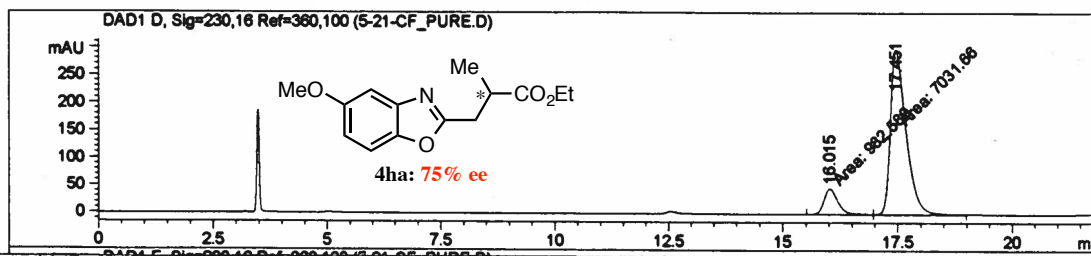


Figure A.2.17 ¹H spectrum of pure **4ca** in CDCl₃ (Chapter 2, Figure 2.11, eq. 19)

Data File C:\CHEM32\1\DATA\5-21-CF_PURE.D

Sample Name: 5-21-CF_pure

```
=====
Injection Date : 10/17/2014 1:09:34 PM      Seq. Line : 2
Sample Name    : 5-21-CF_pure              Location  : Vial 3
Acq. Operator  :                          Inj      : 1
Acq. Instrument: Instrument 1              Inj Volume: 10 µl
Different Inj Volume from Sequence !      Actual Inj Volume : 2 µl
Acq. Method    : C:\CHEM32\1\METHODS\ODH 93-7 HEX-10-1-HEX-IPA 22 MIN.M
Last changed   : 10/1/2014 12:31:18 PM
Analysis Method: C:\CHEM32\1\METHODS\IC 80-20 1ML-1UL 40MIN.M
Last changed   : 12/2/2014 7:06:11 AM
              (modified after loading)
=====
```

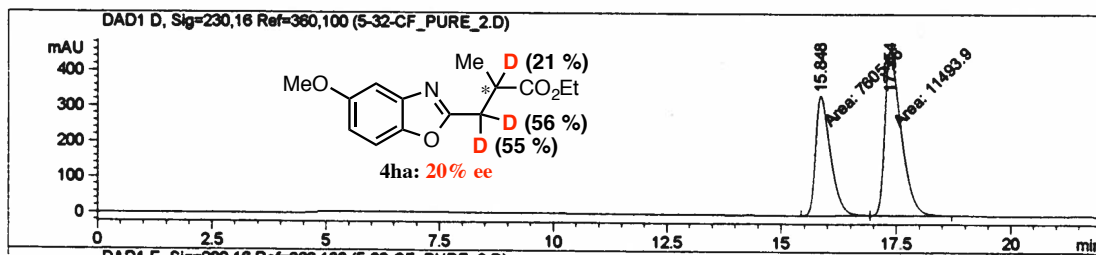


Peak #	RetTime [min]	Type	Width [min]	Area [mAU*s]	Height [mAU]	Area %
1	16.015	MM	0.3500	982.58887	46.79169	12.2605
2	17.451	MM	0.3928	7031.66162	298.32571	87.7395

Data File C:\CHEM32\1\DATA\5-32-CF_PURE_2.D

Sample Name: 5-32-CF_pure

```
=====
Injection Date : 10/20/2014 9:22:35 PM      Seq. Line : 8
Sample Name    : 5-32-CF_pure              Location  : Vial 6
Acq. Operator  :                          Inj      : 1
Acq. Instrument: Instrument 1              Inj Volume: 10 µl
Different Inj Volume from Sequence !      Actual Inj Volume : 3 µl
Acq. Method    : C:\CHEM32\1\METHODS\ODH 93-7 HEX-10-1-HEX-IPA 22 MIN.M
Last changed   : 10/1/2014 12:31:18 PM
Analysis Method: C:\CHEM32\1\METHODS\IC 80-20 1ML-1UL 40MIN.M
Last changed   : 12/2/2014 7:06:11 AM
              (modified after loading)
=====
```

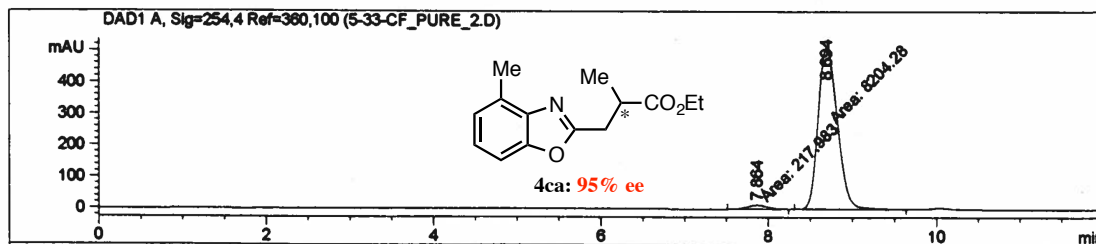


Peak #	RetTime [min]	Type	Width [min]	Area [mAU*s]	Height [mAU]	Area %
1	15.848	MM	0.3766	7605.65967	336.58133	39.8211
2	17.354	MM	0.4139	1.14939e4	462.82819	60.1789

Figure A.2.18 HPLC data from epimerization reaction of **4ha** in CD₃CN (Chapter 2, Figure 2.11, eq. 18). Top: **4ha** (spiked with DTBB) 75% ee; Bottom: purified **4ha** (20% ee) after reaction (Chapter 2, Figure 2.11, eq. 18)

Data File C:\CHEM32\1\DATA\5-33-CF_PURE_2.D
Sample Name: 5-33-CF_pure

```
=====
Injection Date : 10/20/2014 12:28:28 PM      Seq. Line : 6
Sample Name    : 5-33-CF_pure                Location : Vial 3
Acq. Operator  :                             Inj : 1
Acq. Instrument : Instrument 1                Inj Volume : 10 µl
Different Inj Volume from Sequence !          Actual Inj Volume : 2 µl
Acq. Method    : C:\CHEM32\1\METHODS\ODH 94-6 HEX-10-1-HEX-IPA 12 MIN.M
Last changed   : 5/27/2014 11:31:49 AM by TAD
Analysis Method : C:\CHEM32\1\METHODS\IC 80-20 1ML-1UL 40MIN.M
Last changed   : 12/2/2014 7:55:59 AM
                    (modified after loading)
=====
```



Data File C:\CHEM32\1\DATA\5-44-CF_CRUDE_2.D
Sample Name: 5-44-CF_crude

```
=====
Injection Date : 10/30/2014 4:40:05 PM      Seq. Line : 1
Sample Name    : 5-44-CF_crude              Location : Vial 4
Acq. Operator  :                             Inj : 1
Acq. Instrument : Instrument 1                Inj Volume : 10 µl
Different Inj Volume from Sequence !          Actual Inj Volume : 3 µl
Acq. Method    : C:\CHEM32\1\METHODS\ODH 94-6 HEX-10-1-HEX-IPA 15 MIN.M
Last changed   : 1/10/2014 8:22:21 PM by tad
Analysis Method : C:\CHEM32\1\METHODS\IC 80-20 1ML-1UL 40MIN.M
Last changed   : 12/2/2014 7:55:59 AM
                    (modified after loading)
=====
```

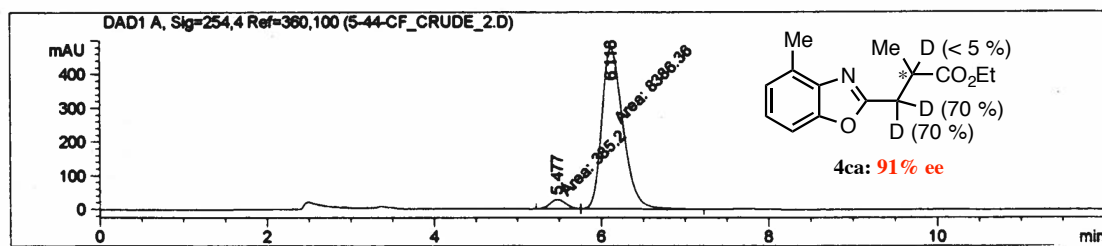
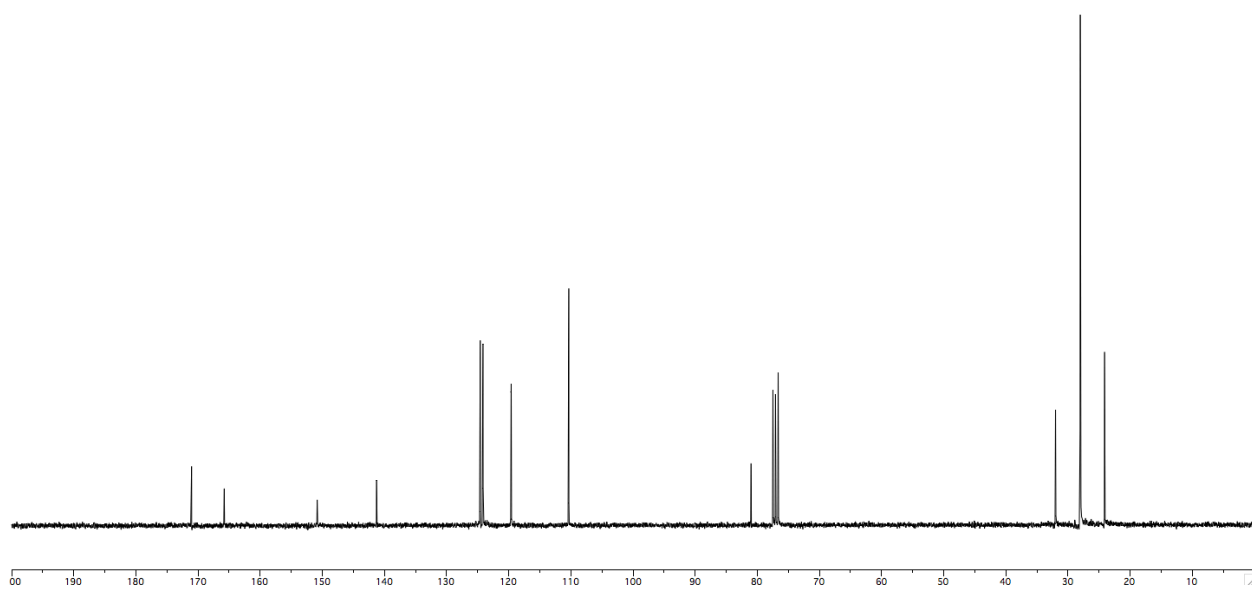
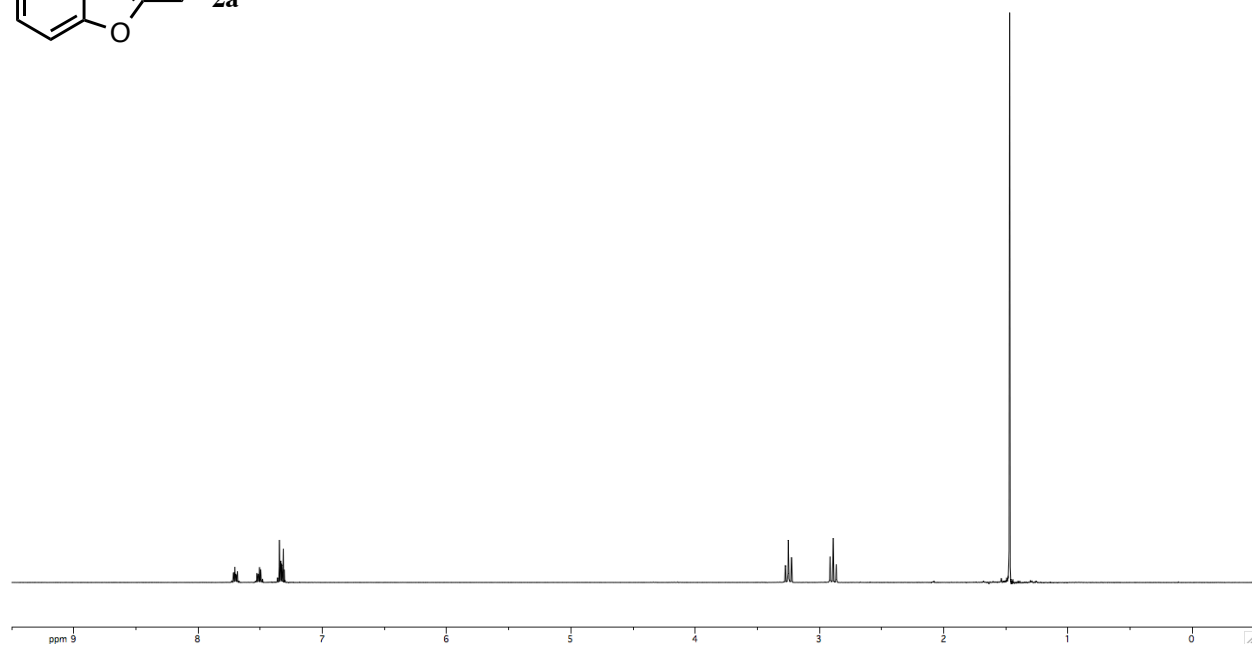
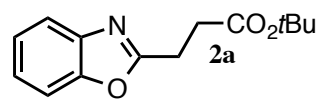
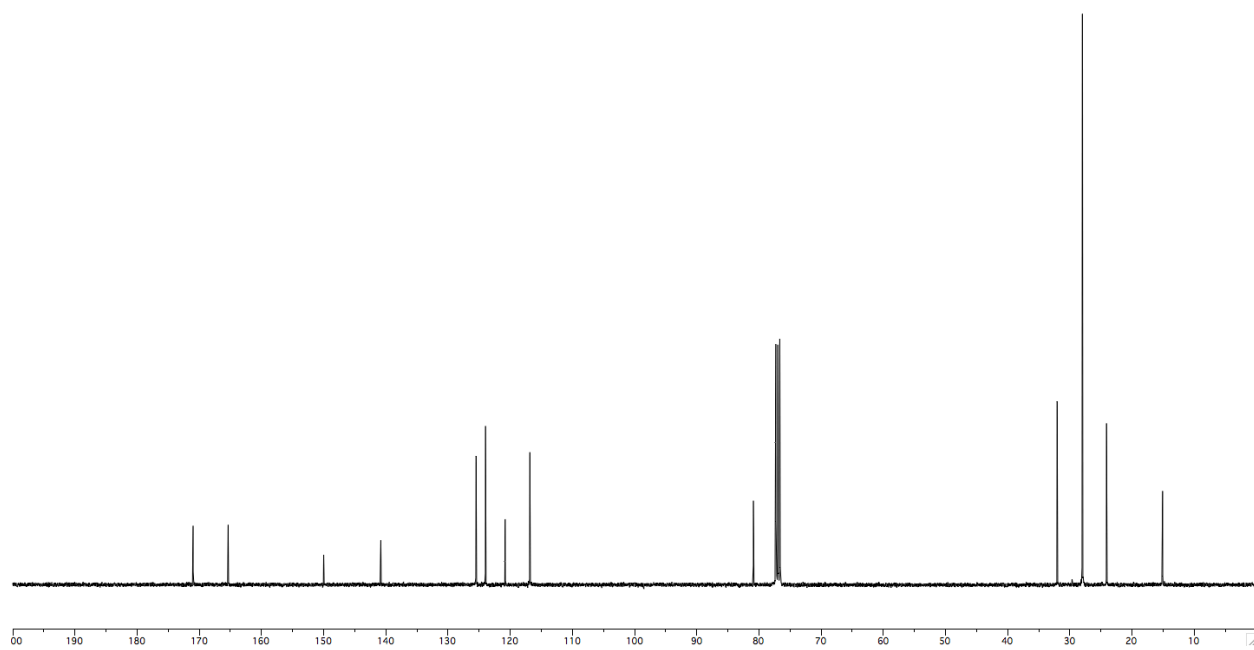
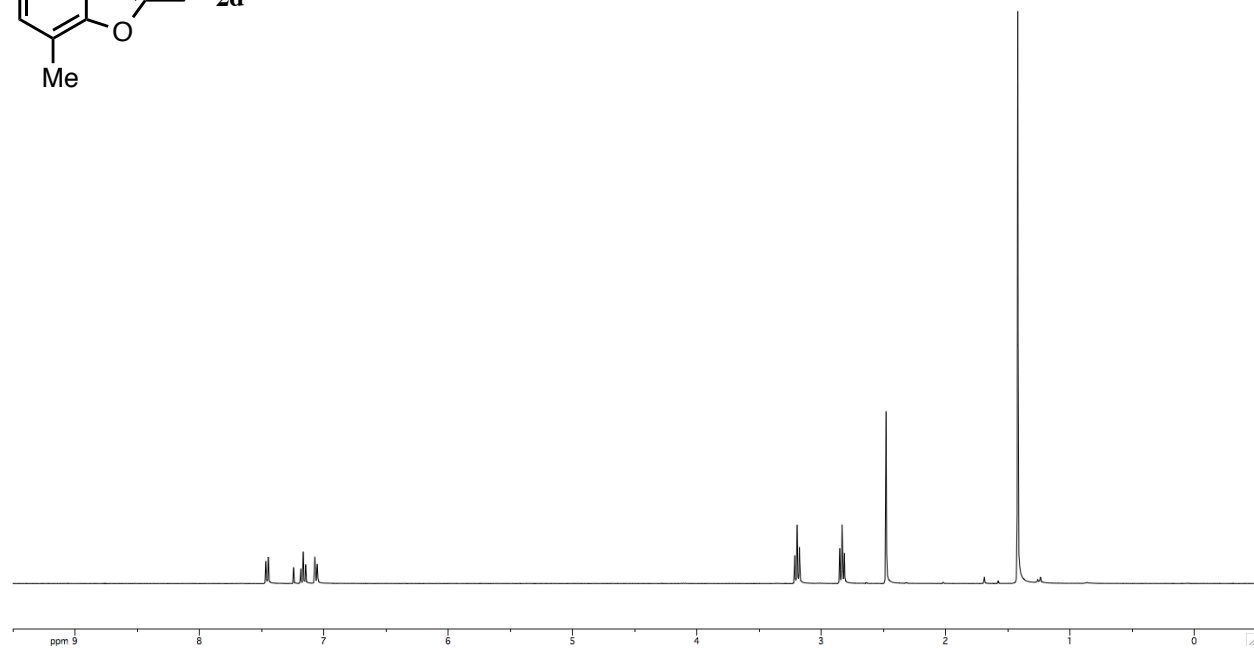
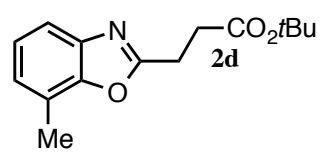
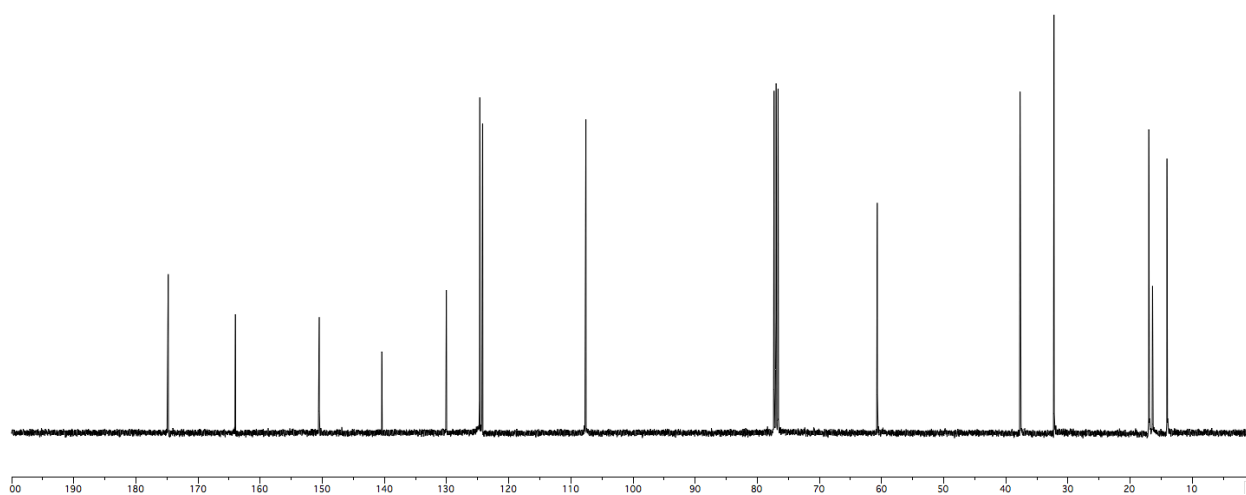
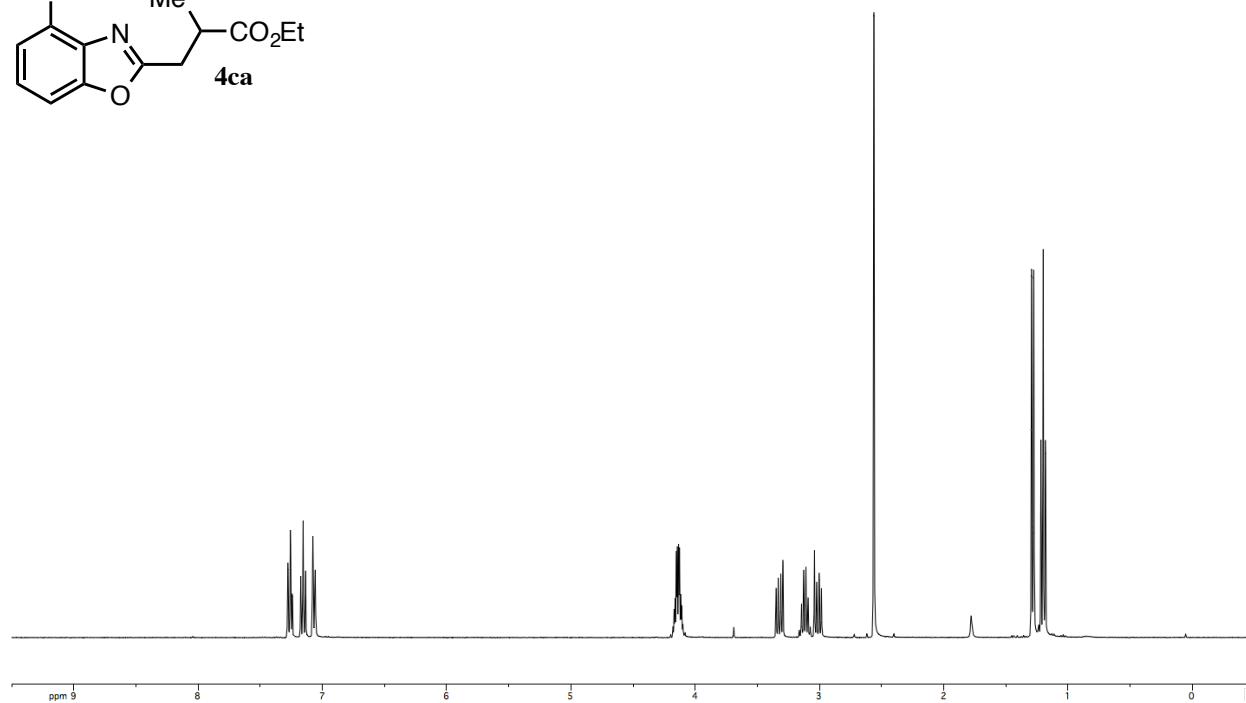
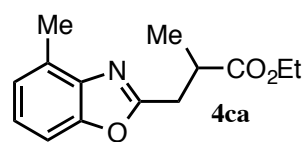
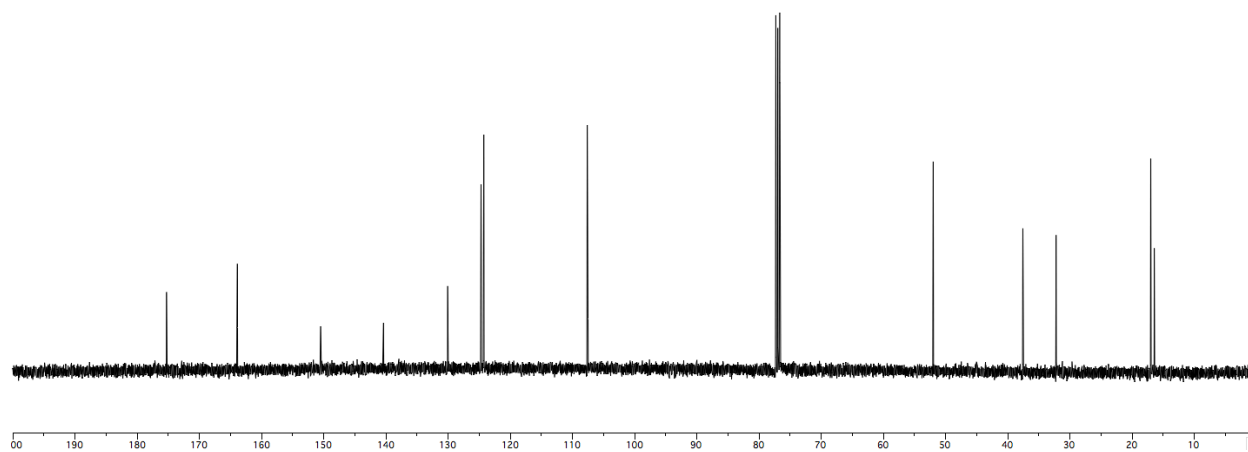
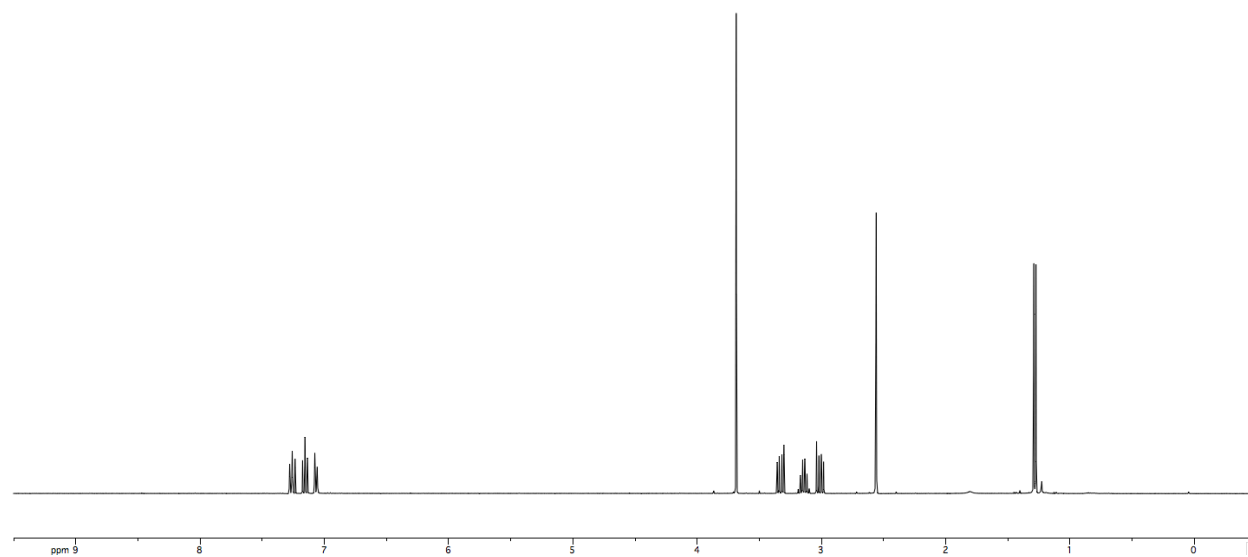
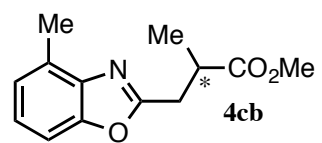


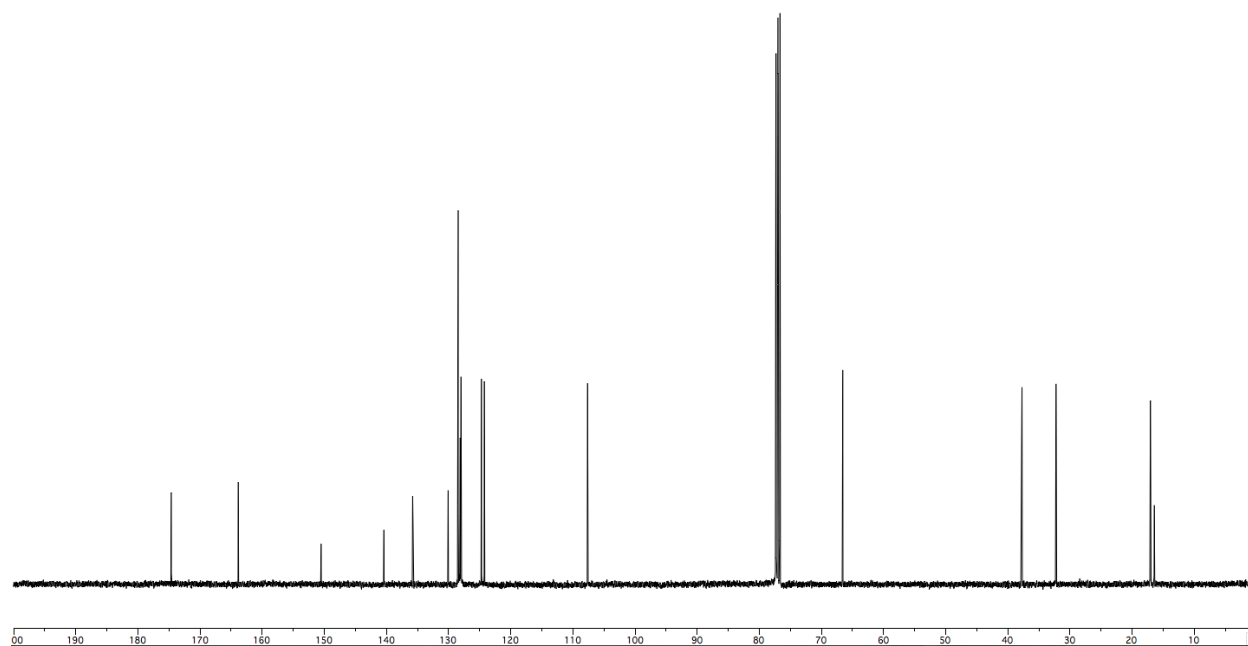
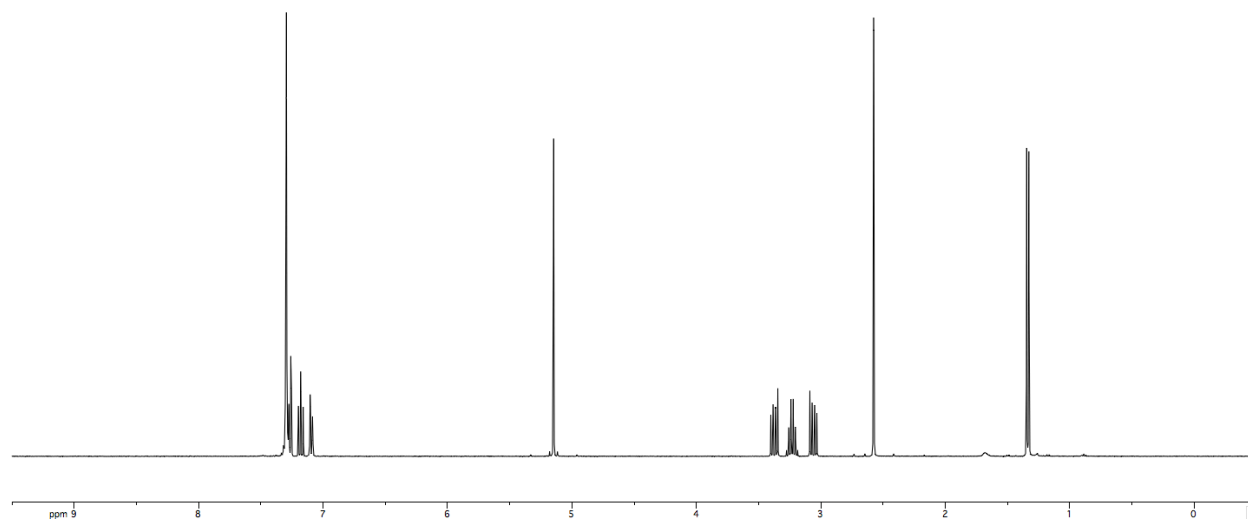
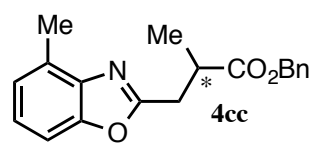
Figure A.2.19 HPLC data from epimerization reaction of **4ca** in CD₃CN (Chapter 2, Figure 2.11, eq. 19). Top: **4ca** (95% ee); Bottom: crude **4ca** (91% ee) after reaction (Chapter 2, Figure 2.11, eq. 19)

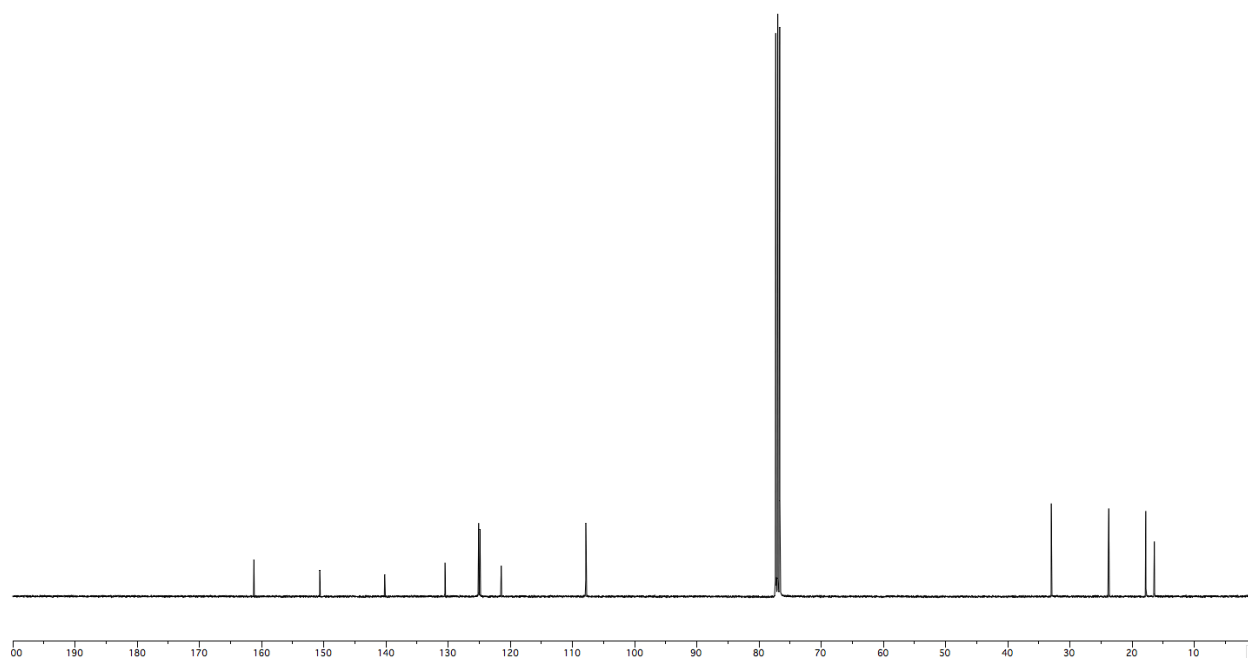
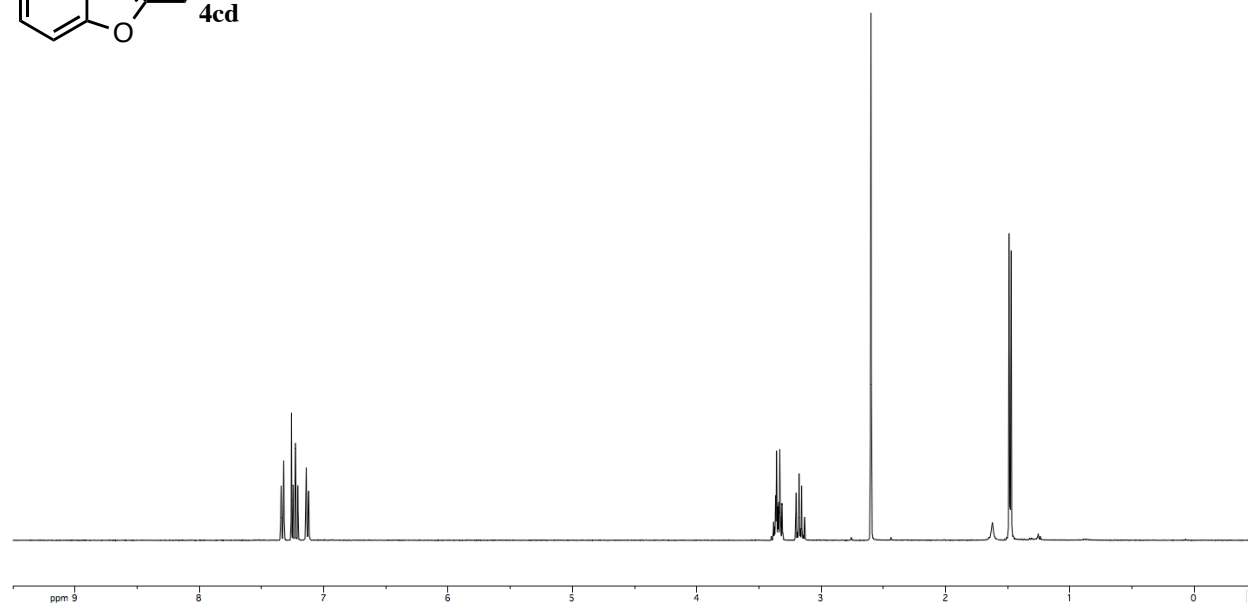
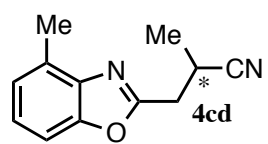


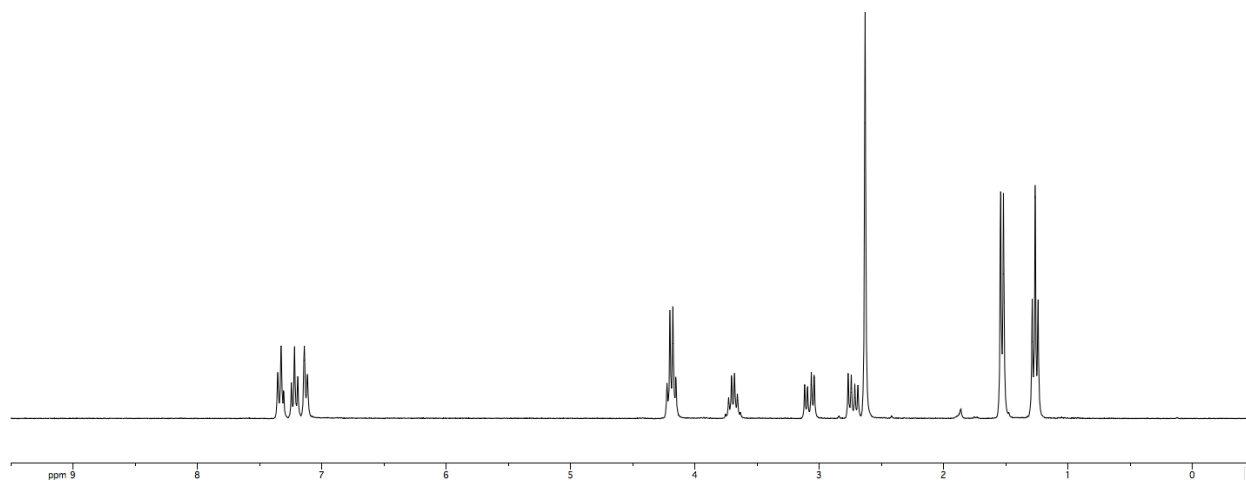


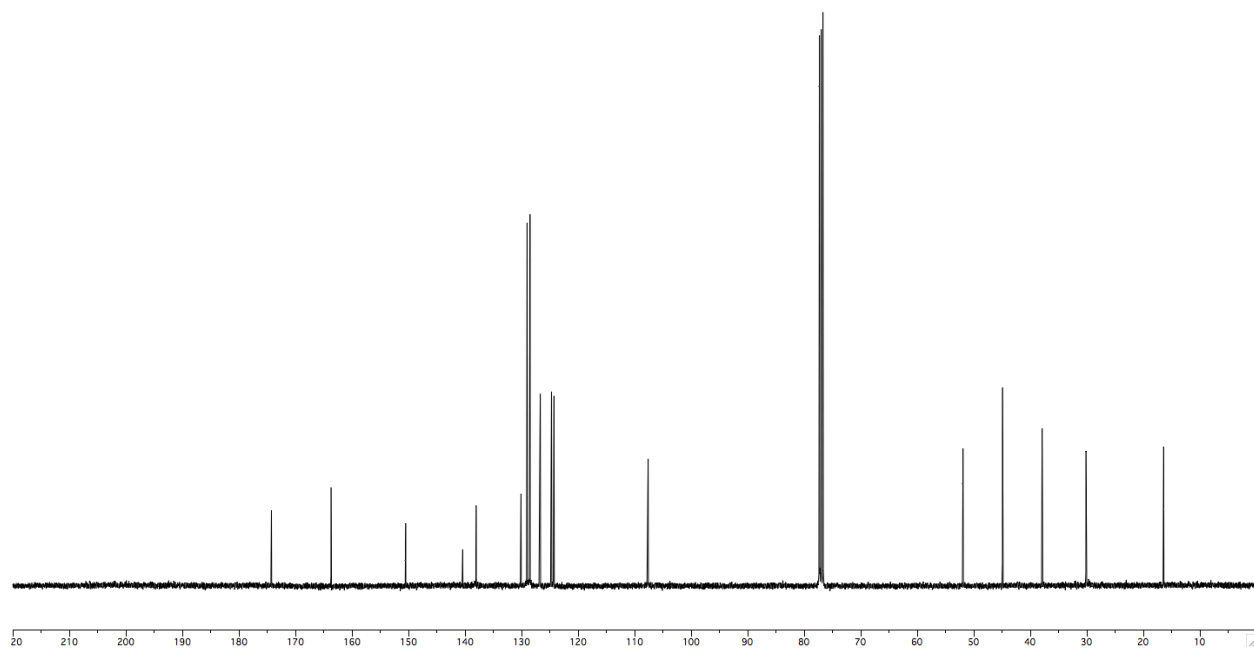
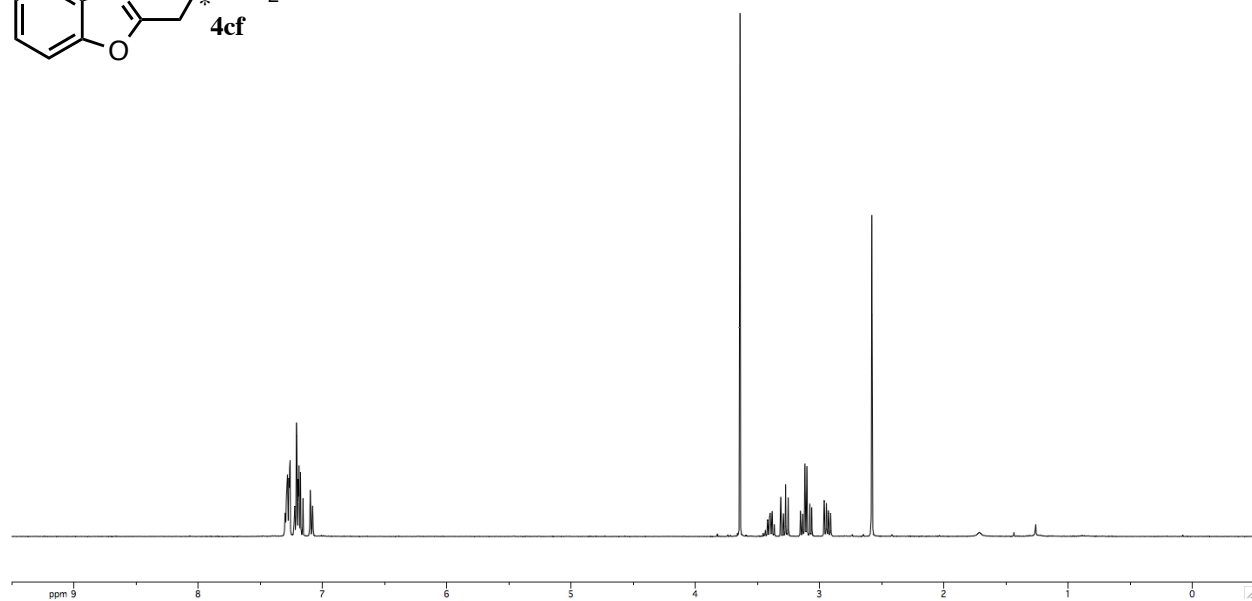
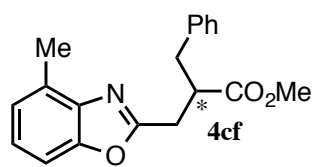


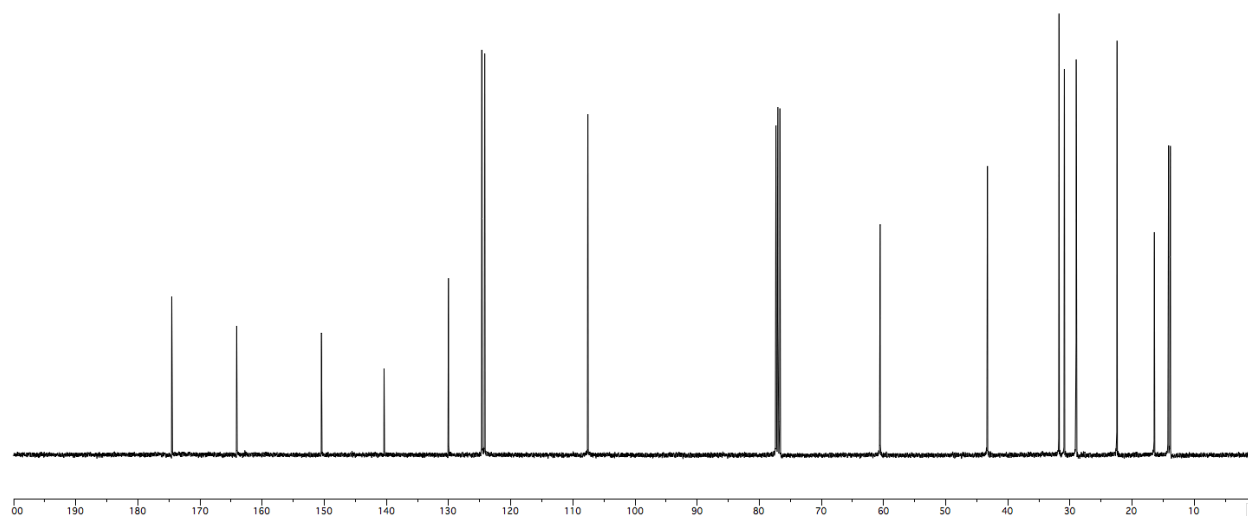
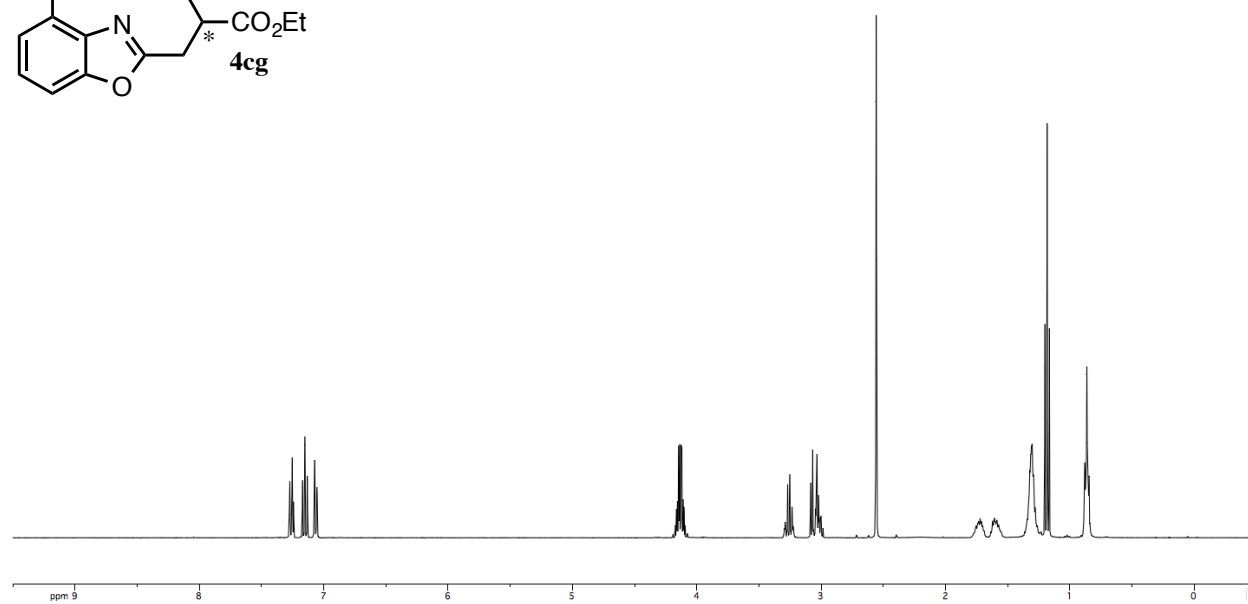
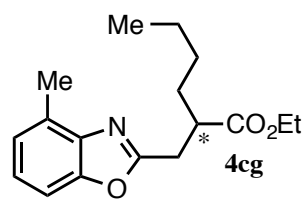


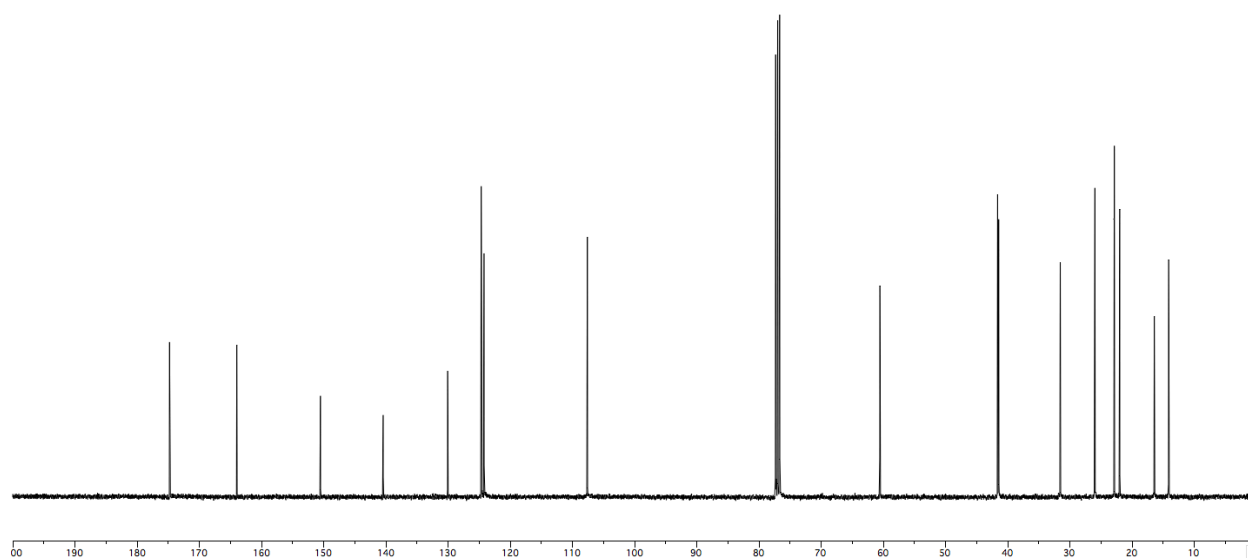
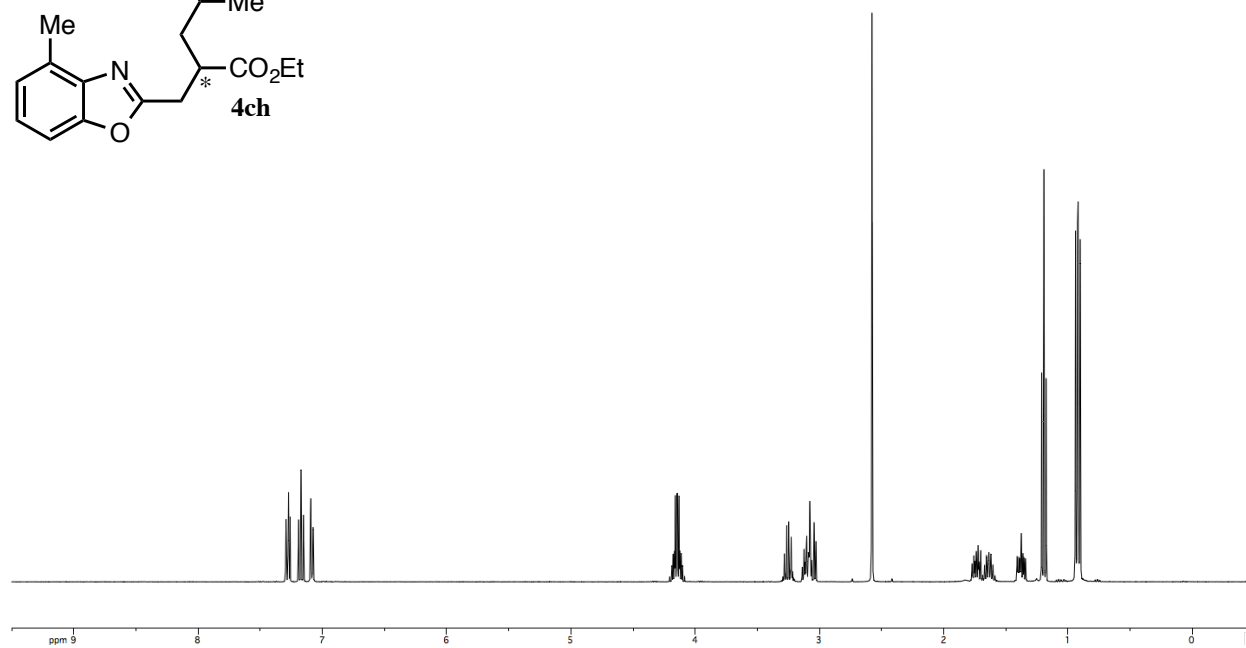
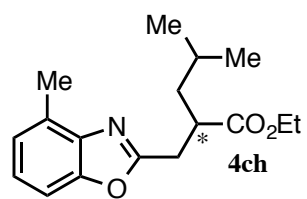


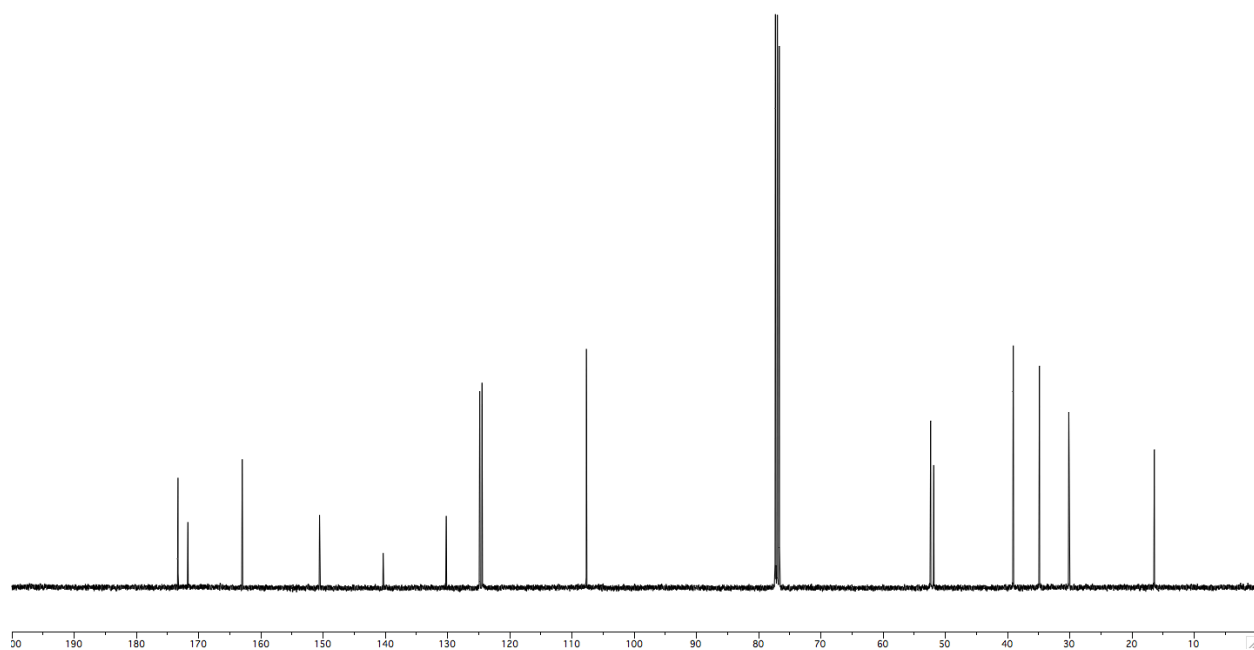
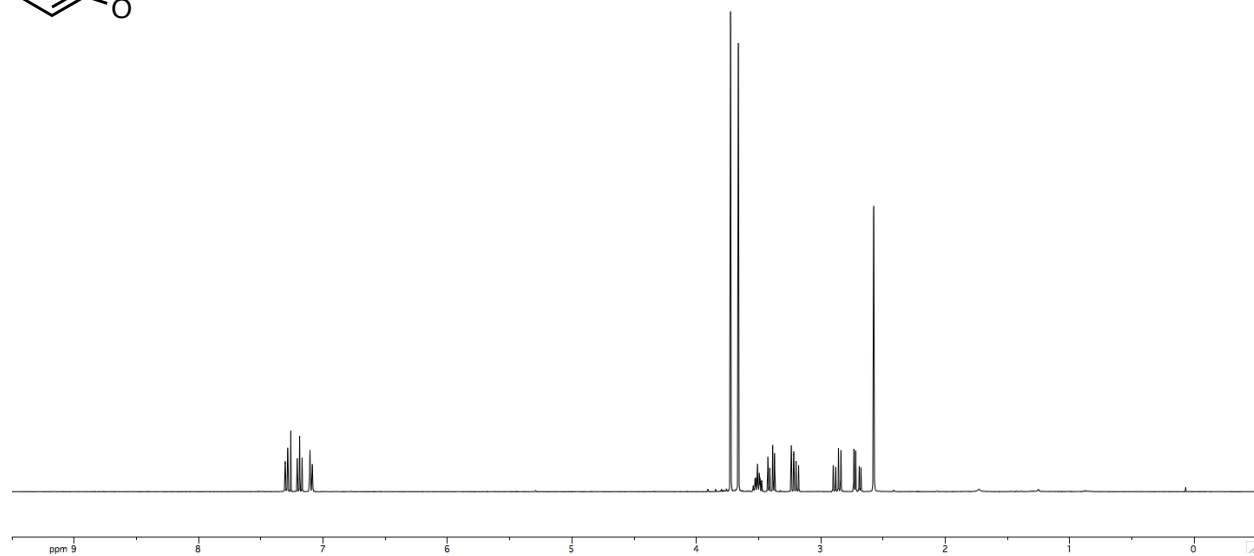
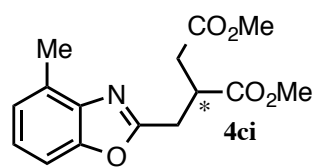


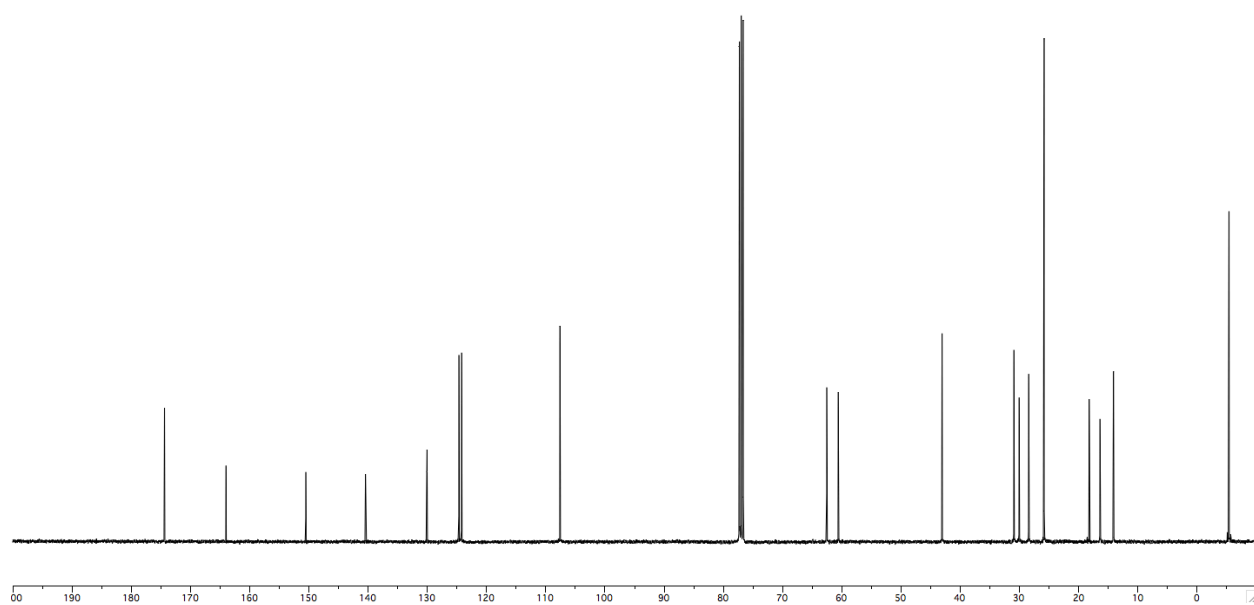
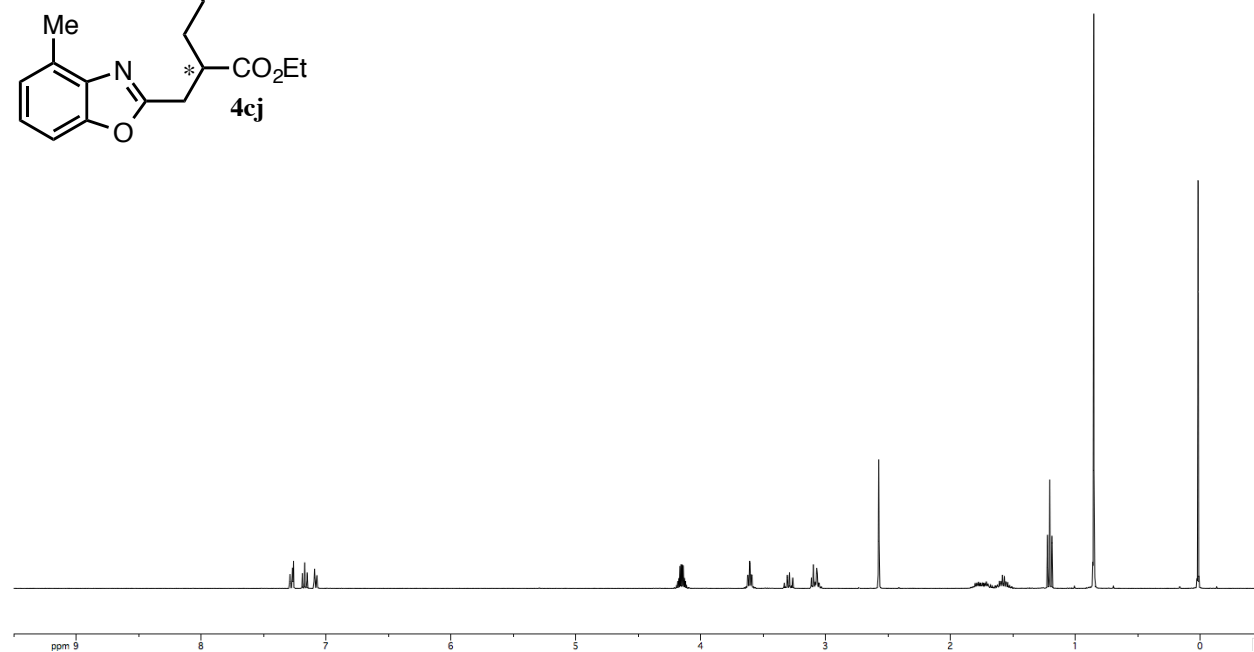
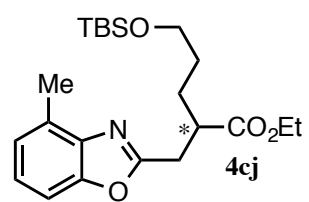


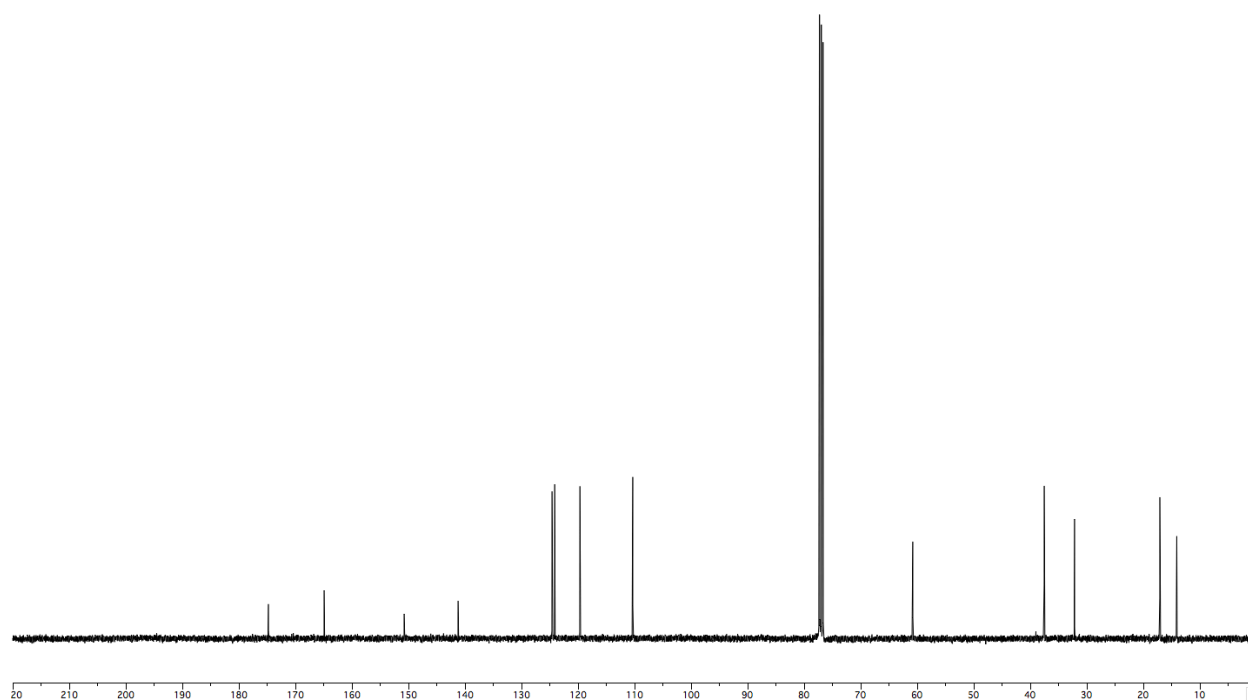
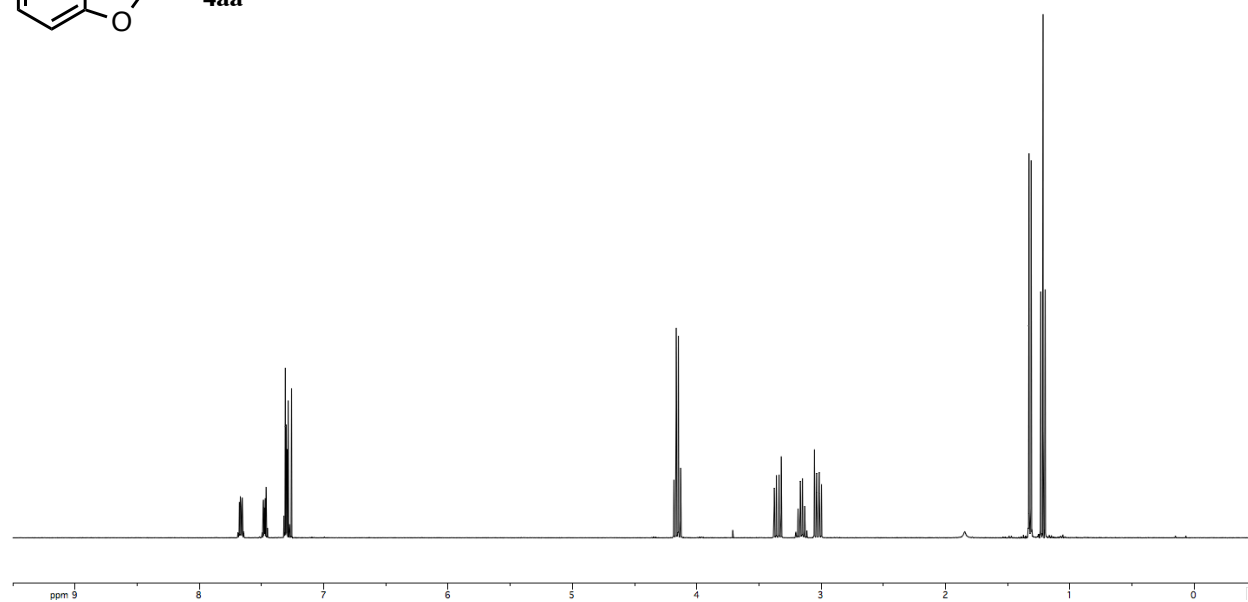
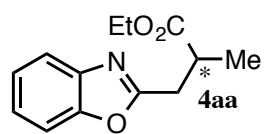


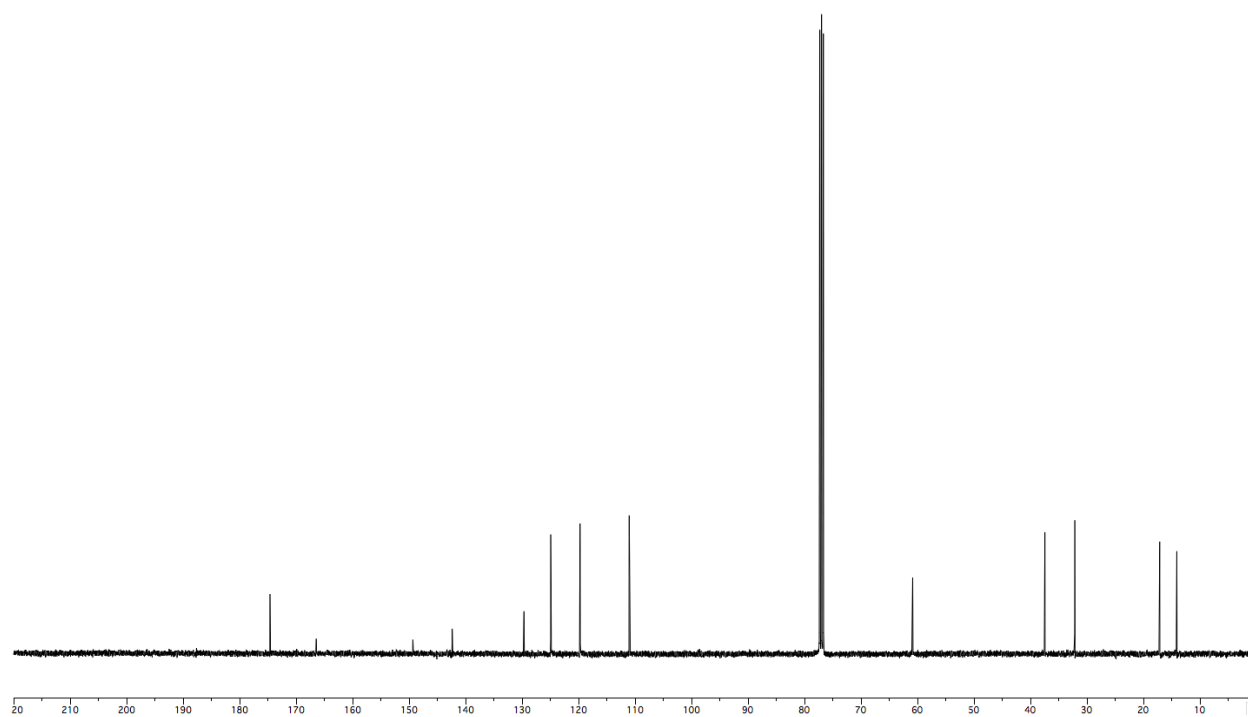
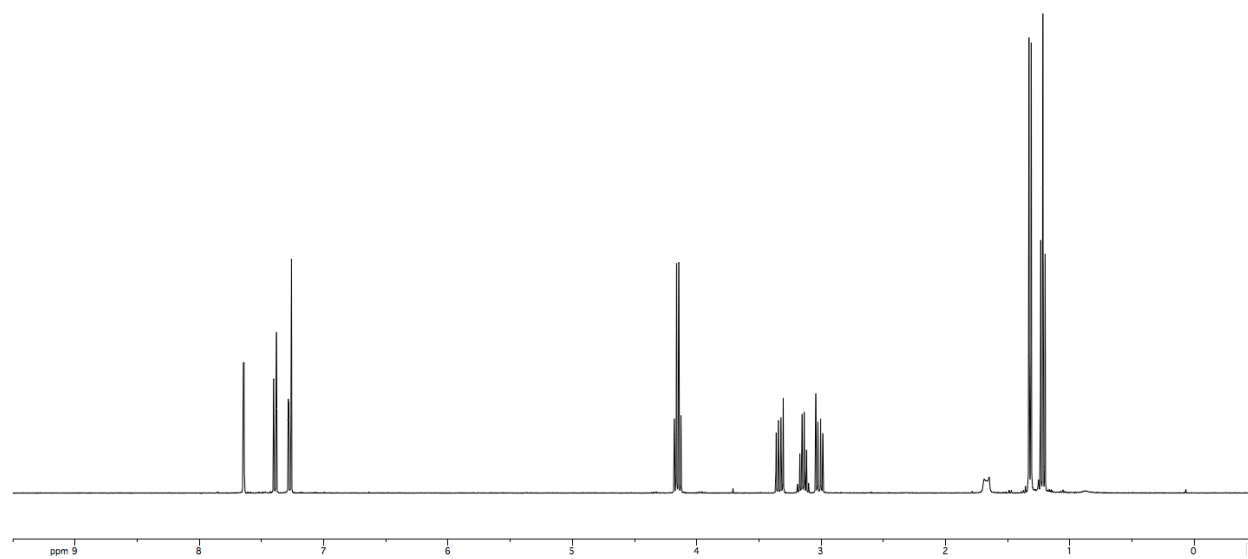
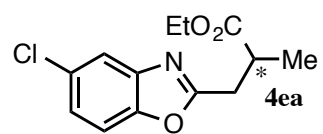


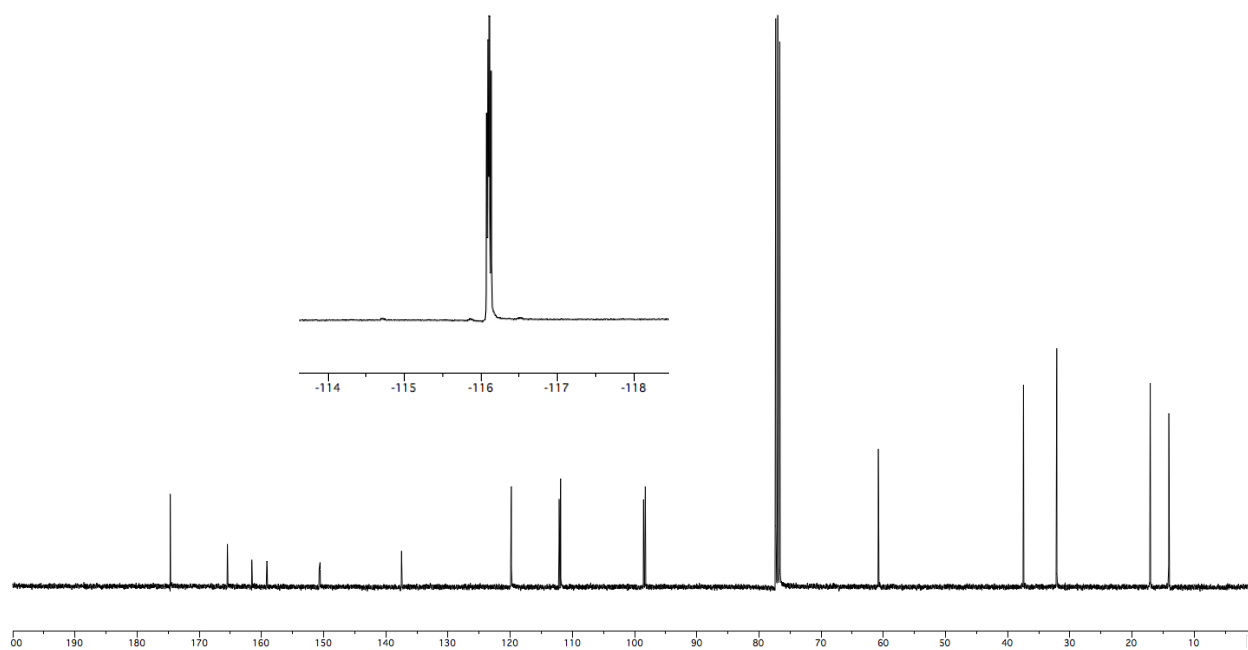
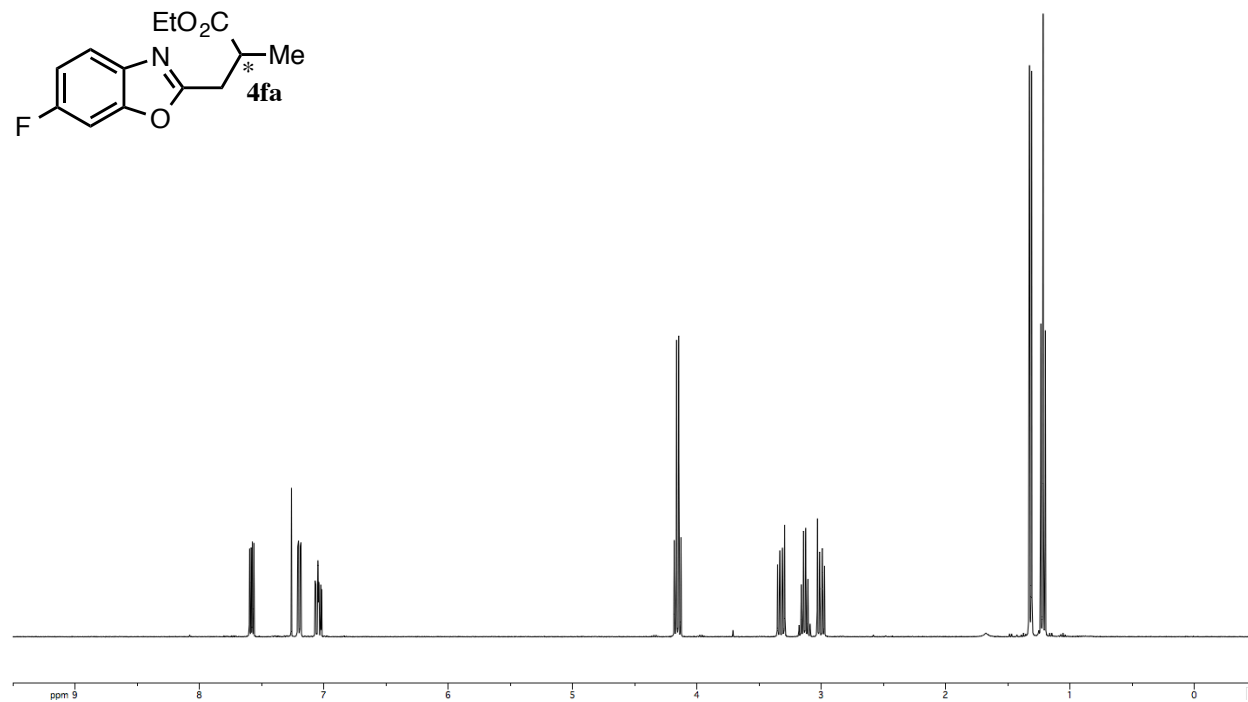
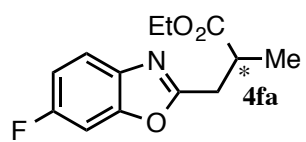


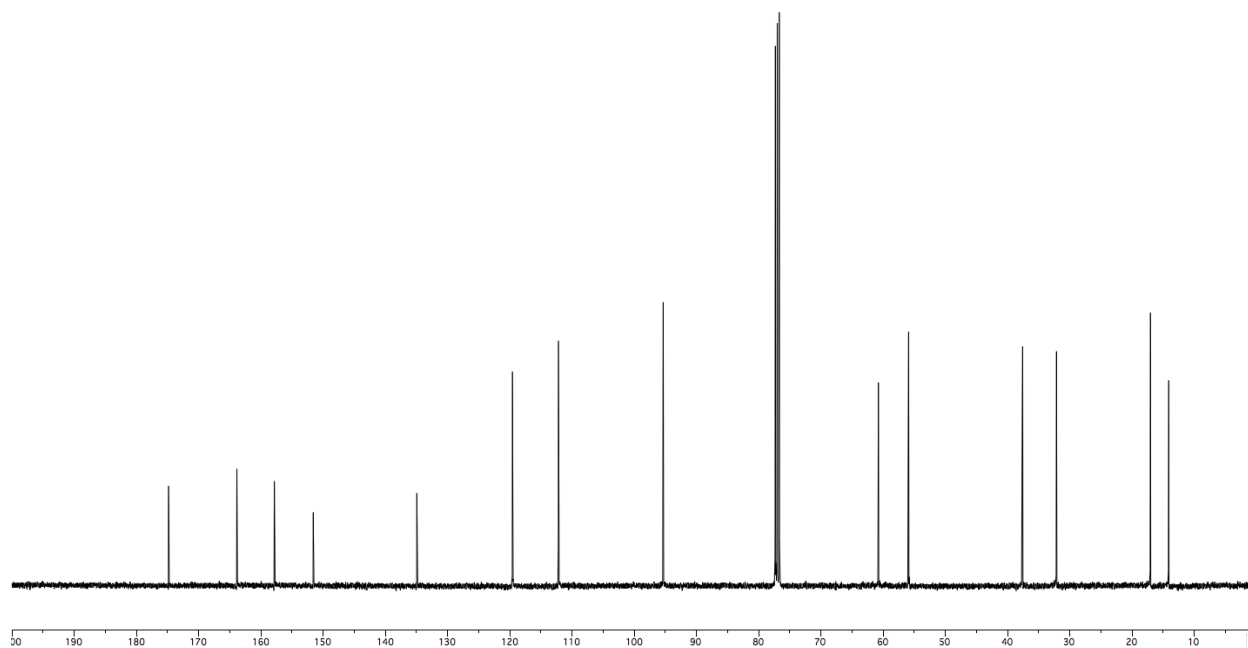
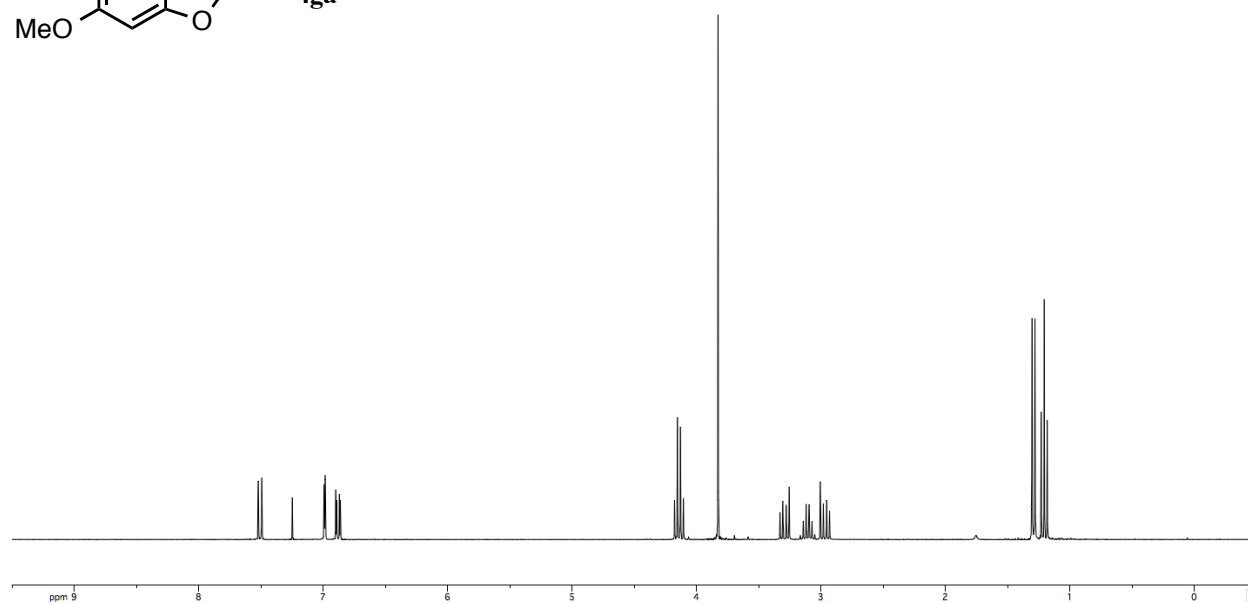
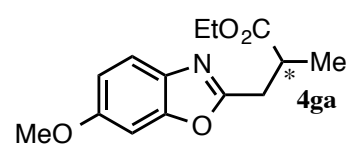


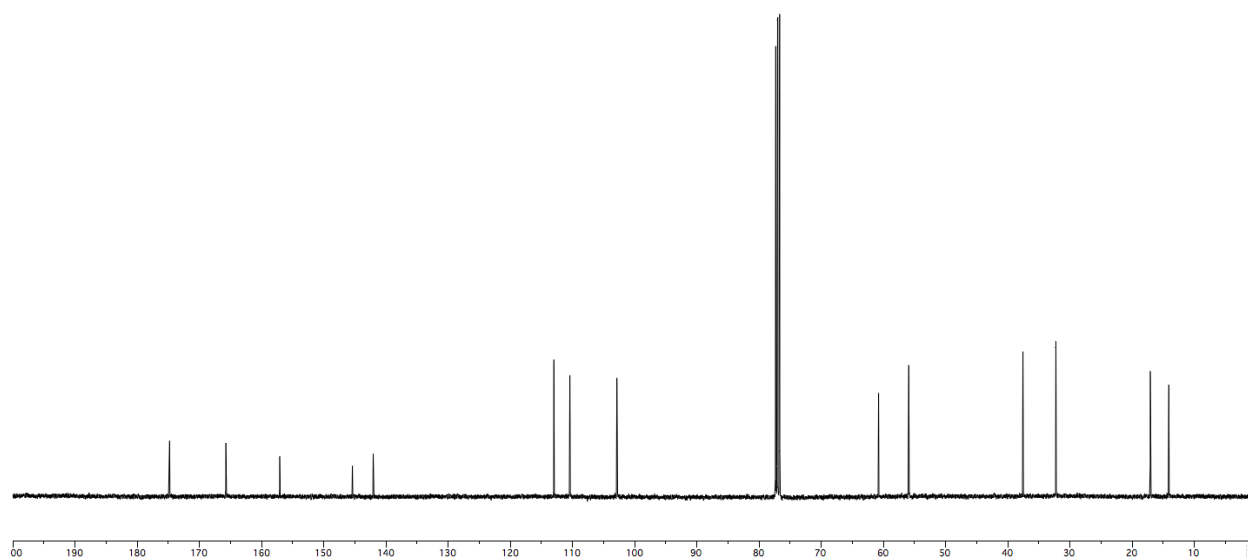
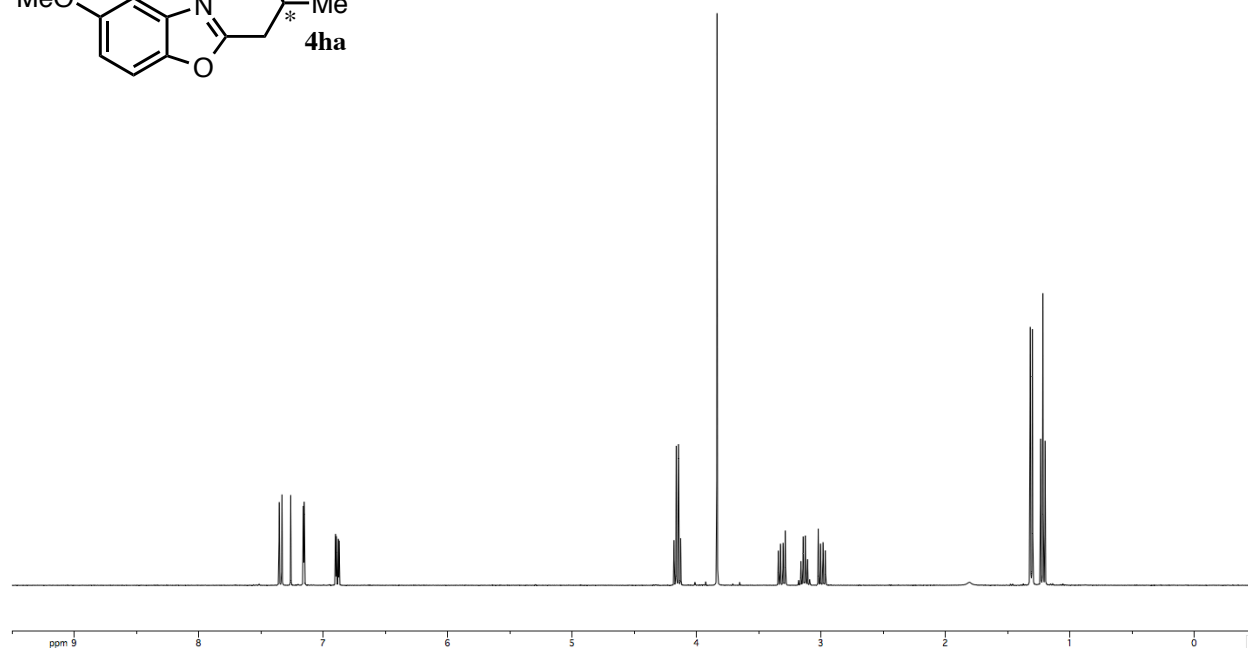
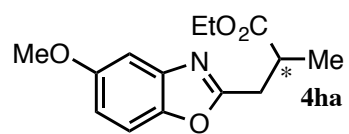




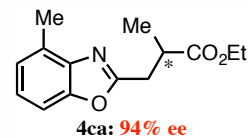




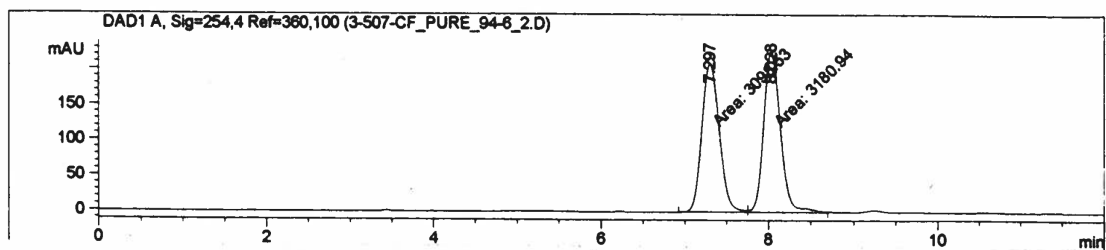




Data File C:\CHEM32\1\DATA\3-507-CF_PURE_94-6_2.D
 Sample Name: 3-507-CF_pure



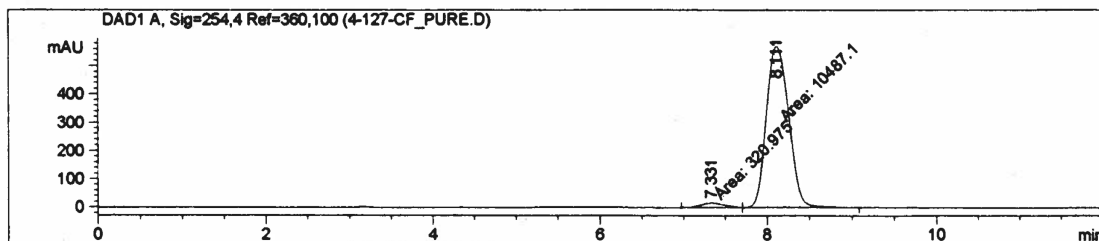
```
=====
Injection Date   : 4/25/2014 6:53:22 PM      Seq. Line :    6
Sample Name      : 3-507-CF_pure             Location  : Vial 1
Acq. Operator    : TAD                      Inj       :    1
Acq. Instrument  : Instrument 1              Inj Volume: 10 µl
Different Inj Volume from Sequence !        Actual Inj Volume: 2 µl
Acq. Method      : C:\CHEM32\1\METHODS\ODH 94-6 HEX-10-1-HEX-IPA 15 MIN.M
Last changed     : 1/10/2014 8:22:21 PM by tad
Analysis Method  : C:\CHEM32\1\METHODS\IC 80-20 1ML-1UL 40MIN.M
Last changed     : 12/1/2014 5:17:49 PM
                  (modified after loading)
=====
```



Peak #	RetTime [min]	Type	Width [min]	Area [mAU*s]	Height [mAU]	Area %
1	7.297	MM	0.2463	3098.53076	209.67038	49.3438
2	8.028	MM	0.2321	3180.93677	228.38246	50.6562

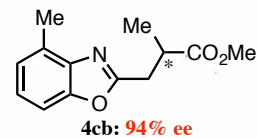
Data File C:\CHEM32\1\DATA\4-127-CF_PURE.D
 Sample Name: 4-127-CF_pure

```
=====
Injection Date   : 7/18/2014 2:48:41 PM      Seq. Line :    1
Sample Name      : 4-127-CF_pure             Location  : Vial 1
Acq. Operator    :                          Inj       :    1
Acq. Instrument  : Instrument 1              Inj Volume: 10 µl
Different Inj Volume from Sequence !        Actual Inj Volume: 2 µl
Acq. Method      : C:\CHEM32\1\METHODS\ODH 94-6 HEX-10-1-HEX-IPA 12 MIN.M
Last changed     : 5/27/2014 11:31:49 AM by TAD
Analysis Method  : C:\CHEM32\1\METHODS\IC 80-20 1ML-1UL 40MIN.M
Last changed     : 12/1/2014 5:18:01 PM
                  (modified after loading)
=====
```

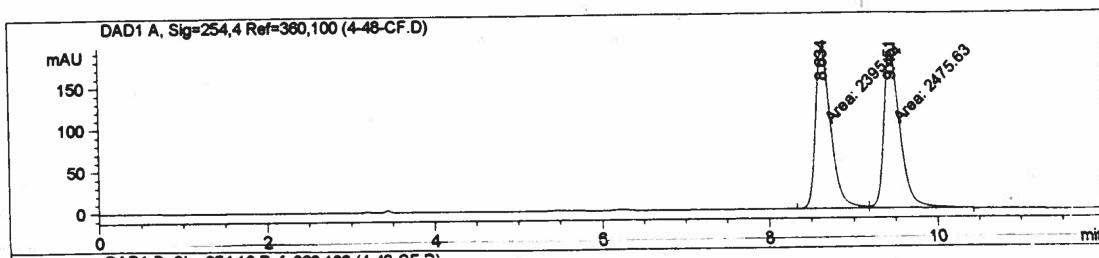


Peak #	RetTime [min]	Type	Width [min]	Area [mAU*s]	Height [mAU]	Area %
1	7.331	MM	0.3365	320.97537	15.89954	2.9698
2	8.111	MM	0.3063	1.04871e4	570.63306	97.0302

Data File C:\CHEM32\1\DATA\4-48-CF.D
 Sample Name: 4-48-CF



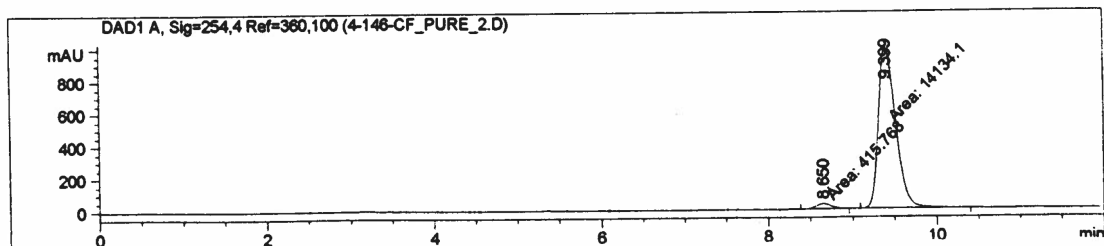
```
=====
Injection Date : 5/26/2014 10:12:57 AM      Seq. Line : 1
Sample Name    : 4-48-CF                    Location  : Vial 1
Acq. Operator  : TAD                        Inj       : 1
Acq. Instrument: Instrument 1                Inj Volume: 10 µl
Different Inj Volume from Sequence !      Actual Inj Volume: 1 µl
Acq. Method    : C:\CHEM32\1\METHODS\ODH 94-6 HEX-10-1-HEX-IPA 15 MIN.M
Last changed   : 1/10/2014 8:22:21 PM by tad
Analysis Method: C:\CHEM32\1\METHODS\IC 80-20 1ML-1UL 40MIN.M
Last changed   : 12/1/2014 5:26:18 PM
                  (modified after loading)
=====
```



Peak #	RetTime [min]	Type	Width [min]	Area [mAU*s]	Height [mAU]	Area %
1	8.634	MM	0.2096	2395.13599	190.41119	49.1737
2	9.451	MM	0.2211	2475.63086	186.57477	50.8263

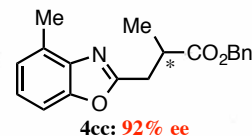
Data File C:\CHEM32\1\DATA\4-146-CF_PURE_2.D
 Sample Name: 4-146-CF_pure

```
=====
Injection Date : 8/31/2014 12:45:25 PM      Seq. Line : 2
Sample Name    : 4-146-CF_pure              Location  : Vial 1
Acq. Operator  :                            Inj       : 1
Acq. Instrument: Instrument 1                Inj Volume: 10 µl
Different Inj Volume from Sequence !      Actual Inj Volume: 2 µl
Acq. Method    : C:\CHEM32\1\METHODS\ODH 94-6 HEX-10-1-HEX-IPA 12 MIN.M
Last changed   : 5/27/2014 11:31:49 AM by TAD
Analysis Method: C:\CHEM32\1\METHODS\IC 80-20 1ML-1UL 40MIN.M
Last changed   : 12/1/2014 5:26:24 PM
                  (modified after loading)
=====
```



Peak #	RetTime [min]	Type	Width [min]	Area [mAU*s]	Height [mAU]	Area %
1	8.650	MM	0.2178	415.76849	31.80896	2.8575
2	9.399	MM	0.2373	1.41341e4	992.65167	97.1425

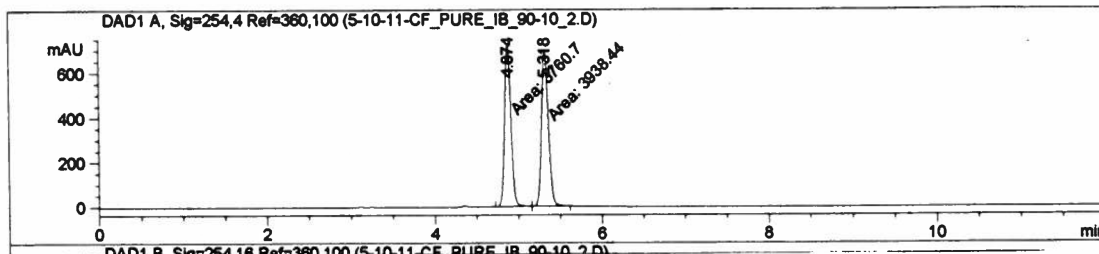
Data File C:\CHEM32\1\DATA\5-10-11-CF_PURE_IB_90-10_2.D
Sample Name: 5-10-11-CF_pure



=====

Injection Date : 9/27/2014 10:32:50 PM	Seq. Line : 5
Sample Name : 5-10-11-CF_pure	Location : Vial 51
Acq. Operator :	Inj : 1
Acq. Instrument : Instrument 1	Inj Volume : 10 µl
Different Inj Volume from Sequence !	Actual Inj Volume : 2 µl
Acq. Method : C:\CHEM32\1\METHODS\ODH 90-10 1ML 20MIN.M	
Last changed : 5/20/2009 7:26:39 PM by Rovis Group	
Analysis Method : C:\CHEM32\1\METHODS\IC 80-20 1ML-1UL 40MIN.M	
Last changed : 12/1/2014 5:30:07 PM	
(modified after loading)	

=====



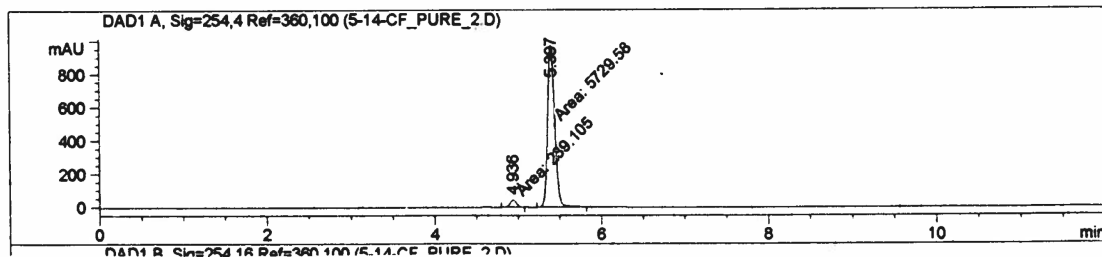
Peak #	RetTime [min]	Type	Width [min]	Area [mAU*s]	Height [mAU]	Area %
1	4.874	MM	0.0870	3760.70068	720.10028	48.8457
2	5.318	MM	0.0942	3938.43896	696.63123	51.1543

Data File C:\CHEM32\1\DATA\5-14-CF_PURE_2.D
Sample Name: 5-14-CF_pure

=====

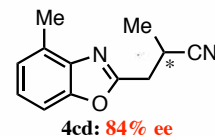
Injection Date : 10/2/2014 1:08:07 PM	Seq. Line : 2
Sample Name : 5-14-CF_pure	Location : Vial 41
Acq. Operator :	Inj : 1
Acq. Instrument : Instrument 1	Inj Volume : 10 µl
Different Inj Volume from Sequence !	Actual Inj Volume : 2 µl
Acq. Method : C:\CHEM32\1\METHODS\ODH 90-10 1ML 12MIN.M	
Last changed : 2/18/2014 4:01:28 PM by KRUHL	
Analysis Method : C:\CHEM32\1\METHODS\IC 80-20 1ML-1UL 40MIN.M	
Last changed : 12/1/2014 5:30:07 PM	
(modified after loading)	

=====

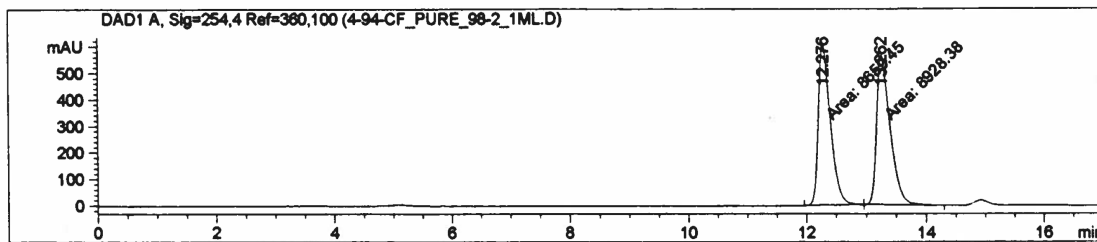


Peak #	RetTime [min]	Type	Width [min]	Area [mAU*s]	Height [mAU]	Area %
1	4.936	MM	0.0883	239.10472	45.14110	4.0060
2	5.397	MM	0.0989	5729.58398	965.79749	95.9940

Data File C:\CHEM32\1\DATA\4-94-CF_PURE_98-2_1ML.D
 Sample Name: 4-94-CF_pure



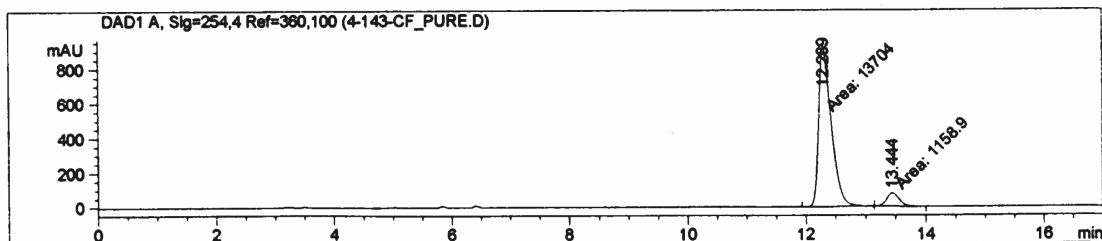
```
=====
Injection Date   : 6/29/2014 1:27:02 PM      Seq. Line :    1
Sample Name      : 4-94-CF_pure              Location  : Vial 23
Acq. Operator    : TAD                      Inj       :    1
Acq. Instrument  : Instrument 1              Inj Volume: 1 µl
Different Inj Volume from Sequence !      Actual Inj Volume: 2 µl
Acq. Method      : C:\CHEM32\1\METHODS\ODH 98-2 1ML 25MIN.M
Last changed     : 12/4/2013 2:07:01 PM
Analysis Method  : C:\CHEM32\1\METHODS\IC 80-20 1ML-1UL 40MIN.M
Last changed     : 12/1/2014 5:45:21 PM
                  (modified after loading)
=====
```



Peak #	RetTime [min]	Type	Width [min]	Area [mAU*s]	Height [mAU]	Area %
1	12.276	MM	0.2381	8659.45020	606.07904	49.2355
2	13.262	MM	0.2628	8928.38379	566.26917	50.7645

Data File C:\CHEM32\1\DATA\4-143-CF_PURE.D
 Sample Name: 4-143-CF_pure

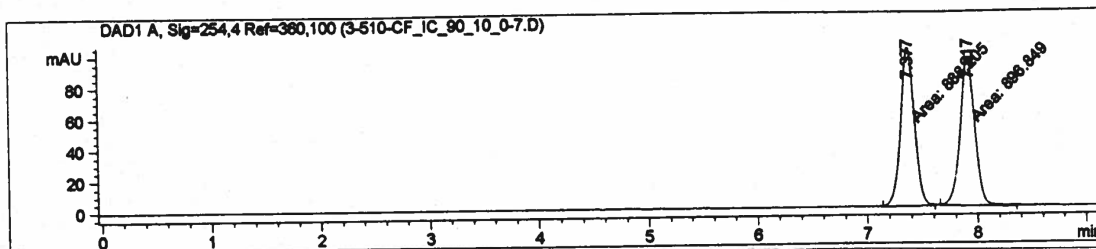
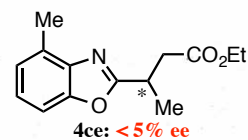
```
=====
Injection Date   : 8/31/2014 1:00:26 PM      Seq. Line :    3
Sample Name      : 4-143-CF_pure              Location  : Vial 2
Acq. Operator    :                          Inj       :    1
Acq. Instrument  : Instrument 1              Inj Volume: 1 µl
Different Inj Volume from Sequence !      Actual Inj Volume: 2 µl
Acq. Method      : C:\CHEM32\1\METHODS\ODH 98-2 1ML 18MIN.M
Last changed     : 8/28/2014 3:03:00 PM
Analysis Method  : C:\CHEM32\1\METHODS\IC 80-20 1ML-1UL 40MIN.M
Last changed     : 12/1/2014 5:45:21 PM
                  (modified after loading)
=====
```



Peak #	RetTime [min]	Type	Width [min]	Area [mAU*s]	Height [mAU]	Area %
1	12.289	MM	0.2454	1.37040e4	930.60889	92.2027
2	13.444	MM	0.2474	1158.89587	78.07531	7.7973

Data File C:\CHEM32\1\DATA\3-510-CF_IC_90_10_0-7.D
 Sample Name: 3-510-CF_pure

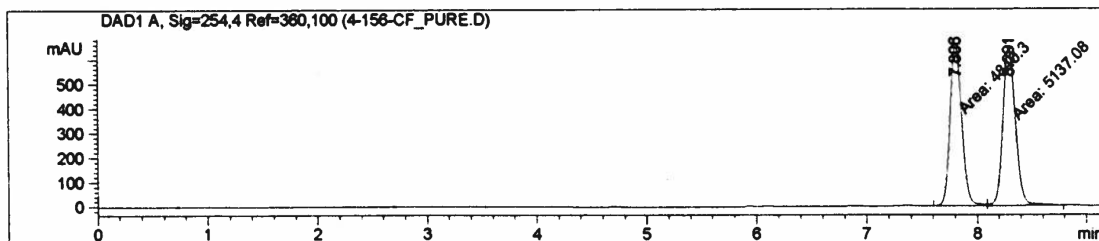
```
=====
Injection Date : 7/15/2013 10:24:07 AM      Seq. Line : 1
Sample Name    : 3-510-CF_pure              Location  : Vial 2
Acq. Operator  :                            Inj      : 1
Acq. Instrument: Instrument 1                Inj Volume: 1 µl
Acq. Method    : C:\CHEM32\1\METHODS\IC 90-10 0-7UL 30MIN.M
Last changed   : 7/15/2013 10:22:34 AM
Analysis Method: C:\CHEM32\1\METHODS\IC 80-20 1ML-1UL 40MIN.M
Last changed   : 4/10/2012 12:17:50 PM
=====
```



Peak #	RetTime [min]	Type	Width [min]	Area [mAU*s]	Height [mAU]	Area %
1	7.377	MM	0.1428	888.20459	103.64252	49.7579
2	7.917	MM	0.1552	896.84924	96.28329	50.2421

Data File C:\CHEM32\1\DATA\4-156-CF_PURE.D
 Sample Name: 4-156-CF

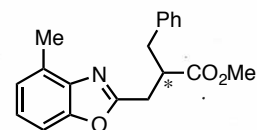
```
=====
Injection Date : 9/10/2014 1:07:46 PM      Seq. Line : 3
Sample Name    : 4-156-CF                  Location  : Vial 14
Acq. Operator  :                            Inj      : 1
Acq. Instrument: Instrument 1                Inj Volume: 1 µl
Different Inj Volume from Sequence !      Actual Inj Volume: 2 µl
Acq. Method    : C:\CHEM32\1\METHODS\IC 90-10 0-7UL 15MIN.M
Last changed   : 7/15/2013 10:55:39 AM
Analysis Method: C:\CHEM32\1\METHODS\IC 80-20 1ML-1UL 40MIN.M
Last changed   : 12/1/2014 6:00:09 PM
                  (modified after loading)
=====
```



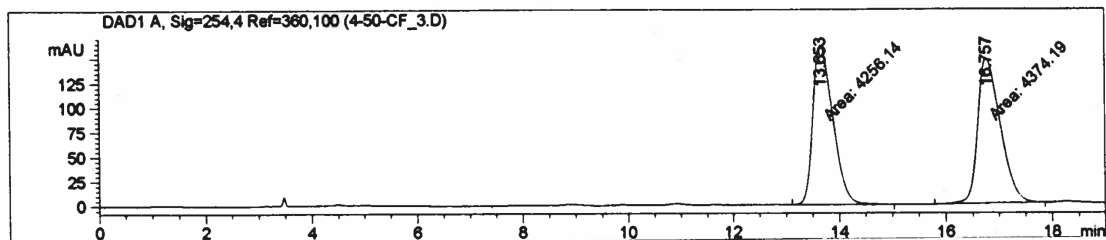
Peak #	RetTime [min]	Type	Width [min]	Area [mAU*s]	Height [mAU]	Area %
1	7.806	MM	0.1221	4840.29541	660.47839	48.5127
2	8.291	MM	0.1317	5137.07959	649.97253	51.4873

Data File C:\CHEM32\1\DATA\4-50-CF_3.D
 Sample Name: 4-50-CF_3

```
=====
Injection Date : 8/25/2014 4:41:00 PM      Seq. Line : 3
Sample Name    : 4-50-CF_3                Location  : Vial 2
Acq. Operator  :                          Inj      : 1
Acq. Instrument: Instrument 1              Inj Volume: 10 µl
Acq. Method    : C:\CHEM32\1\METHODS\ODH 94-6 HEX-10-1-HEX-IPA 20 MIN.M
Last changed   : 9/3/2013 5:25:21 PM
Analysis Method: C:\CHEM32\1\METHODS\IC 80-20 1ML-1UL 40MIN.M
Last changed   : 12/1/2014 6:04:59 PM
                (modified after loading)
=====
```



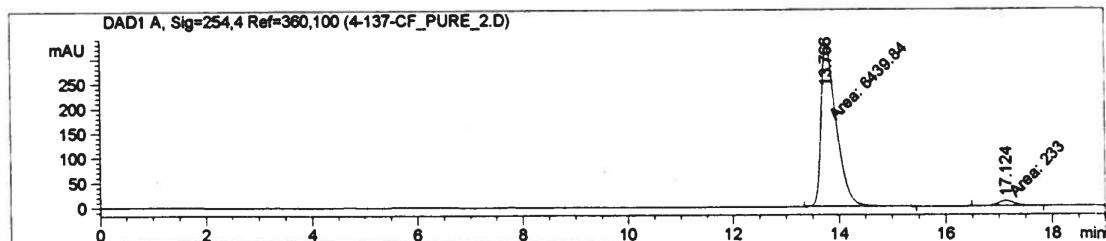
4cf: 93% ee



Peak #	RetTime [min]	Type	Width [min]	Area [mAU*s]	Height [mAU]	Area %
1	13.653	MM	0.4382	4256.13672	161.86275	49.3160
2	16.757	MM	0.4951	4374.19238	147.26196	50.6840

Data File C:\CHEM32\1\DATA\4-137-CF_PURE_2.D
 Sample Name: 4-137-CF_pure_2

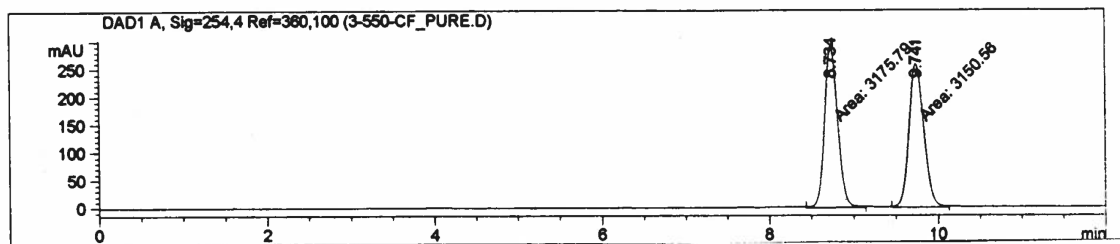
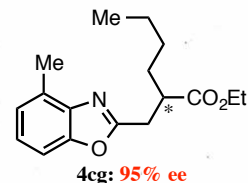
```
=====
Injection Date : 8/25/2014 4:17:58 PM      Seq. Line : 2
Sample Name    : 4-137-CF_pure_2          Location  : Vial 1
Acq. Operator  :                          Inj      : 1
Acq. Instrument: Instrument 1              Inj Volume: 10 µl
Different Inj Volume from Sequence !      Actual Inj Volume : 2 µl
Acq. Method    : C:\CHEM32\1\METHODS\ODH 94-6 HEX-10-1-HEX-IPA 20 MIN.M
Last changed   : 9/3/2013 5:25:21 PM
Analysis Method: C:\CHEM32\1\METHODS\IC 80-20 1ML-1UL 40MIN.M
Last changed   : 12/1/2014 6:04:59 PM
                (modified after loading)
=====
```



Peak #	RetTime [min]	Type	Width [min]	Area [mAU*s]	Height [mAU]	Area %
1	13.766	MM	0.3307	6439.84375	324.54300	96.5082
2	17.124	MM	0.3714	232.99957	10.45665	3.4918

Data File C:\CHEM32\1\DATA\3-550-CF_PURE.D
 Sample Name: 3-550-CF_pure

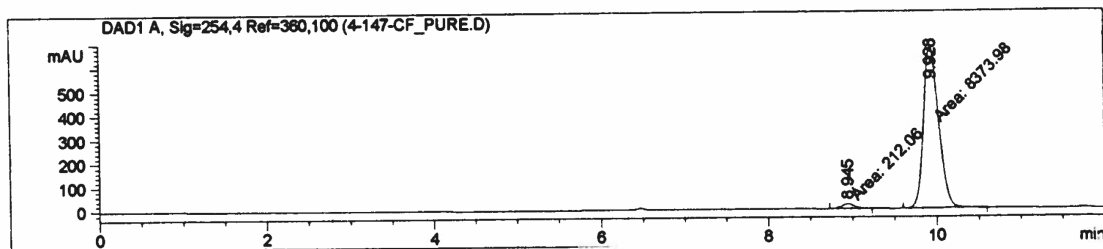
```
=====
Injection Date   : 9/3/2014 9:55:52 AM      Seq. Line :    2
Sample Name      : 3-550-CF_pure            Location  : Vial 2
Acq. Operator    :                          Inj       :    1
Acq. Instrument  : Instrument 1              Inj Volume: 5 µl
Different Inj Volume from Sequence !        Actual Inj Volume: 2 µl
Acq. Method      : C:\CHEM32\1\METHODS\IC 98-2 1ML 13MIN.M
Last changed     : 10/1/2013 10:43:24 AM
Analysis Method  : C:\CHEM32\1\METHODS\IC 80-20 1ML-1UL 40MIN.M
Last changed     : 12/1/2014 6:09:45 PM
                  (modified after loading)
=====
```



Peak #	RetTime [min]	Type	Width [min]	Area [mAU*s]	Height [mAU]	Area %
1	8.734	MM	0.1810	3175.78979	292.37695	50.1994
2	9.741	MM	0.2025	3150.56250	259.32300	49.8006

Data File C:\CHEM32\1\DATA\4-147-CF_PURE.D
 Sample Name: 4-147-CF_pure

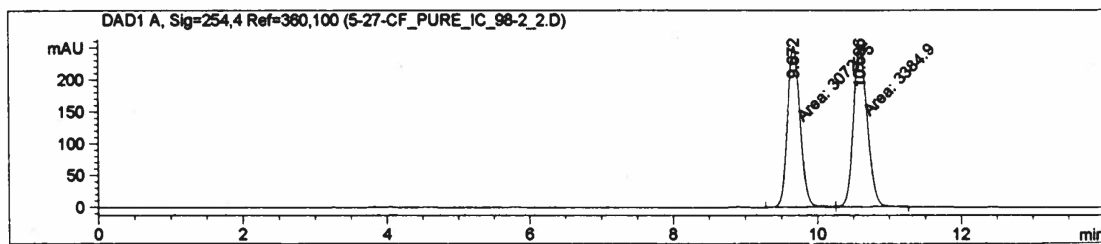
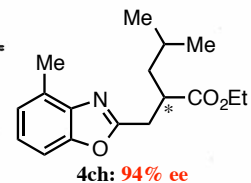
```
=====
Injection Date   : 9/3/2014 9:37:02 AM      Seq. Line :    1
Sample Name      : 4-147-CF_pure            Location  : Vial 1
Acq. Operator    :                          Inj       :    1
Acq. Instrument  : Instrument 1              Inj Volume: 5 µl
Different Inj Volume from Sequence !        Actual Inj Volume: 2 µl
Acq. Method      : C:\CHEM32\1\METHODS\IC 98-2 1ML 13MIN.M
Last changed     : 10/1/2013 10:43:24 AM
Analysis Method  : C:\CHEM32\1\METHODS\IC 80-20 1ML-1UL 40MIN.M
Last changed     : 12/1/2014 6:09:45 PM
                  (modified after loading)
=====
```



Peak #	RetTime [min]	Type	Width [min]	Area [mAU*s]	Height [mAU]	Area %
1	8.945	MM	0.1793	212.06012	19.71037	2.4698
2	9.928	MM	0.2063	8373.97852	676.67206	97.5302

Data File C:\CHEM32\1\DATA\5-27-CF_PURE_IC_98-2_2.D
 Sample Name: 5-27-CF_pure

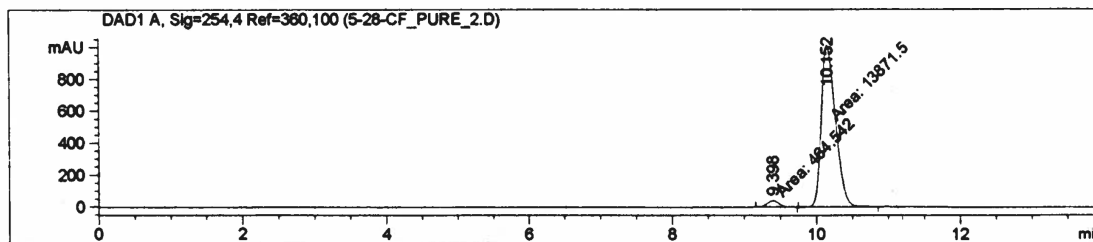
```
=====
Injection Date : 10/19/2014 4:47:56 PM      Seq. Line :    3
Sample Name    : 5-27-CF_pure              Location  : Vial 2
Acq. Operator  :                          Inj      :    1
Acq. Instrument: Instrument 1              Inj Volume: 5 µl
Different Inj Volume from Sequence !      Actual Inj Volume: 2 µl
Acq. Method    : C:\CHEM32\1\METHODS\IC 98-2 1ML 16MIN.M
Last changed   : 10/19/2014 4:40:59 PM
Analysis Method: C:\CHEM32\1\METHODS\IC 80-20 1ML-1UL 40MIN.M
Last changed   : 12/2/2014 6:31:02 AM
                    (modified after loading)
=====
```



Peak #	RetTime [min]	Type	Width [min]	Area [mAU*s]	Height [mAU]	Area %
1	9.672	MM	0.2027	3072.75098	252.70468	47.5831
2	10.596	MM	0.2276	3384.90454	247.89035	52.4169

Data File C:\CHEM32\1\DATA\5-28-CF_PURE_2.D
 Sample Name: 5-28-CF_pure

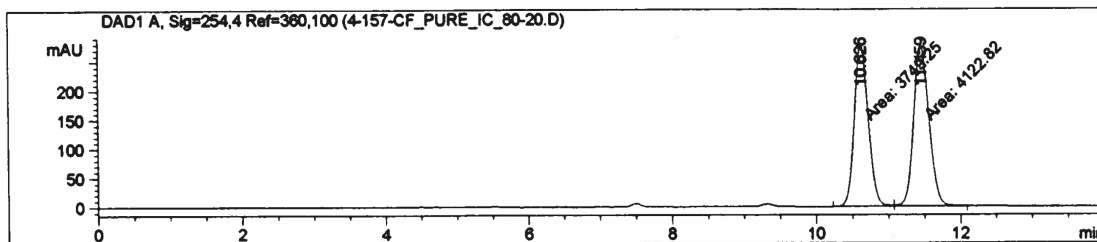
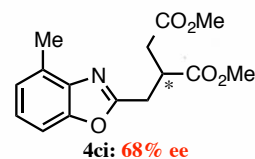
```
=====
Injection Date : 10/20/2014 7:39:38 PM      Seq. Line :    3
Sample Name    : 5-28-CF_pure              Location  : Vial 4
Acq. Operator  :                          Inj      :    1
Acq. Instrument: Instrument 1              Inj Volume: 5 µl
Different Inj Volume from Sequence !      Actual Inj Volume: 2 µl
Acq. Method    : C:\CHEM32\1\METHODS\IC 98-2 1ML 16MIN.M
Last changed   : 10/19/2014 4:40:59 PM
Analysis Method: C:\CHEM32\1\METHODS\IC 80-20 1ML-1UL 40MIN.M
Last changed   : 12/2/2014 6:31:02 AM
                    (modified after loading)
=====
```



Peak #	RetTime [min]	Type	Width [min]	Area [mAU*s]	Height [mAU]	Area %
1	9.398	MM	0.1960	464.54230	39.51024	3.2404
2	10.152	MM	0.2280	1.38715e4	1014.18347	96.7596

Data File C:\CHEM32\1\DATA\4-157-CF_PURE_IC_80-20.D
Sample Name: 4-157-CF_pure

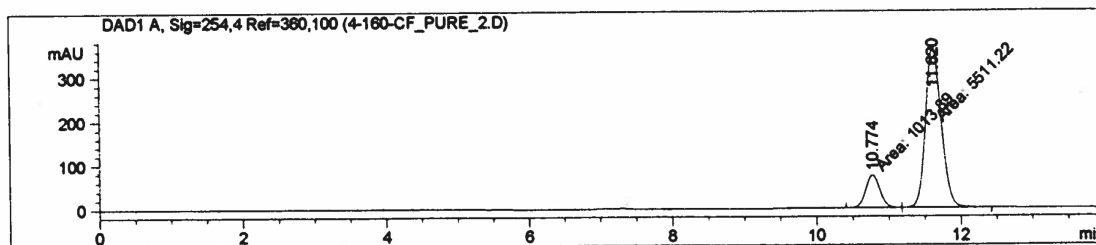
```
=====
Injection Date   : 9/10/2014 9:34:48 PM      Seq. Line :   10
Sample Name      : 4-157-CF_pure             Location  : Vial 15
Acq. Operator    :                          Inj      :    1
Acq. Instrument  : Instrument 1               Inj Volume: 1 µl
Different Inj Volume from Sequence !         Actual Inj Volume: 2 µl
Acq. Method      : C:\CHEM32\1\METHODS\IC 80-20 1ML-1UL 20MIN.M
Last changed     : 8/4/2012 4:38:14 PM
Analysis Method  : C:\CHEM32\1\METHODS\IC 80-20 1ML-1UL 40MIN.M
Last changed     : 12/2/2014 6:31:02 AM
                  (modified after loading)
=====
```



Peak #	RetTime [min]	Type	Width [min]	Area [mAU*s]	Height [mAU]	Area %
1	10.626	MM	0.2244	3749.24927	278.45609	47.6273
2	11.459	MM	0.2478	4122.81689	277.29398	52.3727

Data File C:\CHEM32\1\DATA\4-160-CF_PURE_2.D
Sample Name: 4-160-CF_pure_2

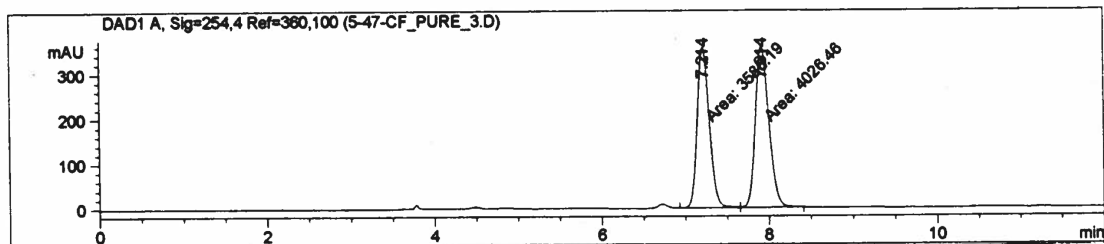
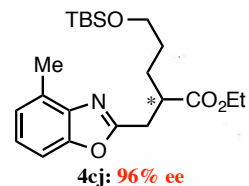
```
=====
Injection Date   : 9/15/2014 11:11:46 AM      Seq. Line :    2
Sample Name      : 4-160-CF_pure_2            Location  : Vial 1
Acq. Operator    :                          Inj      :    1
Acq. Instrument  : Instrument 1               Inj Volume: 1 µl
Different Inj Volume from Sequence !         Actual Inj Volume: 2 µl
Acq. Method      : C:\CHEM32\1\METHODS\IC 80-20 1ML-1UL 15MIN.M
Last changed     : 5/21/2013 8:22:23 PM
Analysis Method  : C:\CHEM32\1\METHODS\IC 80-20 1ML-1UL 40MIN.M
Last changed     : 12/2/2014 6:31:02 AM
                  (modified after loading)
=====
```



Peak #	RetTime [min]	Type	Width [min]	Area [mAU*s]	Height [mAU]	Area %
1	10.774	MM	0.2286	1013.88898	73.93015	15.5383
2	11.620	MM	0.2513	5511.22119	365.47467	84.4617

Data File C:\CHEM32\1\DATA\5-47-CF_PURE_3.D
 Sample Name: 5-48-CF_pure

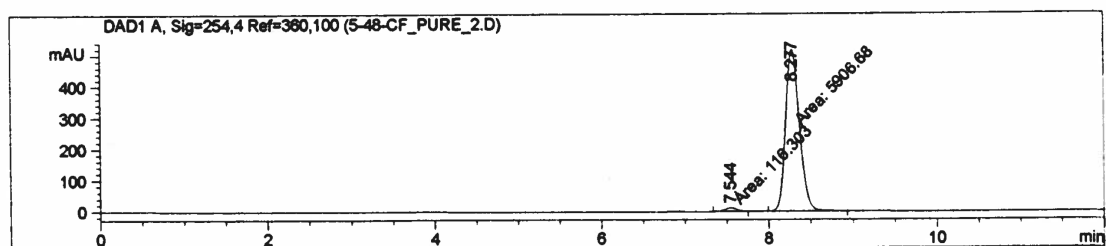
```
=====
Injection Date   : 11/1/2014 9:08:47 PM      Seq. Line :    2
Sample Name     : 5-48-CF_pure              Location  : Vial 1
Acq. Operator   :                          Inj      :    1
Acq. Instrument : Instrument 1               Inj Volume: 5 µl
Different Inj Volume from Sequence !        Actual Inj Volume: 2 µl
Acq. Method     : C:\CHEM32\1\METHODS\IC 98-2 1ML 16MIN.M
Last changed    : 10/19/2014 4:40:59 PM
Analysis Method : C:\CHEM32\1\METHODS\IC 80-20 1ML-1UL 40MIN.M
Last changed    : 12/2/2014 6:40:11 AM
                  (modified after loading)
=====
```



Peak #	RetTime [min]	Type	Width [min]	Area [mAU*s]	Height [mAU]	Area %
1	7.214	MM	0.1673	3586.18506	357.31494	47.1083
2	7.914	MM	0.1872	4026.45532	358.49017	52.8917

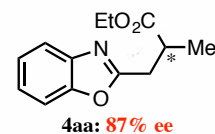
Data File C:\CHEM32\1\DATA\5-48-CF_PURE_2.D
 Sample Name: 5-48-CF_pure

```
=====
Injection Date   : 11/1/2014 8:46:55 PM      Seq. Line :    1
Sample Name     : 5-48-CF_pure              Location  : Vial 2
Acq. Operator   :                          Inj      :    1
Acq. Instrument : Instrument 1               Inj Volume: 5 µl
Different Inj Volume from Sequence !        Actual Inj Volume: 2 µl
Acq. Method     : C:\CHEM32\1\METHODS\IC 98-2 1ML 16MIN.M
Last changed    : 10/19/2014 4:40:59 PM
Analysis Method : C:\CHEM32\1\METHODS\IC 80-20 1ML-1UL 40MIN.M
Last changed    : 12/2/2014 6:40:05 AM
                  (modified after loading)
=====
```

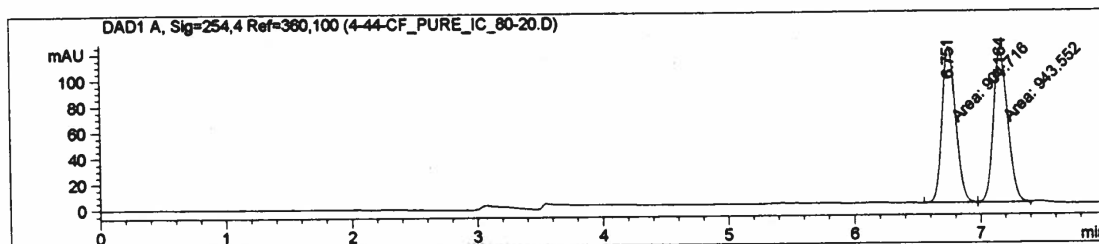


Peak #	RetTime [min]	Type	Width [min]	Area [mAU*s]	Height [mAU]	Area %
1	7.544	MM	0.1696	116.30286	11.42884	1.9310
2	8.277	MM	0.1896	5906.68311	519.35901	98.0690

Data File C:\CHEM32\1\DATA\4-44-CF_PURE_IC_80-20.D
 Sample Name: 4-44-CF_pure



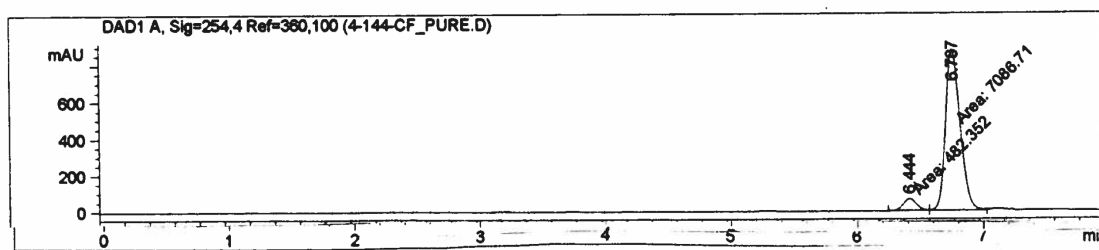
```
=====
Injection Date   : 5/19/2014 2:20:01 PM      Seq. Line :    2
Sample Name      : 4-44-CF_pure              Location  : Vial 3
Acq. Operator    : TAD                      Inj       :    1
Acq. Instrument  : Instrument 1              Inj Volume: 1 µl
Acq. Method      : C:\CHEM32\1\METHODS\IC 80-20 1ML-1UL 20MIN.M
Last changed     : 8/4/2012 4:38:14 PM
Analysis Method  : C:\CHEM32\1\METHODS\IC 80-20 1ML-1UL 40MIN.M
Last changed     : 12/2/2014 6:51:03 AM
                  (modified after loading)
=====
```



Peak #	RetTime [min]	Type	Width [min]	Area [mAU*s]	Height [mAU]	Area %
1	6.751	MM	0.1240	904.71594	121.62111	48.9494
2	7.164	MM	0.1336	943.55182	117.71478	51.0506

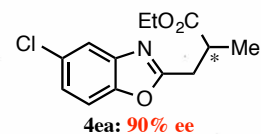
Data File C:\CHEM32\1\DATA\4-144-CF_PURE.D
 Sample Name: 4-144-CF_pure

```
=====
Injection Date   : 8/31/2014 2:25:41 PM      Seq. Line :    1
Sample Name      : 4-144-CF_pure              Location  : Vial 1
Acq. Operator    :                          Inj       :    1
Acq. Instrument  : Instrument 1              Inj Volume: 1 µl
Different Inj Volume from Sequence !      Actual Inj Volume : 4 µl
Acq. Method      : C:\CHEM32\1\METHODS\IC 80-20 1ML-1UL 9_MIN.M
Last changed     : 8/26/2014 2:27:32 PM
Analysis Method  : C:\CHEM32\1\METHODS\IC 80-20 1ML-1UL 40MIN.M
Last changed     : 12/2/2014 6:51:03 AM
                  (modified after loading)
=====
```



Peak #	RetTime [min]	Type	Width [min]	Area [mAU*s]	Height [mAU]	Area %
1	6.444	MM	0.1213	482.35236	66.26153	6.3727
2	6.787	MM	0.1335	7086.70605	884.48328	93.6273

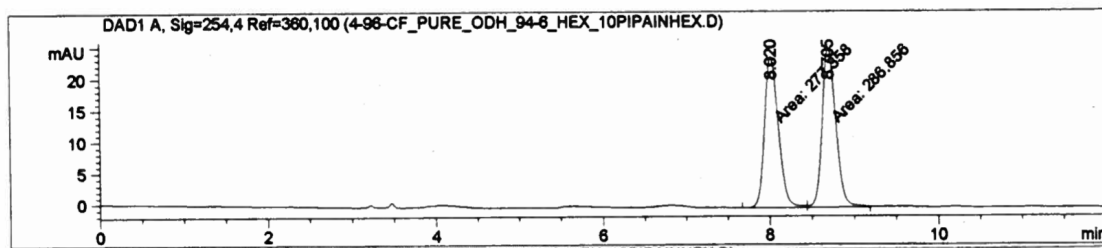
Data File C:\CHEM32\1\DATA\4-96-CF_PURE_ODH_94-6_HEX_10PIPAINHEX.D
 Sample Name: 4-96-CF_pure



=====

Injection Date : 7/2/2014 9:33:03 AM	Seq. Line : 1
Sample Name : 4-96-CF_pure	Location : Vial 1
Acq. Operator : TAD	Inj : 1
Acq. Instrument : Instrument 1	Inj Volume : 10 µl
Different Inj Volume from Sequence ! Actual Inj Volume : 1 µl	
Acq. Method : C:\CHEM32\1\METHODS\ODH_94-6_HEX-10-1-HEX-IPA 15 MIN.M	
Last changed : 1/10/2014 8:22:21 PM by tad	
Analysis Method : C:\CHEM32\1\METHODS\IC 80-20 1ML-1UL 40MIN.M	
Last changed : 12/2/2014 6:55:11 AM	
(modified after loading)	

=====



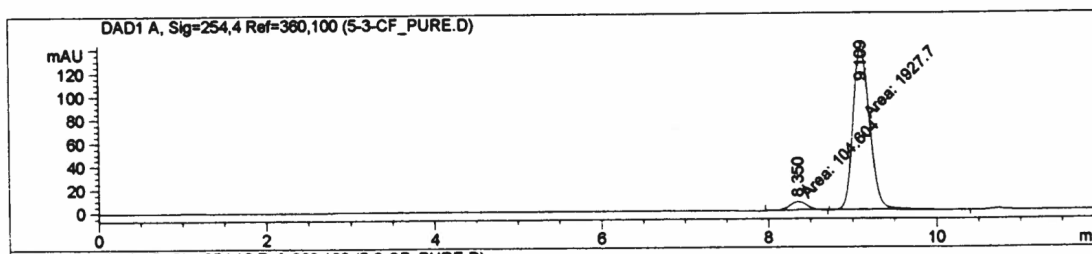
Peak #	RetTime [min]	Type	Width [min]	Area [mAU*s]	Height [mAU]	Area %
1	8.020	MM	0.1915	277.35767	24.14065	49.1583
2	8.705	MM	0.1872	286.85583	25.54341	50.8417

Data File C:\CHEM32\1\DATA\5-3-CF_PURE.D
 Sample Name: 5-3-CF_pure

=====

Injection Date : 9/27/2014 12:31:49 PM	Seq. Line : 2
Sample Name : 5-3-CF_pure	Location : Vial 51
Acq. Operator :	Inj : 1
Acq. Instrument : Instrument 1	Inj Volume : 10 µl
Different Inj Volume from Sequence ! Actual Inj Volume : 2 µl	
Acq. Method : C:\CHEM32\1\METHODS\ODH_94-6_HEX-10-1-HEX-IPA 12 MIN.M	
Last changed : 5/27/2014 11:31:49 AM by TAD	
Analysis Method : C:\CHEM32\1\METHODS\IC 80-20 1ML-1UL 40MIN.M	
Last changed : 12/2/2014 6:55:11 AM	
(modified after loading)	

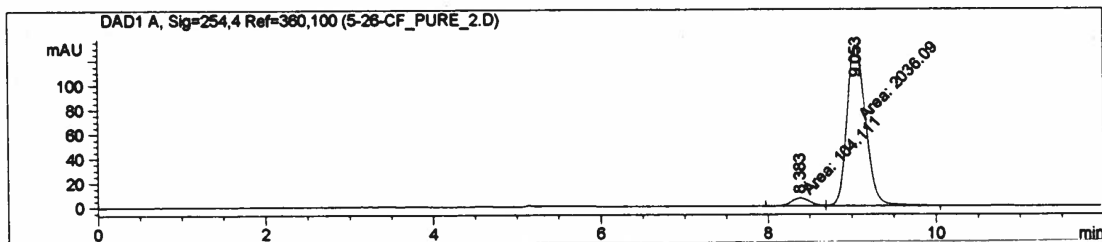
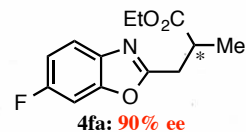
=====



Peak #	RetTime [min]	Type	Width [min]	Area [mAU*s]	Height [mAU]	Area %
1	8.350	MM	0.2441	104.60420	7.14341	5.1471
2	9.109	MM	0.2329	1927.70386	137.92970	94.8529

Data File C:\CHEM32\1\DATA\5-26-CF_PURE_2.D
Sample Name: 5-26-CF_pure

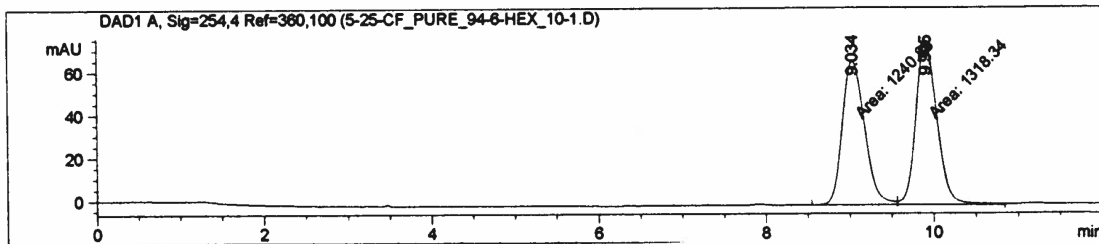
```
=====
Injection Date : 10/20/2014 8:42:38 PM      Seq. Line :    6
Sample Name   : 5-26-CF_pure                Location  : Vial 5
Acq. Operator :                             Inj      :    1
Acq. Instrument : Instrument 1              Inj Volume: 10 µl
Different Inj Volume from Sequence !      Actual Inj Volume : 3 µl
Acq. Method   : C:\CHEM32\1\METHODS\ODH 94-6 HEX-10-1-HEX-IPA 12 MIN.M
Last changed  : 5/27/2014 11:31:49 AM by TAD
Analysis Method : C:\CHEM32\1\METHODS\IC 80-20 1ML-1UL 40MIN.M
Last changed  : 12/2/2014 6:55:11 AM
                    (modified after loading)
=====
```



Peak #	RetTime [min]	Type	Width [min]	Area [mAU*s]	Height [mAU]	Area %
1	9.034	MM	0.3091	1240.87854	66.90951	48.4867
2	9.053	MM	0.2926	1318.33765	75.10188	51.5133

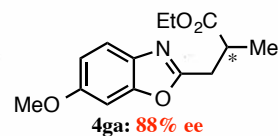
Data File C:\CHEM32\1\DATA\5-25-CF_PURE_94-6-HEX_10-1.D
Sample Name: 5-25-CF_pure

```
=====
Injection Date : 10/19/2014 3:33:30 PM      Seq. Line :    1
Sample Name   : 5-25-CF_pure                Location  : Vial 1
Acq. Operator :                             Inj      :    1
Acq. Instrument : Instrument 1              Inj Volume: 10 µl
Different Inj Volume from Sequence !      Actual Inj Volume : 2 µl
Acq. Method   : C:\CHEM32\1\METHODS\ODH 94-6 HEX-10-1-HEX-IPA 20 MIN.M
Last changed  : 9/3/2013 5:25:21 PM
Analysis Method : C:\CHEM32\1\METHODS\IC 80-20 1ML-1UL 40MIN.M
Last changed  : 12/2/2014 6:55:11 AM
                    (modified after loading)
=====
```

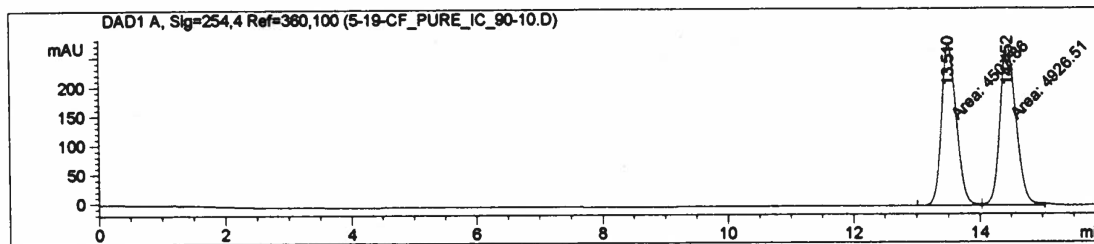


Peak #	RetTime [min]	Type	Width [min]	Area [mAU*s]	Height [mAU]	Area %
1	8.383	MM	0.2671	104.11058	6.49682	4.8645
2	9.053	MM	0.2576	2036.08582	131.74382	95.1355

Data File C:\CHEM32\1\DATA\5-19-CF_PURE_IC_90-10.D
 Sample Name: 5-19-CF_pure



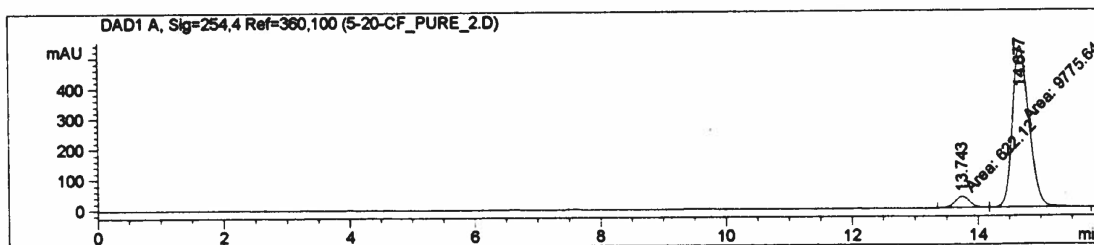
```
=====
Injection Date   : 10/9/2014 8:43:39 AM      Seq. Line :    1
Sample Name      : 5-19-CF_pure              Location  : Vial 21
Acq. Operator    :                          Inj      :    1
Acq. Instrument  : Instrument 1               Inj Volume: 1 µl
Different Inj Volume from Sequence !         Actual Inj Volume : 2 µl
Acq. Method      : C:\CHEM32\1\METHODS\IC 90-10 1ML-1UL 20MIN.M
Last changed     : 8/21/2014 7:51:32 AM
Analysis Method  : C:\CHEM32\1\METHODS\IC 80-20 1ML-1UL 40MIN.M
Last changed     : 12/2/2014 7:02:09 AM
                  (modified after loading)
=====
```



Peak #	RetTime [min]	Type	Width [min]	Area [mAU*s]	Height [mAU]	Area %
1	13.510	MM	0.2718	4507.85986	276.42017	47.7813
2	14.452	MM	0.2996	4926.50635	274.07120	52.2187

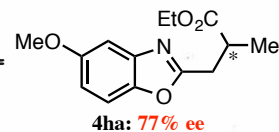
Data File C:\CHEM32\1\DATA\5-20-CF_PURE_2.D
 Sample Name: 5-20-CF_pure

```
=====
Injection Date   : 10/17/2014 2:25:27 PM      Seq. Line :    5
Sample Name      : 5-20-CF_pure              Location  : Vial 4
Acq. Operator    :                          Inj      :    1
Acq. Instrument  : Instrument 1               Inj Volume: 1 µl
Different Inj Volume from Sequence !         Actual Inj Volume : 2 µl
Acq. Method      : C:\CHEM32\1\METHODS\IC 90-10 1ML-1UL 20MIN.M
Last changed     : 8/21/2014 7:51:32 AM
Analysis Method  : C:\CHEM32\1\METHODS\IC 80-20 1ML-1UL 40MIN.M
Last changed     : 12/2/2014 7:02:09 AM
                  (modified after loading)
=====
```



Peak #	RetTime [min]	Type	Width [min]	Area [mAU*s]	Height [mAU]	Area %
1	13.743	MM	0.2779	622.11951	37.31636	5.9832
2	14.677	MM	0.3085	9775.64453	528.16187	94.0168

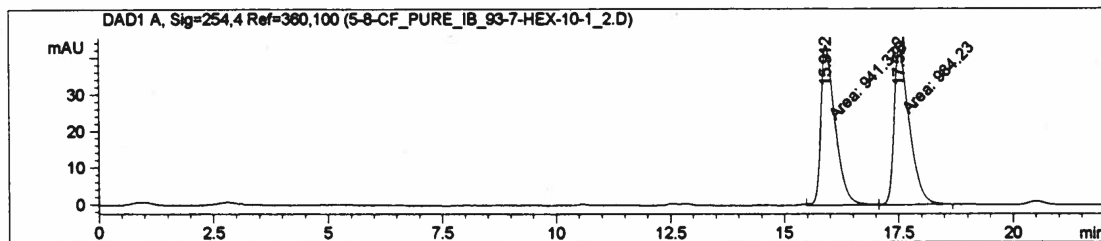
Data File C:\CHEM32\1\DATA\5-8-CF_PURE_IB_93-7-HEX-10-1_2.D
 Sample Name: 5-8-CF_pure



=====

Injection Date : 9/30/2014 10:17:02 AM	Seq. Line : 2
Sample Name : 5-8-CF_pure	Location : Vial 52
Acq. Operator :	Inj : 1
Acq. Instrument : Instrument 1	Inj Volume : 10 µl
Different Inj Volume from Sequence !	Actual Inj Volume : 2 µl
Acq. Method : C:\CHEM32\1\METHODS\ODH 93-7 HEX-10-1-HEX-IPA 15 MIN.M	
Last changed : 9/30/2014 10:17:23 AM	
	(modified after loading)
Analysis Method : C:\CHEM32\1\METHODS\IC 80-20 1ML-1UL 40MIN.M	
Last changed : 12/2/2014 7:06:11 AM	
	(modified after loading)

=====



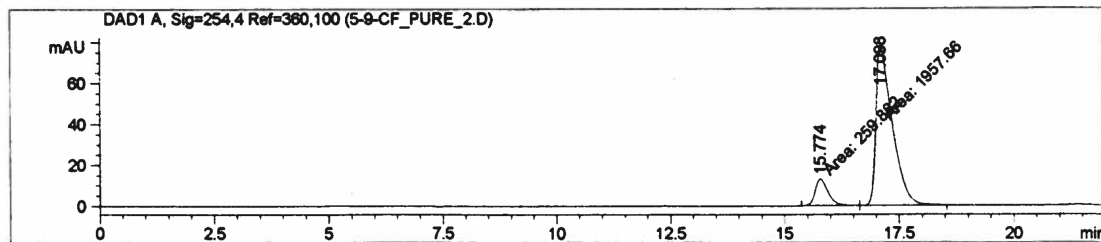
Peak #	RetTime [min]	Type	Width [min]	Area [mAU*s]	Height [mAU]	Area %
1	15.912	MM	0.3600	941.37628	43.57972	48.8873
2	17.522	MM	0.3888	984.23010	42.18650	51.1127

Data File C:\CHEM32\1\DATA\5-9-CF_PURE_2.D
 Sample Name: 5-9-CF_pure

=====

Injection Date : 10/1/2014 10:18:37 AM	Seq. Line : 2
Sample Name : 5-9-CF_pure	Location : Vial 51
Acq. Operator :	Inj : 1
Acq. Instrument : Instrument 1	Inj Volume : 10 µl
Different Inj Volume from Sequence !	Actual Inj Volume : 2 µl
Acq. Method : C:\CHEM32\1\METHODS\ODH 93-7 HEX-10-1-HEX-IPA 15 MIN.M	
Last changed : 10/1/2014 10:08:22 AM	
	(modified after loading)
Analysis Method : C:\CHEM32\1\METHODS\IC 80-20 1ML-1UL 40MIN.M	
Last changed : 12/2/2014 7:06:11 AM	
	(modified after loading)

=====



Peak #	RetTime [min]	Type	Width [min]	Area [mAU*s]	Height [mAU]	Area %
1	15.774	MM	0.3316	259.88199	13.06342	11.7194
2	17.098	MM	0.4143	1957.65564	78.75360	88.2806

Table 1. Crystal data and structure refinement for [Rh(cod)OAc]₂

Identification code	rovis139_0m	
Empirical formula	C ₂₀ H ₃₀ O ₄ Rh ₂	
Formula weight	540.26	
Temperature	120(2) K	
Wavelength	0.71073 Å	
Crystal system	Triclinic	
Space group	<i>P</i> -1	
Unit cell dimensions	<i>a</i> = 8.9223(8) Å	α = 103.826(4)°.
	<i>b</i> = 9.9063(8) Å	β = 90.574(5)°.
	<i>c</i> = 12.6748(11) Å	γ = 112.147(4)°.
Volume	1001.31(15) Å ³	
Z	2	
Density (calculated)	1.792 Mg/m ³	
Absorption coefficient	1.670 mm ⁻¹	
F(000)	544	
Crystal size	0.21 x 0.14 x 0.10 mm ³	
Theta range for data collection	1.66 to 33.41°.	
Index ranges	-13 ≤ <i>h</i> ≤ 13, -15 ≤ <i>k</i> ≤ 15, -19 ≤ <i>l</i> ≤ 19	
Reflections collected	27291	
Independent reflections	7666 [R(int) = 0.0256]	
Completeness to theta = 33.41°	98.3 %	
Absorption correction	Semi-empirical from equivalents	
Max. and min. transmission	0.8495 and 0.7248	
Refinement method	Full-matrix least-squares on F ²	
Data / restraints / parameters	7666 / 0 / 237	
Goodness-of-fit on F ²	1.088	
Final R indices [I > 2σ(I)]	R1 = 0.0324, wR2 = 0.0722	
R indices (all data)	R1 = 0.0604, wR2 = 0.0909	
Largest diff. peak and hole	0.831 and -0.492 e.Å ⁻³	

Table 2. Atomic coordinates ($\times 10^4$) and equivalent isotropic displacement parameters ($\text{\AA}^2 \times 10^3$) for Rovis139_0m. $U(\text{eq})$ is defined as one third of the trace of the orthogonalized U^{ij} tensor.

	x	y	z	U(eq)
C(1)	11185(3)	3719(3)	996(2)	43(1)
C(2)	11027(4)	2227(3)	620(2)	44(1)
C(3)	12303(4)	1664(3)	901(3)	56(1)
C(4)	11961(4)	1056(4)	1908(3)	55(1)
C(5)	11088(3)	1809(3)	2684(2)	43(1)
C(6)	11523(3)	3366(3)	3063(2)	40(1)
C(7)	13027(4)	4514(3)	2762(3)	52(1)
C(8)	12633(4)	4949(3)	1736(3)	52(1)
C(9)	6809(3)	2434(3)	326(2)	33(1)
C(10)	5711(3)	1618(3)	-737(2)	43(1)
C(11)	6606(3)	1843(3)	3161(2)	32(1)
C(12)	5456(3)	824(3)	3773(2)	48(1)
C(13)	9422(4)	6740(3)	2170(2)	41(1)
C(14)	10686(4)	7718(3)	3145(2)	48(1)
C(15)	10581(4)	6895(3)	4048(2)	47(1)
C(16)	8887(4)	5745(3)	4038(2)	41(1)
C(17)	7478(4)	6039(3)	4031(2)	44(1)
C(18)	7485(4)	7585(4)	4051(3)	58(1)
C(19)	7226(4)	7723(3)	2891(3)	52(1)
C(20)	7881(4)	6784(3)	2061(2)	43(1)
O(1)	7876(2)	1635(2)	2960(2)	45(1)
O(2)	6221(2)	2832(2)	2924(2)	44(1)
O(3)	7602(2)	1773(2)	635(2)	46(1)
O(4)	6848(3)	3703(2)	817(2)	46(1)
Rh(1)	7636(1)	4800(1)	2475(1)	31(1)
Rh(2)	9513(1)	2405(1)	1854(1)	30(1)

Table 3. Bond lengths [Å] and angles [°] for Rovis139_0m.

C(1)-C(2)	1.392(4)
C(1)-C(8)	1.509(4)
C(1)-Rh(2)	2.085(2)
C(2)-C(3)	1.517(4)
C(2)-Rh(2)	2.096(3)
C(3)-C(4)	1.524(4)
C(4)-C(5)	1.494(4)
C(5)-C(6)	1.398(4)
C(5)-Rh(2)	2.080(3)
C(6)-C(7)	1.518(4)
C(6)-Rh(2)	2.106(3)
C(7)-C(8)	1.540(4)
C(9)-O(3)	1.244(3)
C(9)-O(4)	1.249(3)
C(9)-C(10)	1.511(3)
C(11)-O(1)	1.245(3)
C(11)-O(2)	1.249(3)
C(11)-C(12)	1.511(3)
C(13)-C(20)	1.398(4)
C(13)-C(14)	1.521(4)
C(13)-Rh(1)	2.107(3)
C(14)-C(15)	1.540(4)
C(15)-C(16)	1.510(4)
C(16)-C(17)	1.393(4)
C(16)-Rh(1)	2.081(3)
C(17)-C(18)	1.524(4)
C(17)-Rh(1)	2.097(3)
C(18)-C(19)	1.532(4)
C(19)-C(20)	1.506(4)
C(20)-Rh(1)	2.087(2)
O(1)-Rh(2)	2.0954(17)
O(2)-Rh(1)	2.0999(17)
O(3)-Rh(2)	2.0894(18)
O(4)-Rh(1)	2.0958(18)

C(2)-C(1)-C(8)	123.8(3)
C(2)-C(1)-Rh(2)	70.98(15)
C(8)-C(1)-Rh(2)	112.41(18)
C(1)-C(2)-C(3)	123.6(3)
C(1)-C(2)-Rh(2)	70.14(15)
C(3)-C(2)-Rh(2)	113.35(19)
C(2)-C(3)-C(4)	111.5(2)
C(5)-C(4)-C(3)	112.7(2)
C(6)-C(5)-C(4)	125.6(3)
C(6)-C(5)-Rh(2)	71.48(15)
C(4)-C(5)-Rh(2)	111.17(19)
C(5)-C(6)-C(7)	122.8(3)
C(5)-C(6)-Rh(2)	69.51(15)
C(7)-C(6)-Rh(2)	114.17(18)
C(6)-C(7)-C(8)	111.5(2)
C(1)-C(8)-C(7)	112.7(2)
O(3)-C(9)-O(4)	125.6(2)
O(3)-C(9)-C(10)	116.5(2)
O(4)-C(9)-C(10)	117.9(2)
O(1)-C(11)-O(2)	126.0(2)
O(1)-C(11)-C(12)	116.4(2)
O(2)-C(11)-C(12)	117.7(2)
C(20)-C(13)-C(14)	123.0(3)
C(20)-C(13)-Rh(1)	69.76(15)
C(14)-C(13)-Rh(1)	113.72(17)
C(13)-C(14)-C(15)	111.6(2)
C(16)-C(15)-C(14)	112.2(2)
C(17)-C(16)-C(15)	124.5(3)
C(17)-C(16)-Rh(1)	71.13(15)
C(15)-C(16)-Rh(1)	112.29(18)
C(16)-C(17)-C(18)	123.3(3)
C(16)-C(17)-Rh(1)	69.90(15)
C(18)-C(17)-Rh(1)	113.54(19)
C(17)-C(18)-C(19)	111.1(2)
C(20)-C(19)-C(18)	112.6(2)

C(13)-C(20)-C(19)	125.5(3)
C(13)-C(20)-Rh(1)	71.29(14)
C(19)-C(20)-Rh(1)	110.90(18)
C(11)-O(1)-Rh(2)	128.95(16)
C(11)-O(2)-Rh(1)	130.66(17)
C(9)-O(3)-Rh(2)	134.42(17)
C(9)-O(4)-Rh(1)	126.41(16)
C(16)-Rh(1)-C(20)	98.92(11)
C(16)-Rh(1)-O(4)	166.32(10)
C(20)-Rh(1)-O(4)	86.42(9)
C(16)-Rh(1)-C(17)	38.97(11)
C(20)-Rh(1)-C(17)	82.51(11)
O(4)-Rh(1)-C(17)	154.70(10)
C(16)-Rh(1)-O(2)	90.32(9)
C(20)-Rh(1)-O(2)	150.92(10)
O(4)-Rh(1)-O(2)	90.99(8)
C(17)-Rh(1)-O(2)	87.81(10)
C(16)-Rh(1)-C(13)	82.28(11)
C(20)-Rh(1)-C(13)	38.94(11)
O(4)-Rh(1)-C(13)	94.43(9)
C(17)-Rh(1)-C(13)	91.15(11)
O(2)-Rh(1)-C(13)	169.37(9)
C(5)-Rh(2)-C(1)	98.68(12)
C(5)-Rh(2)-O(3)	148.89(9)
C(1)-Rh(2)-O(3)	92.22(10)
C(5)-Rh(2)-O(1)	85.55(9)
C(1)-Rh(2)-O(1)	165.06(10)
O(3)-Rh(2)-O(1)	91.35(8)
C(5)-Rh(2)-C(2)	82.31(12)
C(1)-Rh(2)-C(2)	38.88(11)
O(3)-Rh(2)-C(2)	88.38(10)
O(1)-Rh(2)-C(2)	155.82(9)
C(5)-Rh(2)-C(6)	39.00(11)
C(1)-Rh(2)-C(6)	82.13(11)
O(3)-Rh(2)-C(6)	171.62(9)
O(1)-Rh(2)-C(6)	92.60(9)

C(2)-Rh(2)-C(6) 91.03(11)

Symmetry transformations used to generate equivalent atoms:

Table 4. Anisotropic displacement parameters ($\text{\AA}^2 \times 10^3$) for Rovis139_0m. The anisotropic displacement factor exponent takes the form: $-2\pi^2 [h^2 a^{*2} U^{11} + \dots + 2 h k a^* b^* U^{12}]$

	U^{11}	U^{22}	U^{33}	U^{23}	U^{13}	U^{12}
C(1)	43(2)	48(2)	38(2)	18(1)	14(1)	14(1)
C(2)	42(2)	49(2)	32(1)	8(1)	12(1)	11(1)
C(3)	40(2)	48(2)	70(2)	-4(2)	19(2)	17(1)
C(4)	43(2)	51(2)	73(2)	11(2)	-5(2)	25(2)
C(5)	39(2)	50(2)	46(2)	20(1)	0(1)	21(1)
C(6)	36(2)	52(2)	32(1)	7(1)	-1(1)	21(1)
C(7)	34(2)	46(2)	62(2)	-5(2)	-3(1)	11(1)
C(8)	43(2)	41(2)	65(2)	12(2)	20(2)	8(1)
C(9)	29(1)	35(1)	31(1)	11(1)	5(1)	9(1)
C(10)	44(2)	47(2)	32(1)	5(1)	-4(1)	15(1)
C(11)	27(1)	32(1)	35(1)	9(1)	5(1)	9(1)
C(12)	41(2)	54(2)	54(2)	29(2)	18(1)	15(1)
C(13)	51(2)	35(1)	40(2)	16(1)	9(1)	16(1)
C(14)	43(2)	38(1)	53(2)	6(1)	0(1)	9(1)
C(15)	45(2)	47(2)	42(2)	5(1)	-7(1)	15(1)
C(16)	50(2)	46(2)	27(1)	9(1)	0(1)	19(1)
C(17)	51(2)	53(2)	31(1)	7(1)	9(1)	26(1)
C(18)	62(2)	54(2)	57(2)	-3(2)	9(2)	33(2)
C(19)	54(2)	36(1)	70(2)	9(1)	-3(2)	23(1)
C(20)	54(2)	34(1)	42(2)	15(1)	-5(1)	15(1)
O(1)	37(1)	54(1)	59(1)	32(1)	21(1)	22(1)
O(2)	35(1)	42(1)	62(1)	24(1)	10(1)	16(1)
O(3)	43(1)	43(1)	48(1)	-1(1)	-12(1)	20(1)
O(4)	64(1)	38(1)	35(1)	3(1)	-11(1)	21(1)
Rh(1)	36(1)	28(1)	29(1)	7(1)	0(1)	13(1)
Rh(2)	24(1)	35(1)	31(1)	10(1)	4(1)	11(1)

Table 5. Hydrogen coordinates ($\times 10^4$) and isotropic displacement parameters ($\text{\AA}^2 \times 10^{-3}$) for Rovis139_0m.

	x	y	z	U(eq)
H(1)	10685	4075	466	51
H(2)	10429	1707	-129	53
H(3A)	13390	2502	1037	67
H(3B)	12318	855	272	67
H(4A)	11296	-43	1673	66
H(4B)	13005	1204	2292	66
H(5)	10568	1237	3225	51
H(6)	11254	3699	3820	48
H(7A)	13868	4087	2626	63
H(7B)	13473	5431	3381	63
H(8A)	12413	5878	1964	62
H(8B)	13595	5174	1323	62
H(10A)	6363	1419	-1326	64
H(10B)	5165	2247	-905	64
H(10C)	4893	660	-668	64
H(12A)	5226	-233	3399	72
H(12B)	4437	985	3796	72
H(12C)	5958	1057	4520	72
H(13)	9889	6546	1463	49
H(14A)	10518	8662	3446	57
H(14B)	11788	7993	2900	57
H(15A)	11351	6382	3945	56
H(15B)	10913	7647	4769	56
H(16)	8846	4983	4444	49
H(17)	6616	5448	4431	53
H(18A)	8538	8380	4421	69
H(18B)	6610	7743	4473	69
H(19A)	6046	7400	2682	63
H(19B)	7770	8795	2883	63
H(20)	7454	6617	1288	52

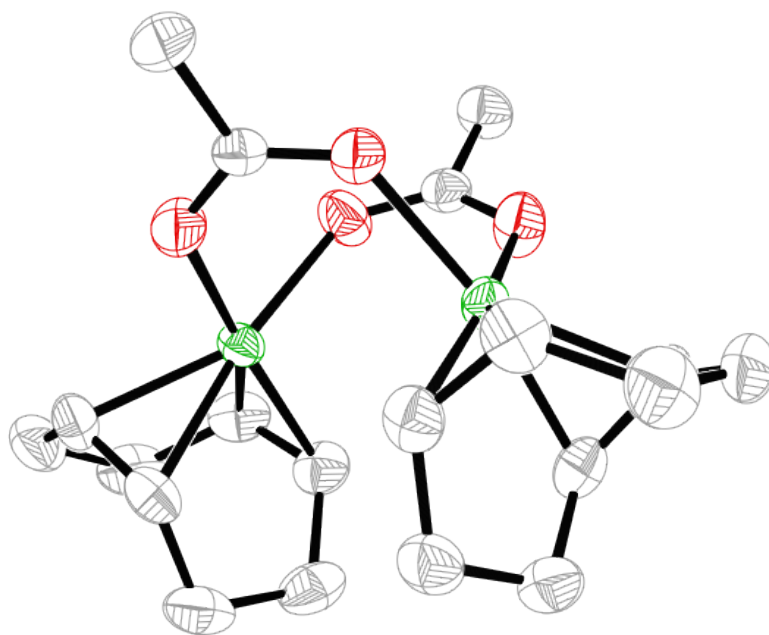


Figure A.2.20 X-ray crystal structure of $[\text{Rh}(\text{cod})\text{OAc}]_2$ (obtained by Dr. Kevin Martin Oberg)